UNIVERSIDADE FEDERAL DO PARÁ
INSTITUTO DE GEOCIÊNCIAS
PROGRAMA DE PÓS-GRADUAÇÃO EM GEOLOGIA E GEOQUÍMICA

TESE DE DOUTORADO

MAGMATISMO GRANITÓIDE ARQUEANO DA ÁREA DE CANAÃ DOS CARAJÁS: IMPLICAÇÕES PARA A EVOLUÇÃO CRUSTAL DA PROVÍNCIA CARAJÁS

Tese apresentada por:

GILMARA REGINA LIMA FEIO
Orientador: Prof. Dr. Roberto Dall'Agnol (UFPA)

BELÉM
2011

Dados Internacionais de Catalogação-na-Publicação (CIP)
Biblioteca Geólogo Raimundo Montenegro Garcia de Montalvão

F299m Feio, Gilmara Regina Lima

Magmatismo granitóide arqueano da área de Canaã dos Carajás: implicações para a evolução crustal da Província Carajás / Gilmara Regina Lima Feio; Orientador: Roberto Dall'Agnol – 2011
xv, 190 f.: il.

Tese (Doutorado em Geoquímica e Petrologia) – Programa de Pós-Graduação em Geologia e Geoquímica, Universidade Federal do Pará, Belém, 2011.

1. Geocronologia. 2. Isótopo de Nd. 3. Geoquímica. 4. Granitóides Arqueanos 5. Evolução crustal. 6. Província Carajás. I. Dall'Agnol, Roberto, *orient*. II. Universidade Federal do Pará. III. Título.

CDD 22º ed.:551.70098115

Universidade Federal do Pará

Instituto de Geociências

Programa de Pós-Graduação em Geologia e Geoquímica

MAGMATISMO GRANITÓIDE ARQUEANO DA ÁREA DE CANAÃ DOS CARAJÁS: IMPLICAÇÕES PARA A EVOLUÇÃO CRUSTAL DA PROVÍNCIA CARAJÁS

TESE APRESENTADA POR

GILMARA REGINA LIMA FEIO

Como requisito parcial à obtenção do Grau de Doutor em Ciências na Área de GEOQUÍMICA E PETROLOGIA

Data de Aprovação: 16/08/2011

Banca Examinadora:

Prof. ROBERTO DALL'AGNOL
(Orientador-UFPA)

Prof. ELSON PAIVA DE OLIVEIRA
(Membro-UNICAMP)

Profa. IGNEZ DE PINHO GUIMARÃES
(Membro-UFPE)

Prof. JEAN MICHEL LAFON
(Membro-UFPA)

Prof. MUDLAPPA JAYANANDA
(Membro-University of Delhi)

Prof. CLAUDIO NERY LAMARÃO
(Membro suplente – UFPA)

Ao mestre com carinho,
com açúcar e com afeto.

AGRADECIMENTOS

A autora expressa seus sinceros e profundos agradecimentos a todas as pessoas e entidades que contribuíram para que este trabalho fosse concluído a contento, em especial:

- Ao Programa de Pós-Graduação em Geociências da Universidade Federal do Pará (UFPA), pelo fornecimento de infra-estrutura.

- Ao CNPq/Universal (Proc. 484524/2007-0) e INCT de Geociências da Amazônia pelo suporte financeiro. E ao CNPq pela concessão da bolsa de estudo de doutoramento;

- Ao Grupo de Pesquisa Petrologia de Rochas Granitóides (GPPG) do Instituto de Geociências (IG) da UFPA, pelo suporte técnico-científico;

- Aos membros do laboratório de estudos geocronológicos, geodinâmicos e ambientais da UNB, em especial Elton, Sérgio, Barbara e Massimo;

- Ao Laboratório de Geologia Isotópica da UFPA pelo suporte na aquisição dos dados isotópicos, em especial aos professores Moacir Macambira e Marco Toro;

- Ao João O. Santos, pela aquisição de dados SHRIMP U-Pb;

- Ao colegiado de Marabá, pela oportunidade de concluir esta tese com tranqüilidade;

- Aos funcionários Cleida, Joelma, Edinelson, Lúcia e Macris da UFPA;

- A Alan Gomes, Alex, Erimar e Marcelo pelo passo inicial nos trabalhos desenvolvidos na região de Canaã dos Carajás; e a Albano, Cadu, Davis, Fabricia, Fernando e Patrick pelo auxílio no mapeamento geológico.

- A Adriel, Albano et al., Alice, Ari et al., Davis et al., Daniel, Eleison, Fabriciana, Ingrid, Lamarão et al., Macris, Mayara, Mara, Marcelo et al., Nathan, Pablo, Patrick, Roseli e Tayla, pelo esforço diário em desenvolver pesquisas na Província Carajás.

- Ao Hilton (MPEG), Régis (UFPA) e Gilvana (VALE), equipe Pitinga, obrigada pelo eterno incentivo;

- Um agradecimento especial ao Carlos Marcello e toda sua família pelo incentivo e apoio.

- Aos amigos Roberta, Marlon, Hérica, Tizzianne, Alex presuntinho e André Bob, pelos momentos de descontração e carinho que vocês me proporcionaram.

- À minha família, que é sem dúvida nenhuma a melhor do mundo, em especial aos meus sobrinhos e minhas mães.

- Por fim, a Roberto Dall'Agnol, meu ídolo, grande professor, pesquisador, orientador e amigo que tive a oportunidade de conviver. Foi Roberto que me despertou a *alegria* de trabalhar com granitos, que me estendeu a mão e me estimulou a procurar um caminho; que sempre me enriquece com sua presença.

Eu tentei evitar
Liguei a tevê
E deitei no sofá
Desde que haja tempo pra sonhar
E assuntos pra desenvolver
Não é muito fácil desligar
...O saldo final de tudo
Foi mais positivo que mil divãs
... Faz-me mais feliz
Dá-me asas pra fluir
(Tiê)

SUMÁRIO

LISTA DE ILUSTRAÇÕES

2 - ARCHEAN GRANITOID MAGMATISM IN THE CANAÃ DOS CARAJÁS AREA: IMPLICATIONS FOR CRUSTAL EVOLUTION OF THE CARAJÁS PROVINCE, AMAZONIAN CRATON, BRAZIL

3 - GEOCHEMISTRY AND PETROGENESIS OF THE GRANITES FROM THE CANAÃ DOS CARAJÁS AREA, CARAJÁS PROVINCE, BRAZIL: IMPLICATIONS FOR THE ORIGIN OF ARCHEAN GRANITES

4 - GEOCHEMISTRY, GEOCHRONOLOGY, AND ORIGIN OF THE NEOARCHEAN PLANALTO GRANITE SUITE, CARAJÁS, AMAZONIAN CRATON: A-TYPE OR HYDRATED CHARNOCKITIC GRANITES?

LISTA DE TABELAS

1 – INTRODUÇÃO

2 - ARCHEAN GRANITOID MAGMATISM IN THE CANAÃ DOS CARAJÁS AREA: IMPLICATIONS FOR CRUSTAL EVOLUTION OF THE CARAJÁS PROVINCE, AMAZONIAN CRATON, BRAZIL

3 - GEOCHEMISTRY AND PETROGENESIS OF THE GRANITES FROM THE CANAÃ DOS CARAJÁS AREA, CARAJÁS PROVINCE, BRAZIL: IMPLICATIONS FOR THE ORIGIN OF ARCHEAN GRANITES

4 - GEOCHEMISTRY, GEOCHRONOLOGY, AND ORIGIN OF THE NEOARCHEAN PLANALTO GRANITE SUITE, CARAJÁS, AMAZONIAN CRATON: A-TYPE OR HYDRATED CHARNOCKITIC GRANITES?

RESUMO

Mapeamento geológico e estudos geocronológicos, geoquímicos e petrológicos realizados nos granitóides arqueanos da área de Canaã dos Carajás na Província Carajás do Cráton Amazônico permitiram a definição de novas unidades granitóides que vieram a substituir inteiramente o Complexo Xingu, outrora dominante naquela área. Quatro grandes eventos magmáticos foram identificados, três de idade mesoarqueana e um de idade neoarqueana: (1) em 3,05-3,0 Ga ocorreu a formação do protólito do Complexo Pium e de rochas com idades similares cuja existência foi deduzida somente a partir de zircões herdados encontrados em diversas unidades; (2) em 2,96-2,93 Ga deu-se a cristalização do Granito Canaã dos Carajás e a formação das rochas mais antigas do Trondhjemito Rio Verde; (3) em 2,87-2,83 Ga foram formados o Complexo Tonalítico Bacaba, o Trondhjemito Rio Verde e os granitos Bom Jesus, Cruzadão e Serra Dourada; (4) no Neoarqueano, em 2,75-2,73 Ga foram originados as suítes Planalto e Pedra Branca e rochas charnoquíticas. Em termos geoquímicos foram distinguidos dois grandes grupos de granitóides: (A) As unidades tonalítico-trodhjemíticas que englobam o Complexo Tonalítico Bacaba e a Suíte Pedra Branca, que são geoquimicamente distintos dos típicos TTG arqueanos, e o Trondhjemito Rio Verde similar às séries TTG; (B) As unidades graníticas que cobrem mais de 60% da superfície de Canaã e incluem cinco unidades distintas. Os granitos mesoarqueanos Canaã dos Carajás, Bom Jesus, Cruzadão e Serra Dourada são compostos essencialmente de biotita leucomonzogranitos, enquanto que as rochas dominantes na Suíte neoarqueana Planalto são biotita-hornblenda monzogranitos a sienogranitos com conteúdo modal de máficos variando de 5% a 20%. Os granitos Canaã dos Carajás e Bom Jesus e a variedade do Granito Cruzadão com razões La/Yb mais elevadas são geoquimicamente similares aos granitos cálcio-alcalinos, enquanto que as outras variedades do Granito Cruzadão são transicionais entre granitos cálcio-alcalinos e alcalinos. O Granito Serra Dourada tem um caráter ambíguo em termos geoquímicos, pois apresenta similaridades ora com granitos cálcio-alcalinos, ora com os peraluminosos. Os granitos Canaã dos Carajás e Bom Jesus de Canaã são similares aos granitos com Alto-Ca, enquanto que os granitos Cruzadão e Serra Dourada se assemelham mais aos granitos Baixo-Ca do Cráton Yilgarn. As características geoquímicas dos granitos mesoarqueanos de Canaã se aproximam daquelas dos biotita granitos arqueanos do Cráton Dharwar, mas os últimos são enriquecidos em HFSE e ETRP quando comparados com os granitos mesoarqueanos de Canaã. As variações acentuadas das razões Sr/Y e $(La/Yb)_N$ observadas nos granitos de Canaã devem refletir dominantemente diferenças composicionais nas fontes dos magmas graníticos com efeito subordinado da pressão. O modelamento geoquímico sugere que a fusão parcial de uma fonte similar em composição a média de basaltos do Proterozóico Inferior ou a média da crosta continental inferior poderia gerar os magmas formadores do Granito Bom Jesus e da

variedade do Granito Cruzadão com razão $(La/Yb)_N$ mais elevada. O resíduo de fusão deveria conter proporções variáveis de plagioclásio, hornblenda, granada, clinopiroxênio ± ortopiroxênio e ilmenita. Nos demais granitos de Canaã, plagioclásio foi a fase dominante, a granada estava muito provavelmente ausente e a hornblenda teve influência limitada no resíduo de fusão. Uma pressão de 8 a 10 kbar e um ambiente crustal foi estimada para a geração dos magmas que apresentaram granada como uma das fases residuais tais como aqueles dos granitos Bom Jesus e similares. Os granitos neoarqueanos da Suíte Planalto são ferrosos e similares geoquimicamente aos granitos reduzidos do tipo-A. Porém, o ambiente tectônico e a associação entre a Suíte Planalto e rochas charnoquíticas levou-nos a propor que tais granitos sejam classificados como biotita-hornblenda granitos hidratados associados às séries charnoquiticas. A Suíte Planalto derivou da fusão parcial de rochas máficas a intermediárias toleiíticas com ortopiroxênio similares àquelas do Complexo Pium. O magmatismo granitóide arqueano de Canaã difere significativamente daquele encontrado na maioria dos crátons arqueanos, incluindo o terreno Rio Maria, porque o magmatismo TTG não é abundante, rochas sanukitóides não foram identificadas e rochas graníticas são dominantes. A Suíte Planalto não possui equivalente no terreno mesoarqueano de Rio Maria, nem tampouco aparentemente nos crátons de Yilgarn e Dharwar. Os contrastes entre Canaã e o Terreno Granito-*Greenstone* de Rio Maria não favorecem a hipótese de uma evolução tectônica idêntica ou muito similar para estes dois domínios arqueanos da Província Carajás. A crosta arqueana de Canaã não mostra caráter juvenil e a curva de evolução do Nd sugere a existência de uma crosta um pouco mais antiga na área de Canaã em comparação ao Terreno Rio Maria. A crosta de Canaã existe pelo menos desde o Mesoarqueano (ca. 3.2 a 3.0 Ga) e foi fortemente retrabalhada durante o Neoarqueano (2.75 a 2.70 Ga). Um terreno similar ao da crosta Mesoarqueana de Canaã ou até mesmo a extensão da mesma deve corresponder ao substrato da Bacia Carajás; e o denominado subdomínio de 'Transição' apresentou, provavelmente, uma evolução distinta daquela do Terreno Rio Maria. A evolução Neoarqueana da Província Carajás foi marcada pela ascensão do manto astenosférico em um ambiente extensional, que provocou a formação da Bacia Carajás. Entre 2.73-2.7 Ga, o calor gerado pela colocação de magmas máficos induziu a fusão parcial da crosta inferior máfica e intermediária originando os granitóides das suítes Planalto e Pedra Branca, e os charnoquitos. A íntima relação entre a suíte Planalto e as rochas charnoquíticas sugerem similaridades de evolução com o magmatismo formado em temperaturas elevadas comumente encontradas em limites de blocos tectônicos ou em sua zona de interação.

Palavras-chave: Geocronologia. Isótopo de Nd. Geoquímica. Granitóides Arqueanos. Evolução crustal. Província Carajás.

ABSTRACT

Geological mapping, geochemical, and geochronological studies undertaken in the Archean granitoids of the Canaã area in the Carajás province, Amazonian craton, Brazil, led to the definition of new granitoid units that entirely replace the Xingu complex in the area. Four major magmatic events are indentified: three of Mesoarchean age and one of Neoarchean age. The succession of events is: (1) at 3.05-3.0 Ga, it occurred the formation of the protolith of the Pium complex and of rocks with similar ages only indicated by inherited zircons found in different units; (2) at 2.96-2.93 Ga, occurred the crystallization of the Canaã dos Carajás granite and the formation of the older rocks of the Rio Verde trondhjemite; (3) at 2.87-2.83 Ga, the Bacaba tonalitic complex, the Rio Verde trondhjemite, and the Cruzadão, Bom Jesus and Serra Dourada granites were formed; (4) in the Neoarchean, at 2.75-2.73 Ga, the Planalto and Pedra Branca suites and charnockite rocks were originated. Geochemically, two groups of granitoid units were distinguished: (1) The tonalitic-trondhjemitic units, which encompass the Bacaba tonalitic complex and the Pedra Branca suite, which are geochemically distinct of typical Archean TTG series, and the Rio Verde trondhjemite, akin to the TTG series; (2) the granitic units which cover more than 60% of the Canaã surface and include five distinct granites. The Mesoarchean Canaã dos Carajás, Bom Jesus, Cruzadão, and Serra Dourada granites are composed dominantly of biotite leucomonzogranites whereas the dominant rocks in the Neoarchean Planalto suite are biotite-hornblende monzogranites to syenogranites with total mafic content between 5% and 20%. The Canaã dos Carajás and Bom Jesus granites and the variety of the Cruzadão granite with higher La/Yb are geochemically akin to the calc-alkaline granites, whereas the other varieties of the Cruzadão granite are transitional between calc-alkaline and alkaline granites. The Serra Dourada granite has an ambiguous geochemical character with some features similar to those of calc-alkaline granites and other to peraluminous granites. The Canaã dos Carajás and Bom Jesus granites of Canaã are similar to the High-Ca granites, whereas the Cruzadão and Serra Dourada are more akin to the Low-CaO granites of the Yilgarn craton. The geochemical characteristics of the Mesoarchean Canaã granites approach those of the biotite granite group of the Dharwar craton but the latter are enriched in HFSE and HREE compared to the Mesoarchean granites of Canaã. The accentuated variation of the Sr/Y and $(La/Yb)_N$ ratios observed in the Canaã granites should reflect dominantly compositional differences in the sources of the granite magmas with a subordinate effect of pressure. Geochemical modeling suggests that partial melting of a source similar in composition to the average of Early Proterozoic basalts or to the average lower continental crust could be able to give origin to the Bom Jesus granite and to the variety of the Cruzadão granite with higher $(La/Yb)_N$. The residue of melting will contain variable proportions of plagioclase, amphibole, garnet, clinopyroxene ± orthopyroxene, and ilmenite.

In the other Canaã granites, plagioclase was dominant, garnet was probably an absent phase in the residue of melting and the influence of amphibole was also apparently limited. A crustal environment and a pressure of 8 to 10 kbar is estimated for the generation of the Bom Jesus and similar granite magmas that left garnet as a residual phase. The Neoarchean Planalto granites have ferroan character and are similar geochemically to reduced A-type granites. The tectonic setting and the association between the Planalto suite and charnockitic series led us to propose classifying these biotite-hornblende granites as hydrated granites of the charnockitic series. The Planalto suite was derived by partial melting of mafic to intermediate tholeitic orthopyroxene-bearing rocks similar to those of the Pium complex. The Archean granitoid magmatism in Canaã significantly differs of that found in most classical Archean cratons, including the Rio Maria terrane, because TTG magmatism is not abundant, sanukitoid rocks are absent and granitic rocks are dominant. The Neoarchean Planalto suite granite has no counterpart in the Mesoarchean Rio Maria terrane of the Carajás province, neither apparently in the Yilgarn and Dharwar cratons. The contrasts between Canaã and the Rio Maria granite-greenstone terrane do not favor a common tectonic evolution for these two domains of the Carajás province. The Archean crust of Canaã has not a juvenile character and the Nd evolution paths suggest the existence of a little older crust in the Canaã area compared to that of Rio Maria. The crust of the Canaã area existed at least since the Mesoarchean (ca. 3.2 to 3.0 Ga) and was strongly reworked during the Neoarchean (2.75 to 2.70 Ga). A similar terrane to that represented by the Canaã Mesoarchean crust or even an extension of it was probably the substratum of the Carajás basin formed during the Neoarchean. Probably there is no an effective transition between Rio Maria and the Carajás basin and the denominated 'Transition' subdomain had more probably an evolution distinct of that of Rio Maria. The Neoarchean evolution of the Carajás province is marked by the upwelling of the asthenospheric mantle in an extensional setting that propitiated the formation of the Carajás basin. Later on, at ca. 2.73-2.70 Ga, the heat input associated with underplate of mafic magma induced the partial melting of mafic to intermediate lower crustal rocks originating the Planalto and Pedra Branca suites, and charnockite rocks. The close association between the Planalto suite and charnockitic rocks suggests similarity between its evolution and that of the high temperature granite magmatism commonly found near the limits between distinct tectonic blocks or in their zone of interaction.

Keywords: Geochronology. Nd isotope, Geochemistry. Archean Granitoids. Crustal evolution. Carajás Province.

1. INTRODUÇÃO

1.1 - APRESENTAÇÃO

A área de Canaã dos Carajás, alvo da presente pesquisa, faz parte do subdomínio de Transição (Dall'Agnol et al. 2006), na porção sul do Domínio Carajás (Vasquez et al. 2008b). Esta área corresponde a um segmento da Província Carajás que, conforme dados obtidos no presente trabalho, é constituído por *greenstone belts* e diversos tipos de granitóides de idade Mesoarqueana (TTG, Tonalitos a granodioritos cálcico-alcalinos, leucogranitos de afinidade cálcico-alcalina); e seqüências metavulcano-sedimentares e granitóides de idade Neoarqueana (granitos subalcalinos, tonalitos e trondhjemitos com alto Zr, Y e Ti e charnoquitos). No Paleoproterozóico, essas rochas foram cortadas por granitos anorogênicos (Huhn et al. 1988, Souza et al. 1990, Dall'Agnol et al. 1997, 2006).

Antes da presente tese, grande parte dos granitóides da área de Canaã dos Carajás era inserida no Complexo Xingu (formado por diversos tipos de rochas). Apenas a porção sudeste da área Canaã (Gomes 2003, Sardinha et al. 2004) e o granito Planalto em sua área-tipo (Oliveira 2003, Huhn et al. 1999) haviam sido caracterizados em termos de sua petrografia, geoquímica e geocronologia, mas não havia uma discussão mais profunda sobre a origem dos granitóides e seu papel na evolução crustal da Província Carajás.

Portanto, o principal objetivo desta tese foi contribuir para esclarecer a petrogênese e o papel dos granitóides na evolução geológica e geotectônica deste segmento da Província Carajás e avançar, assim, na compreensão da evolução crustal desta área e do Domínio Carajás como um todo. Para alcançar esses objetivos, foram obtidos dados geológicos, petrográficos, geoquímicos, geocronológicos e isotópicos.

Este documento foi elaborado seguindo o modelo de tese de integração de artigos. Desta forma, o corpo central da tese apresenta três artigos científicos submetidos a periódicos internacionais, sendo os mesmos apresentados na forma de capítulos (capítulos 2, 3 e 4). Os capítulos com os artigos são precedidos por um texto integrador, que é apresentado em um capítulo introdutório (Capitulo 1), que inclui a apresentação da pesquisa, localização da área de estudo, contexto geológico e tectônico regional, as principais características do magmatismo granitóide da Província Carajás, bem como a apresentação do problema, os objetivos traçados e materiais e métodos usados para alcançar os objetivos. O capitulo final (capitulo 5), sumariza de forma integrada as discussões e as conclusões alcançadas nos três artigos científicos e no desenvolvimento da tese como um todo.

Os artigos serão apresentados de acordo com a seguinte ordem:

Capítulo 2 – *Artigo 1* – **Archean granitoid magmatism in the Canaã dos Carajás area: Implications for crustal evolution of the Carajás Province, Amazonian craton, Brazil.** Submetido para publicação à revista *PRECAMBRIAN RESEARCH*. Este artigo apresenta dados inéditos sobre a geologia, petrografia, geoquímica, geocronologia e isótopos de Nd dos granitóides arqueanos aflorantes na área de Canaã dos Carajás, Província Carajás. Os dados apresentados permitiram definir a natureza do magmatismo granitóide, bem como determinar os principais eventos de formação e/ou retrabalhamento da crosta e desta forma especular sobre a história evolutiva deste segmento da Província Carajás, comparar com a evolução do Terreno granito-*greenstone* de Rio Maria (TGGRM), localizado na porção sul da província e com aquela de outros crátons arqueanos.

Capítulo 3 – *Artigo 2* – **Geochemistry and petrogenesis of the granites from the Canaã dos Carajás area, Carajás province, Brazil: implications for the origin of Archean granites.** Submetido para publicação à revista *LITHOS*. O artigo aborda os aspectos geológicos e o comportamento geoquímico dos granitos da área de Canaã dos Carajás. Este trabalho foi fundamental para distinguir as séries graníticas formadas no Arqueano em Canaã, bem como discutir os prováveis processos e fontes responsáveis pela geração dos mesmos. Além disso, foi realizada comparação entre os granitóides de Canaã e aqueles do TGGRM e de outros crátons arqueanos do mundo.

Capítulo 4 – *Artigo 3* **– Geochemistry, geochronology, and origin of the Neoarchean Planalto Granite suite, Carajás, Amazonian craton: A-type or hydrated charnockitic granites?** Submetido para publicação à revista *LITHOS*. Este artigo apresenta dados petrográficos, geoquímicos e geocronológicos dos granitos da suíte Planalto. Tais rochas são biotita-hornblenda granitos associados com rochas charnoquíticas e apresentam caráter ferroso, com características de granitos tipo-A. Tais granitos são raros em terrenos arqueanos de outros cratons do mundo, inclusive no TGGRM. Foram discutidos a natureza dos granitos, os processos e fonte responsáveis pela formação dos mesmos, bem como a implicação desse tipo de magmatismo para a evolução da crosta arqueana da Província Carajás. Foi questionado se tais granitos não correspondem a granitos hidratados da série charnoquítica, ao invés de verdadeiros granitos tipo-A.

1.2 - LOCALIZAÇÃO E ACESSO À REGIÃO DE CANAÃ DOS CARAJÁS

A área de Canaã dos Carajás está localizada nas cercanias do município homônimo, no sudeste do Estado do Pará, Brasil. Partindo de Belém, o acesso à área pode ser feito por via terrestre ou aérea até a cidade de Marabá, seguindo-se desta em direção à Parauapebas por via

terrestre pelas rodovias PA-150 e PA-275. O acesso para o município de Canaã dos Carajás se dá por estrada pavimentada, ligando o terminal ferroviário de Parauapebas com a cidade de Canaã dos Carajás e com a mina do Sossego. Além dessas vias principais, a área é cortada por uma série de estradas não pavimentadas e caminhos, trafegáveis nos períodos menos chuvosos.

1.3 - CONTEXTO GEOLÓGICO REGIONAL

O Cráton Amazônico tem sido subdividido em províncias geocronológicas com idades e padrões estruturais distintos e evoluções geodinâmicas particulares (Tassinari & Macambira 2004, Santos et al. 2000). Tassinari & Macambira (2004) consideram que a Província Amazônia Central é o segmento mais antigo do Cráton Amazônico, sendo dividida em dois blocos tectônicos principais: Carajás e Xingu-Iricoumé. Santos et al. (2000) consideram o bloco Arqueano de Carajás como uma província independente. Entretanto, os diferentes autores citados concordam que a Província Carajás constitui o principal núcleo arqueano do Cráton Amazônico. Além da Província Carajás, idades arqueanas foram obtidas em granitóides expostos na região do Amapá (Rosa-Costa et al. 2003, 2006, Rosa-Costa 2006) e Bacajá (Vasquez et al. 2008a, Macambira et al. 2009). Além disso, dados de isótopos de Nd mostram evidências de uma crosta arqueana no domínio vulcânico que se estende do Xingu à região próxima de Itaituba (Teixeira et al. 2002, Lamarão et al. 2005).

1.4 - GEOLOGIA DA PROVÍNCIA CARAJÁS

A província Carajás (PC) está localizada na porção sul-oriental do Cráton Amazônico. Para Costa & Hasui (1997), a estruturação do Cráton Amazônico resultou da articulação de blocos crustais que teriam se unido através de colisões no Arqueano/Proterozóico Inferior, compondo parte de um megacontinente. Além das colisões, teriam ocorrido eventos extensionais, acompanhados por intenso magmatismo e formação de bacias, cuja geometria foi controlada por estruturas pré-existentes. Entretanto, Cordani & Sato (1999), Tassinari & Macambira (1999, 2004), Santos et al. (2000) consideram que o Cráton Amazônico é dividido em províncias geocronológicas, formadas em torno de um núcleo arqueano, denominado originalmente Província Amazônia Central (Teixeira et al. 1989). As províncias proterozóicas resultaram de retrabalhamentos e acresção crustal ao longo de cinturões móveis e são, geralmente, alongadas na direção NW/SE.

Santos et al. (2000) denominaram a porção sudeste da Província Amazônia Central de Província Carajás que seria integralmente formada durante o Arqueano. Eles assumiram que

esta província se prolongaria até o sul do Amapá, formando um bloco arqueano de maiores dimensões. Embora trabalhos posteriores tenham demonstrado inequivocamente a existência de um bloco arqueano no sul do Amapá (Bloco Amapá, Rosa-Costa 2006 e Rosa-Costa et al. 2006), e estudos desenvolvidos na região de Bacajá, ao norte de Carajás, revelaram que este domínio formou-se essencialmente durante o Paleoproterozóico, relacionado ao evento Transamazônico, e não no Arqueano (Macambira et al. 2001, Vasquez et al. 2005, 2008a, 2008b, Macambira et al. 2009). Em função disso, modelos mais recentes restringem a Província Carajás até o sul do Domínio Bacajá, correspondente ao extremo sul da província Transamazonas (Santos et al. 2000) ou Maroni-Itacaiunas (Tassinari & Macambira 2004).

1.4.1. Aspectos tectono-estratigráficos e modelos evolutivos

A geologia da Província Carajás foi inicialmente delineada por Hirata et al. (1982) e DOCEGEO (1988), sendo, com o passar dos anos, aperfeiçoada por diversos autores (Araújo & Maia 1991, Machado et al. 1991, Macambira & Vale 1997, Macambira & Lafon 1995, Costa et al. 1995, Dall'Agnol et al. 1997, 2006, Avelar et al. 1999, Neves & Vale 1999, Althoff et al. 2000, Souza et al. 2001, Leite et al. 2004, Pidgeon et al. 2000, Tallarico et al. 2005, et al. 2005, Lobato et al. 2005, Vasquez et al. 2008b, Oliveira, M.A. 2009, Almeida et al. 2011).

Costa et al. (1995) distinguiram três domínios tectônicos na Província Carajás: Cinturão de Cisalhamento Itacaiunas (CCI) a norte, Cinturão de Cisalhamento Pau D'Arco (CCPD) a sul e o Terreno Granito-*Greenstone* de Rio Maria (TGGRM), como um domínio preservado tectonicamente, entre eles. Althoff et al. (1991, 1995), Dall'Agnol et al. (1997) e Rolando & Macambira (2002, 2003) não consideram o CCPD como um domínio distinto e sim como um prolongamento do TGGRM até a região de Redenção e Serra do Inajá. De acordo com Souza et al. (1996), a PC possui dois blocos tectônicos, cujo limite entre eles é incerto, mas estaria localizado a norte do *greenstone belt* de Sapucaia, pertencente ao Supergrupo Andorinhas, situando-se o TGGRM a sul e o domínio Carajás (DC) a norte.

DOCEGEO (1988) considera que a Bacia de Carajás, na qual domina o Supergrupo Itacaiunas, formou-se sobre o terreno Granito-*Greenstone* de Rio Maria. Dall'Agnol et al. (1997, 2006) acreditam que a região entre Xinguara e a porção sul da Bacia de Carajás corresponde a um domínio de transição, pois seria uma extensão do TGGRM, intensamente afetada pelos eventos magmáticos e tectônicos registrados na bacia Carajás. No entanto, o limite entre o TGGRM e a bacia Carajás permanece ainda indefinido. Apesar das indefinições ainda existentes, no texto ora apresentado será adotada a designação de "subdomínio de

Transição" (Dall'Agnol et al. 2006) para a região entre Xinguara e Serra Sul de Carajás, sendo a sua geologia abordada separadamente, sem que isso implique um posicionamento definitivo em relação à evolução deste segmento da Província Carajás. Vasquez et al. (2008b) também distinguem apenas dois grandes domínios na Província Carajás, o Domínio Rio Maria e o Domínio Carajás.

1.4.2. Terreno Granito-*Greenstone* de Rio Maria

O TGGRM é o domínio cuja evolução geológica foi estudada em maior detalhe dentro da Província Carajás. É formado por *greenstone belts* (Supergrupo Andorinhas) e por cinco principais grupos de granitóides arqueanos (Pimentel & Machado 1994, Macambira & Lafon 1995, Althoff et al. 2000, Leite 2001, Leite et al. 2004, Dall'Agnol et al. 2006, Oliveira et al. 2009, Almeida et al. 2010, 2011): (1) Séries TTGs mais antigas formadas em dois episódios distintos, sendo o mais antigo (2,96 ± 0,02 Ga), representado pelo Tonalito Arco Verde e Trondhjemito Mogno, seguido em 2,93 ± 0,02 Ga pela formação do Complexo Tonalítico Caracol, Tonalito Mariazinha e algumas rochas do Tonalito Arco Verde; (2) granitóides dominantemente granodioríticos com alto Mg (2,87 Ga), formado pelo Granodiorito Rio Maria, rochas intermediárias e máficas associadas de afinidade sanukitóide; (3) leucogranodioritos e leucomonzogranitos cálcico-alcalinos enriquecidos em Ba e Sr, representados pela Suíte Guarantã e granitos similares (2,87 Ga); (4) TTGs mais jovens, correspondentes ao Trondhjemito Água Fria (2.86 Ga); (5) leucogranitos potássicos (2,86 Ga), representados pelos granitos Xinguara, Mata Surrão e similares.

1.4.2.1. Greenstone belts

São formados por sequências vulcano-sedimentares (Sapucaia, Identidade, Lagoa Seca, Babaçu, Seringa, Pedra Preta, entre outras) metamorfisadas em condições de fácies xisto-verde a anfibolito (Souza et al. 1997, 2001) e agrupadas no Supergrupo Andorinhas (Huhn et al. 1988, DOCEGEO 1988). Vasquez et al. (2008b) não utilizam o termo Supergrupo Andorinhas, e dividem os *greenstone belts* do TGGRM em seis grupos: Gradaús, Serra do Inajá, Lagoa Seca, Babaçu, Sapucaia e Tucumã.

Souza et al. (1997) individualizaram, na área de identidade, rochas metaultramáficas (talco-tremolita xistos) na base, seguidas por metabásicas (basaltos maciços e gabros porfiríticos) e, no topo, por metadacitos porfiríticos. Metassedimentos terrígenos (grauvacas, siltitos) e vulcano-químicos (cherts e formações ferríferas) se intercalam nas porções basais a

intermediárias, podendo ocorrer em maior volume no topo da sequência, como no caso da área Lagoa Seca (Huhn et al. 1988).

1.4.2.2. TTG

Os granitóides da série tonalítica-trondhjemítica (TTG) do TGGRM (granitóides dos grupos 1 e 4), embora com idades distintas (Tabela 1), apresentam características químicas similares e, portanto, serão aqui descritos em conjunto, sendo ressaltadas apenas as diferenças entre eles.

O Tonalito Arco Verde forneceu originalmente idade de 2957+25/-21 Ma (U/Pb em zircão, Macambira 1992), posteriormente, confirmadas por datações efetuadas em rochas desta unidade da região de Inajá e Pau-D'Arco (2948 ± 7 Ma e 2981 ± 8 Ma, Pb/Pb em zircão; Rolando & Macambira 2002, 2003; 2964 ± 2 Ma, Pb/Pb em zircão, Vasquez et al. 2008b; 2941 ± 5 Ma, 2948 ± 4 Ma, LA-MC-ICPMS U-Pb em zircão e 2937 ± 3 Ma, Pb/Pb em zircão, Almeida et al. 2011). Não foram observadas relações de contato entre o Tonalito Arco Verde e as sequências de *greenstone belts*.

O Trondhjemito Mogno ocorre a sul de Xinguara e se estende até o norte de Bannach. Contém enclaves máficos, interpretados como metabasaltos do Supergrupo Andorinhas (Souza 1994). Esta unidade havia sido anteriormente datada (Tabela 1) pelos métodos Pb-Pb em zircão (2857 ± 13 e 2900 ± 21, Macambira et al. 2000) e U-Pb em titanita (2871 Ma, Pimentel & Machado 1994). Almeida et al. (2011) obtiveram novas idades (Tabela 1) para essa unidade (2962 ± 8 Ma, 2968 ± 2 Ma, 2959 ± 5 Ma, método Pb/Pb em zircão; 2959 ± 2 Ma, 2961 ± 16 Ma e 2972 ± 9 Ma por LA-MC-ICPMS em zircão) que diferem com aquelas obtidas anteriormente. O intervalo de idades entre 2.97-2.95 Ga foi interpretado como o período de cristalização do Trondhjemito Mogno (Almeida et al. 2011) e as idades mais jovens poderiam estar relacionadas a efeitos térmicos causados pelas intrusões da Suíte Sanukitóide Rio Maria, datada em 2.87 Ga (Pimentel & Machado, 1994; Rolando & Macambira, 2003; Oliveira et al., 2009).

O Complexo Tonalítico Caracol, ocorrente a noroeste da cidade de Xinguara, foi individualizado por Leite (2001) a partir do Complexo Xingu. O Complexo Tonalítico Caracol é formado por rochas com idades (Tabela 1) entre 2936 ± 3 Ma e 2948 ± 5 Ma (Pb/Pb em zircão, Leite et al. 2004), de composição tonalítica e trondhjemítica seccionadas pelo Granito arqueano Xinguara. Apresenta contato não exposto com o *Greenstone Belt* de Sapucaia (Leite et al. 1997, Leite et al. 2004). Contém enclaves e megaenclaves de rochas similares aos metabasaltos dos *greenstone belts.*

O Tonalito Mariazinha apresenta uma foliação NE-SW e N-S discordante do *trend* regional NW-SE. Contém enclaves máficos e é cortado pelo Granodiorito Grotão e veios de leucogranitos. Idades (Tabela 1) de 2924 ± 2 Ma, 2925 ± 3 Ma e 2920 ± 11 Ma (Pb/Pb em zircão) e 2912 ± 5 Ma (LA-MC-ICPMS em zircão) foram interpretadas como representativas da idade de cristalização da unidade (Leite et al. 2004, Almeida et al. 2011).

O Trondhjemito Água Fria representa a geração mais jovem de TTG descrito no TGGRM. Exibe bandamento subvertical com direção NW-SE e WNW-ESSE, inclue enclaves tonalíticos e acha-se associado concordantemente com leucogranitos relacionados ao Granito Xinguara (Leite 2001). Foram obtidas idades (Tabela 1) de 2864 ± 21 Ma (Pb/Pb em zircão, Leite et al. 2004) e 2843 ± 10 Ma (LA-MC-ICPMS em zircão, Almeida et al. 2011) para o Trondhjemito Água Fria, o que levou ao seu posicionamento estratigráfico no final da evolução do TGGRM..

Com base na assinatura geoquímica, os granitóides TTG na região de Rio Maria foram divididos em três grupos (Almeida et al. 2011): (1) grupo com altas razões La/Yb, Sr/Y e Nb/Ta, formado fundamentalmente pelo Trondhjemito Mogno e Tonalito Mariazinha, interpretados como formados a partir da fusão de rochas máficas em profundidades elevadas (1,5 GPa), no campo de estabilidade da granada; (2) grupo com razões La/Yb, Sr/Y, Nb/Ta moderadas, o qual engloba o Tonalito Caracol e o Trondhjemito Água Fria, gerados sob pressão entre 1,0-1,5 GPa, mas ainda no campo de estabilidade da granada; (3) TTGs com baixas razões La/Yb, Sr/Y e Nb/Ta, dominados pelo Tonalito Arco Verde, cristalizados de magmas gerados a baixas pressões (1.0 GPa) a partir de uma fonte anfibolítica, tendo plagioclásio como fase residual.

1.4.2.3. Sanukitóide Rio Maria

A suíte sanukitóide Rio Maria é formada dominantemente por granodioríticos, subordinadamente monzogranitos e quartzo-dioritos ou quartzo-monzodioritos (rochas intermediárias), além de rochas acamadadas e enclaves máficos. Apresenta ampla distribuição no Terreno Granito-*Greenstone* de Rio Maria e ocorrências de rochas granodioríticas da região do Xingu e Carajás também foram tentativamente correlacionadas a esta unidade (DOCEGEO 1988, Costa et al. 1995, Avelar et al. 1999). As idades obtidas para esta unidade (Tabela 1) são bastante uniformes e similares àquela de 2874 -9/+10 Ma definida em sua área-tipo (U/Pb em zircão; Macambira & Lancelot 1996).

O Granodiorito Rio Maria apresenta algumas características geoquímicas coincidentes com as das séries cálcio-alcalinas (Medeiros & Dall'Agnol 1988), porém pertence na

realidade às séries de granitóides arqueanos ricos em Mg, pois exibe conteúdos relativamente baixos de Al_2O_3, para as rochas daquela série, além de ser relativamente enriquecido em Ba, Sr, Cr, Ni e terras raras leves (Althoff et al. 1995, 2000, Leite 2001, Oliveira, M.A. et al. 2009, 2010).

Embora Vasquez et al. (2008b) agrupe o Granodiorito Rio Maria com às séries TTG, há muitas diferenças entre eles. O Granodiorito Rio Maria é enriquecido em Ca, Mg e K, além de Cr e Ni, aproximando-se geoquimicamente das séries sanukitóides arqueanas definidas por Stern et al. (1989). Os padrões de elementos terras raras também são desprovidos de anomalias significativas de Eu e são fortemente fracionados, porém o empobrecimento de elementos terras raras pesados é menos pronunciado do que nos granitóides TTG (Dall'Agnol et al. 2006, Oliveira, M.A. et al. 2009, Almeida et al. 2011).

1.4.2.4. Suíte Guarantã

A suíte Guarantã é formada por três plutons (Guarantã, Azulona e Trairão), localizados na região de Pau D'Arco, porção sul do Terreno Granito-*Greenstone* de Rio Maria. Geoquimicamente, as rochas da Suíte Guarantã apresentam razão $K_2O/Na_2O < 1$ e altos conteúdos de Ba e Sr, padrões de TR com fracionamento de ETR pesados em relação aos leves variável e, em geral, anomalias de Eu ausentes ou pouco marcantes (Dias 2009, Almeida et al. 2010). Tais rochas formam interpretadas como produto de mistura em diferentes proporções de magmas de composição trondhjemítica e leucogranítica rica em Ba e Sr, derivadas de magmas sanukitóides (Almeida et al. 2010). As idades de cristalização dessa suíte (Almeida et al. submetido) foram determinadas pelos métodos de evaporação Pb/Pb em zircão (2864 ± 8 Ma) e LA-MC-ICPMS U-Pb em zircão (2875 ± 8 Ma e 2872 ± 7 Ma).

1.4.2.5. Leucogranitos potássicos

Os leucogranitos potássicos fortemente fracionados (Almeida et al. submetido) são representados no Terreno Granito-Greenstone de Rio Maria, principalmente pelos granitos Xinguara (Leite et al. 1997) e Mata Surrão (Duarte et al. 1991, Althoff et al. 2000) e por pequenos stocks graníticos encontrados no TGGRM.

O Granito Xinguara (Leite 2001, Almeida et al. submetido), intrusivo em greenstone belts, Complexo Tonalítico Caracol, Tonalito Mariazinha e Granodiorito Rio Maria, forneceu idades Pb/Pb em zircão de 2865 ± 1 Ma (Tabela 1). Esta idade é similar a do Trondhjemito Água Fria (Tabela 1) e, somada com evidências de campo, indica que esses dois granitóides

são contemporâneos e intrusivos no Complexo Tonalítico Caracol. Uma idade de 2928±2 Ma obtida por Pb/Pb em zircão foi interpretada como herdada de sua fonte (Leite et al. 2004).

O Granito Mata Surrão, intrusivo no Tonalito Arco Verde (Duarte et al. 1991, Duarte & Dall'Agnol 1996, Althoff et al. 2000), forneceu idade Pb/Pb em rocha total de 2872 ± 10 Ma (Rodrigues et al. 1992, Lafon et al. 1994) e de Pb/Pb em zircão de 2871±7 Ma (Althoff et al 1998).

1.4.3. Bacia Carajás

Na Bacia Carajás, o magmatismo não é inteiramente conhecido, restando muitas dúvidas e controvérsias a respeito de sua evolução. Aqui serão descritas apenas as unidades dominantes na bacia, sendo o seu provável embasamento e os granitóides associados a ele discutidos em seguida no item sobre o subdomínio de transição.

O evento magmático amplamente dominante na Bacia Carajás é representado pelo vulcanismo máfico do Supergrupo Itacaiunas (cerca de 2,76 Ga, Wirth et al. 1986, Machado et al. 1991; cf. Tabela 1). Além do mesmo, tem-se o magmatismo máfico-ultramáfico do Complexo Luanga e um grande número de intrusões de granitos subalcalinos (Tabela 1; 2,76 a 2,73 Ga, Complexo Granítico Estrela, Granito Serra do Rabo e similares – Barros et al. 2004, 2009, Sardinha et al. 2006; 2,57 Ga -, e Granito Velho Salobo - Machado et al. 1991), sucedidos por extensa sedimentação (Formação Águas Claras, Nogueira et al. 1995).

1.4.3.1. Supergrupo Itacaiúnas

DOCEGEO (1988) propôs a designação Supergrupo Itacaiunas para englobar o Grupo Grão Pará e unidades supracrustais similares, grupos Igarapé Salobo, Igarapé Pojuca, Igarapé Bahia e Rio Novo, que ocorrem na Serra dos Carajás. A principal característica das unidades deste supergrupo é serem formadas dominantemente por rochas vulcano-sedimentares, de idade arqueana, apresentando graus variáveis de metamorfismo e litologias distintas do Supergrupo Andorinhas (TGGRM). Esta megaunidade não foi reconhecida em síntese recente (Vasquez et al. 2008b) onde se optou por manter a individualidade estratigráfica dos diferentes grupos citados, aos quais foram ainda acrescentados os grupos Aquiri, São Félix e São Sebastião.

O Grupo Grão Pará (CVRD 1972) é formado por uma espessa sequência de rochas vulcânicas, nas quais são geralmente distinguidos dois estratos, superior e inferior (Formação Parauapebas, com idade de 2759 ± 2 Ma, determinada em vulcânicas félsicas, pelo método U/Pb em zircão; Machado et al. 1991) e jaspilitos com minério de ferro associado (Formação

Carajás). Essa unidade preenche a maior parte da Bacia de Carajás. Dois modelos têm sido propostos para explicar a evolução tectônica da Bacia Carajás: (1) ligada a rifte continental (Gibbs et al. 1986, Oliveira et al. 1993, Macambira 2003); (2) relacionada a arco magmático (Meirelles & Dardenne 1991, Lobato et al. 2005, Silva et al. 2005).

O Grupo Igarapé Salobo foi redefinido por DOCEGEO (1988) a partir da Sequência Salobo-Pojuca (Hirata et al. 1982). Ele engloba rochas vulcano-sedimentares ocorrentes na porção NW da mina de ferro Carajás. Entretanto, Vasquez et al. (2008b) sugerem uma nova definição para o Grupo Igarapé Salobo, que passa a incorporar somente rochas vulcano-sedimentares expostas na região de serra do Salobo, enquanto que aquelas das serras Cinzento e Redenção seriam supracrustais do domínio Bacajá.

O Grupo Igarapé Pojuca, formalizado por DOCEGEO (1988), que o definiu em sua área-tipo no igarapé Pojuca, afluente da margem esquerda do igarapé Azul, extremo norte da Serra dos Carajás, é formado por uma sequência metavulcano-sedimentar arqueana, metamorfisada na fácies xisto verde alto a anfibolito baixo, que constitui uma faixa estreita e alongada, segundo a direção N50ºW, com mergulhos variando entre 50°NE e 60°SW (Farias et al. 1984, DOCEGEO 1984).

O Grupo Igarapé Bahia abrange um pacote vulcano-sedimentar, metamorfisado em fácies xisto verde, de direção NNW, subverticalizado, que aflora como janela dentro da formação Águas Claras. Dados geocronológicos em rochas metavulcânicas e metavulcanoclásticas obtidos por Galarza et al. (2008) e Tallarico et al. (2005) mostram idades (Tabela 1) Pb/Pb e U/Pb em zircão entre 2745±1 e 2776±12 Ma. Idades T_{DM} entre 2,96-3,13 Ga, εNd (-0,85 a -2,1) e zircões herdados de 2,96-3,07 Ga sugerem a existência de uma crosta continental mesoarqueana anterior ao magmatismo (Galarza et al., 2008).

1.4.3.2. Complexo Luanga

O Complexo Luanga (DOCEGEO 1988), localizado nas proximidades de Serra Pelada, é formado por rochas máficas acamadadas - anortositos e gabros, metamorfisados em fácies xisto-verde - apresenta idade de 2763 ± 6 Ma (U-Pb em zircão, Machado et al. 1991). Tais rochas cortam as supracrustais do Supergrupo Itacaiunas.

1.4.3.3. Granitos subalcalinos

Os granitos subalcalinos da Bacia Carajás são representados pelo Complexo granítico Estrela, granitos Serra do Rabo, Igarapé Gelado e Velho Salobo. O Complexo Granítico Estrela aflora a sul da PA-275, entre os municípios de Parauapebas e Curionópolis, na porção

norte-nordeste da Bacia Carajás. Foi inicialmente correlacionado, em função de dados aerogeofísicos que mostravam expressivas anomalias radiométricas em seus domínios, aos granitos paleoproterozóicos da Suíte Serra dos Carajás (DOCEGEO 1988). Entretanto, Meireles et al. (1984) chamaram a atenção de que tais rochas eram bastante deformadas e gnaissificadas e destoavam, portanto dos granitos anorogênicos paleoproterozóicos. É formado dominantemente por monzogranitos, com sienogranitos, granodioritos e tonalitos subordinados (Barros et al. 1997). Geoquimicamente, se assemelha aos granitos tipo-A, apresentando concentrações moderadas de $Na_2O + K_2O$ (5,7 a 8,4 %), altas razões $FeO_t/(FeO_t+MgO)$, altas concentrações de elementos incompatíveis do grupo dos HFSE (Zr = 146-640 ppm, Y = 13-404 ppm, Nb = 21–45 ppm), padrões de ETR pouco fracionados [(La/Sm)N = 3,09–7,78; (Gd/Yb)N = 1,22–2,33]. Datações pelo método Pb-Pb em zircão forneceram idades de cristalização de 2763 ± 7 Ma, para o Complexo Granítico Estrela (Barros et al. 2004, 2009). Dados isotópicos de Nd indicaram para suas rochas εNd(t) de -0,38 e -2,06 e idades-modelo T_{DM} de 2,97 e 3,19 Ga, interpretados como indicativos de fontes crustais mesoarqueanas para os magmas geradores deste complexo (Barros et al. 2004).

O Granito Serra do Rabo, um stock alongado na direção EW, localizado próximo à terminação leste da Falha Carajás, nas proximidades da Serra do Rabo, é composto por álcali-feldspato granito e sienogranito (Sardinha et al. 2006). Geoquimicamente apresenta altos teores de SiO_2, K_2O e Na_2O, altas razões $FeO_t/(FeO_t + MgO)$ e altas concentrações de Zr, Ba, Nb, Ga e ETR, o que se reflete em uma assinatura alcalina metaluminosa, similar à dos granitos tipo-A. A idade de colocação do Granito Serra do Rabo é de 2743 ± 1,6 Ma (Tabela 1), obtida através do método U-Pb em zircão (Sardinha et al. 2006).

O Granito Igarapé Gelado, individualizado por Barbosa (2004), está localizado no extremo norte do domínio Carajás. É formado por granodioritos e monzogranitos, com tonalitos, leucomonzogranitos e sienogranitos subordinados. Geoquimicamente contêm rochas de natureza cálcio-alcalina e alcalina, com teores moderados a altos de Nb e Zr. A datação de um monzogranito desta unidade forneceu uma idade de 2731 ± 26 Ma (1 grão), pelo método Pb-Pb em zircão (Barbosa 2004), a qual foi interpretada como idade mínima de cristalização.

O Granito Velho Salobo (2573 ± 3 Ma, U-Pb zircão; Machado et al. 1991) aflora a sul do alvo Salobo, mostra sinais de deformação e assinatura moderadamente alcalina (Lindenmayer et al. 1994).

1.4.3.3. Formação Águas Claras

A Formação Águas Claras é uma cobertura siliciclástica arqueana, não metamorfisada, distribuída amplamente na porção central da estrutura sigmoidal da Serra dos Carajás. A seção-tipo da Formação Águas Claras está localizada na estrada de acesso à mina de Igarapé Bahia, a oeste do igarapé Águas Claras (Nogueira et al. 1995). Acredita-se que a deposição desta unidade ocorreu entre 2778 e 2708 Ma, devido a idades de 2708 ± 37 Ma, obtida em dique (U-Pb em zircão, Mougeot et al. 1996) e de 2778 Ma, obtida em zircões detríticos, através do método U-Pb (Mougeot et al. 1996, Macambira et al. 2001).

1.4.4. Subdomínio de Transição

O domínio situado entre o Terreno Granito-Greenstone de Rio Maria e a bacia Carajás foi definido informalmente por Dall'Agnol et al. (1997, 2006) como Domínio de Transição. Ele se estenderia entre a região situada imediatamente a norte de Xinguara, passando lateralmente por Tucumã e São Félix do Xingu, até a borda sul da Bacia de Carajás, correspondente às exposições mais meridionais do Supergrupo Itacaiunas. Devido à escassez de dados geológicos e geocronológicos, o subdomínio de transição é pouco conhecido, mas esse quadro deve mudar com o avanço dos estudos ora em desenvolvimento nesta região (Oliveira, D.C. et al. 2010). As informações disponíveis apontam a presença do ortogranulito Chicrim-Cateté (Vasquez et al. 2008b), diopsídio-norito Pium (Hirata et al. 1982, Pidgeon et al. 2000, Santos et al. 2008), rochas mais antigas do Tonalito Bacaba (Moreto et al. 2011), granitóides e gnaisses indiferenciados do Complexo Xingu (Machado et al. 1991), seguidos no tempo pelas intrusões da Suíte Intrusiva Cateté (Macambira & Vale 1997), da Suíte Pedra Branca (Sardinha et al. 2004, Gomes & Dall'Agnol 2007) e dos plutons das Suítes Plaquê e Planalto (Avelar et al. 1999, Huhn et al. 1999, Oliveira 2003, Gomes 2003, Sardinha et al. 2004, Vasquez et al. 2008b).

1.4.4.1. Ortogranulito Chicrim-Cateté

Araújo & Maia (1991) descreveram, ao longo do rio Cateté, ortogranulitos correlacionáveis ao então Complexo Pium. Entretanto, Ricci & Carvalho (2006) e Santos & Oliveira (2010) não consideram que o Complexo Pium seja formado por granulitos e sim por rochas ígneas gabróicas. Neste sentido, os granulitos - charnockito a enderbito - da região entre a Aldeia Indígena Chicrim e rio Cateté seriam considerados os únicos representantes do embasamento granulítico do Domínio Carajás, denominados por Vasquez et al. (2008b) como ortogranulito Chicrim-Cateté.

1.4.4.2. Diopsídio-norito Pium

O diopsídio-norito Pium (Vasquez et al. 2008b), anteriormente descrito na literatura como Complexo Pium (DOCEGEO 1987), compreende fundamentalmente gabros e dioritos, maciços a foliados, com variedades ricas em quartzo. Engloba enclaves de granulitos charnockíticos a enderbíticos, considerados por Ricci (2006) como pertencentes à unidade ortogranulito Chicrim-Cateté.

A idade e o significado genético do granulito Chicrim-Cateté e do diopsídio-norito Pium são controversos. Pidgeon et al. (2000) obtiveram pelo método U-Pb em SHRIMP idades variadas, em cristais de zircão zonados de uma rocha de composição enderbítica na área-tipo Pium. A idade mais antiga, de 3002±14 Ma, foi interpretada como idade de cristalização do protolito do suposto granulito e a idade mais jovem, de 2859±9 Ma, corresponderia ao metamorfismo granulítico. No entanto, Ricci & Carvalho (2006) argumentam que a rocha datada por Pidgeon et al. (2000) seria, na realidade, um xenólito do ortogranulito Chicrim-Cateté incluso no diopsídio-norito Pium. Já Santos et al. (2008) concluíram, com base em observações de campo e petrográficas, que as ocorrências de rochas básicas noríticas no domínio do Complexo Pium são mais antigas e possível fonte do ortopiroxênio-quartzo-diorito. Desta forma, a rocha datada por Pidgeon et al. (2000) seria possivelmente da variedade quartzo-diorítica, cujos cristais de zircão conservariam em seu núcleo restos de zircão da rocha norítica de idade mais antiga (3002±14 Ma), enquanto suas bordas, com idade de 2859±9 Ma, marcariam a idade de geração e cristalização do quartzo-diorito.

1.4.4.3. Complexo Xingu

O Complexo Xingu inclui corpos gnáissico-migmatíticos (tonalitos, trondhjemitos e/ou granodioritos), granulitos e granitóides, além de supracrustais. Esta unidade se estendia desde o rio Xingu, no domínio Bacajá, até o sudeste do Pará, no Domínio Rio Maria. O avanço do conhecimento geológico permitiu demonstrar que o referido complexo era na realidade formado por diversos corpos de granitóides, passíveis de serem individualizados, e, conseqüentemente, levou ao abandono do termo Complexo Xingu no domínio Bacajá (Macambira et al. 2001, Vasquez et al. 2005, Vasquez et al. 2008a) e no Domínio Rio Maria (Leite 2001, Dall'Agnol et al. 2006, Vasquez et al. 2008b). Portanto, o termo Complexo Xingu acha-se atualmente restrito apenas ao Domínio Carajás (Vasquez et al. 2008b), correspondendo aqui à Bacia Carajás e ao subdomínio de Transição (cf. Fig 1, artigo 1).

Avelar et al. (1999) obtiveram na região de Tucumã uma idade de 2972±16 Ma (Pb/Pb em zircão) para um gnaisse de composição granodiorítica incluído por eles no Complexo

Xingu. Por sua vez, nos arredores da cidade de Curionópolis, Machado et al. (1991) obtiveram uma idade de 2859±2 e 2860±2 Ma, em um leucossoma, interpretado como último episódio de migmatização, afetando rocha daquele complexo. Estas idades são de difícil interpretação, tendo em vista as limitações existentes quanto à definição do Complexo Xingu.

1.4.4.4. Suíte Intrusiva Cateté

A suíte Intrusiva Cateté, formalizada por Macambira & Vale (1997), é composta por um conjunto de corpos máfico-ultramáficos (gabros, noritos, piroxenitos, serpentinitos e peridotitos), alongados e alinhados preferencialmente segundo E-W e N-S. Estão incluídos nesta unidade os corpos conhecidos como Serra da Onça, Serra do Puma, Serra do Jacaré, Serra do Jacarezinho, Igarapé Carapanã, Fazenda Maginco, Ourilândia e Vermelho, e outros sem denominação formal. A principal característica desta suíte é a ausência de deformação e metamorfismo (Macambira & Vale 1997). Estudos geocronológicos realizados por Macambira & Tassinari (1998) no corpo Serra da Onça, pelo método Sm-Nd (rocha e minerais) forneceram uma idade isocrônica de 2378 ± 55,5 Ma, admitida como idade mínima de cristalização desta suíte. Lafon et al. (2000) obtiveram pelo método U-Pb em zircão uma idade de 2766 ± 6 Ma no gabro do corpo Serra da Onça.

1.4.4.5. Suíte Plaquê

A Suíte Plaquê foi inicialmente definida por Araújo et al. (1988), sendo formada por corpos lenticulares de granitóides deformados, distribuídos no Domínio Carajás. Araújo & Maia (1991) interpretaram estes corpos como tendo sido gerados concomitantemente à evolução do Cinturão Itacaiúnas, redefinindo a unidade como Granito Estratóide Plaquê. Os corpos que definem esta unidade seriam compostos dominantemente por granitos, com biotita e/ou anfibólio ± muscovita, de coloração rosa clara a rosa avermelhada, granulação média a grossa, equi ou inequigranulares, com tipos pouco foliados ou apresentando pronunciada foliação milonítica e exibindo microtexturas porfiroclásticas ou granolepidoblásticas (Araújo & Maia 1991, Macambira & Vale 1997). Estudos petroquímicos de corpos desta unidade indicaram caráter cálcio-alcalino a alcalino (Jorge João et al. 1991, Macambira et al. 1996). Dados geocronológicos, obtidos na região de Tucumã, forneceram idades de 2729 ± 29 Ma (Avelar 1996) e 2736 ± 24 Ma (Avelar et al. 1999) pelo método Pb-Pb por evaporação em zircão.

1.4.4.6. Suíte Planalto

O termo Granito Planalto foi empregado por Huhn et al. (1999) para designar um corpo situado na região a oeste da Serra do Rabo, próximo da localidade de Vila Planalto. Corpos graníticos lenticulares localizados a leste da cidade de Canaã dos Carajás foram correlacionados a esta unidade (Gomes 2003). São formados por sienogranitos, monzogranitos e álcali-feldspato granitos, com hornblenda e biotita. Geoquimicamente são rochas subalcalinas, metaluminosas a fracamente peraluminosas, com características de granitos tipo-A. Datações geocronológicas efetuadas por Huhn et al. (1999) e Sardinha et al. (2004), através do método Pb-Pb em zircão, resultaram, respectivamente, em idades de 2747±2 Ma e 2734±4 Ma, ambas interpretadas como idade de cristalização.

1.4.4.7. Outros granitóides Arqueanos

Gomes (2003) identificou na região a leste de Canaã dos Carajás diversos granitóides, divididos em três grupos: leucomonzogranitos potássicos de afinidade cálcico-alcalina (2928 ± 1 Ma, Sardinha et al. 2004), Associação Tonalítica-Trondhjemítica com alto Zr, Y e Ti (2750 ± 3 Ma e 2765 ± 39 Ma, Sardinha et al. 2004) e granitos subalcalinos (2734 ± 4 Ma, Sardinha et al. 2004), correlacionados ao Granito Planalto. Oliveira, D.C. et al. (2010) identificaram na porção sul do subdomínio de Transição, granitóides da série TTG de idade ~2,87 Ga, leucomonzogranitos formados entre 2,88-2,85 Ga e, durante o Neoarqueano, ortopiroxênio-trondhjemitos com ~2,75 Ga, leucogranodioritos (2,74-2,73) e granitos subalcalinos correlacionados a Suíte Planalto (2.73-2.75 Ga).

1.4.5. Magmatismo tipo-A Paleoproterozóico

Durante o Paleoproterozóico, mais precisamente em torno de 1,88 Ga, a Província Mineral de Carajás foi palco de um amplo magmatismo granítico anorogênico, que afetou os seus diferentes domínios. Os granitos tipo-A oxidados intrusivos em rochas arqueanas do TGGRM foram agrupados na Suíte Jamon, e os granitos tipo-A moderadamente reduzidos, intrusivos em rochas arqueanas da bacia Carajás e do subdomínio de transição foram englobados na Suíte Serra dos Carajás (Dall'Agnol et al. 1999, 2005, 2006). Embora, na área de Canaã dos Carajás, o granito paleoproterozóico Rio Branco apresente características petrográficas e geoquímicas semelhantes aos granitos evoluídos da Suíte Velho Guilherme. Diques félsicos a máficos, contemporâneos dos granitos proterozóicos, seccionam tanto as unidades arqueanas quanto os granitos paleoproterozóicos (Gastal 1987, Huhn et al. 1988, Souza et al. 1990).

Tabela 1 - Síntese dos dados geocronológicos dos granitóides arqueanos da Província Carajás.

Unidades Estratigráficas	Tipo de Rocha	Método	Material Analisado	Idade/Referência
BACIA CARAJÁS				
Granitos Foliados Subalcalinos				
Granito Velho Salobo	Granitóide	U-Pb	Zircão	2573± 3 Ma [2]
Granito Igarapé Gelado	Granitóide	Pb-Pb	Zircão	2731±26 Ma [17]
Granito Serra do Rabo	Granitóide	U-Pb	Zircão	2743±1,6 Ma [11]
Complexo Granítico Estrela	Granitóide	Pb-Pb	Zircão	2763±7 Ma [3]
Supergrupo Itacaiunas				
Grupo Salobo	Anfibolito	U-Pb	Zircão	2761±3 Ma [2]
		U-Pb	Titanita	2497±5 Ma [2]
	Anfibolito	U-Pb	Zircão	2555+4/-3 Ma [2]
Grupo Igarapé Pojuca	Anfibolito	U-Pb	Zircão	2732±3 Ma [2]
Grupo Grão Pará	Formação Carajás	U-PbShrimp	Zircão	2743±11[22]
	Formação	U-Pb	Zircão	2759±2 Ma[2]
	Parauapebas	U-Pb	Zircão	2758±39 Ma[19]
Grupo Igarapé Bahia	Metavulcânicas	U-PbShrimp	Zircão	2748±34 Ma[21]
	Metavulcânicas	Pb-Pb	Zircão	2745±1 Ma[20]
	Metavulcanoclásticas	U-Pb	Zircão	2776±12 Ma[20]
Complexo Luanga	Gabro	U-Pb	Zircão	2763±6 Ma[2]
Suíte Intrusiva Cateté	Gabro	U-Pb	Zircão	2766±6 Ma[16]
Complexo Xingu	Leucossoma granítico	U-Pb	Zircão	2859±2 Ma[2]
	Gnaisse félsico	U-Pb	Zircão	2974±15 Ma[2]
ÁREA DE CANAÃ DOS CARAJÁS E DOMÍNIO DE TRANSIÇÃO				
Suíte Plaquê	Granitóide	Pb-Pb	Zircão	2729±29 Ma [4]
				2736±24 Ma [4]
Intrusivas dioríticas	Diorito	Pb-Pb	Zircão	2738±6 Ma [6]
Granito Planalto	Granitóide	Pb-Pb	Zircão	2747±2 Ma [6]
				2734±4 Ma [13]
Associação tonalítica-trondhjemítica	Trondhjemito	U-Pb	Zircão	2750±3 Ma [13]
		Pb-Pb	Zircão	2765±39 Ma [13]
Granodiorito Rio Maria	Granitóide	Pb-Pb	Zircão	2850±17 Ma [4]
Granito Canaã dos Carajás	Leucogranito	Pb-Pb	Zircão	2929±1 Ma [13]
Complexo Xingu	Gnaisse	Pb-Pb	Zircão	2972±15 Ma [4]
Diopsídio Norito Pium	Granulito	Pb-Pb	Rocha total	3050±114 Ma [18]
	Granulito (enderbito)	SHRIMP	Zircão	3002±14 Ma [9]
				2859±9 Ma [9]
TERRENO GRANITO-*GREENSTONE* DE RIO MARIA				
Granito Mata Surrão	Leucogranito	Pb-Pb	Rocha total	2872±10 Ma [24]
			Zircão	2871± 7 Ma [8]
Trondhjemito Água Fria	TTG	Pb-Pb	Zircão	2864±21 Ma [10]
		U-Pb		2854±17Ma [28]
Granito Xinguara	Granito	Pb-Pb	Zircão	2865±1 Ma [10]
Grupo do leucogranodioritos-leucogranitos Suíte Guarantã	Granodiorito	Pb-Pb	Zircão	2868±5[8]
	Leucogranito			2870±5 [28]
	Granito Guarantã	Pb-Pb	Zircão	2864±8Ma [28]
	Granito Guarantã	U-Pb	Zircão	2875±8Ma [28]
	Granodiorito Trairão	U-Pb	Zircão	2872±7Ma [28]
Granito Rancho de Deus	Granito	U-Pb	Zircão	2888±27Ma [28]
Granodiorito Rio Maria	Granodiorito	U-Pb	Zircão	2874+9/-10 Ma [5]
		U-Pb	Zir, Titan.	2872±5 Ma [1]
		Pb-Pb	Zircão	2877±6 Ma [12]
	Quartzo-diorito	Pb-Pb	Zircão	2878± 4 Ma [7]
Tonalito Parazônia	Quartzo-diorito	Pb-Pb	Zircão	2876±2 [26]
	Tonalito	U-Pb	Titanita	2858 [1]
Tonalito Mariazinha	TTG	U-Pb	Zircão	2925±3Ma [28]
	TTG	U-Pb	Zircão	2918±13Ma [28]
Complexo Tonalítico Caracol Cont.	Tonalito	Pb-Pb	Zircão	2948±5 Ma [10]
				2936±3 Ma [10]

Unidades Estratigráficas		Tipo de Rocha	Método	Material Analisado	Idade/Referência
TERRENO GRANITO-*GREENSTONE* DE RIO MARIA					
Trondhjemito Mogno		TTG	Pb-Pb	Zircão	2857±13[20]
		TTG	Pb-Pb	Zircão	2900±21[20]
		Granitóide	U-Pb	Titanita	2871±? Ma [1]
		TTG	Pb-Pb	Zircão	2962±8Ma [28]
		TTG	U-Pb	Zircão	2965±7Ma [28]
		TTG	Pb-Pb	Zircão	2968±2Ma [28]
		TTG	U-Pb	Zircão	2968±3Ma [28]
		TTG	Pb-Pb	Zircão	2959±5Ma [28]
		TTG	Pb-Pb	Zircão	2959±2Ma [28]
Tonalito Arco Verde		Tonalito	Pb-Pb	Zircão	2964±2 Ma [23]
		TTG	Pb-Pb	Zircão	2948±7 Ma [14]
		TTG	Pb-Pb	Zircão	2952±2Ma [28]
		TTG	U-Pb	Zircão	2936±13Ma [28]
		TTG	Pb-Pb	Zircão	2926±2Ma [28]
		TTG	U-Pb	Zircão	2935±5Ma [28]
		TTG	Pb-Pb	Zircão	2937±3Ma [28]
		TTG	U-Pb	Zircão	2973±11Ma [28]
Supergrupo Andorinhas	*(Gr. Lagoa Seca)*	Metagrauvacas	U-Pb	Zircão	2971±18 Ma [5]
		Metavulcânica félsica	U-Pb	Zircão	2904+29/-22 Ma [5] 2979±5 Ma [1]
	(Gr. Gradaús)	Dacito	U-Pb	Zircão	3002±3 Ma [25]

Fonte dos dados: [1]Pimentel & Machado (1994); [2]Machado et al. (1991); [3]Barros et al. (2004); [4]Avelar et al. (1999); [5]Macambira and Lancelot (1996); [6]Huhn et al. (1999); [7]Dall'Agnol et al. (1999); [8]Althoff et al. (2000); [9]Pidgeon et al. (2000); [10]Leite et al. (2004); [11]Sardinha et al. (2006); [12]Rolando & Macambira (2002), [13]Sardinha et al. (2004); [14]Rolando & Macambira (2003), [15]Althoff (2000); [16]Lafon et al. (2000); [17]Barbosa (2004); [18]Macambira & Lafon (1995); [19]Wirth et al. (1986); [20]Galarza et al. (2008); [21]Tallarico et al. (2005); [22]Trendall et al. (1998); [23]Vasquez et al. (2008b); [24]Rodrigues et al. (1992); [25]Althoff et al. (1998); [26] Almeida (dados inéditos); [27] Almeida et al. 2008; [28]Almeida et al. (2011);[29] Macambira et al. (2000).

1.4.6. Breve comparação entre o TGGRM e a Bacia Carajás

São listadas a seguir as principais diferenças entre o TGGRM e a BC (cf. Dall'Agnol et al. 2006), que tornam mais evidentes os contrastes evolutivos existentes entre eles.

1- As sequências supracrustais do TGGRM e da BC diferem em idade e características petrológicas. No TGGRM, os *greenstones belts* do Supergrupo Andorinhas têm idades entre 2,97 e 2,90 Ga e são compostos dominantemente por basaltos toleíticos e komatiítos metamorfisados. Na BC, as sequências supracrustais estão incluídas no Supergrupo Itacaiunas, possuem idades próximas de 2,76 Ga e são compostas essencialmente de metavulcânicas máficas e intermediárias e formações ferríferas bandadas.

2- As rochas expostas no TGGRM foram formadas entre 2,98 e 2,86 Ga (Macambira 1992, Pimentel & Machado 1994, Rolando & Macambira 2003, Leite et al. 2004) e o principal evento deformacional que as afetou ocorreu em torno de 2,87 Ga (Althoff et al. 2000, Souza et al. 2001, Leite 2001, Leite et al. 2004). Na BC, as principais unidades estratigráficas foram formadas no período de 2,76 a 2,70 Ga e o último evento deformacional teria ocorrido entre 2,58 a 2,50 Ga (Machado et al. 1991). Esses dados indicam que a estabilização tectônica do TGGRM precedeu a da BC.

3- Os granitóides do TGGRM foram formados entre 2,98 e 2,86 Ga. Já na BC, embora os eventos de formação de granitos não tenham sido inteiramente definidos, há ocorrências muito expressivas de granitos subalcalinos tipo-A, com idades entre 2,75 Ga e 2,57 Ga.

4- Leite (2001) admite que a evolução geológica do TGGRM ocorreu em dois estágios. O primeiro começou em 2,96-2,92 Ga com a geração de TTG por fusão da base de espessa pilha de metabasaltos. O segundo estágio começou em 2,88 Ga e coincidiu com uma grande mudança no comportamento crustal, que resultou no espessamento e estabilização da crosta primitiva, redundando em processos de convergência e, conseqüentemente, subducção. Oliveira, M.A. (2010), Almeida et al. (2011) e Dall'Agnol et al. (2011) admitem a ocorrência de subducção de crosta oceânica já em torno de 2.98 a 2.96 Ga, a qual seria responsável pela formação da maioria dos TTGs mais antigos do TGGRM. Nesse contexto, a cunha mantélica acima da placa subductante seria metassomatizada por líquidos TTG. Em 2,87 Ga, a fusão parcial deste manto enriquecido teria gerado o magma sanukitóide granodiorítico Rio Maria. A ascensão deste para níveis crustais profundos levaria à fusão parcial de metabasaltos transformados em granada-anfibolito e produziria o magma formador dos TTGs mais jovens. O movimento de ascensão e colocação na crosta desses magmas levou a um aporte expressivo de calor e induziu a fusão de TTGs antigos na crosta inferior, permitindo assim a geração dos magmas leucograníticos.

5- Na BC, Gibbs et al. (1986) e DOCEGEO (1988) acreditam que as sequências supracrustais estariam relacionadas à ambiente de rifte continental, enquanto Meirelles & Dardenne (1991), Teixeira & Egler (1994), Lindenmayer et al. (2005) e Lobato et al. (2005) propuseram um modelo envolvendo ambiente de margem continental, cuja evolução estaria relacionada à subducção de uma crosta oceânica, seguida por colisão continente-continente.

1.4.7. Geologia isotópica Sm-Nd da Província Carajás

1.4.7.1. Terreno granito-greenstone de Rio Maria

No domínio Rio Maria, os *greenstone belts* foram datados e forneceram idades de 3046 ± 32 Ma e 2943 ± 88 Ma através do método Sm-Nd em rocha total (Souza et al. 2001), idades interpretadas como referência para formação desta unidade. Idades obtidas por U-Pb em zircões detríticos, dacitos e metagrauvacas forneceram valores de 3002 ± 3 Ma e 2904 ± 29/-22 Ma (Tassinari et al. 2005 e Macambira & Lancelot 1996, respectivamente), interpretados como idades mínimas de formação desta unidade. Os valores de εNd variam entre positivos (+0,22 a +3,15; t = 3,0 Ga) até negativos (-0,34; t=3,0 Ga), indicando que estas rochas são

juvenis e derivaram de fonte mantélica com leve contaminação crustal durante sua colocação (Souza et al. 2001, Rolando & Macambira 2003, Tassinari et al. 2005).

Os granitóides TTG mais antigos de Rio Maria (Arco Verde, Mogno, Caracol e Mariazinha) apresentam idades de cristalização entre 2,98 e 2,92 Ga (Tabela 1, Macambira & Lancelot 1996, Rolando & Macambira 2003, Almeida et al. 2011). Estudos isotópicos de Nd revelaram idades T_{DM} variáveis de 2,93 a 3,01 Ga, com $\varepsilon Nd_{(2.94\ Ga)}$ positivos e negativos (+0,87 a +2,21), sugerindo fonte juvenil para os magmas formadores dos granitóides (Leite 2001).

Os granitóides TTG mais jovens (Água Fria) forneceram idades próximas de 2,86 Ga (Tabela 1), interpretadas como idade mínima de cristalização, ao passo que as idades T_{DM} variam entre 2,89 e 2,95 Ga com $\varepsilon Nd_{(2,86\ Ga)}$ de +1,4 a +2,0 (Leite et al. 2004) e sugerem fonte com pequeno tempo de residência crustal para a formação dos magmas destes granitóides.

A suíte sanukitóide Rio Maria apresenta valores de $\varepsilon Nd_{(2.87\ Ga)}$ de +1,2 a -0,53 e idades T_{DM} de 2,92 a 3,07 Ga (Leite 2001, Rämo et al. 2002, Rolando & Macambira 2003), que, aliados à presença de zircões herdados com idades entre 2970 e 3100 Ma (Rolando & Macambira 2003), indicam a provável participação de material mantélico e crustal na formação deste granitóide.

Os leucogranitos encontram-se, ainda, pobremente caracterizados isotopicamente. Para o Granito Xinguara foi obtida uma idade T_{DM} de 2,88 Ga com εNd de + 1,6 (Leite et al. 2004), que, aliada a idades de 2928±2 Ma em zircões herdados presentes neste granito, indicam que o Granito Xinguara foi originado por fusão de uma crosta já existente, possivelmente similar ao Tonalito Caracol (Leite 2001, Almeida et al. submetido).

1.4.7.2. Domínio Carajás

No domínio Carajás, as rochas do Supergrupo Itacaiunas forneceram idades entre 2745 ± 1 Ma e 2776 ± 12 Ma (Tallarico et al. 2005, Galarza et al. 2008, Santos 2002). Por sua vez, as idades T_{DM} para esta unidade situam-se entre 2,96 e 3,13 Ga e, juntamente como os valores negativos de εNd (– 0,85 a – 3,2), indicam provável contaminação por uma crosta continental mesoarqueana pré-existente, quando da colocação dos magmas máficos formadores dos atuais metabasaltos (Galarza et al. 2003, Santos 2002, Pimentel et al. 2003).

Os granitos alcalinos do Domínio Carajás são pobremente caracterizados isotopicamente, dispondo-se de dados somente para o Complexo Granítico Estrela (2763 ± 7 Ma,), para o qual foram obtidas idades-modelo T_{DM} de 2,97 a 3,19 Ga e valores de εNd(t) de -0,38 a -2,06

(Barros et al. 2004, Barros et al. 2009), interpretados como indicativo de fontes crustais mesoarqueanas para os magmas geradores deste complexo.

1.4.7.3. Magmatismo Anorogênico Paleoproterozóico

Os dados isotópicos de Nd das suítes Jamon (Domínio Rio Maria) e Serra dos Carajás (Domínio Carajás) com idades próximas de 1880 Ma, obtidos por Dall'Agnol et al. (1999, 2005) e Ramö et al . (2002), revelaram valores negativos de εNd entre -7,9 a -10,5 e idades T_{DM} variáveis entre 3,35 e 2,60 Ga. Com base nesses dados e outras evidências petrológicas, foi assumida a hipótese de que os magmas formadores dos granitos paleoproterozóicos foram derivados de fontes crustais mesoarqueanas (Dall'Agnol et al. 1999, 2005).

1.5 - APRESENTAÇÃO DO PROBLEMA

A área selecionada para pesquisa localiza-se no sudeste do Estado do Pará, nos arredores de Canaã dos Carajás. Geologicamente está inserida na porção sul do Domínio Carajás (Vasquez et al. 2008b) ou no sub-domínio de Transição, localizado a norte do Terreno Granito-*Greenstone* de Rio Maria e a sul da Bacia Carajás.

O sub-domínio de Transição é considerado por Dall'Agnol et al. (2006) como uma extensão do TGGRM, que foi intensamente afetada pelos eventos magmáticos e tectônicos ocorridos durante o Neoarqueano e registrados na Bacia Carajás, porém ausentes nos domínios do TGGRM propriamente dito. No entanto, o real significado do sub-domínio de Transição não foi ainda compreendido, devido, entre outras coisas, à carência de informações geológicas, geoquímicas e geocronológicas que permitam esclarecer as relações entre as unidades do sub-domínio de Transição e aquelas do TGGRM e da BC. Pela mesma razão, não é possível definir de modo mais consistente a evolução crustal do sub-domínio de Transição e tampouco deduzir suas implicações para a Província Carajás como um todo.

No sub-domínio de Transição, a maioria das rochas granitóides está inserida no Complexo Xingu (DOCEGEO 1988, Vasquez et al. 2008b). Somente rochas do Complexo Pium e de alguns corpos granitóides foram estudadas, ainda assim, localmente. Em função disso, há incertezas quanto ao posicionamento tectono-estratigráfico das rochas granitóides e dos corpos máficos-ultramáficos, bem como das associações metavulcanossedimentares, possíveis *greenstone belts,* ocorrentes na área.

Anteriormente aos estudos do Grupo de Pesquisa Petrologia de Granitóides (GPPG), a maioria das rochas granitóides expostas na região de Canaã dos Carajás estava inserida no Complexo Xingu. Isso demonstrava o grande desconhecimento existente sobre a natureza e

origem dessas rochas. Os estudos preliminares efetuados anteriormente ao presente trabalho permitiram individualizar rochas da série TTG, granitóides cálcico-alcalinos, granitos alcalinos tipo-A (metaluminosos a peraluminosos) e uma associação tonalítica-trondhjemítica com alto Zr, Y e Ti. Associadas às rochas granitóides, há rochas máficas e ultramáficas cuja origem e posicionamento estratigráfico também são ainda obscuros. Esta grande variedade de rochas sugere uma complexidade evolutiva que só poderá ser esclarecida com base em estudos detalhados dos diferentes tipos de rochas aí identificados.

Quanto ao Complexo Pium, embora Ricci & Carvalho (2006) e Vasquez et al. (2008b) o tenham redefinido como diopsídio-norito Pium na região de Canaã dos Carajás e diversos autores estejam estudando petrograficamente tais rochas (Ricci & Carvalho 2006, Santos et al. 2008), ainda não há uma definição clara sobre o real significado desta unidade, sua origem e seu papel como possível fonte de rochas graníticas neoarqueanas. Há controvérsias na literatura sobre a natureza magmática (Ricci & Carvalho 2006, Santos et al. 2008) ou metamórfica (Pidgeon et al. 2000) do Complexo Pium, bem como sobre o significado das idades obtidas em suas rochas.

Quanto aos prováveis *greenstone belts*, não há uma definição clara quanto à sua origem, nem tampouco quanto à idade de sua formação. A questão fundamental é se essas rochas estariam relacionadas às sequências supracrustais do Supergrupo Itacaiunas, pertencentes à Bacia Carajás, com idade <2,8 Ga, ou se seriam equivalentes temporalmente às rochas do Supergrupo Andorinhas, mais antigas (>2,9 Ga), existentes na região de Rio Maria.

Outro problema em foco é se os granitóides, previamente inseridos na Suíte Plaquê, são realmente granitos a duas micas e, além disso, se a Suíte Plaquê existe de fato na área de Canaã dos Carajás, pois granitos com as características tidas como típicas desta suíte não foram ainda identificados na área.

Assim, as informações a serem obtidas acerca da natureza e idades das diferentes associações magmáticas, bem como os resultados do mapeamento geológico, deverão permitir um avanço considerável na compreensão dos processos de formação, evolução e estabilização da crosta arqueana da área de Canaã dos Carajás. Será obtido, ao mesmo tempo, um grande avanço na caracterização petrográfica e geoquímica dos diferentes granitóides arqueanos expostos naquela área

Abaixo estão listadas algumas dentre as inúmeras questões que carecem de respostas sobre a geologia daquela área e, de modo mais amplo, do sub-domínio de Transição:

1. O Complexo Xingu existe efetivamente ou deverá ser desmembrado em diferentes unidades como já ocorreu em outras áreas da província?

2. Qual a natureza das séries magmáticas e as idades do magmatismo granitóide presente na área de Canaã dos Carajás? Qual o posicionamento estratigráfico dessas séries magmáticas? Qual é a assinatura geoquímica dos diferentes granitóides e quais seriam as fontes de seus magmas?

3. Quais são as relações em termos de idade e séries magmáticas existentes entre as associações do domínio de transição, na área de Canaã dos Carajás, com as do TGGRM? Idem com aquelas da Bacia Carajás? Existe alguma relação entre a formação das rochas do domínio de transição, na área de Canaã dos Carajás, com os processos tectônicos neoarqueanos que afetaram a Bacia Carajás?

4. Como podem ser explicadas as características geoquímicas particulares da associação tonalítica-trondhjemítica com alto Zr, Y e Ti? Qual a sua origem e o seu papel na evolução geológica da área de Canaã dos Carajás? Por que as rochas desta associação são distintas geoquimicamente das associações TTG arqueanas clássicas, incluindo aquelas do TGGRM?

5. Quais as características petrográficas e geoquímicas do Granito Planalto e corpos afins? Os vários corpos de granitos arqueanos subalcalinos podem ser enquadrados em uma única suíte? Qual o significado tectônico dessa suíte na evolução neoarqueana da área de Canaã dos Carajás? Em que ambiente tectônico se deu a sua formação? Esses granitos podem ser correlacionados aos granitos subalcalinos similares já estudados na Bacia Carajás (Complexo Estrela, granitos Serra do Rabo e Igarapé Gelado)? A Suíte Planalto pode ser enquadrada entre os granitos tipo-A apesar da colocação sintectônica de seus corpos ou haveria outro enquadramento em termos de tipologia para ela?

6. Rochas granitóides com as características petrográficas e geoquímicas da Suíte Plaquê, conforme definida originalmente, ocorrem efetivamente na região delimitada para este estudo ou a definição e a própria existência desta suíte devem ser revistas? Caso se confirme a sua existência, qual é a sua origem e seu significado na evolução desta porção do sub-domínio de transição?

7. Quais são as relações temporais e em termos de processos de formação entre as associações máficas presentes na região e o magmatismo granitóide?

8. Qual o papel do corpo ultramáfico do Vermelho e das diferentes associações máfico-ultramáficas na evolução da crosta arqueana do domínio de transição?

9. O Complexo Pium é constituído por que tipos de rochas? Foi formado em condições magmáticas ou metamórficas? O Complexo Pium ou os Granulitos Chicrim-Cateté serviram como fonte dos magmas geradores de granitos neoarqueanos? Quais?

10. Quando se deu a formação da crosta exposta em Canaã dos Carajás, em que cenário geológico-tectônico se deu sua evolução e qual é o seu papel dentro do sub-domínio de transição? Trata-se de uma crosta juvenil mesoarqueana ou neoarqueana ou foi formada a partir de retrabalhamento crustal? Se foi produto de retrabalhamento, em que momento aconteceu este retrabalhamento e que processos foram responsáveis por ele?
11. Como se deu a integração tectônica entre o TGGRM e a Bacia Carajás e qual o papel da zona de transição neste período?
12. Há relação direta entre o magmatismo granitóide arqueano e as mineralizações de Cu e Au, amplamente disseminadas na região de Canaã de Carajás?

1.6 - OBJETIVOS

As discussões e questões levantadas no item precedente serviram de base para definir os objetivos do presente trabalho que, obviamente, não podem visar responder a todas elas. Procura-se a seguir destacar os objetivos primordiais a serem alcançados que devem responder a parte das questões levantadas anteriormente.

O principal objetivo desta tese é caracterizar as associações granitóides dominantes na área de Canaã dos Carajás, situada dentro do sub-domínio de Transição, definir suas idades e esclarecer os processos petrogenéticos responsáveis pela geração dos seus magmas. Pretende-se com base nisso, em dados isotópicos e em conceitos modernos sobre a gênese e evolução de terrenos arqueanos, elaborar um modelo de evolução crustal deste segmento da Província Carajás e avaliar, por extensão, as implicações desse modelo na evolução geológica e tectônica do sub-domínio de Transição e da Província Carajás como um todo.

Para tanto, pretende-se atingir os seguintes objetivos específicos:

(1) Integração e aperfeiçoamento dos mapas geológicos (escala 1:100.000) produzidos anteriormente na área de Canaã dos Carajás por membros do Grupo de Petrologia de Granitóides (Soares 2002, Gomes 2003, Oliveira 2003, Sardinha 2005);

(2) Caracterização petrográfica e classificação dos diversos granitóides arqueanos ocorrentes na área de Canaã dos Carajás;

(3) Caracterização geoquímica das diferentes associações granitóides, definição de suas tipologias e séries magmáticas e discussão dos processos magmáticos que controlaram a sua evolução;

(4) Definição das idades de cristalização e idades-modelo (TDM), bem como obtenção da assinatura isotópica Sm-Nd das associações granitóides da área de Canaã dos Carajás;

(5) Proposição de uma coluna estratigráfica para a área estudada;

(6) Discussão de modelos tectônicos e definição da evolução crustal arqueana da área de Canaã dos Carajás, avaliação de sua possível extensão para o sub-domínio de Transição e comparação com a evolução do TGGRM e da BC, bem como de outros crátons arqueanos.

1.7 - MATERIAIS E MÉTODOS

Para alcançar os objetivos propostos foram utilizados vários métodos e técnicas de investigação, relacionadas ao tema e compatíveis com os assuntos abordados.

1.7.1. Pesquisa Bibliográfica

Levantamento bibliográfico referente à geologia da Província Carajás, principalmente no que concerne à granitogênese arqueana, com ênfase em evolução crustal, geocronologia e geoquímica isotópica. Foram pesquisados também artigos que versam sobre geoquímica e petrogênese de rochas granitóides em geral, bem como sobre séries magmáticas arqueanas do mundo. Adicionalmente, foi dada atenção à literatura geológica que versa sobre processos deformacionais sin- e pós-magmáticos em corpos ígneos e seus reflexos nas texturas de rochas magmáticas.

1.7.2. Trabalhos de Campo e Mapa Geológico Integrado

Aproveitou-se para esta pesquisa todo material coletado pelos geólogos do Grupo de Pesquisa Petrologia de Granitóides em cinco campanhas de campo realizadas entre os anos de 1999 e 2004. Adicionalmente, foram realizadas duas campanhas de campo com a participação da autora, para complementar a amostragem em geral, aprimorar o levantamento de dados estruturais e efetuar a amostragem para estudos geocronológicos e isotópicos. Essas campanhas foram realizadas. em outubro de 2008 e outubro de 2009, com a participação de diversos membros do GPPG.

O mapa geológico integrado preliminar tem como base mapas prévios elaborados por Soares (2002), Gomes (2003), Oliveira (2003) e Sardinha (2005). Para aprimorar o mapa foram usadas imagens de satélite, radar e cartas aero-radiométricas (canais do potássio, tório, urânio e contagem total) que serviram de apoio para individualizar os domínios das diferentes unidades geológicas. As informações de campo foram confrontadas com as obtidas na petrografia, geoquímica e geocronologia, de modo a refinar as interpretações preliminares. É importante ressaltar que todas as informações levantadas foram lançadas em um sistema de informação geográfica (SIG).

1.7.3. Petrografia

O estudo petrográfico contou com a descrição mesoscópica de todas as amostras coletadas no campo, representativas dos diferentes tipos de rochas ocorrentes na área de Canaã dos Carajás. A descrição mesoscópica envolveu os principais aspectos das rochas visíveis a olho nu, tais como cor, forma, textura e estrutura. Esta etapa foi realizada com o intuito de selecionar amostras representativas dos diferentes grupos de rochas para estudos microscópicos.

Foram preparadas cerca de 300 lâminas delgadas e polidas para descrição em microscópio ótico de luz polarizada. As composições modais (Chayes 1956; Hutchison 1974) foram obtidas através de contador automático de pontos (1500 pontos por amostra) e serviram de base para a classificação das rochas, efetuada seguindo as orientações da nomenclatura e classificação das rochas ígneas estabelecidas pela *International Union of Geological Sciences* (IUGS - Le Maitre et al. 2002). A abreviação dos nomes de minerais segue a designação adotada por Kretz (1983) e recomendada pela *American Mineralogical Society*. Tais estudos foram fundamentais para a seleção criteriosa de amostras para análises geoquímicas em rocha total. Todas as amostras analisadas quimicamente e datadas tiveram suas composições modais previamente determinadas. O estudo de microtexturas e estruturas foi baseado o em Passchier & Trouw (1996) e Vernon (2004) e em outros autores referenciados naqueles trabalhos.

1.7.4. Geoquímica em rocha total

As análises químicas em rocha foram realizadas no *Acme Analytical Laboratories Ltda* (Vancouver, CANADÁ). Os conteúdos de elementos maiores e menores (SiO_2, Al_2O_3, Fe_2O_3t, MgO, CaO, Na_2O, TiO_2, Cr_2O_3, P_2O_5, PF), foram dosados por ICP-ES e os elementos-traço (Zn, Cu, Ni, Au, Pb, Ba, Be, Cs, Ga, Hf, Nb, Rb, Sn, Sr, Ta, Th, U, W, Zr, Bi), incluindo terras raras (La, Ce, Pr, Nd, Sm, Eu, Gd, Tb, Dy, Ho, Er, Tm, Yb e Lu), foram determinados por ICP-MS.

1.7.5. Geocronologia

Os concentrados de zircão foram extraídos a partir de cerca de 10 kg de amostra triturada usando método convencional de separação de minerais pesados no Laboratório de Geologia Isotópica da Universidade Federal do Pará (Pará-Iso). Os zircões foram separados manualmente em lupa binocular.

No método Pb-Pb em zircão (Kober, 1987), colocado em rotina no laboratório Pará-Iso por Gaudette et al. (1998), o zircão selecionado é depositado em um filamento de rênio,

em forma de canoa. As canoas contendo os cristais de zircão foram montadas em um "tambor" constando de treze posições, sendo doze de canoas com zircão e um com o padrão NBS-982, que foram todos analisados no espectrômetro de massa Finnigan MAT262. O Pb é extraído por aquecimento em três etapas de evaporação a temperaturas de 1450º, 1500º e 1550 °C e então ionizadas. A contagem foi feita com 5 blocos de 5 ciclos de massa cada, perfazendo um total de 25 razões $^{207}Pb/^{206}Pb$. O efeito da presença de ^{204}Pb oriundo do interior do cristal sobre a idade foi corrigido a partir da curva de evolução do Pb de Stacey & Kramers (1975). As idade calculadas são apresentadas no presente trabalho com erros de 2σ. Idades que se afastaram muito da idade platô do conjunto foram eliminadas subjetivamente.

As análises U-Pb por LA-MC-ICP-MS (*laser ablation multi-collector inductively coupled plasma mass spectrometry*) foram realizadas usando o equipamento *Thermo Finnigan Neptune multi-colletor* no Laboratório de Geocronologia da Universidade de Brasília (UNB). O método U-Pb LA-MC-ICP-MS em zircão consiste inicialmente na confecção de montagens dos grãos de zircão em epoxy. Após a secagem do epoxy, é feito o polimento da montagem com lixa e pasta de diamante (3 μm) até que o zircão fique exposto e a superfície esteja límpida. Esse procedimento é seguido pela obtenção de imagens por catodoluminescência no microscópio eletrônico de varredura, realizada no Laboratório de Microscopia Eletrônica de Varredura do IG-UFPA. Após essa etapa, as montagens são banhadas em ultrasom com 3% HNO_3 e após lavadas com água destilada. A montagem é colocada junto com os padrões no equipamento e os grãos de zircão analisados conforme rotina do laboratório (Buhn et al. 2009). O método U-Pb por LA-MC-ICP-MS se baseia em análises por espectrômetro de massa multi-coletor com ionização por plasma acoplada e ablação a laser e utiliza feixe de laser de diâmetro de 30 micrômetros (*spot analyses*) para ionização da superfície de amostra. Padrões são analisados em paralelo para controle e a precisão analítica fica entre 1,9 e 3,7% (2σ desvio padrão) com uma exatidão de 0,6 a 3,8% (2σ de desvio padrão). A interferência de chumbo comum (^{204}Pb) foi corrigida pelo monitoramento das massas de ^{202}Hg e ^{204}Pb ($^{204}Hg+^{204}Pb$) durante as análises, usando o modelo de composição do Pb (Stacey & Kramers 1975).

As análises U-Pb pelo método SHRIMP (*Sensitive High-mass Resolution Ion MicroProbe*) em zircão foram realizadas na Universidade do Oeste da Austrália. O padrão usado é o zircão BR 266 (559 Ma, U=903 ppm). A composição isotópica do zircão foi determinada pelo SHRIMP II (De Laeter and Kennedy, 1998), usando métodos baseados em Compston et al. (1992). Um feixe preliminar de íons de ~3nA, 10 kVO22 e diâmetro de ~25 μm é focalizado no mineral. Cada análise U-Pb SHRIMP faz cinco varreduras e nove medidas

em cada ponto analisado (196Zr2O, 204Pb, padrão, 206Pb, 207Pb, 208Pb, 238U, 248ThO e 254UO). Correções para Pb comum foram efetuadas pela composição isotópica da galena de Broken Hill. Os dados foram calculados usando o programa SQUID (Ludwig, 2002).

Os resultados das análises de U-Pb por LA-MC-ICPMS e SHRIMP foram plotados em diagramas concordia usando o programa ISOPLOT (Ludwig 2002).

1.7.5. Análise isotópica Sm-Nd

As análises foram realizadas no Laboratório de Geocronologia na Universidade de Brasília e no Laboratório de Geologia Isotópica da Universidade Federal do Pará (Pará-Iso), sendo em ambos os casos usado espectrômetro de massa Finnigan MAT 262.

O método Sm-Nd da Universidade de Brasília é descrito em Gioia and Pimentel (2000). 50 mg de rocha pulverizada são misturados com uma solução *spike* ^{149}Sm–^{150}Nd e dissolvidos em cápsulas de savillex. A extração de Sm e Nd seguiu a técnica de troca catiônica, usando coluna de teflon contendo resina L-N spec (*HDEHP–diethylhexyl phosphoric acid supported on PTFE powder*). O Sm e Nd separados foram depositados em filamento de Re e analisados em modo estático no espectrômetro. A precisão das razões Sm/Nd e $^{143}Nd/^{144}Nd$ é superior a ± 0.5% (2σ) e ± 0.005% (2σ), respectivamente, baseado em repetições de análises de padrões internacionais de rocha (BHVO-1 and BCR-1).

As análises isotópicas Sm-Nd em rocha total obtidas no laboratório de Geologia Isotópica da UFPA seguiram a metodologia descrita por Oliveira, E.M. et al. (2009), que consiste em adicionar o *spike* ^{150}Nd–^{149}Sm em 100 mg de rocha. A esta solução foi adicionado HF + HNO_3 em frasco de Teflon dentro de recipiente PARR a 150º C por uma semana. Após a evaporação, uma nova adição de HF + HNO_3 foi realizada e a solução foi colocada para secar e em seguida diluída com HCl (6N). Concluída a secagem foi diluída com HCl (2N). Após a ultima evaporação, os elementos terras raras (ETR) foram separados dos outros elementos por troca cromatográfica usando a resina Dowex 50WX-8, HCl (2N) e HNO_3 (3N). Após isso, Sm e Nd foram separados dos outros ETR por troca cromatográfica aniônica usando resina Dowex AG1-X4 com a mistura de HNO_3 (7N) e metanol.

Em ambos os laboratórios, a razão $^{143}Nd/^{144}Nd$ foi normalizada para $^{146}Nd/^{144}Nd$ igual a 0,7219, e a constante de decaimento usada foi $6{,}54 \times 10^{-12}$ a^{-1}. O valor das idades-modelo TDM foi calculado usando o modelo de DePaolo (1981).

Capítulo – 2

2. ARCHEAN GRANITOID MAGMATISM IN THE CANAÃ DOS CARAJÁS AREA: IMPLICATIONS FOR CRUSTAL EVOLUTION OF THE CARAJÁS PROVINCE, AMAZONIAN CRATON, BRAZIL

Gilmara Regina Lima Feio
Roberto Dall'Agnol
Elton L. Dantas
M.J.B. Macambira
J.O.S Santos
F.J. Althoff
J.E.B. Soares

Submetido: Precambrian research

Dear Mrs Feio,

Your submission entitled "Archean granitoid magmatism in the Canaã dos Carajás area: implications for crustal evolution of the Carajás province, Amazonian craton, Brazil" has been received by Precambrian Research

Please note that submission of an article is understood to imply that the article is original and is not being considered for publication elsewhere. Submission also implies that all authors have approved the paper for release and are in agreement with its content.

You will be able to check on the progress of your paper by logging on to http://ees.elsevier.com/precam/ as Author.

Your manuscript will be given a reference number in due course.

Thank you for submitting your work to this journal.

Kind regards,

Precambrian Research

Archean granitoid magmatism in the Canaã dos Carajás area: implications for crustal evolution of the Carajás province, Amazonian craton, Brazil

G.R.L. Feio[1,2*], R. Dall'Agnol[1,2], E.L. Dantas[3], M.J.B. Macambira[2,4], J.O.S. Santos[5], F.J. Althoff[1,6], J.E.B. Soares[1]

[1]Grupo de Pesquisa Petrologia de Granitóides, Instituto de Geociências (IG), Universidade Federal do Pará (UFPA), Rua Augusto Corrêa, 01, Belém, PA. Brazil. CEP 66075-110.

[2]Programa de pós-graduação em Geologia e Geoquímica, IG – UFPA.

[3]Laboratório de Estudos Geocronológicos, Geodinâmicos e Ambientais, Universidade de Brasília, Brasília, DF, CEP 70910-900, Brazil.

[4]Laboratório de Geologia Isotópica, IG – UFPA.

[5]Centre for Exploration Targeting, University of Western Australia, Crawley 6009, Western Australia

[6]Departamento de Geociências, Centro de Filosofia e Ciências Humanas, Universidade Federal de Santa Catarina, Campus Universitário Reitor João David Ferreira Lima. CEP: 88040-970. Brazil.

*Corresponding author

ABSTRACT

Geological mapping, geochemical, and geochronological studies undertaken in the Archean granitoids of the Canaã area in the Carajás province, Amazonian craton, Brazil, led to the definition of new granitoid units that entirely replace the Xingu complex in the area. Four major magmatic events are indentified: three of Mesoarchean age and one of Neoarchean age. The succession of events is: (1) at 3.05-3.0 Ga, it occurred the formation of the protolith of the Pium complex and of rocks with similar ages only indicated by inherited zircons found in different units; (2) at 2.96-2.93 Ga, occurred the crystallization of the Canaã dos Carajás granite and the formation of the older rocks of the Rio Verde trondhjemite; (3) at 2.87-2.83 Ga, the Bacaba tonalitic complex, the Rio Verde trondhjemite, and the Cruzadão, Bom Jesus and Serra Dourada granites were formed; (4) in the Neoarchean, at 2.75-2.73 Ga, the Planalto and Pedra Branca suites and charnockite rocks were originated. Two groups of granitoid units were distinguished: (1) The tonalitic-trondhjemitic units, which encompass the Bacaba tonalitic complex and the Pedra Branca suite, which are geochemically distinct of typical Archean TTG series, and the Rio Verde trondhjemite, akin to the TTG series; (2) the granitic units, which cover more than 60% of the Canaã surface and encompass the calc-alkaline Canaã dos Carajás, Bom Jesus, and Serra Dourada granites, the transitional between calc-alkaline and alkaline Cruzadão granite, and the ferroan, alkaline Planalto granite. The Archean granitoid magmatism in Canaã significantly differs

of that found in most classical Archean cratons, including the Rio Maria terrane, because TTG magmatism is not abundant, sanukitoid rocks are absent and granitic rocks are dominant. The contrasts between Canaã and the Rio Maria granite-greenstone terrane do not favor a common tectonic evolution for these two Archean domains of the Carajás province. The Archean crust of Canaã has not a juvenile character and the Nd evolution paths suggest the existence of a little older crust in the Canaã area compared to that of Rio Maria. The Planalto suite is present in the entire Carajás domain and has no equivalent in the Rio Maria terrane. The crust of the Canaã area existed at least since the Mesoarchean (ca. 3.2-3.0 Ga) and was strongly reworked during the Neoarchean (2.75 to 2.70 Ga). A similar terrane to that represented by the Canaã Mesoarchean crust or even an extension of it was probably the substratum of the Carajás basin formed during the Neoarchean. Probably there is no an effective transition between Rio Maria and the Carajás basin and the denominated 'Transition' subdomain had more probably an evolution distinct of that of Rio Maria. The evolution of the Carajás province approach in some aspects the Neoarchean evolution described in the Limpopo belt, a terrain situated between the Zimbabwe and Kaapvaal craton on Southern Africa, because both were strongly reworked during the Neoarchean and generate in hot zones of the deep crust high temperature granitoid magmas, possibly due to collisional tectonic processes.

Keywords: Geochronology, Nd isotope, Geochemistry, Archean Granitoids, Crustal evolution, Carajás Province.

1. Introduction

The Carajás province, the largest and best preserved Archean segment of the Amazonian craton (Fig. 1a), north Brazil, comprises two main tectonic domains: (1) The Rio Maria granite-greenstone terrane (RMGGT) and (2) the Carajás domain (Souza et al., 1996; Dall'Agnol et al., 2006; Vasquez et al., 2008). The granitoid magmatism and evolution of the RMGGT was more deeply studied (Macambira and Lafon, 1995; Macambira and Lancelot, 1996; Althoff et al., 2000; Souza et al., 2001; Leite et al., 2004; Oliveira, M.A. et al., 2009, 2010; Almeida et al., 2010, 2011) than that of the Carajás domain, where two distinct sub-domains were distinguished. To the north, it is exposed the Carajás basin formed essentially by Neoarchean supracrustal units (Gibbs et al., 1986; Machado et al., 1991; Teixeira and Eggler, 1994; Nogueira et al., 1995; Lobato et al., 2005; Dall'Agnol et al., 2006) and, to the south, a terrane dominated by Archean granitoids with subordinate granulitic and charnockitic rocks (Vasquez et al., 2008; Oliveira, D.C. et al., 2010). This south terrane was denominated informally as 'Transition' sub-domain, interpreted as a probable Mesoarchean substratum, similar to the RMGGT, that was intensely affected by the magmatic and tectonic Neoarchean

events recorded in the Carajás basin (Dall'Agnol et al., 2006 and references therein; Domingos, 2009).

The absence of systematic geochemical, geochronological and isotope studies on the Archean granitoid magmatism of the Carajás domain, reflected in the undefined ages and geochemical signature of the major granitoid units exposed in that area, which were encompassed in the Xingu complex, do not allow to constrain the proposed models for the crustal evolution of the Carajás domain and, consequently, of the Carajás Province.

This paper reports the results of an integrated geochemical, geochronological and Nd isotope study on granitoids of the Canaã dos Carajás region, a key area for the understanding of the Carajás domain crustal evolution, because of its diversified Archean granitoid magmatism and location in the border between the Carajás basin and the 'Transition' sub-domain. The obtained data will also allow the characterization of the nature, age, and composition of some of the main Archean granitoids formed in the Carajás domain. Besides, this work contributes to clarify the tectonic relationships between the Carajás and Rio Maria domains of the Carajás Province and to the knowledge of the Mesoarchean to Neoarchean transition in Archean cratons.

2. Tectonic setting and regional geology of the Carajás province

The Carajás Province is located in the southeastern part of the Amazonian craton (Fig. 1a, Machado et al., 1991; Santos et al., 2000; Tassinari and Macambira, 2004; Dall'Agnol et al., 2006) and their two distinct domains are separated for approximately E-W shear zones (Fig. 1b; Vasquez et al., 2008): To the south, it is exposed the Mesoarchean Rio Maria granite-greenstone terrane (RMGGT; 3.0 to 2.86 Ga; Macambira and Lafon, 1995; Althoff et al., 2000; Souza et al., 2001; Almeida et al., 2011) and, to the north, the Carajás domain (3.0 to 2.55 Ga; Gibbs et al., 1986; Machado et al., 1991; Dall'Agnol et al., 2006), which corresponds approximately to the Itacaiúnas shear belt (Araújo and Maia, 1991; Costa et al., 1995). The exact limit between the RMGGT and the Carajás domain is still undefined, but it is located approximately to the North of the Sapucaia belt, where there is geophysical evidence of a major tectonic discontinuity (Fig. 1b), separating the more strongly deformed and EW elongated plutonic bodies of the 'Transition' sub-domain to those of the RMGGT.

The Mesoarchean Rio Maria granite-greenstone terrane is composed of greenstone belts (3.0-2.90 Ga; Macambira and Lafon, 1995; Souza et al., 2001 and references therein) and several granitoid series: (1) An older TTG series (2.98-2.93 Ga; Macambira and Lancelot,

1996; Althoff et al., 2000; Leite et al., 2004; Almeida et al., 2011); (2) The sanukitoid Rio Maria suite (~2.87 Ga; Macambira, 1992; Oliveira, M.A. et al., 2009, 2010 and references therein); (3) An younger TTG series (~2.87-2.86 Ga; Leite et al., 2004; Almeida et al., 2011); (4) A high Sr- and Ba-bearing leucogranodiorite-granite suite (~2.87 Ga; Almeida et al., 2010); and (5) Potassic leucogranites of calc-alkaline affinity (~2.87-2.86 Ga; Leite et al., 1999, 2004; Almeida et al., submitted). Despite their diversity, the magmatic units of this terrane were generated in a relatively short period of ~120 Ma.

Compared to the RMGGT, the Carajás domain has a more complex evolution. The 'Transition' sub-domain is formed by strongly deformed Mesoarchean to Neoarchean units, whereas its northern part corresponds essentially to the Neoarchean Carajás basin. The southern 'Transition' sub-domain has been poorly studied so far and their Archean granitoid and gneissic rocks were generally grouped in the Xingu Complex (Fig. 1b). In the Canaã area, located in the 'Transition' sub-domain (Fig. 2), before the present work, the oldest rocks exposed were those of the Xingu complex (Fig. 1b), associated with the granulites of the Pium Complex (protolith crystallization age of 3002±14 Ma and granulite facies metamorphism at 2859±9 Ma; SHRIMP U-Pb on zircon; Pidgeon et al., 2000), the Bacaba tonalite (ca 3.0 Ga; U-Pb LA-MC-ICPMS on zircon; Moreto et al., 2011), and the Canaã dos Carajás potassic leucogranite (Fig. 2; 2928±1 Ma; Pb-evaporation on zircon; Sardinha et al., 2004). These Mesoarchean units were followed during the Neoarchean (cf. Fig. 2) by the Vermelho mafic-ultramafic stratified complex (Vasquez et al., 2008, and references therein), a trondhjemitic-tonalitic association (ca. 2.75 Ga; Sardinha et al., 2004; Gomes and Dall'Agnol, 2007) designated as Pedra Branca suite in the present work, the Planalto suite granites (2734±4 Ma; Pb-evaporation on zircon; Huhn et al., 1999; Sardinha et al., 2004; Feio et al., submitted), Neoarchean charnockitic rocks (2.75-2.73 Ga; Gabriel et al., 2010; Feio et al., submitted) and undifferentiated gabbros. The Neoarchean Carajás basin (Fig. 1b) is formed by banded iron formations, accompanied by a bimodal volcanism metamorphosed in greenschist conditions (Itacaiúnas Supergroup; 2.76-2.74 Ga; Machado et al., 1991; Trendall et al., 1998; Tallarico et al., 2005), and followed by the fluvial to marine siliciclastic deposits of the Águas Claras formation (Nogueira et al., 1995).

Several Neoarchean subalkaline granite plutons occur in the basin or in adjacent areas (Figs. 1b, 2) and are intrusive in the Itacaiúnas supergroup (~2.76-2.57 Ga; Machado et al., 1991; Barros et al., 2004, 2009; Sardinha et al., 2004, 2006; Feio et al., submitted).

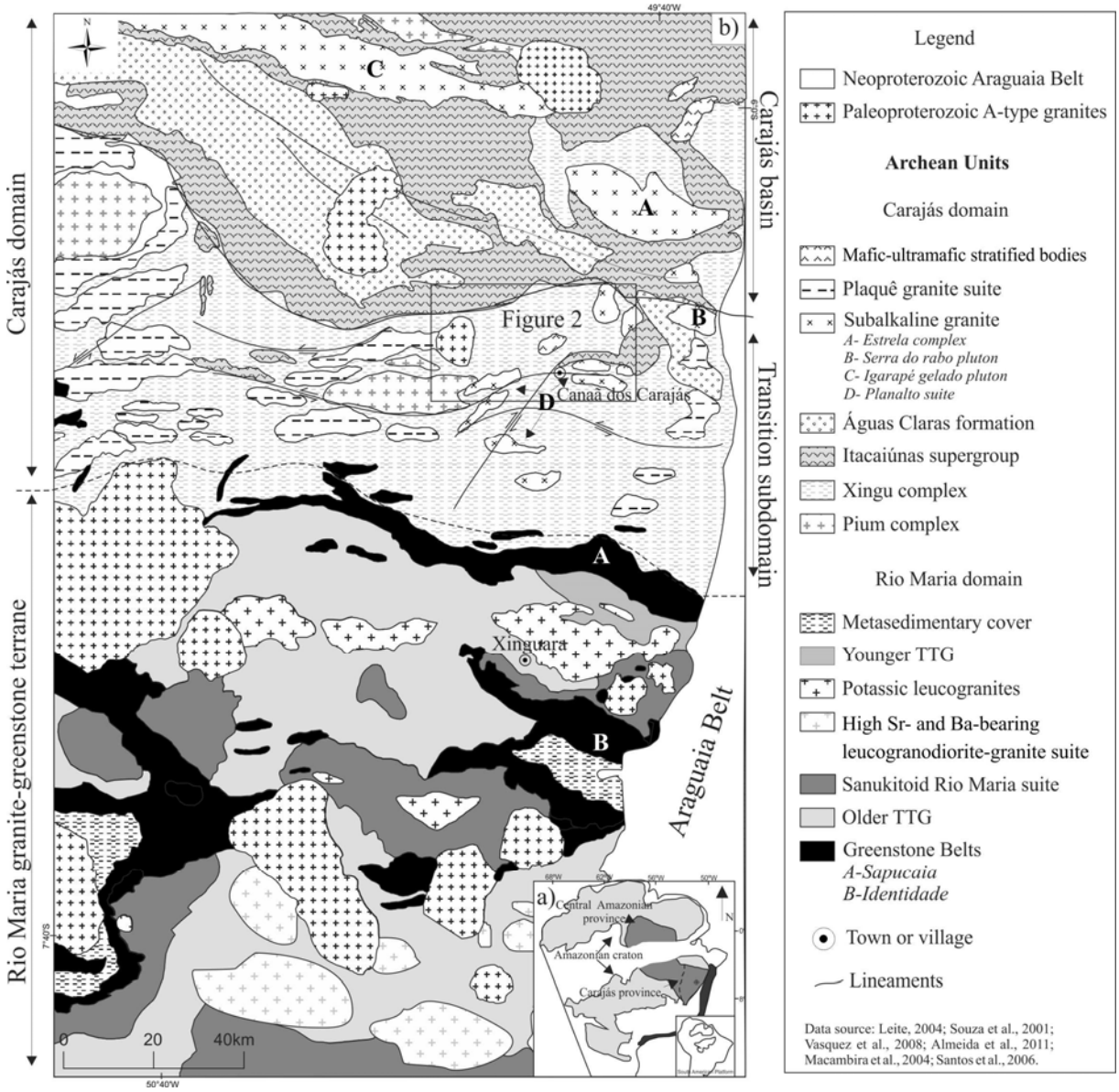

Figure 1 - Simplified geological map of the Carajás province (Leite et al., 2001; Vasquez et al., 2008; Almeida et al., 2011). The dashed line is the proposed boundary between the Carajás domain and the Rio Maria granite-greenstone terrane; the continuous line divides the Carajás domain in Carajás basin and 'Transition' subdomain (Dall'Agnol et al., 2006).

Near the borders of the Carajás basin (Figs. 1b, 2) are also exposed several Neoarchean mafic-ultramafic stratified bodies (Vasquez et al., 2008 and references therein), generally mineralized in nickel. Sills and dykes of Neoarchean hydrothermal-altered gabbros cross-cut all these rocks. The few isotope data available on the Neoarchean subalkaline granites of the Estrela Complex (Barros et al., 2009), mafic rocks of the Carajás basin (Galarza et al., 2008), and Paleoproterozoic A-type granites (Serra dos Carajás suite, Dall'Agnol et al., 2005) indicate that the Carajás basin was formed over a Mesoarchean crustal substratum (~3.0 Ga).

It is clear that, differently of the RMGGT, a large part of the evolution of the Carajás domain was concentrated during the Neoarchean when the Carajas basin and a widespread dominantly subalkaline plutonic magmatism and charnockitic rocks were formed. This implies that the tectonic stabilization of the RMGGT terrane preceded that of the Carajás domain (Dall'Agnol et al., 2006).

3. Geology of the Canaã dos Carajás area

3.1. Introduction

The Canaã dos Carajás area is located in the border between the Carajás basin and the 'Transition' sub-domain and the results of its geological mapping are presented in Figure 2. To the northern and northeastern of the mapped area are exposed the Neoarchean metavolcanic rocks and banded iron formations of the Itacaiunas supergroup. The northeastern and eastern areas are part of the Serra do Rabo, an extension to southeast of the Carajás basin, that was affected by the Serra dos Carajás fault and is related to a structure of horsetail splays which show different orientations (Pinheiro and Holdsworth, 1997; Domingos, 2010). There are also some occurrences of the Itacaiunas supergroup in the central-southern part of the Canaã area which show a strong structural control and correspond to expositions along NE-SW shear zones related to the splays of the Serra dos Carajás fault.

The geological mapping demonstrated that the study area, excluded the Itacaiunas supergroup, is composed essentially of granitoids and orthopyroxene-bearing rocks, with subordinate mafic and ultramafic rocks, small plutons of Paleoprotezoic anorogenic granites (Rio Branco and similar granites) and lateritic covers (Fig. 2). The areas originally occupied by the Xingu complex are in fact formed by different kind of granitoids, many of them characterized by the first time in the present work. As it will be show by the geochronological data presented hereafter, excluding the anorogenic granites and lateritic covers, the other units

were formed in the Mesoarchean and Neoarchean with ages comprised in the interval between 3.00 and 2.65 Ga.

Poorly exposed, local remnants of Mesoarchean(?) greenstone belts were identified in the northern part of the area, apparently intruded by different granitoids. The Vermelho mafic-ultramafic intrusion is a Neoarchean layered complex derived from original mafic magmas that has associated secondary nickel deposits. Small stocks, sills and dikes of gabbros are also common. Their ages were not defined so far, but field relationships and their probable correlation with the Aguas Claras gabbros of the Carajás basin (Barros et al., 1994; Dias et al., 1996; Mougeot et al., 1996) suggest an age of ca. 2.65 for them. The units mentioned above and the anorogenic granites will not be further discussed in detail in the present work that is focused in the Archean granitoid rocks identified in the Canaã area.

3.2. Geological and petrographic aspects of the Archean granitoids of the Canaã area

3.2.1. Mesoarchean granitoids

3.2.1.1. The Pium complex

The Pium complex forms a large EW elongated body, disposed parallel to the regional foliation and partially exposed in the southwestern part of the mapped area (Fig. 2). It was described as a Mesoarchean granulitic complex (Pidgeon et al., 2000, and references therein) composed of norite, gabbro, and subordinate quartz-orthopyroxene-bearing rocks, all of them with massive or foliated aspect, generally displaying igneous textures modified by ductile deformation and recrystallization (Ricci and Carvalho, 2006; Santos and Oliveira, 2010). The presence of partially assimilated or angular enclaves of the mafic rocks (Araújo and Maia, 1991; Santos and Oliveira, 2010) included in the quartz-orthopyroxene-bearing rocks suggests that the latter were emplaced after the gabbros and could be significantly younger in age.

An enderbite of the Pium complex was dated by SHRIMP U-Pb on zircon and ages of 3002 ± 14 Ma and 2859 ± 9 Ma were obtained, respectively, for the core and rim zones of zircon crystals (Pidgeon et al., 2000). The older age was interpreted as the crystallization age of the protolith of the enderbite and the younger one as the granulite facies metamorphism.

The igneous or metamorphic origin of the Pium complex is now controversial (Vasquez et al., 2008), among other things, because Neoarchean orthopyroxene-bearing igneous rocks have been recently identified associated with it (2754 ± 1 Ma, Pb-evaporation on zircon, Gabriel et al., 2010; 2735 ± 5 Ma, LA-MC-ICPMS on zircon, Feio et al., submitted). This indicates the existence of a generation of charnockitic rocks that is clearly

younger than the rocks of the Pium complex studied by Pidgeon et al. (2000) and points to the need for additional studies of this complex.

3.2.1.2. Canaã dos Carajás granite

The Canaã dos Carajás granite occurs in the southeastern part of the study area in the proximities of the Canaã dos Carajás town (Fig. 2). It consists of strongly deformed, folded and mylonitized rocks showing penetrative E-W foliation with vertical dip and crosscut by dextral EW or, locally, NE-SW shear zones (Fig. 3a). A SE-dipping inverse fault cut the foliation. Field relationships between the Canaã dos Carajás granite and other units were not observed, but the inferred western and northern contacts are limited by large shear zones (Fig. 2). Locally, the granite includes metric enclaves of amphibolite.

The granite is a hololeucocratic rock (M'<5%), displaying gray color and medium- to fine-grained seriated texture. It is a biotite monzogranite, with zircon, magnetite, titanite ± apatite ± allanite as primary accessory minerals and muscovite, and chlorite as secondary ones. In thin section, quartz occurs as elongated polygonal aggregates and plagioclase and alkali feldspar crystals are augen shaped and generally enveloped by fine-grained recrystallized aggregates (core and mantle structures; Vernon, 2004). Bulbous myrmekite intergrowths (Phyllips, 1980) replacing alkali feldspar grains are common.

3.2.1.3. Rio Verde trondhjemite

The major occurrences of the Rio Verde trondhjemite are located near the Planalto village and extend to the west of the Vermelho intrusion in the center of the Canaã area and to northeast near the type area of the Planalto granite (Fig. 2). It makes contact with the Bom Jesus granite, Bacaba tonalitic complex and the Serra Dourada and Planalto granites. The latter gave comparatively younger ages compared to the Rio Verde trondhjemite (see geochronology section). Along the contact with the Serra Dourada granite, the Rio Verde trondhjemite was affected by metassomatism probably related to the intense sodic and subordinate potassic alteration registered in the northern part of the Canaã area (Sousa, 2007; Moreto et al., 2011).

The dominant trondhjemite varies from texturally homogeneous (Fig. 3b) to banded rocks in which trondhjemitic layers alternate with biotite tonalite. Most of the rocks are strongly foliated and the foliation strikes EW to N and has a vertical dip. These rocks show also complex folds with vertical or E-dipping axes and are cut by leucogranite veins, sinistral shear

zones, and thrust faults. The trondhjemite includes metric enclaves of amphibolites that are possibly related to the greenstone belts.

The trondhjemite displays white to gray color, fine to medium-grained equigranular texture and brown biotite is the main mafic mineral. Allanite, ilmenite, and zircon are minor minerals. The secondary phases are albite, chlorite, scapolite, greenish biotite, apatite, epidote, carbonate, magnetite, and rutile.

In the less deformed rocks, plagioclase form sub-euhedral crystals involved by aggregates of fine grains of recrystallized quartz whereas in the more strongly deformed ones, the feldspar appears as porphyroclasts surrounded by a fine-grained matrix which contains quartz recrystallized aggregates that form oriented elongated ribbons with intense undulant extinction.

3.2.1.4. Bacaba Tonalitic complex

This complex occurs as an elongated EW-strip in the northern part of the study area. It makes contact with the Itacaiúnas supergroup that is exposed in the southern border of the Serra dos Carajás. Its southern contact is done with the Rio Verde trondhjemite, Bom Jesus, Serra Dourada and Cruzadão granites (Fig. 2). Small stocks of gabbros are intrusive in this unit (Moreto et al., 2011). It was better studied in its eastern segment located near Vila Planalto where two distinct associations were distinguished: (1) biotite tonalite to granodiorite (Fig. 3d) with subordinate diorite and monzogranite that dominate into the north domain of the unit, and (2) biotite-hornblende tonalite with subordinate granodiorite and monzogranite, exposed in the quarry near Vila Planalto (Fig. 3e) and extending to the west in the southern domain of the unit near the contact with the Serra Dourada granite. The main mineralogical contrast between these associations is the presence or not of amphibole as a major mafic phase but they show also important geochemical differences (see below). In the western segment of the complex, the rocks are poorly exposed but both varieties with or without amphibole were identified. Leucogranite veins cut all these rocks.

In addition, hornblende tonalites, similar in mineralogy to those of the southern domain of the complex, occur intimately associated with the Cruzadão granite (Fig. 3f) in the central-western part of the area, near the Rio Branco granite (Fig. 2). The different rock varieties of the tonalitic complex are characterized by a remarkable magmatic ~EW-foliation due to the orientation of plagioclase and mafic minerals. Locally, the foliation is oriented along NS or NE-SW.

A contradictory aspect of this unit is related to the fact that in the iron oxide-Cu-Au Bacaba deposit, the hydrothermally altered tonalite sampled in drill cores from the mineralized area gave ages around 3.0 Ga (Moreto et al., 2011). That tonalite is a foliated, phaneritic fine-grained rock with hornblende and biotite as main mafic minerals. Moreto et al. (2011) have denominate Bacaba tonalite the mentioned rock and included in this unit the tonalites exposed in adjacent areas which are superposed spatially with those studied in the present work. These 3.0 Ga ages are significantly older and not coincident with those obtained in the present work (~2.85 Ga; see geochronological section) for rocks representative of, apparently, the same unit, but sampled in its extreme eastern domain, not adjacent to the mineralized area. It is impossible to individualize so far in the geological map these possible two generations of tonalites. For this reason, our option was to denominate the unit as Bacaba tonalitic complex, leaving implicit that more detailed future work will be necessary to better evaluate this question and possibly to distinguish the different kind of tonalites that compose this complex.

Both tonalite associations have medium- to coarse-grained granular texture and display gray color changing to dark gray in strongly altered rocks. The biotite granodiorite and monzogranite show porphyritic texture due to the presence of centimetric (~1-2 cm) phenocrysts of alkali feldspar. In these rocks, the phenocrysts show a strong preferential orientation, and are set in a medium-grained matrix composed of quartz + plagioclase + biotite ± microcline. The rocks of the biotite-hornblende tonalite association include elongated mafic xenoliths oriented parallel to the magmatic foliation and, in the most deformed rocks, the quartz crystals are intensely deformed and recrystallized. The accessory minerals found in both associations are zircon, apatite, allanite, titanite, and magnetite. The different rock varieties of the complex show secondary formation of scapolite, albite, biotite, apatite, magnetite, actinolite, ± epidote ± muscovite ± sulfides ± chlorite ± quartz that was due to the intense Na- and subordinate K-metasomatism registered in a regional scale in the northern sector of the Canaã area and, more particularly, near the Sossego copper mine (Sousa, 2007; Moreto et al., 2011).

3.2.1.5. Bom Jesus granite

The Bom Jesus granite is exposed in the central-eastern part of the mapped area. It consists essentially of banded and foliated granite oriented along NE-SW to EW with vertical or steep SE- to S-dips. Sinistral mylonitic EW to NE-SW shear zones crosscut the granite and apparently controls the strike of their major structures. Locally, isoclinals folds with SE-

dipping axes were registered. Quartz-feldspar pegmatoid or fine-grained veins are present in the granites.

The Bom Jesus granite and the Rio Verde trondhjemite are disposed in semi parallel NE-oriented strips in the map scale (Fig. 2) and they show strong interaction along the contacts. In the field, the rocks of both units occur intimately associated and intercalated bands of granite and trondhjemite composition are commonly observed (Fig. 3c). This suggests that both units were submitted to a same event of intense ductile deformation. The Bom Jesus granite contains enclaves of amphibolites and is cut by epidote and quartz-feldspar veins. Except for the contact with the Rio Verde trondhjemite, the relationships between the Bom Jesus granite and the other units were not observed in the field.

The Bom Jesus granite has monzogranite to syenogranite composition and shows pink to gray color and fine- to medium- or medium- to coarse-grained seriated to porphyroclastic texture. Biotite is the main mafic mineral, accompanied by accessory allanite, titanite, zircon, magnetite ± ilmenite, and apatite. The secondary mineralogy is chlorite, rutile, hematite, epidote, carbonates, scapolite, and muscovite. In thin section, this granite exhibits (1) intensely recrystallized lenticular aggregates of quartz, disposed along the rock foliation and generally surrounding the augen shaped porphyroclasts; (2) porphyroclasts of K-feldspar and plagioclase set in a fine-grained recrystallized matrix; (3) plagioclase grains with polysynthetic twinning and concentric zoning, generally displaying deformed curved twin lamellae; (4) subordinate myrmekite intergrowths in the border of K-feldspar grains.

3.2.1.6. Cruzadão granite

The Cruzadão granite shows dominant NW-SE- to EW-striking foliation and was locally affected by NW-SE- to EW shear zones and mylonitized. It was distinguished for the first time in the present work and two distinct areas of its occurrence were identified. The first one is located in the centre-western part of the mapped area, where the granite is in contact to the north with the Bacaba tonalite and Itacaiúnas supergroup, to the south with the Pium complex and to the east with the Bom Jesus granite (Fig. 2). In this sector, the Cruzadão granite is exposed generally is small hills and is intruded by the Paleoproterozoic Rio Branco granite. It is also locally associated with hornblende tonalites which are tentatively correlated with the Bacaba tonalite. Both rocks define strongly banded structures with intercalated bands of granitic and tonalitic composition (Fig. 3f) which were folded, suggesting that these rocks had a coeval emplacement and were submitted to similar ductile deformational processes.

The second large occurrence of the Cruzadão granite defines a NE-SW-oriented strip located in the central-southern part of the area (Fig. 2). To the east, this intrusion has a tectonic contact with the Canaã dos Carajás granite and the Itacaiúnas supergroup, and to the north with the Bom Jesus granite. It is intruded by the Vermelho mafic body, a pluton of the Planalto suite and a small stock of the Pedra Branca suite. The field relationships between different units were not observed in the field and the local stratigraphy was defined on the basis of geochronological data.

The Cruzadão granite is a hololeucocratic rock (M'<7%), displaying pink to gray color and coarse- to medium- or medium- to fine-grained seriated texture. It is a biotite monzogranite to syenogranite, with zircon, allanite, apatite, and magnetite as common accessory minerals. Some samples of the west sector contain also magmatic epidote and titanite is found in those of the central-southern sector. Chlorite, epidote, muscovite ± carbonates are the secondary minerals. In thin section, the plagioclase and perthitic alkali feldspar form porphyroclasts, generally showing core-mantle microstructures (Vernon, 2004). Some plagioclase grains show deformed twins and develop myrmekite intergrowths with quartz along the contacts with alkali feldspar. The quartz consists of polygonal recrystallized grains with undulant extinction or forms elongated ribbons that surround the feldspar porphyroclasts. The biotite is generally fine-grained and oriented along the rock foliation.

3.2.1.7. Serra Dourada granite

The Serra Dourada granite is a sub-circular stock, located near the Serra Dourada village in the northern part of the Canaã area (Fig. 2). Remnants of greenstone belts are involved by the granite. It is intrusive in the Bacaba tonalitic complex as observed in the northwestern contact between both granitoids and in a quarry immediately to the west of Vila Planalto (Fig. 3e). Conclusive field relationships between it and the Rio Verde trondhjemite and Bom Jesus granite were not observed. This granite show also a spatial association with abundant small bodies of mafic rocks, that apparently cut the granite but their contact relationships are not exposed.

The Serra Dourada granite displays pink color rocks and medium- to coarse-grained (Fig. 3g) or subordinate fine-grained texture. The major part of the stock is formed by little deformed rocks. A not pervasive EW-striking vertical foliation is observed locally and mylonitized rocks are found along shear zones. Pegmatite and aplitic veins cut the granite which has monzogranite composition and biotite, with accessory allanite, zircon ± magnetite and ilmenite as mafic minerals. Secondary phases, mostly related to hydrothermal alteration,

are common and include albite, muscovite, biotite, chlorite, epidote, opaque, titanite, quartz, scapolite, and tourmaline.

The plagioclase is calcic oligoclase (An_{30-20}) and it forms, alike the alkali feldspar, subeuhedral crystals. The alkali feldspar is perthitic and myrmekite quartz-plagioclase intergrowths are seen along the border of its crystals. Quartz consists of locally fractured and partially recrystallized anhedral grains, and biotite is subeuhedral and interstitial to the feldspars and quartz.

3.2.2. Neoarchean granitoids

3.2.2.1. Pedra Branca suite

The Pedra Branca suite is composed of sodic granitoids exposed into the southern part of the study area. It occurs as small stocks spatially associated with the Planalto Suite (Fig. 2) but the contact relationships between this suite and the Planalto one and also with other Archean units are not clearly exposed in the field.

The rocks of the Pedra Branca suite are strongly deformed and commonly show a magmatic banding, with alternation of decimeter- to meter-thick tonalitic and trondhjemitic bands and subvertical EW foliation related to a ductile deformation. A high angle SSE-dipping thrust fault was identified in the stock located in the southeastern part of the mapped area (Fig. 2). It intercepts the primary foliation and is apparently related to the action of a late NS-compressive strain (Gomes and Dall'Agnol, 2007). A high-angle stretching lineation dipping to SE quadrant is also locally present (Fig. 2, 3h).

It is composed dominantly of tonalite and trondhjemite, with hornblende and biotite as major mafic minerals, and titanite, allanite, zircon, apatite, and, locally, clinopyroxene as accessory minerals (Gomes and Dall'Agnol, 2007).

3.2.2.2 Charnockite rocks

Neoarchean charnockite rocks occur intimately associated with the Pium complex and cannot be individualized in the scale adopted for geological mapping. However, outside the study area, relatively large bodies of such rocks were recognized (Gabriel et al., 2010) and there is increasing evidence that they can have an important role in the evolution of the 'Transition' sub-domain. In that sub-domain, these orthopyroxene-bearing rocks have quartz norite to leucoenderbite composition and occur associated with the Pium complex and Planalto suite (Feio et al., submitted). The field relationships between the charnockite rocks

and the Planalto granite are complex but apparently some interaction between both magmas has happened suggesting that they coexisted in the partially molten state.

3.2.2.3. Planalto suite

The Planalto suite was described in great detail by Feio et al. (submitted) and just a synthesis of its main aspects will be given here. It consists of several lenticular granite stocks with less than 10 km in the largest dimension, located in the areas of stronger deformation and oriented concordantly to the dominant EW-trending regional structures or, eventually to NE-SW or NS (Fig. 2). This Neoarchean Planalto suite is intrusive in the Mesoarchean granitoid units, in the mafic Pium complex, and in the Neoarchean supracrustal Itacaiúnas supergroup (Fig. 2). In general, this suite is associated spatially with the Pium complex and the Pedra Branca suite.

The Planalto granite shows penetrative EW- to NNW-subvertical foliation locally accompanied by a high angle stretching mineral lineation and C-type shear bands. Mylonites are found along sinistral or subordinate dextral EW to NE-SW shear zones. The Planalto suite is composed of biotite-hornblende monzogranite to syenogranite (Fig. 3i), with subordinate alkali feldspar granite. Relics of clinopyroxene with coronae of amphibole are present in some samples. The primary accessory minerals are zircon, apatite, allanite, ilmenite ± magnetite ± titanite ± fluorite. Complementary information can be found in Feio et al. (submitted).

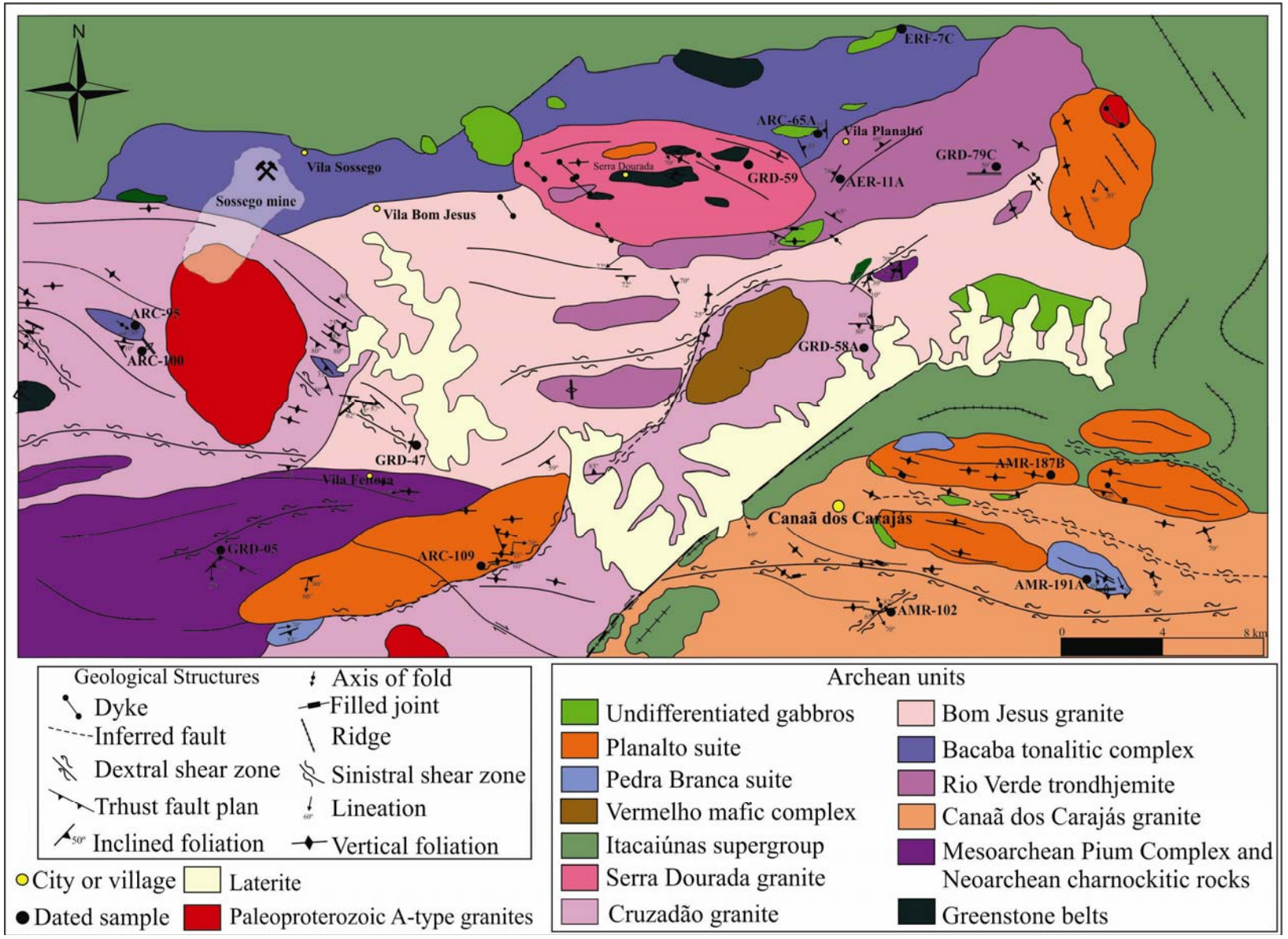

Figure 2 - Geological map of the Canaã area of the Carajás province. Dated samples are indicated by small black circles. The location of this figure is shown in Fig. 1.

Figure 3 - Field aspects of the granitoids of the Canaã area. (a) Foliated Canaã dos Carajás granite crosscut by dextral shear zones; (b) Regular banding in the Rio Verde trondhjemite (c) intercalated bands of Bom Jesus granite and trondhjemite correlated with the Rio Verde trondhjemite; (d) detail of the biotite granodiorite facies of the Bacaba tonalitic complex; (e) the Serra Dourada granite cutting the biotite-hornblende tonalite facies of the Bacaba tonalitic complex in a quarry near the Planalto village; (f) intercalated bands of Cruzadão granite and Bacaba tonalite; (g) Isotropic aspect of the Serra Dourada granite; (h) Subvertical mineral lineation in a trondhjemite of the Pedra Branca suite; (i) Oval-shaped, deformed K-feldspar megacrysts in the Planalto granite.

4. Geochemistry

4.1. Introduction

In this section, it will be done just a broad geochemical characterization of the Archean granitoid units identified in the Canaã area, because a detailed discussion on this subject is beyond the scope of the present work. Our goal is to give a general ideal about the major geochemical aspects of the different granitoids, in order to distinguish their magmatic series and to establish a preliminary comparison between them. Representative chemical analyses of the studied granitoid units are shown on Table 1 and the analytical methods are presented in the Appendix A. For the discussion of the geochemical data, these granitoids will be assembled in two different groups according to the dominant rocks and independent of their ages: (1) essentially granitic rocks; (2) tonalite-trondhjemite and subordinate associated rocks. Five granite units have been distinguished in the first group. Four of them are of Mesoarchean age (the Canaã dos Carajás, Cruzadão and Serra Dourada granites and the Bom Jesus granite) and one was formed during the Neoarchean (Planalto suite). The second group encompasses two Mesoarchean units, the Rio Verde trondhjemite and the Bacaba tonalitic complex, and the Neoarchean Pedra Branca suite. A more detailed geochemical characterization of the Planalto suite and Pium complex and associated charnockite rocks was presented, respectively, by Feio et al. (submitted) and Santos (2009).

4.2. General geochemical aspects

Some classical geochemical diagrams were selected to present the main characteristics of the studied granitoid units (Fig. 4). In the normative An-Ab-Or plot (O'Connor, 1965; modified by Barker, 1979), all analyzed samples of the five granite groups plot effectively in the granite field and the areas occupied by the samples of the different units tend to be partially superposed. The rocks of the tonalitic-trodhjemitic units plot mostly in the tonalite and trondhjemite fields but they occupy distinct areas of the diagram (Fig. 4a). A similar distribution is observed in the PQ diagram (Debon and LeFort, 1983), where the granitic rocks plot in the granite field but with some distinction between the different suites (Fig. 4b), that can vary from granodiorite to monzogranite (Canaã dos Carajás and Serra Dourada granites) or from monzogranite to syenogranite (Cruzadão and Planalto granites), or concentrate in the monzogranite field (Bom Jesus granite). On the other hand, the rocks of the second group plot dominantly in the tonalite (trondhjemite) field with the varieties of the

Bacaba tonalite complex showing more variable composition from tonalite to granodiorite with subordinate quartz diorite, quartz monzodiorite and monzogranite (Fig. 4b).

In the K-Na-Ca plot (Fig. 4c), all granite units are disposed along the calc-alkaline trend (Barker and Arth, 1976), but can be distinguished by their variable K-contents. The Pedra Branca suite is akin of the low-K series and the Rio Verde trondhjemite samples are concentrated in the field of Archean TTGs (Martin, 1994). Finally, the Bacaba tonalitic complex samples are dispersed in the diagram with a clear distinct distribution of the hornblende- or biotite-dominated varieties (Fig. 4c). In the AB diagram (Debon and LeFort, 1983), except for the Planalto suite granites that are dominantly metaluminous, the other granite units are peraluminous and plot in the biotite-bearing or, in the case of the Serra Dourada granite, into the muscovite-biotite-bearing rocks field (Fig. 4d). The rocks of the Pedra Branca suite are metaluminous and show a large chemical variation, whereas those of the Bacaba tonalitic complex can be metaluminous (amphibole-bearing varieties) or peraluminous (biotite-dominated facies) and those of the Rio Verde trondhjemite are essentially peraluminous rocks (Fig. 4d). The SiO_2 vs. FeOt/(FeOt+MgO) diagram (Fig. 4e) also allows a good discrimination of the studied granitoids. The Planalto suite granites show the highest values of FeOt/(FeOt+MgO) (generally > 0.9) and are clearly separated of the remaining granite units that show values varying from 0.8 to 0.9 for that ratio. The Planalto granites are typical ferroan granites (Frost et al., 2001). The nature of the other granite units is unclear because they are high silica assemblages that can represent oxidized ferroan granites or, more probably, strongly fractionated magnesian granites. The Pedra Branca suite has also relatively high FeOt/(FeOt+MgO) compared to the other units of the second group and can be classified as a ferroan series (Frost et al., 2001). The Rio Verde trondhjemite and the Bacaba tonalitic complex show the lowest FeOt/(FeOt+MgO) and are magnesian granitoids.

The samples of the granite group were also plotted in the $100*(MgO+FeO+TiO_2)/SiO_2$ vs. $(Al_2O_3+CaO)/(FeO+K_2O+Na_2O)$ diagram of Sylvester (1989). The Planalto suite granites plot into the alkaline field, whereas the Canaã dos Carajás, Serra Dourada and Bom Jesus granites plot in the calc-alkaline and strongly peraluminous field and straddles the strongly fractionated field (Fig. 4f). The Cruzadão granite samples plot mostly in the strongly fractionated field and show a more accentuated alkaline character than the other Mesoarchean granites. The mentioned diagram is not able to distinguish calc-alkaline from strongly peraluminous evolved granites. However, the studied granites do not show strongly peraluminous character (Fig. 4d) and their Sr and Ba contents are more compatible with those found in calc-alkaline better than strongly peraluminous Archean granites (Sylvester, 1994).

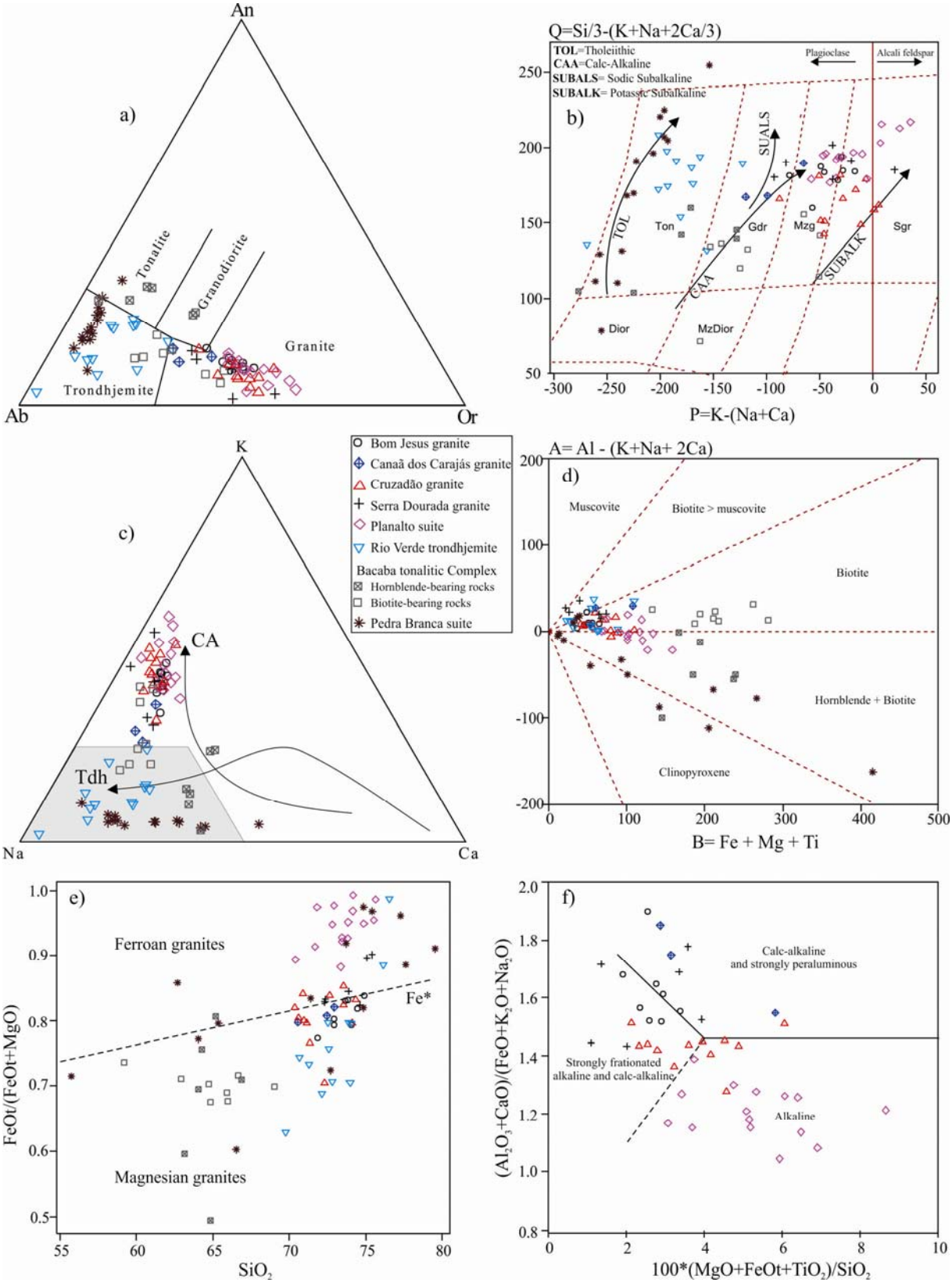

Figure 4 – Geochemical diagrams showing the distribution of the granitoids of the Canaã area. (a) Normative feldspar triangle (O'Connor, 1965) with fields from Barker (1979); (b)) P-Q diagram (Debon and Le Fort, 1988); (c) K–Na–Ca plot with trends for calc-alkaline (CA) and trondhjemite (Tdh) series (Barker and Arth, 1976) and gray field of Archean TTG (Martin, 1994); (d) B-A diagram (Debon and Le Fort, 1988); (e) SiO2 vs. FeO/(FeO+MgO) plot (ferroan and magnesian granites fields of Frost et al., 2001); (f) Major element discrimination diagram for leucogranites (Sylvester, 1989).

4.3. Specific geochemical aspects

4.3.1. Granitic units

Some additional trace element diagrams are presented for a better distinction of the granite units (Fig. 5). In the Zr vs. Rb/Sr plot (Fig. 5a), the Zr-enriched character of the Planalto suite is remarkable, whereas the Mesoarchean granite units are distinguished for their variable Rb/Sr ratios or, in the case, of the Bom Jesus and Canaã dos Carajás granites, also for their contrast in Zr contents. In the La/Yb vs. Sr/Y plot (Fig. 5b), the Planalto and Bom Jesus granites are distinguished by their, respectively, lowest and highest La/Yb and Sr/Y ratios compared to the other units. These show similar Sr/Y but distinct La/Yb which increases from the Canaã dos Carajás to the Serra Dourada and attains maximum values in the Cruzadão granite. In the La/Yb vs. Eu/Eu* diagram (Fig. 5c), it can be seen that the Canaã dos Carajás and Bom Jesus granites have relatively higher Eu/Eu* values when compared to the other granite units. This reflects the discrete or absent Eu anomalies observed in the former granites and the moderate to accentuated negative Eu anomalies shown by the Planalto, Serra Dourada and Cruzadão granites (Fig. 5d). Besides the contrast in the Eu anomalies, the studied granites differ also by their distinct $(La/Yb)_N$ ratios and total REE contents (Figs. 5b,c,d; Table 1).

4.3.2. Tonalitic-trondhjemitic units

The AFM diagram (Fig. 6a; fields of Irvine and Baragar, 1971) shows that the Pedra Branca suite rocks plot in the border between the tholeiitic and calc-alkaline fields, whereas the Rio Verde trondhjemite and the Bacaba tonalitic complex define trends that are compatible with calc-alkaline series. In the K_2O-SiO_2 diagram (Fig. 6b; fields of Pecerillo and Taylor, 1976), the Pedra Branca suite plot in the low-K_2O calc-alkaline series field, the Rio Verde trondhjemite in the low- to medium-K_2O calc-alkaline series and the Bacaba tonalite complex rocks show a strong variation of K_2O for not very distinct SiO_2 contents (dioritic to monzogranitic samples), with the amphibole-bearing varieties being impoverished in K_2O compared to those with biotite as the main mafic mineral. The TiO_2 vs. SiO_2 and Rb vs. Zr diagrams (Figs. 6c, d) also allow a clear distinction between the three units. The Pedra Branca suite differs of the others units by its higher TiO_2 and Zr and lower Rb contents (cf. Gomes and Dall'Agnol, 2007). The Rio Verde trondhjemite and the Bacaba complex show a clear contrast in SiO_2 and the Rb contents of the latter tend to be higher.

The REE patterns (Fig. 7a) of the three units are also clearly distinct due to the contrast in the degree of fractionation of heavy REE (HREE). Eu anomalies are absent or discrete (positive

or negative) in all three units. The geochemical differences between the three units are also evident in the La/Yb vs. Sr/Y (Fig. 7b). These ratios tend to increase from the Pedra Branca suite to the Bacaba complex and attain the highest values in the Rio Verde trondhjemite.

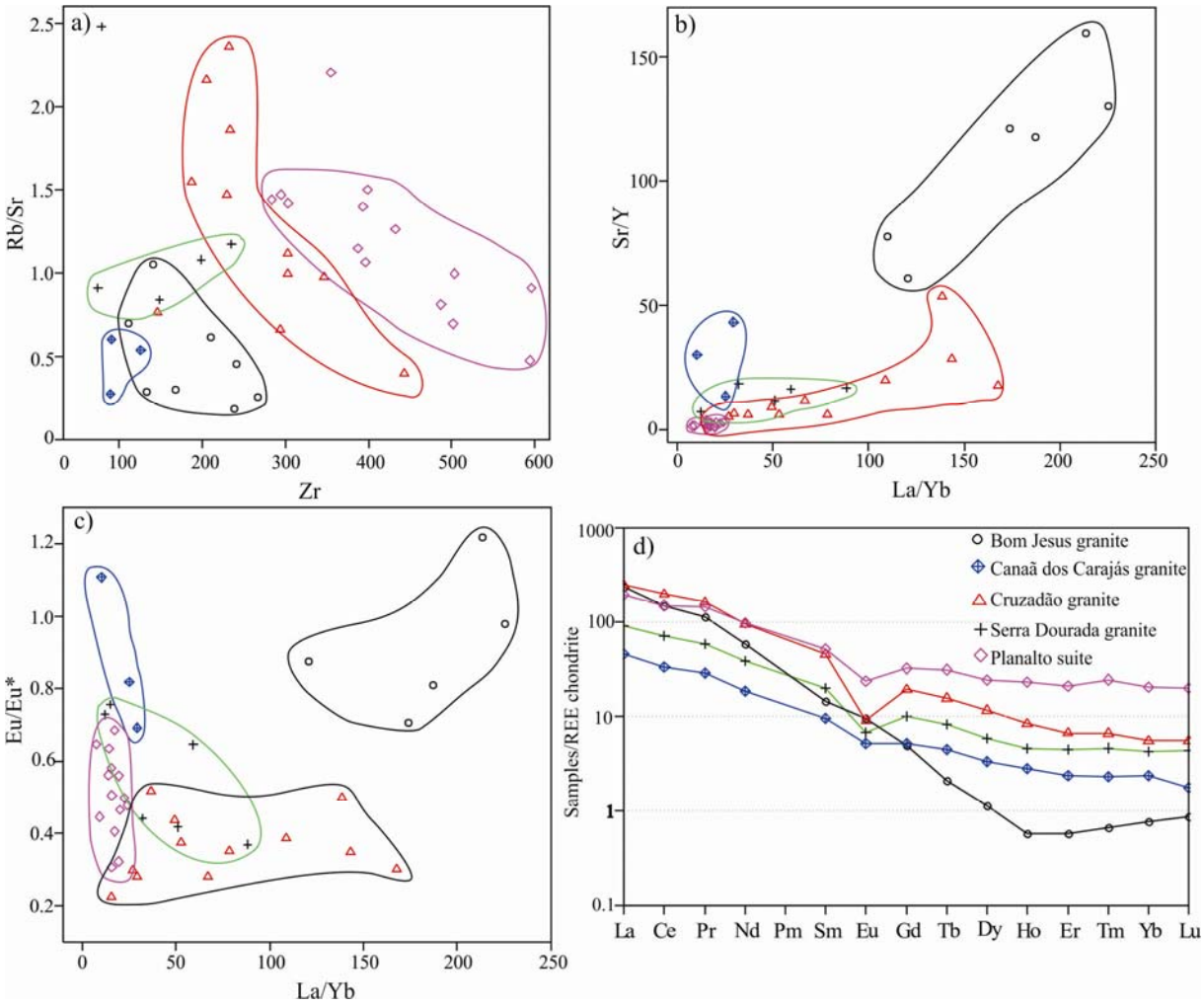

Figure 5 - Geochemical diagrams of the Archean granites of the Canaã area: (a) Zr vs. Rb/Sr plot; (b) La/Yb vs. Sr/Y; (c) La/Yb vs. Eu/Eu*; (d) REE patterns of representative selected samples of the different granite units.

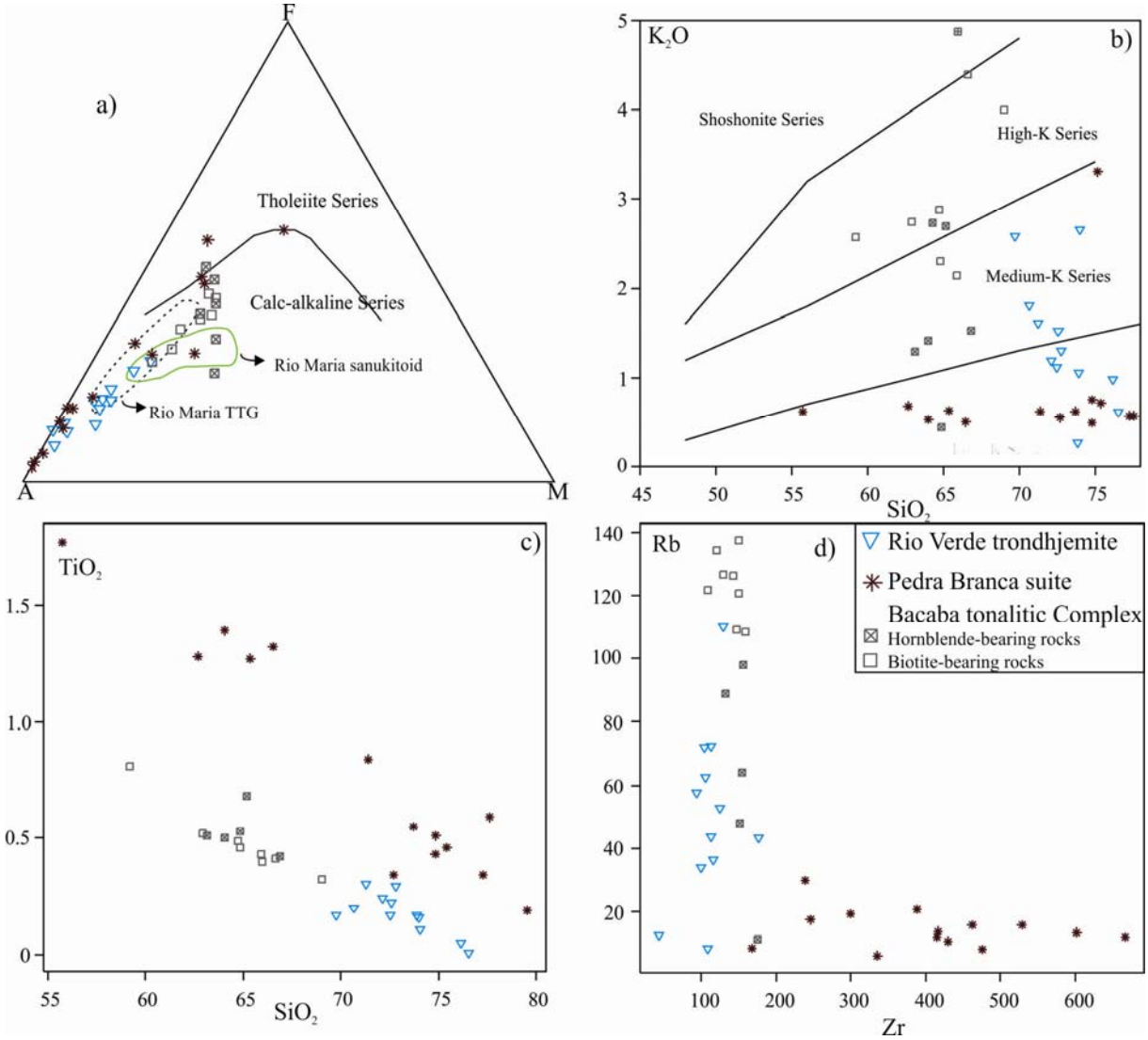

Figure 6 – Geochemical diagrams of the tonalitic-trondhjemitic units of the Canaã area: (a) AFM diagram (fields of tholeiites and calc-alkaline series of Irvine and Baragar, 1971); (b) K_2O vs. SiO_2 diagram (fields of Peccerillo and Taylor, 1976); (c) SiO_2 vs. TiO_2 diagram; (d) Zr vs. Rb diagram.

4.4. Preliminary geochemical conclusions

The dominantly tonalitic-trondhjemitic units show clear geochemical contrasts that point for their independent origin. The Pedra Branca suite, despite its dominant lithologies, is enriched in TiO_2, Zr, and Y, has no geochemical affinities with the Archean TTG series and should have been originated by different processes or derived from distinct sources than TTGs (Gomes and Dall'Agnol, 2007). The Bacaba tonalitic complex differs also from the classical Archean TTG series because it defines an expanded magmatic series that has affinity with calc-alkaline series (Fig. 6a). Besides, its amphibole- and biotite-dominated varieties tend to follow two distinct near vertical trends in the K-Na-Ca plot (Fig. 4c) and are not concentrated exclusively in the field of classical Archean TTGs (Martin, 1994). Only the Rio Verde

trondhjemite has geochemical affinities with the latter, including those of the Rio Maria terrane (Fig. 6a).

The Planalto suite granites are easily distinguished in function of its ferroan and more accentuated alkaline character from all other granite units (Fig. 4f; cf. also Feio et al., submitted). The remainder granites, despite their highly evolved nature, show also significant geochemical contrasts. The Canaã dos Carajás, Serra Dourada and Bom Jesus granites have affinity with evolved Archean calc-alkaline granites (Sylvester, 1994), whereas the Cruzadão granite is apparently transitional between calc-alkaline and alkaline (Fig. 4f). The five granite units have also distinct geochemical signatures pointing to distinct origins for them.

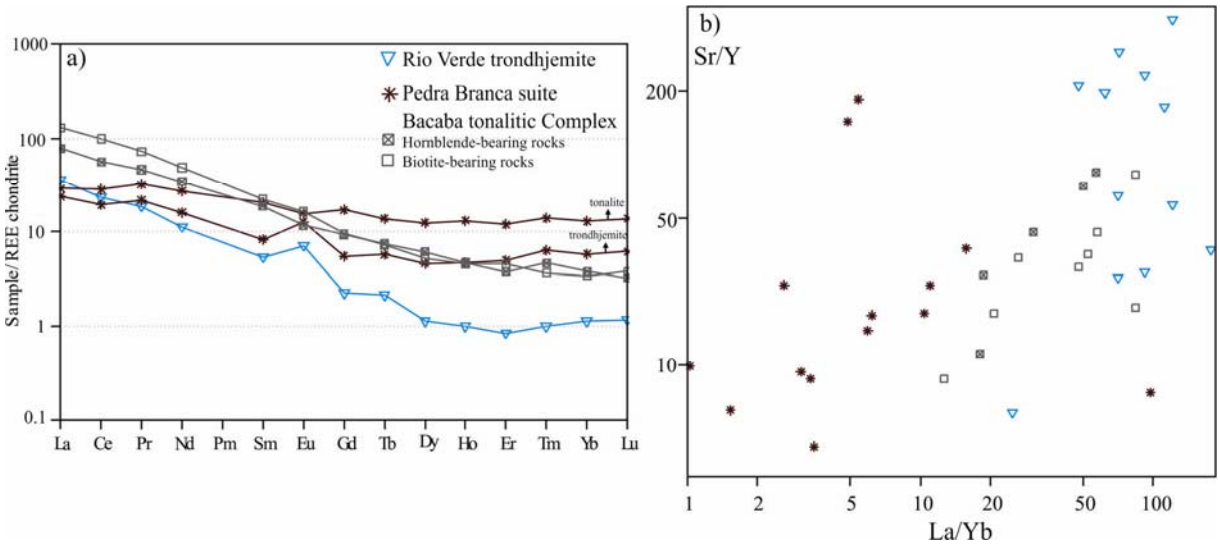

Figure 7 - Geochemical diagrams of the tonalitic-trondhjemitic units of the Canaã area: (a) Chondrite normalised REE patterns (Nakamura, 1974); (b) La/Yb vs. Sr/Y diagram.

Table 1 - Representative chemical compositions of the granitoids of the Canaã dos Carajás area.

Sample	AER-79A	AER-11A	AMR-213	AMR-102	ERF-123	AE-47	ARC-65A	AER-7C	ARC-100	ERF-102	AER-59	AER-27	ARC-109	AMR-187B	AMR-121D	AMR-191A
Petrology	BTr	BTr	BGrd	BLMzG	BMzG	BLSG	BHTon	BMzG	BLSG	BLSG	BLMzG	LMzG	HBSG	HSG	CpxHTon	Tr
Unidade	Rio Verde Trondhjemite		Canaã dos Carajás granite		Bom Jesus gneiss granite		Bacaba tonalitic complex		Cruzadao granite		Serra Dourada granite		Planalto suite*		Pedra Branca suite	
SiO_2	72,10	73,87	70,56	72,44	71,83	74,43	63,14	69,03	70,90	74,10	72,35	74,61	71,66	72,91	64,03	77,26
TiO2	0,24	0,17	0,31	0,16	0,18	0,15	0,51	0,32	0,22	0,15	0,27	0,08	0,44	0,31	1,39	0,34
Al_2O_3	14,80	15,22	14,74	14,84	14,47	13,79	16,23	14,31	14,25	13,35	14,42	13,50	12,77	11,67	14,29	13,25
FeO_t	1,52	0,75	3,03	1,55	1,39	1,03	4,00	3,34	2,55	1,13	1,93	1,17	3,79	4,32	5,33	0,25
Fe_2O_{3t}	1,69	0,83	3,37	1,72	1,55	1,15	4,44	3,71	2,83	1,26	2,15	1,30	4,21	4,80	5,92	0,28
MnO	0,02	0,01	0,01	0,04	0,01	0,01	0,03	0,02	0,03	0,02	0,01	0,01	0,03	0,05	0,07	<0,01
MgO	0,69	0,19	0,77	0,37	0,41	0,23	2,71	1,44	0,48	0,29	0,39	0,25	0,36	0,10	1,58	0,01
CaO	2,71	0,51	1,50	2,02	1,59	1,56	5,11	1,15	0,76	1,03	1,94	0,26	1,71	1,67	6,22	2,39
Na_2O	5,21	8,13	4,29	4,54	3,83	3,53	4,92	3,99	3,62	3,54	3,95	3,64	3,25	2,99	4,92	5,19
K_2O	1,19	0,27	3,17	3,02	4,51	4,56	1,29	4,00	5,60	4,83	3,32	4,80	4,49	4,44	0,53	0,57
P_2O_5	0,07	0,01	0,08	0,05	0,07	0,06	0,21	0,11	0,12	0,05	0,12	0,04	0,09	0,04	0,40	<0.01
LOI	1,20	0,70	1,0	0,7	1,30	0,40	1,20	1,40	0,80	1,30	1,00	1,40	0,70	0,70	0,50	0,60
Total	98,6	99,1	98,5	99,0	98,3	99,4	98,1	97,7	98,5	98,5	98,7	98,4	98,6	98,5	98,8	99,3
Ba	407,2	95,0	961,0	684,0	1658,1	915,0	510,0	889,0	1531,0	519,5	610,1	911,2	1627,0	1459,0	193,0	102,0
Rb	57,5	8,4	108,7	77,6	140,1	135,2	48,1	121,7	227,5	152,8	172,3	149,4	117,3	102,3	6,2	10,8
Sr	763,6	109,9	202,3	282,4	462,5	194,0	704,5	205,8	343,0	200,0	205,2	60,3	144,8	102,9	299,0	193,0
Zr	94,4	108,4	125,6	89,4	167,4	110,6	151,0	107,9	293,2	146,3	148,6	78,2	487,1	503,6	335,8	429,7
Nb	4,0	2,9	6,9	4,9	5,8	3,2	5,6	5,1	3,7	8,6	15,9	25,3	20,9	21,4	25,0	8,2
Y	2,5	3,1	14,8	6,5	2,9	2,5	9,9	6,1	6,4	16,9	11,1	14,2	47,9	66,4	34,6	11,1
Th	5,9	7,8	9,9	5,3	62,6	2,6	6,4	17,7	67,0	63,4	16,8	25,4	23,8	23,4	15,1	8,8
U	0,5	1,4	2,0	0,7	6,7	1,2	2,6	4,2	3,1	18,1	14,4	14,0	3,6	3,4	2,5	2,7
Ga	18,9	17,1	15,7	18,9	17,9	17,3	20,2	20,1	18,2	16,2	22,3	18,5	18,1	19,5	24,1	11,8
Cu	4,6	36,0	28,4	0,8	2,5	7,0	60,0	18,5	165,5	4,8	135,3	66,5	19,4	9,6	1,9	5,1
Pb	2,9	1,1	3,5	2,8	11,0	2,9	5,9	8,8	18,7	14,1	13,4	3,3	5,7	6,6	2,7	3,0
La	19,30	44,30	32,0	15,3	51,30	23,10	43,20	27,40	125,90	81,70	30,20	24,30	64,40	130,00	9,60	7,90
Ce	37,40	44,00	58,8	29,0	87,80	36,90	78,00	52,20	238,90	172,50	62,10	46,70	130,40	249,70	24,50	16,80
Pr	3,54	5,92	6,55	3,23	7,51	3,71	8,92	4,63	26,23	18,35	6,63	4,85	16,31	26,51	3,61	2,45
Nd	11,50	17,50	23,7	11,8	20,90	12,00	31,60	16,90	81,00	59,80	24,20	17,80	62,50	99,60	17,30	10,10
Sm	1,60	1,55	3,69	1,97	2,00	1,35	4,63	2,60	10,85	9,30	4,10	3,30	10,62	15,73	4,14	1,69
Eu	0,53	0,70	0,91	0,40	0,62	0,69	1,21	0,69	1,40	0,71	0,52	0,75	1,84	2,67	1,21	0,98
Gd	0,75	1,10	2,93	1,45	0,92	0,85	3,14	1,29	5,26	5,38	2,81	2,59	8,93	12,67	4,72	1,53
Tb	0,08	0,12	0,43	0,21	0,10	0,10	0,40	0,16	0,62	0,74	0,39	0,42	1,48	2,08	0,65	0,27
Dy	0,47	0,52	2,35	1,15	0,46	0,41	1,88	1,15	2,35	4,02	2,01	2,02	8,36	11,31	4,26	1,59
Ho	0,08	0,09	0,46	0,20	0,07	0,08	0,32	0,19	0,29	0,59	0,32	0,45	1,64	2,24	0,92	0,33
Er	0,21	0,26	1,36	0,54	0,25	0,19	0,90	0,55	0,70	1,51	1,01	1,42	4,73	6,75	2,69	1,12
Tm	0,05	0,04	0,19	0,07	0,05	0,03	0,13	0,08	0,13	0,20	0,14	0,22	0,74	1,02	0,42	0,19
Yb	0,27	0,25	1,27	0,52	0,24	0,21	0,86	0,52	0,91	1,22	0,94	1,61	4,56	6,62	2,84	1,28
Lu	0,05	0,04	0,20	0,06	0,04	0,03	0,12	0,10	0,13	0,19	0,15	0,24	0,68	0,99	0,47	0,21
K_2O/Na_2O	0,23	0,03	0,74	0,67	1,18	1,29	0,26	1,00	1,55	1,36	0,84	1,32	1,38	1,48	0,11	0,11
Rb/Sr	0,08	0,08	0,54	0,27	0,30	0,70	0,07	0,59	0,66	0,76	0,84	2,48	0,81	0,99	0,02	0,06
Sr/Y	305,4	35,5	13,7	43,4	159,5	77,6	71,2	33,7	53,6	11,8	18,5	4,2	3,0	1,5	8,6	17,4
La/Yb	71,5	177,2	25,2	29,4	213,8	110,0	50,2	52,7	138,4	67,0	32,1	15,1	14,1	19,6	3,4	6,2
*Mg	0,45	0,31	0,31	0,30	0,34	0,28	0,55	0,43	0,25	0,31	0,26	0,28	0,14	0,04	0,35	0,07
FeOt/(FeOt+MgO)	0,69	0,80	0,80	0,81	0,77	0,82	0,60	0,70	0,84	0,80	0,83	0,82	0,91	0,98	0,77	0,96
(La/Yb)N	51,3	127,1	18,1	21,1	153,3	78,9	36,0	37,8	99,2	48,0	23,0	10,8	10,1	14,1	2,4	4,4
Eu/Eu*	1,30	1,56	0,82	0,69	1,22	1,84	0,92	1,02	0,50	0,28	0,44	0,76	0,56	0,56	0,83	1,83
A/CNK	1,00	1,04	1,12	1,03	1,03	1,02	0,86	1,10	1,06	1,03	1,06	1,16	0,96	0,91	0,72	0,98

BTr - Biotite trondhjemite; BHTon - Biotite-hornblende tonalite; CpxHTon - Clinopyroxene-hornblende tonalite; Tr- Trondhjemite; BLMzG - Biotite leucomonzogranite;
BLSG - Biotite leucosyenogranite; BMzG - Biotite monzogranite; LMzG - Leucomonzogranite; HBSG - Hornblende-biotite syenogranite; HSG - Hornblende syenogranite.
*Feio et al. (submitted)

5. Pb-evaporation and U–Pb LA-MC-ICPMS on zircon geochronology

5.1. Previous geochronological data and new dated samples

The available geochronological data on the Archean granitoids of the Carajás domain, including the 'Transition' sub-domain and the Canaã dos Carajás area, and the new ages obtained in this work are presented on Table 2 together with the methods employed for dating. The Pium complex yielded ages of 3002 ± 14 Ma and 2859 ± 9 Ma, interpreted, respectively, as the age of the protolith formation and that of its metamorphism (Pidgeon et al., 2000). Hydrotermally altered tonalites of the Bacaba complex and the Serra Dourada granite gave, respectively, ages of ca. 3.0 Ga and 2860 ± 22 Ma (Moreto et al., 2011). Additional ages were given for the Canaã dos Carajás granite (2928 ± 1 Ma) and Pedra Branca suite (2749 ± 6 Ma, 2765 ± 39 Ma) by Sardinha et al. (2004). The Planalto suite and associated charnockitic rocks were studied recently in more detail and gave ages of ca. 2.73 Ga (Feio et al., submitted).

In order to get complementary geochronological data on the main granitoid units of the Canaã area, we have studied by new methods or collected additional representative samples of the Bom Jesus granite (GRD-47), Canaã dos Carajás granite (AMR-102), Rio Verde trondhjemite (AER-11A and GRD-79C), Bacaba tonalitic complex (ARC-65A, ERF-07C, and ARC-95A), Cruzadão granite (ARC-100 and GRD-58), Serra Dourada granite (GRD-59), Pedra Branca suite (AMR-191A), and Planalto suite (ARC-109 and AMR-187B). The geochronological methods are described in Appendix B and the isotope data are presented in supplementary tables (Tables A, B, C).

5.2. Canaã dos Carajás granite

In the biotite leucomonzogranite (AMR-102 sample) of the Canaã dos Carajás granite the largely dominant population of zircon is composed of intensely fractured, translucent to transparent prismatic crystals with slightly rounded edges and brown color. Subordinate crystals have short prismatic or rounded shape and brown color. Under cathodoluminescence (CL), the crystals show marked magmatic zoning. This sample was dated for the Pb-evaporation method (Sardinha et al., 2004) and additional LA-MC-ICPMS dating was performed in the same sample. 21 zircon grains were analyzed and, when possible, analyses of core and border zones were performed in the same grain. The obtained results are shown in Table A and Figure 8a. Most analyses show high discordance degree or high error, and therefore were eliminate of the age calculation. Seven analyses obtained in five grains

resulted in a discordance age with superior intercept of 2952 ± 24 (MSWD = 2.3). Reducing the discordance to a maximum of 3%, the remainder five analyses in four distinct zircon grains plot in the concordia curve and yielded an age of 2959 ± 6 Ma (MSWD = 1.5). This age is a little older than the Pb-evaporation age and is interpreted as the crystallization age of the Canaã dos Carajás granite. An inherited zircon gave a concordia age of 3030 ± 15 Ma (MSWD = 1.3). Another zircon yielded a concordia age of 2864 ± 12 Ma (MSWD = 1.2), probably due to an opening of the U-Pb system. The presence of an older inherited zircon in the dated rock indicates a probable crustal source for the magma of this granite. The younger age of ca. 2.86 could be related to reworking of the granite during the important magmatic and tectonic events identified in the Canaã area at that time (cf. Table 2).

5.3. Rio Verde trondhjemite

Two samples of biotite trondhjemite (AER-11A) and biotite granodiorite (GRD-79C) were both dated by the Pb-evaporation on zircon and U–Pb LA-MC-ICPMS methods.

AER-11A and GRD-79C display similar pinkish elongated prismatic zircon crystals (Fig. 9a, b), with euhedral to subhedral shape and, in some cases, rounded terminations. Under cathodoluminescence, these crystals show well developed oscillatory zoning and low luminescence (Fig. 8b, c), but some grains also have U-enriched, bright zones, preferentially located at the cores, that, in some crystals, are strongly metamict.

Twelve zircon grains of AER-11A were analyzed by Pb-evaporation and three grains (Fig. 9a; Table B) yielded an age of 2929 ± 3 Ma (MSWD = 3.0). Forty-two analyses on twenty-six zircons were performed by the U–Pb LA-MC-ICPMS method. Most analyzes were strongly discordant and were discarded of the age calculation. Reducing the degree of discordance to a maximum of 3%, seven spots in different zircon grains (Fig. 8b; Table A) defined a concordia age of 2923 ± 15 (MSWD = 6.8). This age is similar to that obtained by the Pb-evaporation method. Moreover, four spots in the border of distinct zircon crystals with less than 2% of discordance provided a concordia age of 2868 ± 6 Ma (MSWD = 2.3).

Eleven zircon grains of GRD-79 were analyzed by Pb-evaporation and four grains gave an age of 2868 ± 4 Ma (MSWD = 1.13). Forty spot analyses on twenty-five zircon grains were performed by the U–Pb LA-MC-ICPMS method. Almost all analyses are strongly discordant and do not define a clear age. A concordant analyzed zircon yielded an age of 2841 ± 9 Ma (MSWD = 2.4) and the spot analyses aligned with that grain (Fig. 8c) gave an upper intercept age of 2820 ± 22 Ma (MSWD = 4.8). The age obtained by the Pb-evaporation

method is a little older than that indicated by the concordant zircon grain (U–Pb LA-MC-ICPMS method).

The different ages obtained in the two analyzed samples are difficult to interpret. The older age yielded by the AER-11A sample could indicate the existence of older trondhjemitic rocks associated with the dominant Rio Verde trondhjemite that were strongly deformed during the ca. 2.87 Ga event. An alternative would be to admit that the dated zircons of AER-11A were inherited but this hypothesis is not favored because a large number of zircon grains were analyzed and a significant number of spot analyses were employed to define the concordia age of 2923 ± 15 Ma (Fig. 8b). The geochronological data obtained on the sample GRD-79 are also not conclusive about its crystallization age. Apparently the most confident age is the Pb-evaporation age of 2868 ± 4 Ma that is coincident with the younger age given by the AER-11A sample. The 2820 ± 22 Ma upper intercept age of GRD-79 is apparently too younger and probably not representative of the crystallization age of the Rio Verde Trondhjemite. It is concluded that the rocks dominant in the Rio Verde trondhjemite were formed at ca. 2.87-2.85 Ga, a period of intense tectono-magmatic activity in the Canaã area.

5.4. Bacaba tonalitic complex

Two samples of the Bacaba tonalitic complex representative of the biotite tonalite to granodiorite and biotite-hornblende tonalite varieties were selected for dating, a biotite granodiorite (ERF-7C) collected along the road between Vila Planalto and Parauapebas (Fig. 2) and a biotite-hornblende tonalite (ARC-65A) from a quarry located at ca. 1 km to the west of Vila Planalto. A third sample of biotite-hornblende tonalite (ARC-95) associated with the Cruzadão granite, located to the west of the Rio Branco granite (Fig. 2), was also dated.

The zircon crystals of three dated samples are similar and show colorless to pale brown subeuhedral short prismatic crystals with rounded edges (Fig. 9c, d, e) and few inclusions and fractures. CL pictures (Figs. 8d, e) reveal that the crystals show well-developed oscillatory-zone.

The biotite granodiorite (ERF-7C) was dated only by the Pb-evaporation method. Twelve zircon crystals were analyzed and five of them (Fig. 9b; Table B) defined a mean age of 2868 ± 2 Ma (MSWD = 1.3).

The biotite-hornblende tonalite (ARC-65A) was dated by the Pb-evaporation method. Fourteen crystals were analyzed and five were used to calculate a mean age of 2872 ± 1 Ma (MSWD = 1.2; Fig. 9c; Table B). The same sample was also analyzed by the U-Pb LA-MC-ICPMS method on zircon. Eliminating all spots with more than 3% of discordance, the

remainder nine spot analyzes yielded a concordant age of 2850 ± 7 Ma (MSWD = 2.7; Fig. 8c; Table A). That age is a little younger than the Pb-evaporation age. Three analyzed spots in the outer zone of zircon grains yielded an age of 2724 ± 15 Ma (MSWD = 3.0), suggesting an opening of the U-Pb system probably related to an event of Neoarchean age in the Canaã area. One analyzed zircon grain, interpreted as inherited, provided an age of 3002 ± 23 Ma (MSWD = 1.6).

The sample ARC-95 was also dated by the Pb-evaporation and U-Pb LA-MC-ICPMS methods on zircon. Fifteen zircon crystals were analyzed by Pb-evaporation and six of them defined a mean age of 2853 ± 2 Ma (MSWD = 3.1; Fig. 9e; Table B). One analyzed zircon provided an age of 2966 ± 5 Ma and most likely represents an inherited grain. Twenty-three zircon grains were analyzed by the U-Pb LA-MC-ICPMS method. Reducing the degree of discordance to a maximum of ~10%, the twelve remainder spots defined an upper intercept age of 2851 ± 18 Ma (MSWD = 2.9) and eight concordant analyzes (Fig. 8e) gave a concordia age of 2849 ± 18 Ma (MSWD = 0.13). An isolated zircon grain yielded a concordia age of 2647 ± 23 Ma (MSWD = 0.047)

The ages obtained in this work for the different dated samples of the Bacaba tonalitic complex are similar. However the ages provided by the Pb-evaporation method are a little older than those yielded by the U-Pb method (ca. 2.87 Ga vs. ca. 2.85 Ga). On the other hand, the results obtained by Moreto et al. (2011) for, apparently, the same unit are quite different (3001 ± 4 Ma, MSWD = 1.8; 2991 ± 6 Ma, MSWD = 1.9; 3005 ± 9 Ma, MSWD = 2.2). The rocks dated by Moreto et al. (2011) are potassic altered samples of the Bacaba tonalite and two of them have also Cu-Au mineralization and the three ages correspond to upper intercept ages obtained by LA-MC-ICPMS U-Pb on zircon. Despite the fact that these rocks are drill hole hydrothermally altered samples, the resulting ages look confident. Thus, the contrast between the ages obtained in the present work for the Bacaba tonalitic complex and those available in the literature suggests that this unit is not uniform and could encompass distinct tonalitic rocks that have not been individualized in the field so far. The morphological characteristics of the zircon grains analyzed by Moreto et al. (2011; their Fig.11) are apparently distinct of those of the Bacaba tonalite samples dated in the present work and this makes more plausible the mentioned hypothesis.

We consider that most of the rocks exposed in surface in the domain of the Bacaba tonalitic complex (Fig. 2) correspond to the biotite tonalite to granodiorite and biotite-hornblende tonalite varieties studied in the present work. For these rocks, despite their contrast in geochemistry, a crystallization age of ca. 2.85 Ga is assumed. A coeval age was

obtained for the ARC-95 sample associated with the Cruzadão granite which was apparently emplaced and deformed simultaneously with that tonalite.

5.5. Bom Jesus granite

A biotite leucosyenogranite (GRD-47) of the Bom Jesus granite was selected for dating. The dominant zircons of this sample are prismatic, light brownish in color, and show strong zoning that is more marked in the grain cores. Some grains are rounded and do not show clear faces. The outer zones are commonly darker in CL images and some crystals are not zoned and show a more uniform darker aspect. Partial metacmitization and fractures are observed in many grains.

Dating of this sample by the U-Pb LA-MC-ICPMS method was performed and the obtained results (Table A) show that most analyzed spots were strongly discordant. Discarding grains with more than 5% of discordance the remainder grains are still extremely dispersed in the age diagram and did not define a unique age for this granite. Several analyzed spots are disposed near the concordia curve but they are dispersed and isolated grains define extremely variable ages: 3005 ± 15 Ma (MSWD = 0.15), 2963 ± 13 Ma (MSWD = 1.8), 2914 ± 14 Ma (MSWD = 1.5), 2847 ± 13 Ma (MSWD = 1.6), 2699 ± 11 Ma (MSWD = 0.71), 2588 ± 15 Ma (MSWD = 1.3).

Owing to the complexity of the results obtained by the U-Pb LA-MC-ICPMS method, it was decided to date this sample also by U-Pb SHRIMP techniques. Ten analyzed zircon grains provided an upper intercept discordia age of 2833 ± 6 Ma (MSWD = 1.8; 1σ) with two grains yielding ages of 3017 ± 5 Ma and 3074 ± 6 Ma (Fig. 10a). The lower intercept defined an age of 525 ± 44 Ma possibly related to uplift of the Canaã area during the Brasiliano cycle.

The whole results are not entirely conclusive. They suggest that 2833 ± 6 Ma could correspond to the age of crystallization of the Bom Jesus granite, but this is not entirely consistent with the field relationships between the Bom Jesus granite and the Rio Verde trondhjemite that suggest coeval ages for both units (see above). It is evident that the Bom Jesus granite evolution was complex as indicated by the presence of zircon of different ages on it. On the other hand, the stronger deformation of this unit compared to the other Archean units could also be seen as evidence of an older age for it, but this is obviously not conclusive. A sedimentary source for the Bom Jesus granite would be able to explain the diversity of zircon ages but the geochemical characteristics of this rock are not consistent with such origin (cf. geochemistry section). It is concluded that additional field, geochemical and geochronological data are necessary to solve this puzzle. By the moment, the 2833 ± 6 Ma

age can be seen as a minimum crystallization age for the Bom Jesus granite. It is probable that the age of this granite approaches those of the Cruzadão granite (see below) and Rio Verde trondhjemite.

5.6. Cruzadão granite

Two samples of the Cruzadão granite were selected for dating by the U-Pb LA-MC-ICPMS method. The sample ARC-100 (biotite leucosyenogranite) is located in the western and GRD-58 (biotite syenogranite) in the central-southern occurrence of that granitic unit.

The zircon grains of the analyzed samples are prismatic, light pinkish in color, and zoned. In the sample ARC-100, the dominant zircon grains have smaller size between 125-75 mm than GRD-58 (size: 180-125 mm). The outer zones are commonly darker in CL images and some crystals are not zoned and show a more uniform darker aspect. Partial metacmitization and fractures are observed in many grains.

The 21 analyzed zircon grains of ARC-100 show with a few exceptions a high degree of discordance. Reducing the discordance to a maximum of 50%, the thirteen remainder zircon grains (Fig. 8f) define an upper intercept discordia age of 2879 ± 37 Ma (MSWD = 5.8) and one isolated grain yielded a 2875 ± 12 Ma (MSWD = 1.16) concordia age. Three grains gave an older concordia age of 3056 ± 9 Ma (MSWD = 1.6). In the sample GRD-58, twenty-five zircon grains were analyzed. Eliminating the more strongly discordant grains, 16 remainder spot analyzes (Fig. 8g) did not define an upper intercept age. However, the six zircon analyzes with less than 5% of discordance gave a concordia of 2857 ± 8 Ma (MSWD = 13). These same six grains yielded a mean weighted average $^{207}Pb/^{206}Pb$ age of 2845 ± 15 Ma (MSWD = 2.1). Other four zircon grains with low-discordance yielded a concordia age of 2751 ± 56 Ma (MSWD = 3.8).

Apparently the ages of ca. 2.85 Ga obtained for GRD-58 are more confident and could be assumed as representative of the crystallization age of the Cruzadão granite. The concordia age of 3056 ± 9 Ma is probably due to the presence of inherited zircon grains and that of 2751 ± 56 Ma suggest opening of the isotope system during the Neoarchean.

5.7. Serra Dourada granite

A biotite leucomonzogranite (GRD-59) of the central area of the Serra Dourada pluton (Fig. 2) was sampled for dating. The dominant zircon crystals are fractured, euhedral to subhedral, pinkish, elongated prismatic grains which could be slightly rounded; the

subordinate grains are short prismatic and rounded. CL pictures (Fig. 8h) reveal that most crystals have well-developed oscillatory-zoning.

The U-Pb LA-MC-ICPMS method was employed to date this unit. Fifty-five analyses performed on thirty-one zircon grains yielded in general strongly discordant analytical points (Table A). Reducing the discordance to a maximum of 3%, the remainder eight zircon grains (Fig. 8e) provided a concordia age of 2831 ± 6 Ma (MSWD = 1.3).

This age is significantly younger than the upper intercept age of 2860 ± 22 Ma (MSWD = 11.5) obtained for the same granite unit (Moreto et al., 2011). The fact that the age presented in this work is a concordia age with a relatively low MSWD makes it more confident and it is interpreted as the crystallization age of the Serra Dourada granite.

5.8. Pedra Branca suite

The previous geochronological study performed in the Pedra Branca Suite (Sardinha et al., 2004) did not define a precise age for that unit. Looking for a better definition of its age, the LA-MC-ICPMS method was employed for a detailed isotope study of the sample AMR-191 (trondhjemite).

The dominant zircon crystals of that sample are elongated, prismatic, euhedral or slightly rounded. There is also a subordinate population of crystals that have short prismatic or rounded shape. All of them have light brown color, are translucent to transparent, intensely fractured and sometimes show metamictic cores. Under cathodoluminescence, the crystals show a gray core surrounded by lighter and thicker outer zones with well developed oscillatory zoning (Fig. 8i). Many crystals exhibit also thin dark irregular rims and in some cases convolute zoning. The second population of zircon crystals shows lighter irregular weakly zoned cores surrounded by thinner dark rims.

Twenty-nine zircon grains were analyzed by LA-MC-ICPMS and, when possible, analyses of core and border zones were performed in the same grain. The obtained results are shown in Table A and Figure 8i. The zircon analyses show a diversified distribution in the concordia diagram and a significant number of analyzed spots is discordant (Fig. 8i). In a preliminary approach, the analyses with more than 10% of discordance were discarded and the remainder data yielded an upper intercept age of 2762 ± 13 Ma (MSWD = 1.0; Fig. 8i). Reducing the discordance to a maximum of 2.5%, 6 zircon analyses, performed in core and border zones and in bright and darker zones of the crystals, gave a concordia age of 2750 ± 5 Ma (MSWD = 3.9; Fig. 8i). Three zircon grains similar in aspect to those of the dominant population yielded an upper intercept age of 2954 ± 52 Ma (MSWD= 0.11) and where

interpreted as inherited zircons. Finally, two zircons grains defined a younger concordia age of 2701 ± 6 Ma (MSWD = 0.9).

The geochronological data available in the literature added to those presented in this work reveal that the Pedra Branca sodic granitoids had a complex geologic evolution. This is indicated by the presence of inherited and rejuvenated zircon grains and abundant fractures in the zircon crystals. The ages of the inherited zircons are coincident within errors with important events of the Canaã area crustal evolution (2.96 to 2.93 Ga). The concordia age of 2750 ± 5 Ma obtained in the dominant zircon population is interpreted as the crystallization age of the Pedra Branca granitoids. The two zircon crystals younger than the dominant population probably register an opening of the U-Pb system possibly related to the emplacement of the Planalto suite (Feio et al., submitted).

5.9. Planalto suite

The available geochronological data and new dating on this unit were reported by Feio et al. (submitted). Three samples of the Planalto granite yielded extremely similar Pb-evaporation on zircon ages (2733 ± 2 Ma, AMR-187B; 2731 ± 1 Ma, AMR-109; and 2736 ± 4 Ma, GRD-77; Feio et al., submitted). These ages are a little younger that those of the Planalto suite of its type area (2747 ± 2 Ma, Huhn et al., 1999) and of two stocks located in the 'Transition' sub-domain (2754 ± 2 Ma, Silva et al., 2010; 2748 ± 2 Ma and 2749 ± 3 Ma, Souza et al., 2010), all dated by the Pb-evaporation method. The Estrela complex, the Igarapé Gelado and the Serra do Rabo plutons of the Carajás domain, which are geochemically similar to the Planalto suite, yielded, respectively, zircon ages of 2763 ± 7 Ma and 2731 ± 26 Ma (Pb-evaporation; Barros et al., 2009) and of 2743 ± 2 Ma (U-Pb TIMS age; Sardinha et al., 2006).

Additional ages were obtained for three distinct plutons of the Planalto suite by the U-Pb LA-MC-ICPMS method (Feio et al., submitted). It resulted concordia ages of 2729 ± 17 Ma (AMR-187B), 2710 ± 10 Ma (ARC-109), and 2706 ± 5 Ma (GRD-77).

Due to the relevance of the age definition of this suite for the understanding of the crustal evolution of the Canaã area, it was decided to obtain also U-Pb SHRIMP on zircon ages on two samples (AMR-187B and ARC-109) previously dated by Feio et al. (submitted). The analytical procedures are described in Appendix 2 and isotope data are presented in the supplementary Table C. The sample AMR-187B came from a stock to the east of Canaã dos Carajás town and ARC-109 from another stock in the southwestern part of the study area (Fig. 2). Both samples have fractured, translucent to transparent, prismatic slightly rounded zircon crystals with pale brown color. Under cathodoluminescence (Fig. 10b, c) , the zircon crystals

show most commonly irregular dark gray cores surrounded by larger outer zones with well developed oscillatory zoning and local dark rims. Eight analyzed zircon grains of the sample AMR-187B (Fig. 10b) yielded an upper intercept age of 2738 ± 3 Ma (MSWD = 2.5; 2σ). Sixteen analyses were done on zircon grains of sample ARC-109. Discarding the seven more discordant data (Fig. 10c), it resulted an upper intercept age of 2730 ± 5 Ma (MSWD = 1.6; 1σ).

The new ages obtained in the present work for sample AMR-187B are almost coincident within error with those yielded by the Pb-evaporation on zircon and U-Pb LA-MC-ICPMS methods (Feio et al., submitted). The same is true in the case of the Pb-evaporation on zircon and U-Pb SHRIMP on zircon ages of the sample ARC-109. However, the U-Pb LA-MC-ICPMS zircon age obtained for that sample (Feio et al., submitted) is comparatively a little younger. Comparing the different results obtained, it is concluded that the crystallization age of the Planalto suite should have occurred more probably in between 2740 and 2730 Ma.

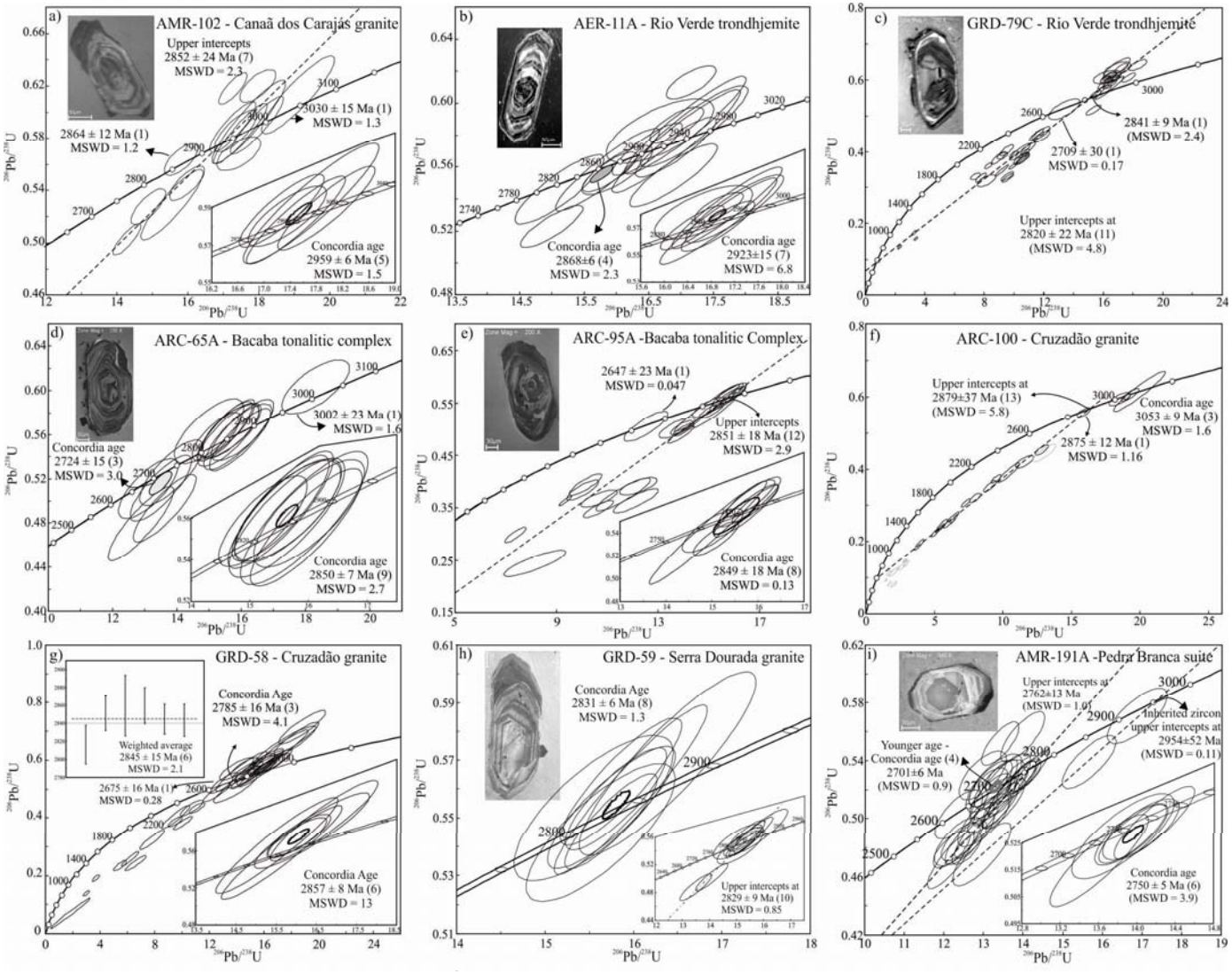

Figure 8 - LA-MC-ICPMS U–Pb concordia diagram for the samples of the Archean granitoids of the Canaã area: (a) Canaã dos Carajás granite (AMR-102); (b) Rio Verde trondhjemite (AER-11A); (c) Rio Verde trondhjemite (GRD-79C); (d) Bacaba tonalitic complex (ARC-65A); (e) Bacaba tonalitic complex (ARC-95A); (f) Cruzadão granite (ARC-100); (g) Cruzadão granite (GRD-58); (h) Serra Dourada granite (GRD-59); (i) Pedra Branca suite (AMR-191A).

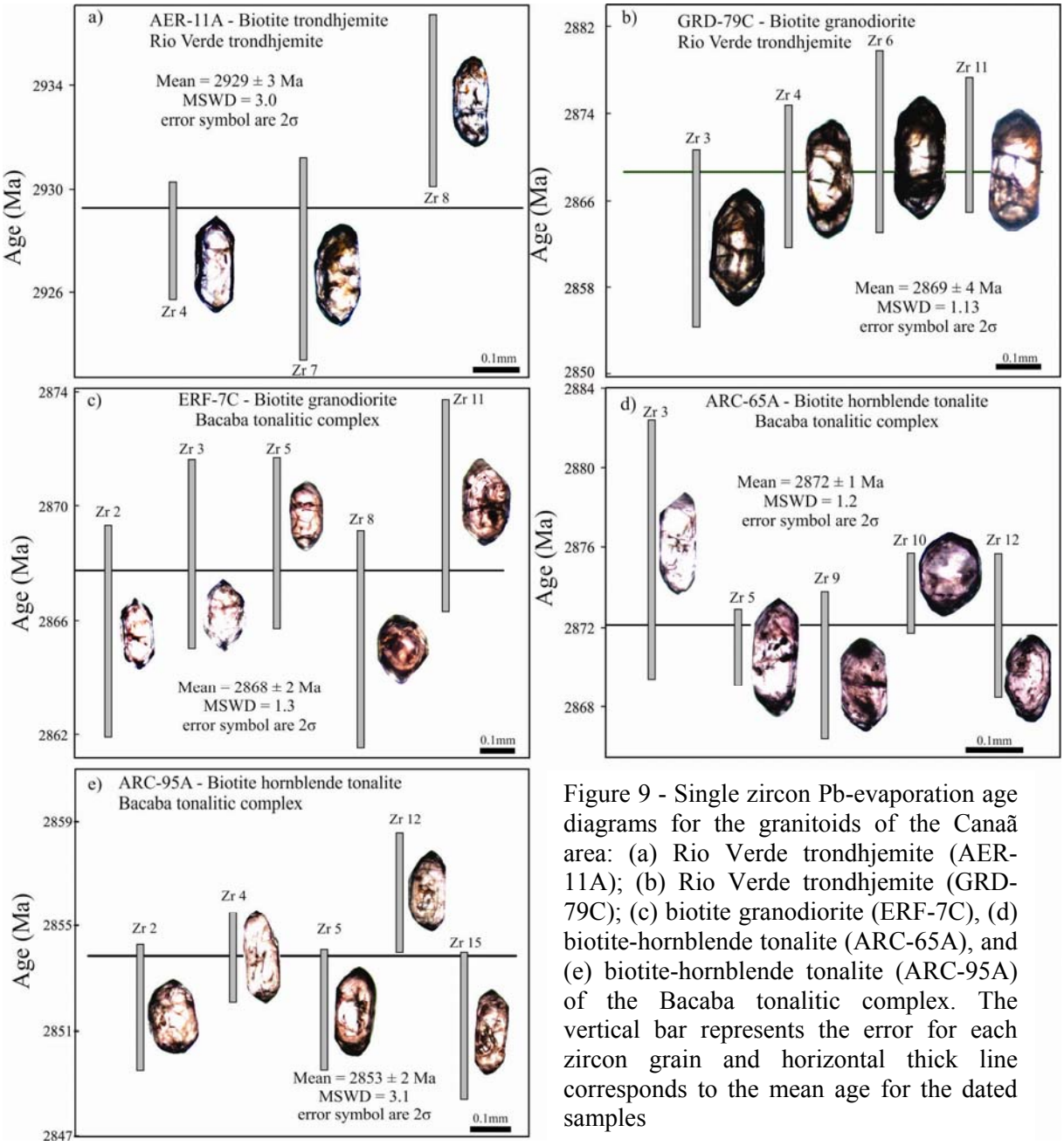

Figure 9 - Single zircon Pb-evaporation age diagrams for the granitoids of the Canaã area: (a) Rio Verde trondhjemite (AER-11A); (b) Rio Verde trondhjemite (GRD-79C); (c) biotite granodiorite (ERF-7C), (d) biotite-hornblende tonalite (ARC-65A), and (e) biotite-hornblende tonalite (ARC-95A) of the Bacaba tonalitic complex. The vertical bar represents the error for each zircon grain and horizontal thick line corresponds to the mean age for the dated samples

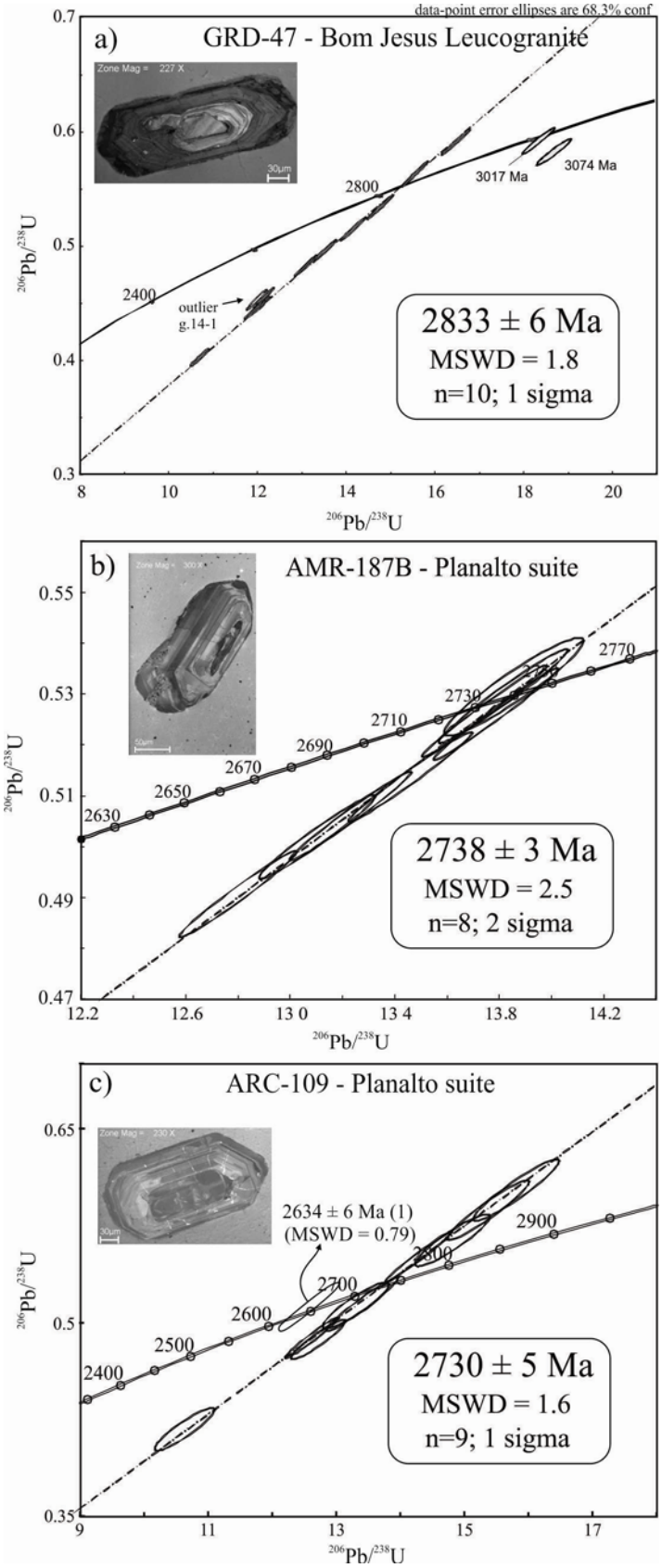

Figure 10 - Concordia plot showing SHRIMP U-Pb zircon data. (a) Bom Jesus granite (GRD-47); (b) Planalto suite (AMR-187B); (c) Planalto suite (ARC-109).

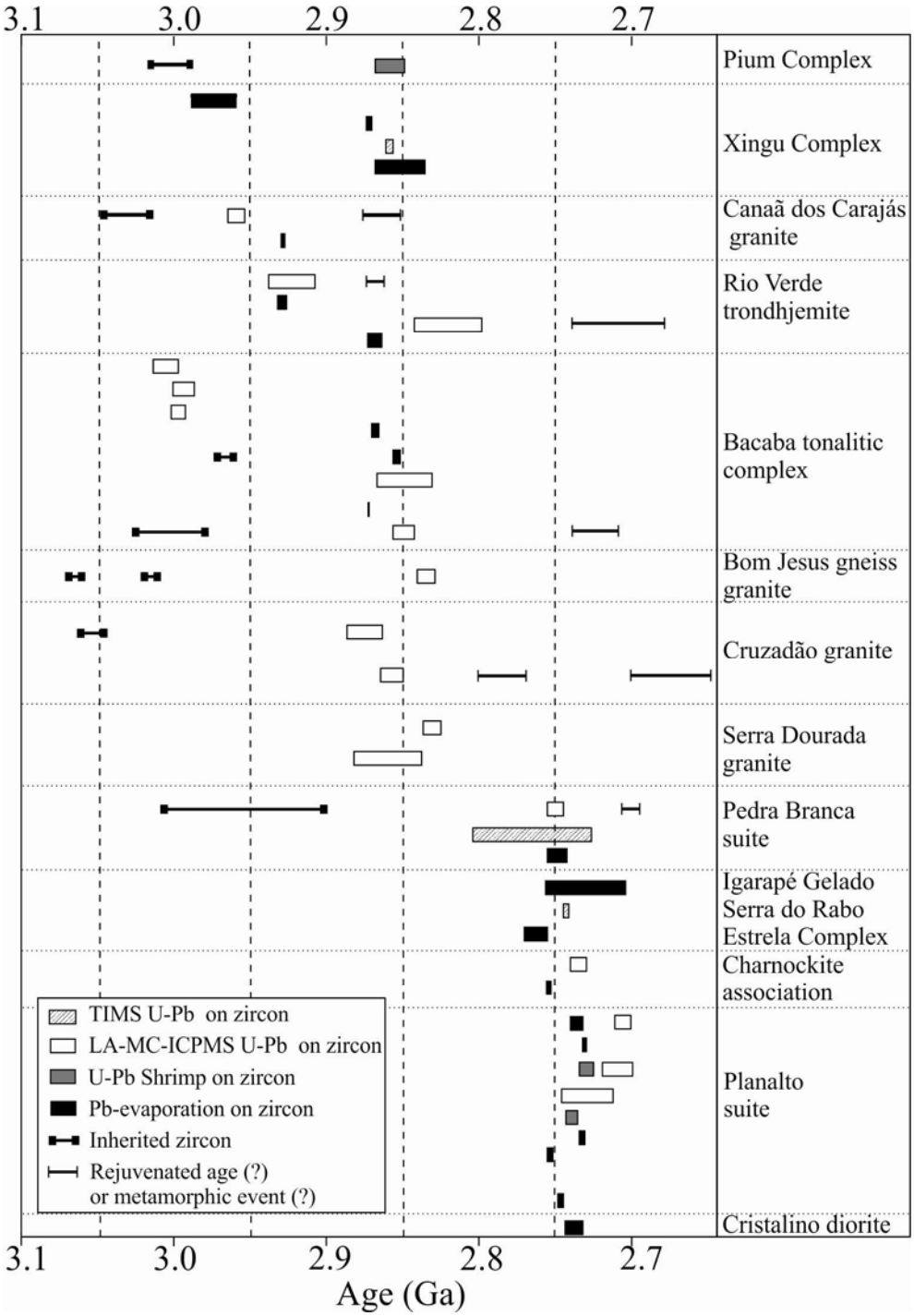

Figure 11 - Summary of geochronological data of the 'Transitional' subdomain available in the literature (data source are given in Table 2), including the new data obtained in this study.

Table 2 - Summary of the available geochronological data of the 'Transitional' subdomain and new data obtained in this work.

Maria granite-greenstone terra	Rock type	Method	Zircon age	Ref.
Cristalino diorite	Diorite	Pb-evaporation	2738±6	1
Planalto suite	Granite	Pb-evaporation	2747±2	1
	Hb-Bt monzogranite	Pb-evaporation	2734±2	2
	Bt-Hb sienogranite	Pb-evaporation	2754±2	2
	Bt-Hb syenogranite (AMR-187B)	Pb-evaporation	2733±2	3
		U-Pb LA-MC-ICPMS	2729±17	3
		U-Pb SHRIMP	2738±3	9
	Hb-Bt syenogranite (ARC-109)	Pb-evaporation	2731±1	3
		U-Pb LA-MC-ICPMS	2710±10	3
		U-Pb SHRIMP	2730±5	9
	Bt syenogranite (GRD-77)	Pb-evaporation	2736±4	3
		U-Pb LA-MC-ICPMS	2706±5	3
Charnockite association	Opx-trondhjemite	Pb-evaporation	2754±1	2
	Qtz-gabbro	U-Pb LA-MC-ICPMS	2735±5	3
Estrela Complex	Granite	Pb-evaporation	2763±7	4
Serra do Rabo pluton	Hb syenogranite	U-Pb TIMS	2743±2	4
Igarapé Gelado pluton	Granite	Pb-evaporation	2731±26	4
Pedra Branca suite	Trondhjemite	Pb-evaporation	2749±6#	5
	Trondhjemite	U-Pb TIMS	2765±39	5
	Trondhjemite (AMR-191A)	U-Pb LA-MC-ICPMS	2750±5	9
		U-Pb LA-MC-ICPMS	2954±52*	9
		U-Pb LA-MC-ICPMS	2701±6**	9
Serra Dourada granite	Granite	U-Pb LA-MC-ICPMS	2860±22	7
	Leucomonzogranite (GRD-59)	U-Pb LA-MC-ICPMS	2831±6	9
Cruzadão granite	Bt syenogranite (GRD-58A)	U-Pb LA-MC-ICPMS	2845±15	9
		U-Pb LA-MC-ICPMS	2857±8	9
		U-Pb LA-MC-ICPMS	2785±16**	9
		U-Pb LA-MC-ICPMS	2675±26**	9
	Bt leucosyenogranite (ARC-100)	U-Pb LA-MC-ICPMS	2875±12	9
		U-Pb LA-MC-ICPMS	3053±8	9
Bom Jesus gneissic granite	Bt leucosyenogranite (GRD-47)	U-Pb SHRIMP	2833±6	9
		U-Pb SHRIMP	3017±5 and 3074±6 Ma*	9
Bacaba tonalitic Complex	Bt-Hb tonalite (ARC-65A)	Pb-evaporation	2872±1	9
		U-Pb LA-MC-ICPMS	2850±7	9
		U-Pb LA-MC-ICPMS	3002±23*	9
		U-Pb LA-MC-ICPMS	2724±15**	9
	Bt-Hb tonalite (ARC-95A)	Pb-evaporation	2854±2	9
		Pb-evaporation	2966±5*	9
		U-Pb LA-MC-ICPMS	2849±18	9
	Bt granodiorite (ERF-07C)	Pb-evaporation	2868±2	9
	Tonalite	U-Pb LA-MC-ICPMS	2997±5	7
	Tonalite	U-Pb LA-MC-ICPMS	2993±7	7
	Tonalite	U-Pb LA-MC-ICPMS	3005±8	7
Rio Verde trondhjemite	Bt granodiorite (GRD-79C)	U-Pb LA-MC-ICPMS	2820±22	9
		U-Pb LA-MC-ICPMS	2709±30**	9
		Pb-evaporation	2869±4	9
	Bt trondhjemite (AER-11A)	Pb-evaporation	2929±3	9
	Bt trondhjemite (AER-11A)	U-Pb LA-MC-ICPMS	2923±15	9
		U-Pb LA-MC-ICPMS	2868±6**	9
Canaã dos Carajás granite	Bt leucomonzogranite (AMR-102)	Pb-evaporation	2928±1	5
	Bt leucomonzogranite (AMR-102)	U-Pb LA-MC-ICPMS	2959±6	9
		U-Pb LA-MC-ICPMS	3030±15*	9
		U-Pb LA-MC-ICPMS	2864±12**	9
Xingu complex	Granodiorite	Pb-evaporation	2852±16	8
	Granitic leucossoma	U-Pb TIMS	2859±2	8
	Bt trondhjemite	Pb-evaporation	2872±2	6
	Gneiss granodiorite	Pb-evaporation	2974±15	8
Pium complex	Protolith of the enderbite	U-Pb SHRIMP	3002±14	10
	Enderbite	U-Pb SHRIMP	2859±9**	10

Data source: 1-Huhn et al. 1999; 2-Oliveira et al. 2010, 3- Feio et al. submitted; 4- Barros et al. 2009; 5- Sardinha et al.
recalculed age for 2 sigma; * inherited zircon; ** openning of the isotopic system or metamorphism
Bt - biotite; Hb - hornblende; opx - orthpyroxene; qtz - quartz

6. Sm-Nd isotopic data

The Nd isotope data and the ages assumed for the different units are presented in Table 3. The Sm and Nd contents are quite variable in the different granitoid units. They are relatively low in the analyzed samples (1.2 to 4.9 ppm of Sm and 10 to 31 ppm of Nd), except for the Planalto and Cruzadão granites, in the orthopyroxene quartz gabbro and in the sample ARC-142 of the Pedra Branca suite, where the Sm and Nd contents are higher (6 to 17 ppm of Sm and 42 to 124 ppm of Nd). The $^{147}Sm/^{144}Nd$ ratios show strong variations with some granitoids with ratios varying between 0.09 to 0.12 (Canaã dos Carajás, Serra Dourada, Planalto granites, Bacaba tonalitic complex, orthopyroxene quartz gabbro and the samples GRD-58 of the Cruzadão granite and AMR-191 of the Pedra Branca suite; Table 3) and others with comparatively lower ratios of 0.050 to 0.075 (Rio Verde trondhjemite, Bom Jesus granite and the samples ARC-113 of the Cruzadão granite and ARC-142 of the Pedra Branca suite).

Among the Mesoarchean units, the Canaã dos Carajás granite and Bacaba tonalitic complex show a broadly similar behavior of the Sm-Nd isotopes. The Nd model ages of the analyzed rocks vary in general from 3162 Ma and 3050 Ma and their εNd(t) values (Table 3) are slightly negative from -0.04 to –4.09, except for an isolated sample (ERF-07C with T_{DM} of 2944 Ma and εNd of +0.94). On the other hand, the εNd(t) values for the Bom Jesus, Cruzadão and Serra Dourada granites are positive (+2.31 and +0.12) with T_{DM} depleted-mantle model ages varying from 2999 Ma to 2932 Ma. The Neoarchean granitoids (Planalto and Pedra Branca suites and Charnockitic rock) show T_{DM} varying from 3136 Ma to 2952 Ma and εNd always negative (–0.85 to –2.25; Table 3), except for the sample AMR-152 of the Planalto suite (T_{DM} of 2813 Ma and εNd of +1.38).

7. Discussion

7.1. Ages of the Archean granitoids of the Canaã area

The new ages obtained for the Archean granitoids of the Canaã area, integrated with those available in the literature, allow us to constrain the timing of the major magmatic events that had took place in that area (Table 2, Fig. 11). Four major events of rock formation are distinguished: at 3.05-3.0, 2.96-2.93, 2.87-2.83, and 2.75-2.73 Ga (Fig. 12). The 3.05-3.0 Ga event was marked by the formation of the Pium complex, by ages obtained in the mineralized area of the Bacaba tonalitic complex, and by several inherited zircon ages shown by different granitoids (Table 2). During the second event, the crystallization of the Canaã dos Carajás granite and the formation of the older rocks of the Rio Verde trondhjemite took place.

Table 3 - Sm-Nd isotopic data for the granitoids of the Canaã dos Carajás area.

Sample	Sm (ppm)	Nd (ppm)	$^{147}Sm/^{144}Nd$	$^{143}Nd/^{144}Nd$ (±2σ)	f(Sm/Nd)	εNd(0)	εNd(t)	T_{DM} (Ma)
2.95 Ga Canaã dos Carajás granite								
AMR-102	1,94	11,14	0,1050	0.51082 (6)	-0,4661	-35,46	-0,66	3162
AMR-213	3,84	23,49	0,0988	0.510691 (5)	-0,4977	-37,98	-0,51	3162
2.93 Ga Rio Verde Trondhjemite								
AER-11	1,78	18,70	0,0572	0.509949(22)	-0,7092	-52,5	0,19	3042
AER-77B	2,55	21,17	0,0741	0.510399(17)	-1,0000	-43,7	2,61	2913
2.86 Ga Rio Verde trondhjemite								
GRD-79C	1,21	10,08	0,0723	0.510421(12)	-0,4977	-43,2	2,75	2850
2.85 Ga Bacaba tonalitic complex								
AER-29A	3,21	17,47	0,1111	0.511008(8)	-0,4352	-31,80	-0,38	3064
ARC-65A	4,98	31,65	0,0951	0.510651(9)	-0,5165	-38,76	-1,48	3113
ARC-95A	4,44	23,74	0,1131	0.511033(13)	-0,4250	-31,31	-0,63	3088
ERF-113	3,75	19,03	0,1192	0.511178 (14)	-0,3940	-28,48	-0,04	3050
ERF-07C	2,48	16,47	0,0910	0.510697(22)	-0,5374	-37,86	0,94	2944
ERF-134	4,90	29,04	0,1021	0.51065(26)	-0,4809	-38,78	-4,09	3321
2.85 Ga Cruzadão granite								
ARC-113	7,68	70,78	0,0655	0.510217(14)	-0,6670	-47,2	2,31	2932
GRD-58A	13,33	82,55	0,0976	0.510793(1)	-0,5038	-36,0	0,38	2987
2.85 Ga Bom Jesus gneiss granite								
AE-47	1,45	12,04	0,0729	0.510337(19)	-0,6294	-44,9	0,55	2957
ARC-116	2,6	31,0	0,0508	0.509899(17)	-0,7417	-53,4	0,12	2967
2.83 Ga Serra Dourada granite								
AER-27	3,02	16,85	0,1084	0.510996 (16)	-0,4489	-32,03	0,15	2999
AER-59	3,47	22,22	0,1025	0.510925 (11)	-0,4789	-33,42	0,92	2935
2.75 Pedra Branca suite								
AMR-191A	1,72	8,94	0,1164	0.51107(6)	-0,4085	-30,59	-2,16	3136
ARC-142	12,84	124,27	0,0625	0.510141(7)	-0,6823	-48,71	-1,21	2952
2.73 Ga Orthopyroxene-quartz gabbro								
GRD-05	11,78	64,64	0,1102	0.51099(7)	-0,4398	-31,97	-1,59	3049
2.73 Ga Planalto suite								
ARC-108	6,02	42,00	0,0867	0.510573(9)	-0,5592	-40,28	-1,64	2996
ARC-109	11,35	63,00	0,1089	0.511013(7)	-0,4464	-31,70	-0,85	2988
AMR-152	13,82	77,83	0,1073	0.511098(12)	-0,4545	-30,04	1,38	2813
AMR-187B	17,09	100,52	0,1027	0.510901(17)	-0,4779	-33,88	-0,86	2975
GRD-77	13,40	77,29	0,1048	0.510868(23)	-0,4672	-34,53	-2,25	3084

During the third stage, the dominant rocks of the Bacaba tonalitic complex and Rio Verde trondhjemite, as well as the Cruzadão, Bom Jesus and Serra Dourada granites were crystallized. Finally, the fourth event occurred during the Neoarchean and involved the crystallization of the Planalto and Pedra Branca suites and of the charnockites associated with the Pium complex.

It is concluded that three major events of rock formation in the study area occurred during the Mesoarchean and are not very distinct in age of those registered so far in the Carajás province as a whole. On the other hand, the fourth Neoarchean magmatic event identified in Canaã is also present in the Carajás basin but absent in the Rio Maria granite greenstone terrane.

7.2. Geochemical signature of the Archean granitoids of the Canaã area: geologic and tectonic implications

Before the present work, most of the Archean granitoid rocks exposed in the Canaã area were encompassed in the Xingu complex. This was entirely modified due to the new granitoid units identified in the present work which lead to the vanishing of the Xingu complex in the Canaã area. In the supposed domains of the Xingu complex (Vasquez et al., 2008), the Canaã dos Carajás, Bom Jesus, Cruzadão, and Serra Dourada granites, the Rio Verde trondhjemite, and the Bacaba tonalitic complex were individualized (Fig. 2).

The granitoid magmatism identified in the Canaã area is diversified in age and geochemical signature. Two groups of units were recognized: the tonalitic-trondhjemitic units and the granitic ones. The Bacaba tonalitic complex and the Pedra Branca suite do not have geochemical affinity with TTG suites such as those of the Rio Maria terrane (Almeida et al., 2011) or other Archean cratons (Martin, 1994; Smithies, 2000; Condie, 2005; Moyen and Stevens, 2006; Clemens et al., 2006). Only the Rio Verde trondhjemite has affinity with the TTG suites but its areal distribution is relatively limited in Canaã, contrarily to the observed in the adjacent Rio Maria terrane, where TTG units cover large areas. Thus, it is concluded that the TTG magmatism was far more limited in Canaã than in classical Archean terranes. Also relevant is the absence in Canaã of sanukitoid suites (Fig. 2). The latter are common in the later stages of evolution of many Archean cratons (Stern and Hanson, 1991; Smithies and Champion, 2000; Halla, 2005; Lobach-Zhuchenko et al., 2005; Heilimo et al., 2011) and are widespread in the Rio Maria terrane (Althoff et al., 2000; Oliveira, M.A. et al., 2009, 2010).

On the other hand, the granitic units, which constitute the second geochemical group, are diversified in age and geochemical signature and occupy large areas in Canaã (more than

60% of the surface covered by granitoids). All granite units are formed essentially by monzogranites and syenogranites and generally contain associated evolved leucogranites (mafic content < 5%). Except for the Serra Dourada granite, the other granite units are strongly deformed, showing penetrative foliation and sometimes lineation and folded structures. The Mesoarchean granite units encompass the Canaã dos Carajás, Serra Dourada, Bom Jesus granites, which have affinity with evolved Archean calc-alkaline granites, and the Cruzadão granite that is transitional between calc-alkaline and alkaline (Sylvester, 1994; cf. our Fig. 4f). The Neoarchean granites are represented by several granitic stocks that constitute the Planalto suite, which has a ferroan and accentuated alkaline character and is thus distinct from the Mesoarchean granites found in the same area in age and geochemical signature (Fig. 4f; Feio et al., submitted). Neoarchean granites similar to those of the Planalto suite are also common in the Carajás basin, being represented by the Estrela complex and the Serra do Rabo and Igarapé Gelado plutons (Sardinha et al., 2006; Barros et al., 2009), and in other areas of the 'Transition' sub-domain to the south of the studied area (Oliveira, D.C. et al., 2010).

The dominance of granites (stricto sensu), the absence of sanukitoids and the scarcity of typical TTGs in Canaã demonstrate that, despite the similarities in the ages of Mesoarchean rocks of that area and those the Rio Maria terrane, the magmatic series present in those terranes are very distinct and do not favor a common tectonic evolution for them. Typical Archean terranes are dominated by TTG and greenstone belts with subordinate volumes of sanukitoid and granite rocks (Goodwin, 1991; Condie, 1993; Sylvester, 1994; Jayananda et al., 2006). Granites are commonly formed in the later stages of evolution of Archean terranes and are generally associated with the stabilization of the oldest cratons (Nisbet, 1987; Kröner, 1991; Davis et al., 1994; Jayananda et al., 2006; Almeida et al., submitted). Thus, the larger abundance of granitic rocks in Canaã suggests that the Archean crust of that area and possibly also of the 'Transition' sub-domain has not a dominant juvenile character (Fig. 12), and possibly derived from an older crust that was tending to stabilization during the Mesoarchean. This is reinforced by the Nd isotope data (see below). The Planalto suite is a peculiar feature of Canaã and of the entire Carajás domain, which has no equivalent in the Rio Maria terrane. The Planalto suite records a remarkable magmatic and deformational Neoarchean event that intensely affected the Mesoarchean crust of the Carajás domain and was responsible for the generation of relatively large volumes of ferroan granites associated with charnockite series.

7.3. Crustal evolution of the Canaã area: implications for the Carajás Province

The obtained data are not conclusive about the evolution of the 'Transition' sub-domain of the Carajás domain, but they establish some constraints and allow some preliminary conclusions. Geochronological and Nd isotope data (Fig. 12a, b) indicate that the crust of the Canaã area existed at least since the Mesoarchean (a minimum age of ca. 3.2-3.0 Ga can be estimated for it) and was strongly reworked during the Neoarchean (2.75 to 2.70 Ga). Differently of the Rio Maria terrane which rocks have crystallization ages concentrated between 2.98 and 2.86 Ga and show similar Nd T_{DM} ages which is an evidence of their juvenile character, the dated rocks of the Carajás domain show more variable crystallization and also T_{DM} ages. Moreover, the T_{DM} ages of the Canaã granitoids are significantly older than those of Rio Maria, extending to ca. 3.2 Ga (Fig. 12b) and εNd values are commonly negative, although positive values have been obtained in the case of some granite units, possibly derived from juvenile crustal sources with low crustal residence times.

It is probable that a terrane similar to that represented by the Canaã Mesoarchean crust or even an extension of it was the substratum of the Carajás basin that was formed during the Neoarchean. The tectonic events responsible for the origin of the Carajás rift and the subsequent formation of the Carajás basin and the compressional stage that followed it, both occurring in a short period during the Neoarchean, were also registered in the Canaã area. The intense magmatic activity responsible for the origin of the Pedra Branca and Planalto suite and charnockite rocks and the main deformational structures shown by these units are related to this major tectono-magmatic event. These rocks show penetrative foliation and local subvertical lineation and were affected by thrust faults. This indicates that they were emplaced in a transpressional regime (Fossen and Tikoff, 1998) related to the regional Neoarchean deformation that affected the Carajás domain (Pinheiro and Holdsworth, 1997). This Neoarchean event is not registered in the Rio Maria terrane in the southern of the Carajás province (Fig. 12a).

The available data on the Carajás domain allow us to evaluate the hypothesis of existence of a 'Transition' sub-domain in between the Rio Maria terrane and the Carajás basin (Dall'Agnol et al., 2006). In others words, we should evaluated whether the Canaã crust could correspond to an extension of the Rio Maria terrane strongly reworked during the Neoarchean or not. Despite the reasonable coincidence in ages between the Mesoarchean rocks of Canaã and the Rio Maria, it is demonstrated that the Rio Maria evolution was concentrated in a shorter period of time (Fig. 12a). Additionally, the contrast in dominant lithologies and Nd

isotope behavior (Fig. 12b) between these terranes is remarkable and point to distinct evolution for both. In the εNd(t) vs age diagram (Fig. 13), it can be observed more clearly the contrasts between the Archean rocks of Rio Maria and Canaã, including the subalkaline granites of the Carajás basin. The evolution paths defined by the rocks of these two domains are partially superposed but they suggest the existence of a distinct and significantly older crust for the Canaã domain compared to that of Rio Maria.

This conclusion should be verified by the geological and geochronological studies now being developed to the south of Canaã in other areas of the 'Transition' sub-domain (Oliveira, D.C. et al., 2010). However, the common presence of orthopyroxene-bearing rocks, the limited occurrence of TTG, the absence of sanukitoid, and the large volume of granites in Canaã are strong evidences of remarkable contrasts with the Rio Maria evolution. The presence of many granitic units in Canaã formed during the Mesoarchean and with ages varying between 2.96 and 2.83 Ga suggest the existence in Canaã of a continental crust older than that of Rio Maria. It is probable that the Mesoarchean crust of Canaã had initiated its tectonic stabilization before that of Rio Maria. However, the Canaã crust, and by extension that of the entire Carajás domain, was submitted to intense crustal reworking during the Neoarchean. This late Archean event was not registered in the Rio Maria terrane.

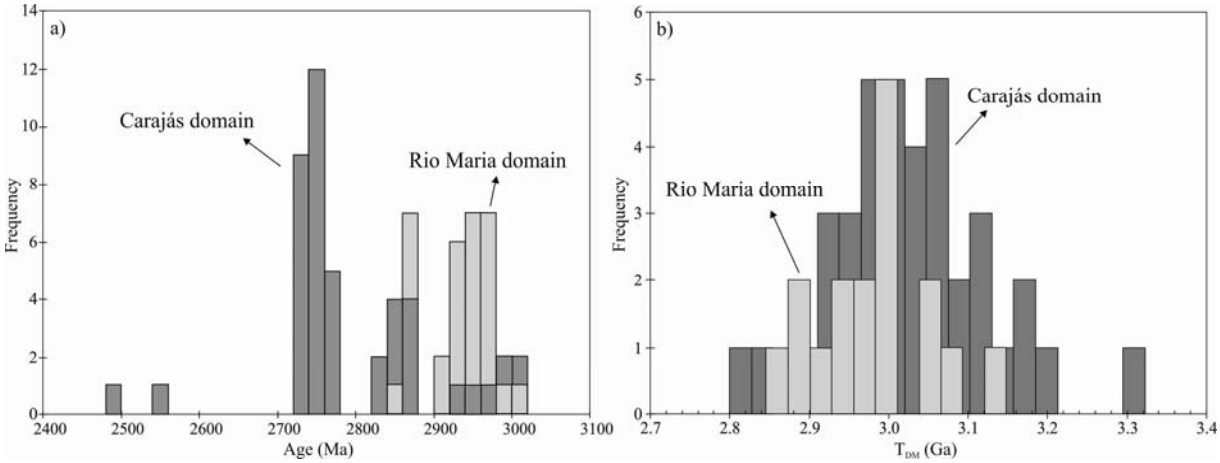

Figure 12 - Histograms of frequency showing (a) the crystallization ages and (b) the depleted mantle (T_{DM}) ages obtained for the Archean rocks of the Carajás and Rio Maria domains, of the Carajás province.

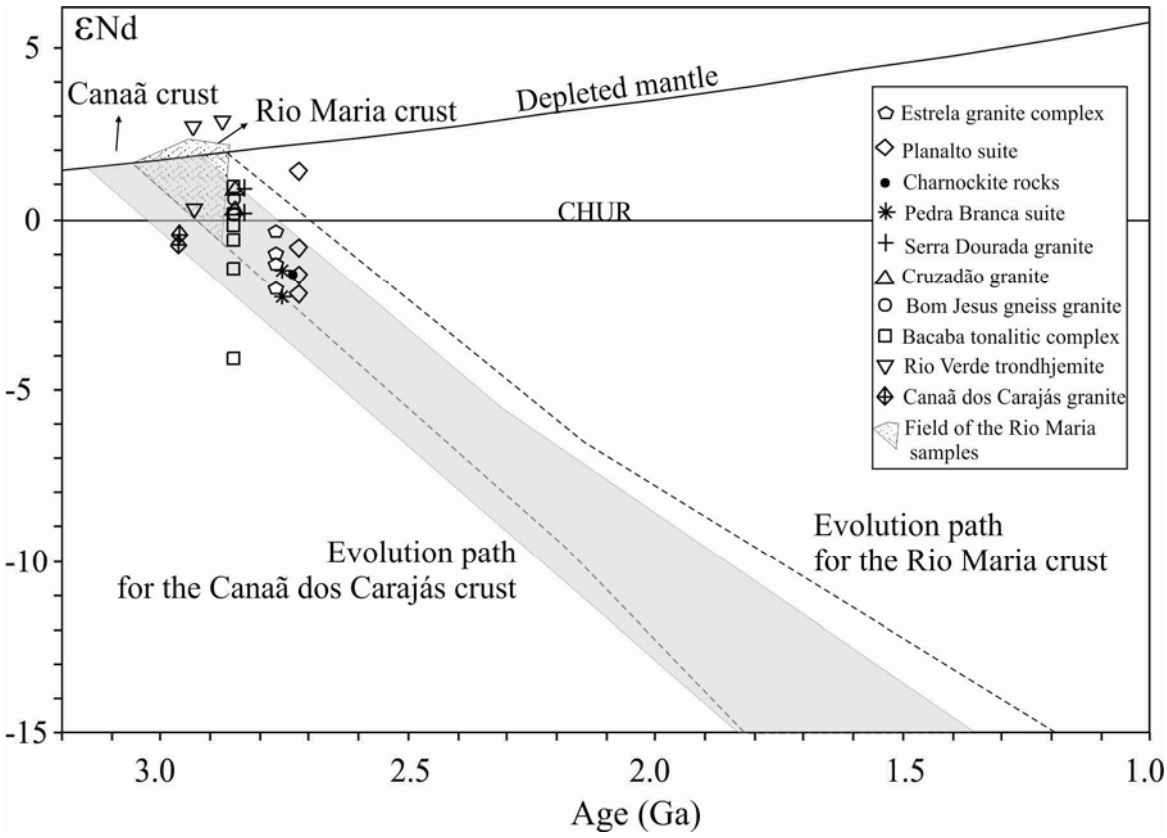

Figure 13 - εNd vs. age diagram for the Archean granitoids of the Canaã area of the Carajás province. The field of the Archean rocks of the Rio Maria granite-greenstone terrane and the evolution paths for the rocks of Rio Maria (Rämö et al., 2002) and Canaã (this work) are indicated. Data of the Estrela granite complex (Barros et al., 2009) are shown for comparison.

7.4. A brief comparison with other Archean cratons

Archean cratons are commonly composed of three main lithologic units (Windley, 1995): (1) a gneissic basement of tonalitic–trondhjemitic–granodioritic (TTG) composition; (2) greenstone belts; (3) K-rich granites, generated generally late in the geological evolution of the craton (Moyen et al., 2003). This general picture is quite similar to that registered in the Rio Maria terrane but it differs substantially of that observed in the Canaã area of the Carajás province. In the following, a preliminary comparison between the evolution of the Carajás province and those of other Archean terranes is presented. We have selected arbitrarily the Dharwar and Karelian cratons and the Limpopo belt for comparison.

The Dharwar craton (Jayananda et al., 2006; Jayananda and Chardon, 2011) is divided in two large domains, the western and eastern Dharwar craton, and has a longer evolution in time compared to the Carajás province. In the western Dharwar craton, the dominant rocks are TTG series (3.4 to 3.2 Ga, Peninsular gneisses) and supracrustal greenstone sequences (the 3.6 to 3.2 Ga, Sargur Group, and the the 3.0 to 2.6 Ga, Dharwar Supergroup). Potassic plutons were formed during the Mesoarchean (ca. 3.0 Ga) and Neoarchean (ca. 2.6 Ga). In the eastern

Dharwar craton, > 3.0 Ga old basement relicts of TTG and 2.7 to 2.55 Ga greenstone belts were identified but the dominant rocks are the 2.56 to 2.51 Ga Neoarchean dominantly calc-alkaline to potassic granitoids, which include the classical Closepet granite (Moyen et al., 2003). The southern part of the craton was affected by granulitic metamorphism at the end of the Neoarchean (2.56 to 2.50 Ga). The evolution of the Dharwar craton extended over a large period of time (ca. 1.0 Ga) compared to the Carajás province (Fig. 12a). It is concluded that the tectonic and magmatic evolution of the Dharwar craton differs in its essence of that registered in the Carajás province.

The evolution of the Karelian province in Finland (Käpyaho et al., 2006; Heilimo et al., 2011) was concentrated in the Mesoarchean and Neoarchean (generally 2.95 to 2.50 Ga; Heilimo et al., 2011) and involved the rock types generally found in classical Archean terranes. The kind of magmatic rocks and their succession in time is quite similar to that described in the Rio Maria terrane (Oliveira, M.A. et al., 2009, 2010; Almeida et al., 2011), however the main geological units in Karelia were formed in between 2.83 and 2.68 Ga (Käpyaho et al., 2006), whereas the main period of new crust formation is a little older in Rio Maria (2.98 to 2.86 Ga). The contrasts between the Karelia province evolution and that of the Carajás province are even stronger in the case of the Carajás domain, including the Canaã area. In this case, besides the difference in ages between both terranes, the main rocks formed during the Neoarchean are quite distinct in both provinces, suggesting contrasting tectonic evolution for them.

The Limpopo Belt is a polymetamorphic terrain situated between the Zimbabwe and Kaapvaal craton on southern Africa (Kröner et al., 1999). It was divided into three zones: a central zone bordered by two marginal zones that resulted of the crustal reworking of the adjacent Zimbabwe (to the North) and Kaapvaal cratons (to the South). This belt was interpreted as the result of a tectonic collision between the Kaapvaal and Zimbabwe cratons at ca. 2.70 to 2.65 Ga (Barton and Van Reenen, 1992; Rollinson, 1993). The two marginal zones should represent the equivalent lithologies of the adjacent cratons submitted to higher deformation and metamorphic grade (Kreissig et al., 2000). A high-grade metamorphism occurred at 2.7-2.5 Ga (Holzer et al., 1999) and its age is coincident with a main event of granitoid magmatism across the Limpopo belt. During this event pyroxene-bearing and pyroxene-free granitoids, as exemplified by the Matok pluton (Rapopo, 2010), were generated. Despite the unequivocal contrasts, there are apparently some relevant similarities between the Limpopo belt and Carajás domain tectonic evolution. The most relevant aspect is that both provinces were strongly reworked during the Neoarchean and produced at that time

an assemblage of pyroxene-bearing and pyroxene-free granitoids that are related to the generation of magmas in hot zones of the deep crust, possibly due to collisional tectonic processes. The analogies in evolution of the study area with hot magmatic zones, not only in the Archean but also during the Proterozoic (Smithies et al., 2011), should be deeper investigated in the future to clarify the origin of the Neoarchean magmatism found in the Canaã area.

8. Conclusions

1. Systematic geological mapping, petrographic, geochemical and geochronological studies undertaken in the Canaã area of the Carajás domain allowed the identification of various new granitoid units that replaced entirely the Xingu complex in that area.

2. Four major magmatic events, three of Mesoarchean age and one of Neoarchean age, were distinguished: (1) at 3.05-3.0 Ga, it occurred the formation of the protolith of the Pium complex and of rocks with similar ages indicated only by inherited zircons found in different units; (2) the second event, at 2.96-2.93 Ga, was marked by the crystallization of the Canaã dos Carajás granite and the formation of the older rocks of the Rio Verde trondhjemite; (3) a third event was identified at 2.87-2.83 Ga and, during it, were formed the Bacaba tonalitic complex, Rio Verde trondhjemite, and the Cruzadão, Bom Jesus and Serra Dourada granites; (4) in the Neoarchean, at 2.75-2.73 Ga, a large magmatic event was responsible for the origin of the Planalto and Pedra Branca suites and of charnockite rocks. The three Mesoarchean events are not very distinct in age of those registered so far in the Carajás province as a whole. However, the Neoarchean event is present only in the Carajás domain and absent in the Rio Maria granite greenstone terrane.

3. In terms of geochemical signature, two groups of granitoid units were distinguished in the Canaã area: (1) The tonalitic-trondhjemitic units, which encompass the Rio Verde trondhjemite, the Bacaba tonalitic complex and the Pedra Branca suite, and (2) the granitic units, which include the Canaã dos Carajás, Bom Jesus, Cruzadão, Serra Dourada, and Planalto granites. The Bacaba tonalitic complex and the Pedra Branca suite are geochemically distinct of typical Archean TTG series, whereas the Rio Verde trondhjemite has affinity with the latter. Sanukitoid series were not so far identified in the studied area. The granitic units are formed essentially by monzogranites and syenogranites and occupy more than 60% of the surface covered by granitoids in Canaã. The Mesoarchean granite units encompass the calc-alkaline Canaã dos Carajás, Serra Dourada, Bom Jesus granites, and the Cruzadão granite which is transitional between calc-alkaline and alkaline. The Planalto suite is formed by

metaluminous to peraluminous, ferroan, alkaline Neoarchean granites, similar geochemically to the Estrela complex and the Serra do Rabo and Igarapé Gelado plutons also exposed in the Carajás domain. It is concluded that the Archean granitoid magmatism in Canaã differs significantly of that found in most classical Archean cratons, including the Rio Maria terrane, because TTG magmatism is little relevant, sanukitoid rocks are absent and granitic rocks are the dominant rocks in Canaã. The contrast in granitoid magmatism between Canaã and Rio Maria do not favor a common tectonic evolution for these two Archean domains of the Carajás province. The relatively high areal distribution of Mesoarchean granites in Canaã suggests that it has not a juvenile character and was probably derived of a crust formed before than that of Rio Maria. The Planalto suite is a peculiar feature of Canaã and of the entire Carajás domain. It records a remarkable magmatic and deformational event which has no equivalent in the Rio Maria terrane.

4. The crust of the Canaã area existed at least since the Mesoarchean (ca. 3.2-3.0 Ga) and was strongly reworked during the Neoarchean (2.75 to 2.70 Ga). A terrane similar to that represented by the Canaã Mesoarchean crust or even an extension of it was probably the substratum of the Carajás basin formed during the Neoarchean. The evolution of Canaã during the Archean is clearly distinct of that of Rio Maria as indicated by the contrast in dominant lithologies and Nd isotope behavior in both domains. The Nd evolution paths suggest the existence of an older crust in the Canaã area compared to that of Rio Maria. If this conclusion could be extrapolated for the entire 'Transition' subdomain of Carajás, it implies that there is no an effective transition between Rio Maria and the Carajás basin and the dominantly granitoid terrane denominated 'Transition' subdomain had more probably an magmatic and tectonic evolution entirely distinct of that of Rio Maria. This preliminary conclusion should be verified in the future studies now being developed to the south of Canaã.

5. The evolution of the Carajás province differs significantly of those registered in the Dharwar and Karelian cratons and approach in some aspects of its Neoarchean evolution to that described in the Limpopo belt, a polymetamorphic terrain situated between the Zimbabwe and Kaapvaal craton on southern Africa. The Carajás domain and the Limpopo belt were both strongly reworked during the Neoarchean and generate in hot zones of the deep crust pyroxene-bearing and pyroxene-free granitoid magmas, possibly due to collisional tectonic processes.

Acknowledgements

A.A.S. Leite, D.C. Oliveira, and C.E.M Barros, are acknowledged for support in field work and A.S. Sardinha, A.K.B. Gomes, J.E.B. Soares and M.A. Oliveira for previous work in the studied area; M.A. Galarza Toro, P.A. Santos, J.A.C. Almeida, M. Matteini, and B. Lima, for their assistance on Pb-evaporation and U-Pb LA-MC-ICPMS analyses; C.N. Lamarão and I.M.O. Ramalho are thanked for their assistance in the cathodoluminescence imaging and the team of the Geochronological Laboratory of the Brasília University for Nd isotope analyses. O.T. Rämö discussed a preliminary set of our geochronological data. This research received financial support from CNPq (R. Dall'Agnol – Grants 0550739/2001-7, 476075/2003-3, 307469/2003-4, 484524/2007-0; PRONEX – Proc. 66.2103/1998-0; G.R.L. Feio – CNPq scholarship), and Federal University of Pará (UFPA). This paper is a contribution to the Brazilian Institute of Amazonia Geosciences (INCT program –CNPq/MCT/FAPESPA – Proc. 573733/2008-2) and to the project IGCP-SIDA 599.

Appendix A- Analytical procedures for whole-rock chemical analyses **-** The chemical analyses were performed by ICP-ES for major elements and ICP-MS for trace-elements, including the rare-earth elements, at the Acme Analytical Laboratories Ltd. in Canada.

Appendix B- Analytical methods of Geochronology - Zircon concentrates were extracted from ca. 10 kg rock samples using conventional gravimetric methods of heavy mineral separation and magnetic (Frantz isodynamic separator) techniques at the Geochronology Laboratory of the University of Pará (Pará-Iso). Final purification was achieved by hand selecting through a binocular microscope and the zircon grains of each sample were then photographed under reflected light. For U-Pb LA-MC-ICPMS analyses, the zircons grains of each sample were mounted in epoxy resin, polished, and. their internal structures were examined by cathodoluminescence (CL) imaging technique in a scanning electron microscope LEO 1430 at the Scanning Electron Microscopy Laboratory of the Geosciences Institute of Federal University of Pará (UFPA).

For the Pb-evaporation method (Kober, 1987), individual selected zircon grains were encapsulated in the Re-filament used for evaporation, which was placed directly in front of the ionization filament. The Pb is extracted by heating in three evaporation steps at temperatures of 1450º, 1500º, and 1550 °C and loaded on an ionization filament. The Pb intensities were measured by each peak stepping through the 206–207–208–206–207–204 mass sequence for five mass scans, defining one data block with eight $^{207}Pb/^{206}Pb$ ratios. The weighted $^{207}Pb/^{206}Pb$ mean for each block is corrected for common Pb using appropriate age values derived from the two-stage model of Stacey and Kramers (1975), and results with $^{204}Pb/^{206}Pb$ ratios higher than 0.0004 and those that scatter more than two standard deviations

from the average age value were discarded. The calculated age for a single zircon grain and its error, according to Gaudette et al. (1998), is the weighted mean and standard error of the accepted blocks of data. The ages are presented with 2σ error.

The U–Pb LA-MC-ICPMS analyses were carried out using a New Wave UP213 Nd:YAG laser (λ - 213 nm), linked to a Thermo Finnigan Neptune multi-collector ICPMS at the Geochronology Laboratory of the University of Brasília. The analytical procedures were described by Buhn et al. (2009). The laser was run at a frequency of 10 Hz and energy of 0.4 mJ/pulse, ablation time of 40 s and a spot size of 30 μm in diameter. Plotting of U–Pb data was performed by ISOPLOT (Ludwig, 2001) and errors for isotopic ratios are presented at the 1σ level.

The analyses have been carried out using raster ablation method (Bühn et al., 2009) to prevent laser induced mass bias fractionation. The U-Pb raw data are translated to an Excel spreadsheet for data reduction and, when necessary, the laser induced mass bias was corrected using the method of Kosler et al. (2002). Common lead (^{204}Pb) interference and background correction, when necessary were carried out by monitoring the ^{202}Hg and 204 mass (^{204}Hg+^{204}Pb) during the analytical sessions and using a model Pb composition (Stacey and Kramers, 1975) when necessary. Reported errors are propagated by quadratic addition [$(2SD^2+2SE^2)^{1/2}$] of external reproducibility and within-run precision. The external reproducibility is represented by the standard deviation (SD) obtained by repeated analyses (n=20, ~ 0.8% for ^{207}Pb/^{206}Pb and ~ 1% for ^{206}Pb/^{238}U) of standard zircon GJ-1, performed during analytical session, and the within-run precision is represented by the standard error (SE) that was calculated for each analysis.

For the exclusion of spot analyses on the calculation of U-Pb ages we have employed the general criteria adopted in the literature: (1) the common lead content (the ^{206}Pb/^{204}Pb ratio should not be lower than 1000); (2) the degree of discordance (not using data where the discordance is higher than 10%); (3) the analytical precision (not using the data where the isotopic ratios have error greater than 3%). These general criteria were refined for each specific sample.

In the case of the samples dated by SHRIMP, sample GRD-47 was crushed, milled and sieved at 60 mesh and the heavy minerals were separated using heavy liquid (TBE tetra-bromo-ethane) and magnetic separation techniques. For the preparation of the samples ARC-109 and AMR-187B the techniques employed for zircon concentration were identical to those for Pb-evaporation and LA-MC-ICPMS methods. The final separation of the minerals was by hand picking the grains. These were mounted on epoxy discs (UWA 11-04 and UWA-06)

with fragments of standards, ground and polished until nearly one third of each grain was removed, and imaged (backscattered electrons) for their internal morphology using a scanning electron microscope at the Centre for Microscopy and Microanalysis at the University of Western Australia. The epoxy mounts were then cleaned and gold-coated to have a uniform electrical conductivity during the SHRIMP analyses.

The zircon standard used was BR266 zircon (559 Ma, 903 ppm U). The isotopic composition of zircon was determined using SHRIMP II (De Laeter and Kennedy, 1998), using methods based on those of Compston et al. (1992). A primary ion beam of ~3nA, 10 kVO22− with a diameter of ~25μm was focused onto the mineral. Each zircon U-Pb analysis on SHRIMP (Sensitive High-mass Resolution Ion MicroProbe) used five scans collecting nine measurements on each (196Zr2O, 204Pb, background, 206Pb, 207Pb, 208Pb, 238U, 248ThO, and 254UO). Corrections for common Pb were made using the measured 204Pb and the Pb isotopic composition of Broken Hill galena. For each spot analysis, initial 60–90 s were used for pre-sputtering to remove the gold, avoiding the analysis of common Pb from the coatings. Zircons data are reduced using SQUID (Ludwig, 2002) software. Data were plotted on concordia diagrams using ISOPLOT/Ex software (Ludwig, 2001), which error ellipses on Concordia plots are shown at the 95% confidence level (2σ). All ages given in text are weighted mean 207Pb/206Pb ages. Details of U–Pb data are presented in Table C.

Appendix C- Sm–Nd isotopic analyses - the analyses were performed at the Geochronology Laboratory of the University of Brasília and at the Isotope Geology Laboratory of the Federal University of Pará (Pará-Iso), Brazil, either using a Finnigan MAT 262 mass spectrometer.

Sm-Nd isotopic method of the Laboratory of the University of Brasília is described by Gioia and Pimentel (2000). Whole rock powders (ca. 50 mg) were mixed with 149Sm–150Nd spike solution and dissolved in Savillex capsules. Sm and Nd extraction of whole rock samples followed conventional cation exchange techniques, using teflon columns containing LN-Spec resin (HDEHP–diethylhexyl phosphoric acid supported on PTFE powder). Sm and Nd samples were loaded on Re evaporation filaments of double filament assemblies and the isotopic measurements were carried out on a multi-collector Finnigan MAT 262 mass spectrometer in static mode. Uncertainties for Sm/Nd and $^{143}Nd/^{144}Nd$ ratios are better than ± 0.5% (2σ) and ± 0.005% (2σ), respectively, based on repeated analyses of international rock standards BHVO-1 and BCR-1.

For the Sm–Nd analysis obtained in the Isotope Geology Laboratory of the Federal University of Pará (Pará-Iso), was utilized the employed routine by Oliveira, E.M. et al.

(2009), that consists of add 150Nd–149Sm spike to the ca. 100 mg of rock and attack with HF + HNO_3 in Teflon vials inside PARR containers at 150º C for one week. After evaporation, new additions of HF + HNO_3 are made, the solutions are dried, followed by dissolution with HCl (6 N), drying, and finally dissolution with HCl (2N). After the last evaporation, the REE are separated from other elements by cation exchange chromatography (Dowex 50WX-8 resin) using HCl (2 N) and HNO_3 (3 N). After that, Sm and Nd were separated from the other REE by anion exchange chromatography (Dowex AG1-X4 resin) using a mixture of HNO3 (7 N) and methanol. In both cases, the $^{143}Nd/^{144}Nd$ ratios were normalized to $^{146}Nd/^{144}Nd$ of 0.7219, and the decay constant used was 6.54×10^{-12} to $^{-1}$. The T_{DM} values were calculated using the model of DePaolo (1981).

References

Almeida, J.A.C., Dall'Agnol, R., Dias, S.B., Althoff, F.J., 2010. Origin of the Archean leucogranodiorite–granite suites: Evidence from the Rio Maria terrane and implications for granite magmatism in the Archean. Lithos 120, 235-257.

Almeida, J.A.C., Dall'Agnol, R., Oliveira, M.A., Macambira, M.J.B., Pimentel, M.M., Rämö, O.T., Guimarães, F.V., Leite, A.A.S., 2011. Zircon geochronology and geochemistry of the TTG suites of the Rio Maria granite-greenstone terrane: Implications for the growth of the Archean crust of Carajás Province, Brazil. Precambrian Research 187, 201-221.

Almeida, J.A.C., Dall'Agnol, R., Leite, A.A.S., submitted for publication. Geochemistry and zircon geochronology of the Archean granite suites of the Rio Maria granite-greenstone terrane, Carajás Province, Brazil. Journal of South American Earth Sciences.

Althoff, F.J., Barbey, P., Boullier, A.M., 2000. 2.8–3.0 Ga plutonism and deformation in the SE Amazonian craton: the Archean granitoids of Marajoara (Carajás Mineral province, Brazil). Precambrian Research 104, 187–206.

Araújo, O.J.B., Maia, R.G.N., 1991. Programa de levantamentos geológicos básicos do Brasil, Serra dos Carajás, folha SB-22-Z-A, Estado do Pará. Texto explicativo, Brasília, DNPM/CPRM. 164p (in Portuguese).

Barker, F., Arth, J.G., 1976. Generation of trondhjemite-tonalite liquids and Archean bimodal trondhjemite-basalt suites. Geology 4, 596–600.

Barker, F., 1979. Trondhjemite: a definition, environment and hypotheses of origin. In: Barker, F. (Ed.), Trondhjemites, Dacites and Related Rocks. Elsevier, Amsterdam, pp. 1–12.

Barros, C.E.M.; Dall'Agnol, R.; Soares, A.D.V.; Dias, G.S. 1994. Metagabros de Águas Claras, Serra dos Carajás: petrografia, geoquímica e transformações metamórfico-hidrotermais. Acta Geol. Leopoldensia 40, 31-70

Barros, C.E.M., Macambira, M.J.B., Barbey, P., Scheller, T., 2004. Dados isotópicos Pb–Pb em zircão (evaporação) e Sm-Nd do Complexo Granítico Estrela, Província Mineral de Carajás, Brasil: Implicações petrológicas e tectônicas. Revista Brasileira de Geociências 34, 531–538 (in Portuguese).

Barros, C.E.M., Sardinha, A.S., Barbosa, J.P.O., Macambira, M.J.B., 2009. Structure, Petrology, Geochemistry and zircon U/Pb and Pb/Pb geochronology of the synkinematic Archean (2.7 Ga) A-type granites from the Carajás Metallogenic Province, northern Brazil, Canadian Mineralogist 47, 1423-1440.

Barton, J.M., Jr., Van Reenen, D.D. 1992. When was the Limpopo Orogeny? Precambrian Research 55: 7-16.

Buhn, B., Pimentel, M.M., Matteini, M., Dantas, E.L., 2009. High spatial resolution analysis of Pb and U isotopes for geochronology by laser ablation multi-collector inductively coupled plasma mass spectrometry (LA-MC-ICP-MS). Anais da Academia Brasileira de Ciências 81, 1-16.

Clemens, J.D., Yearron, L.M., Stevens, G., 2006. Barberton (South Africa) TTG magmas: Geochemical and experimental constraints on source-rock petrology, pressure of formation and tectonic setting. Precambrian Research 151, 53-78.

Compston, W., Williams, I.S., Kirschvink, J.L., Zichao, Z., Guogan, M., 1992. Zircon ages for the Early Cambrian timescale. Journal of Geological Society, London 149, 171–184.

Condie, K.C., 1993. Chemical composition and evolution of the upper continental crust: Contrasting results from surface samples and shale. Chemical Geology, 104, 1-37.

Condie, K.C., 2005. TTGs and adakites: are they both slab melts? Lithos 80, 33-44.

Costa, J.B.S., Araújo, O.J.B., Santos, A., Jorge João, X.S., Macambira, M.J.B., Lafon, J.M., 1995. A Província Mineral de Carajás: aspectos tectono-estruturais, estratigráficos e geocronológicos. Boletim do Museu Paraense Emílio Goeldi 7, 199-235 (in Portuguese).

Dall'Agnol, R., Teixeira, N.P., Rämö, O.T., Moura, C.A.V., Macambira, M.J.B., Oliveira, D.C., 2005. Petrogenesis of the Paleoproterozoic, rapakivi, A-type granites of the Archean Carajás Metallogenic Province, Brazil. Lithos 80, 01-129.

Dall'Agnol, R., Oliveira, M.A., Almeida, J.A.C., Althoff, F.J., Leite, A.A.S., Oliveira, D.C., Barros, C.E.M., 2006. Archean and Paleoproterozoic granitoids of the Carajás Metallogenic Province, eastern Amazonian Craton. In: Dall'Agnol, R., Rosa-Costa, L.T. and Klein, E.L. (Eds.) Symposium on magmatism, crustal evolution, and metallogenesis of the Amazonian Craton. Volume and Field Trip Guide. Belém, PRONEX-UFPA-SBGNO, 99-150.

Davis, W.J., Fryer, B.J., King, J.E. 1994. Geochemistry and evolution of late Archean plutonism and its significance to the tectonic development of the Slave Craton. Precambrian Research 67, 207-241.

Debon, F., Le Fort, P., 1983. A chemical-mineralogical classification of common plutonic rocks and associations. Trans. Roy. Soc. Soc. Edinb-Earth Sci., 73:135-149.

De Laeter, J.R., Kennedy, A.K., 1998. A double focusing mass spectrometer for geochronology. International Journal of Mass Spectrometry 178, 43–50.

De Paolo, D.J., 1981. Neodymium isotope in the Colorado Front Range and crust–mantle evolution in the Proterozoic. Nature 291, 193-196.

Dias, G.S., Macambira, M.J.B., Dall'Agnol, R., Soares, A.D.V., Barros C.E., M., 1996. Datação de zircões de sill de metagabbro: comprovação da idade Arqueana da Formação Águas Claras, Carajás-Pará. In: SBGEO, V Simpósio de Geologia da Amazônia, Belém, 376–379 (in Portuguese).

Domingos, F.H., 2009. The structural setting of the Canaã dos Carajás region and Sossego-Sequeirinho deposits, Carajás – Brazil. University of Durham, England, 483p. (Ph.D. Thesis)

Feio, G.R.L., Dall'Agnol, R., Dantas, E.L., Macambira, M.B., Gomes, A.C.B., Sardinha, A.S., Santos, P.A. submitted for publication. Geochemistry, geochronology, and origin of the Neoarchean Planalto Granite suite, Carajás, Amazonian craton: A-type or hydrated charnockitic granites? Lithos.

Fossen, H., Tikoff, B., 1998. Extended models of transpression and transtension, and application to tectonic settings. In: Holdsworth, R.E., Strachan, R.A., Dewey, J. F. (Eds.), Continental transpressional and transtensional tectonics. Geological Society of London, Special Publication 135, p. 15-33.

Frost, B.R., Barnes, C., Collins, W., Arculus, R., Ellis, D., Frost, C., 2001. A chemical classification for granitic rocks. Journal of Petrology 42, 2033-2048.

Gabriel, E.O., Oliveira, D.C., Macambira, M.J.B., 2010. Caracterização geológica, petrográfica e geocronológica de ortopiroxênio-trondhjemitos (leucoenderbitos) da região de Vila Cedere III, Canaã dos Carajás-PA, Província Mineral de Carajás. In: SBG, Congresso Brasileiro de Geologia, 45, CDrom (in Portuguese).

Galarza, M.A., Macambira, M.J.B., Villas, R.N., 2008. Dating and isotopic characteristics (Pb and S) of the Fe oxide–Cu–Au–U–REE Igarapé Bahia ore deposit, Carajás mineral province, Pará state, Brazil. Journal of South American Earth Sciences 25, 377-397.

Gaudette, H.E., Lafon, J.M., Macambira, M.J.B., Moura, C.A.V., Scheller, T., 1998. Comparison of single filament Pb evaporation/ionization zircon ages with conventional U–Pb results: examples from the Precambrian of Brazil. Journal of South American Earth Sciences 11(4), 351-363.

Gibbs, A.K., Wirth, K.R., Hirata, W.K., Olszewski Jr., W.J., 1986. Age and composition of the Grão Pará Group volcanics, Serra dos Carajás. Revista Brasileira de Geociências 16, 201–211.

Gomes, A.C.B., Dall'Agnol, R., 2007. Nova associação tonalítica-trondhjemítica Neoarqueana na região de Canaã dos Carajás: TTG com altos conteúdos de Ti, Zr e Y. Revista Brasileira de Geociências 37, 182-193 (in Portuguese).

Goodwin, A.M., 1991. Precambrian Geology: the dynamic evolution of the continental crust. Academic Press, London, 666 pp.

Halla, J., 2005. Late Archean high-Mg granitoids (sanukitoids) in the Southern Karelian craton, Eastern Finland. Lithos 79, 161-178.

Heilimo, E., Halla, J., Huhma, H. 2011. Single-grain zircon U–Pb age constraints of the western and eastern sanukitoid zones in the Finnish part of the Karelian Province. Lithos 121, 87–99.

Holzer, L., Barton, J.M.Jr., Paya, B.K., Kramers, J.D., 1999. Tectonothermal history in the western part of the Limpopo belt: test of the tectonic models and new perspectives. Journal of African Earth Sciences 28, 383-402.

Huhn, S.B., Macambira, M.J.B., Dall'Agnol, R., 1999. Geologia e geocronologia Pb/Pb do granito alcalino arqueano Planalto, região da Serra do Rabo, Carajás-PA. In: Simpósio de Geologia da Amazônia, 6, 463-466 (in Portuguese).

Irvine, T.N., Baragar, W.R.A., 1971. A guide to the chemical classification of the common volcanic rocks. Canadian of Journal Earth Sciences 8, 523-547.

Jayananda, M., Chardon, D., Peucat, J.J., Capdevila, R. 2006. 2.61 Ga potassic granites and crustal reworking in the western Dharwar craton, southern India: Tectonic, geochronologic and geochemical constraints. Precambrian Research 150, 1-26.

Jayananda, M., Chardon, D., 2011. Geology of the Dhawar Craton. In: Jayananda, M., Ahmad, T., Chardon, D., 2011 (Eds.), International Symposium on Precambrian Accretionary Orogens and Field workshop in the Dharwar craton, southern India, India, University of Delhi and Geological society of India, 51p.

Käpyaho, A. Mänttäri, I., Huhma, H., 2006. Growth of Archean crust in the Kuhmo district, Eastern Finland: U-Pb and Sm-Nd isotope constraints on plutonic rocks. Precambrian Research 146, 95-119.

Kober, B., 1987. Single-grain evaporation combined with Pb+ emitter bedding for $^{207}Pb/^{206}Pb$ age investigations using thermal ion mass spectrometry, and implications to zirconology. Contributions to Mineralogy and Petrology 96, 63-71.

Kosler, J., Fonneland, H., Sylvester, P., Tubrett, M., Pedersen, R.B., 2002. U-Pb dating of detrital zircons for sediment provenance studies - A comparison of laser ablation ICPMS and SIMS techniques. Chemical Geology 182, 605-618.

Kreissig, K., Nägler, T.F., Kramers, J.D., Van Reenen, D.D., Smit, C.A., 2000. An isotopic and geochemical study of the northern Kaapvaal Craton and the Southern Marginal Zone of the Limpopo Belt: are they juxtaposed terranes? Lithos 50, 1-25.

Kröner, A. 1991. Tectonic evolution in the Archean and Proterozoic. Tectonophysics 87, 393-410.

Kröner, A., Jaeckel, P., Brandl, G., Nemchin, A.A., Pidgeon, R.T., 1999. Single zircon ages for granitoid gneisses in the Central Zone of the Limpopo Belt, southern Africa and geodynamic significance. Precambrian Research 93, 299-337.

Leite, A.A.S., Dall'Agnol, R., Althoff, F.J., 1999. Geoquímica e aspectos petrogenéticos do Granito Xinguara, terreno granito-greenstone de Rio Maria – Cráton Amazônico. Revista Brasileira de Geociências, 23(3), 429-436 (in Portuguese).

Leite, A.A.S., Dall'Agnol, R., Macambira, M.J.B., Althoff, F.J., 2004. Geologia e Geocronologia dos granitóides Arqueanos da região de Xinguara (PA) e suas implicações na evolução do Terreno Granito-Greenstone de Rio Maria. Revista Brasileira de Geociências 34, 447-458 (in Portuguese).

Lobach-Zhuchenko, S.B., Rollinson, H.R., Chekulaev, V.P., Arestova, N.A., Kovalenko, A.V., Ivanikov, V.V., Guseva, N.S., Sergeev, S.A., Matukov, D.I., Jarvis, K.E., 2005. The Archaean sanukitoid series of the Baltic Shield: geological setting, geochemical characteristics and implications for their origin. Lithos 79, 107-128.

Lobato, L.M., Rosière, C.A., Silva, R.C.F., Zucchetti, M., Baars, F.J., Sedane, J.C.S., Javier Rios, F., Pimentel, M., Mendes, G.E., Monteiro, A.M., 2005. A mineralização hidrotermal de ferro da Província Mineral de Carajás – controle estrutural e contexto na evolução metalogenética da província. In: Marini, O.J., Queiroz, E.T., Ramos, B.W. (Eds.). Caracterização de Depósitos Minerais em Distritos Mineiros da Amazônia, DNPM, CT-Mineral / FINEP, ADIMB, pp. 25-92 (in Portuguese).

Ludwig, K.R., 2001. User's manual for Isoplot/Ex Version 2.49 A geochronological toolkit for Microsoft Excel. Berkeley Geochronological Center Special Publication 1, 1-55.

Ludwig, K.R., 2002. Squid 1.02, a user's manual. Berkeley Geochronological Center Special Publication 2 (Berkeley, California, USA), 21 pp.

Macambira, M.J.B. 1992. Chronologie U/Pb, Rb/Sr, K/Ar et croissance de la croûte continentale dans L'Amazonie du sud-est; exemple de la région de Rio Maria, Province de Carajas, Brésil. Université Montpellier II - France. 212p. (Ph.D. thesis; in French)

Macambira, M.J.B., Lafon, J.M., 1995. Geocronologia da Província Mineral de Carajás; Síntese dos dados e novos desafios. Boletim do Museu Paraense Emílio Goeldi 7, 263-287 (in Portuguese).

Macambira, M.J.B., Lancelot, J., 1996. Time constraints for the formation of the Archean Rio Maria crust, southeastern Amazonian Craton, Brazil. International Geology Review 38, 1134-1142.

Machado, N., Lindenmayer, Z.G., Krogh, T.E., Lindenmayer, D., 1991. U-Pb geochronology of Archean magmatism and basement reactivation in the Carajás area, Amazon shield, Brazil. Precambrian Research 49, 329-354.

Martin, H., 1994. The Archean grey gneisses and the gneisses of continental crust. In: Condie, K.C. (Ed.), Developments in Precambrian Geology. Archean crustal Evolution, v.11. Elsevier, Amsterdam, pp. 205–259.

Moreto, C.P.N., Monteiro, L.V.S. Xavier, R.P., Amaral, W.S., Santos, T.J.S., Juliani, C., Souza Filho, C.R., 2011. Mesoarchean (3.0 and 2.86 Ga) host rocks of the iron oxide–Cu–Au Bacaba deposit, Carajás Mineral Province: U–Pb geochronology and metallogenetic implications. Mineralium Deposita, DOI 10.1007/s00126-011-0352-9.

Mougeot, R., Respaut, J.P., Brique, L., Ledru, P., Milesi J.P., Lerouge, C., Marcoux, E., Huhn, S.B., Macambira, M.J.B. 1996. Isotope geochemistry constrains for Cu, Au mineralizations and evolution of the Carajás Province (Para, Brazil). In: SBG, Congresso Brasileiro de Geologia, 39, Salvador, Anais, 7, 321-324 (in Portuguese).

Moyen, J.F., Martin, H., Jayananda, M., Auvray, B., 2003. Late Archean granites: A typology based on the Dharwar Craton (India). Precambrian Research 127, 103-123.

Moyen, J.F., Stevens, G., 2006. Experimental constraints on TTG petrogenesis: implications for Archean geodynamics. In: Benn, K., Mareschal, J.C., Condie, K.C. (Eds.), Archean geodynamics and environments. AGU, pp. 149–178.

Nisbet, E.G. 1987. The young Earth: an introduction to Archean geology. Boston, Allen and Unwin. 402p.

Nogueira, A.C.R., Truckenbrodt, W., Pinheiro, R.V.L., 1995. Formação Águas Claras, Pré-Cambriano da Serra dos Carajás: redescrição e redefinição litoestratigráfica. Boletim Museu Paraense Emílio Goeldi 7, 177-277 (in Portuguese).

O'Connor, J.T., 1965. A classification for quartz-rich igneous rocks based on feldspar rations. US Geological Survey Profissional Papers 525, 79–84.

Oliveira, E.M., Lafon, J.M., Gioia, S.M.C.L., Pimentel, M.M., 2008. Datação Sm-Nd em rocha total e granada do metamorfismo granulítico da região de Tartarugal Grande, Amapá Central. Revista Brasileira de Geologia 38(1), 114-127 (in Portuguese).

Oliveira, D.C., Santos, P.J.L., Gabriel, E.O., Rodrigues, D.S., Faresin, A.C., Silva, M.L.T., Sousa, S.D., Santos, R.V., Silva, A.C., Souza, M.C., Santos, R.D., Macambira, M.J.B., 2010. Aspectos geológicos e geocronológicos das rochas magmáticas e metamórficas da região entre os municípios de Água Azul do Norte e Canaã dos Carajás – Província Mineral de Carajás, In: SBG, Congresso Brasileiro de Geologia, 45, CDrom (in Portuguese).

Oliveira, M.A., Dall'Agnol, R., Althoff, F.J., Leite, A.A.S., 2009. Mesoarchean sanukitoid rocks of the Rio Maria Granite-Greenstone Terrane, Amazonian craton, Brazil. Journal of South American Earth Sciences 27, 146-160.

Oliveira, M.A., Dall'Agnol, R., Scaillet, B. 2010. Petrological Constraints on Crystallization Conditions of Mesoarchean Sanukitoid Rocks, Southeastern Amazonian Craton, Brazil. Journal of Petrology 51, 2121-2148.

Peccerillo, A., Taylor, S.R., 1976. Geochemistry of Eocene calc-alkaline volcanic rocks from the Kastamonu area, Northern Turkey. Contribution to Mineralogy and Petrology 58, 63-81.

Phillips, E.R., 1980. On polygenetic myrmekite. Geological Magazine 117(1), 29-36.

Pidgeon, R.T., Macambira, M.J.B., Lafon, J.M., 2000. Th-U-Pb isotopic systems and internal structures of complex zircons from an enderbite from the Pium Complex, Carajás Province, Brazil: evidence for the ages of granulites facies metamorphism and the protolith of the enderbite. Chemical Geology 166, 159-171.

Pinheiro, R.V.L., Holdsworth, R.E., 1997. Reactivation of Archean strike-slip fault systems, Amazon region, Brazil. Journal of the Geological Society 154, 99-103.

Rapopo, M., 2010. Petrogenesis of the Matok pluton, South Africa: implications on the heat source that induced regional metamorphism in the Southern Marginal Zone of the Limpopo Belt. University of Stellenbosch, South Africa, 117p. (Master thesis).

Ricci, P.S.F., Carvalho, M.A., 2006. Rocks of the Pium-Area, Carajás Block, Brazil – A Deep seated High-T Gabbroic Pluton (Charnockitoid-Like) with Xenoliths of Enderbitic Gneisses Dated at 3002 Ma – The Basement Problem Revisited. In: VIII Simpósio de Geologia da Amazônia, CDroom (in Portuguese).

Rollinson, H.R. 1993. A terrane interpretation of the Archean Limpopo Belt – Geological Magazine 130, 755-765.

Santos, J.O.S., Hartmann, L.A., Gaudette, H.E., Groves, D.I., McNaughton, N.J., Fletcher, I.R., 2000. A new understanding of the provinces of the Amazon Craton based on integration of field mapping and U-Pb and Sm-Nd geochronology. Gondwana Research 3, 453-488.

Santos, R.D., Geologia, petrografia e caracterização geoquímica das rochas máficas (granulitos?) do Complexo Pium – regiões de Vila Feitosa e Cedere III, Canaã dos Carajás – Província Mineral de Carajás. Undergraduate dissertation, Universidade Federal do Pará, Brazil, 73p. (in portuguese).

Santos, R.D., Oliveira, D.C., 2010. Geologia, petrografia e caracterização geoquímica das rochas máficas do Complexo Pium - Província mineral de Carajás. In: Congresso Brasileiro de Geologia, 45, CDrom (in Portuguese).

Sardinha, A.S., Dall'Agnol, R., Gomes, A.C.B., Macambira, M.J.B., Galarza, M.A., 2004. Geocronologia Pb-Pb e U-Pb em zircão de granitóides arqueanos da região de Canaã dos Carajás, Província Mineral de Carajás. In: Congresso Brasileiro de Geologia, 42, CDrom (in Portuguese).

Sardinha, A.S., Barros, C.E.M., Krymsky, R., 2006. Geology, Geochemistry, and U-Pb geochronology of the Archean (2.74 Ga) Serra do Rabo granite stocks, Carajás Province, northern Brazil. Journal of South American Earth Sciences 20, 327-339.

Silva, M.L.T., Oliveira, D.C., Macambira, M.J.B., 2010. Geologia, petrografia e geocronologia do magmatismo de alto K da região de Vila Jussara, Água Azul do Norte - Província Mineral de Carajás. In: SBG, Congresso Brasileiro de Geologia, 45, CDrom (in Portuguese).

Smithies, R.H., 2000. The Archean tonalite–trondhjemite–granodiorite (TTG) series is not an analogue of Cenozoic adakite. Earth and Planetary Science Letters 182, 115-125.

Smithies, R.H., Champion, D.C., 2000. The Archean high-Mg diorite suite: links to tonalite–trondhjemite–granodiorite magmatism and implications for early Archean crustal growth. Journal of Petrology 41 (12), 1653-1671.

Smithies, R.H., Howard, H.M., Evins, P.M., Kirkland, C.L., Kelsey, D.E., Hand, M., Wingate, M.T.D., Collins, A.S., Belousova, E. 2011. High-Temperature Granite Magmatism, Crust-Mantle Interaction and the Mesoproterozoic Intracontinental Evolution of the Musgrave Province, Central Australia. Journal of Petrology 52, 931-958.

Sousa, F.D.S., 2007. Estudo da alteração hidrotermal, com ênfase no metamorfismo sódico, de rochas granitóides e máficas da região de Canaã dos Carajás, Província Mineral de Carajás. Master thesis, Universidade Federal do Pará, Brazil, 195pp. (in portuguese).

Souza, M.C., Oliveira, D.C., Macambira, M.J.B., Galarza, M.A. 2010. Geologia, petrografia e geocronologia do granito de alto K da região de Velha Canadá, município de Água Azul do Norte - Província Mineral de Carajás. In: SBG, Congresso Brasileiro de Geologia, 45, CDrom (in Portuguese).

Souza, S.Z., Dall'Agnol, R., Althoff, F.J., Leite, A.A.S., Barros, C.E.M., 1996. Carajás mineral province: geological, geochronological and tectonic contrasts on the Archean evolution of the Rio Maria Granite- Greenstone Terrain and the Carajás block. In: Symposium Archean Terrane South American Platform, Brasília, extended abstracts, Brasília, SBG, pp. 31-32.

Souza, Z.S., Potrel, A., Lafon, J.M., Althoff, F.J., Pimentel, M.M., Dall'Agnol, R., Oliveira, C.G., 2001. Nd, Pb and Sr isotopes in the Identidade Belt, an Archean greenstone belt of Rio Maria region (Carajás Province, Brazil): implications for the geodynamic evolution of the Amazonian Craton. Precambrian Research 109, 293–315.

Stacey, J.S., Kramers, J.D., 1975. Approximation of terrestrial lead isotope evolution by a two stage model. Earth and Planetary Science Letters 26, 207-221.

Stern, R.A., Hanson, G.N., 1991. Archean high-Mg granodiorites: a derivative of light rare earth enriched monzodiorite of mantle origin. Journal of Petrology 32, 201-238.

Sylvester, P.J., 1989. Post-collisional alkaline granites. Journal of Geology 97, 261–280.

Sylvester, P.J., 1994. Archean granite plutons. In: Condie K. (ed.), Archean Crustal Evolution, Elsevier, Amsterdam, pp. 261–314.

Tallarico, F.H.B., Figueiredo, B.R., Groves, D.I., Kositcin, N., McNaughton, N.J., Fletcher, I.R., Rego, J.L., 2005. Geology and Shrimp U-Pb geochronology of the Igarapé Bahia deposit, Carajás Copper-Gold belt, Brazil: an Archean (2.57 Ga) example of iron-oxide Cu-Au-(U-REE) mineralization. Economic Geology 100, 7-28.

Tassinari, C.C.G., Macambira, M., 2004. A evolução tectônica do Craton Amazônico. In: Mantesso-Neto, V., Bartorelli, A., Carneiro, C.D.R., Brito Neves, B.B. (eds.). Geologia do Continente Sul Americano: Evolução da obra de Fernando Flávio Marques Almeida. São Paulo, p. 471-486 (in Portuguese).

Teixeira, J.B.G., Eggler, D.H., 1994. Petrology, geochemistry, and tectonic setting of Archean basaltic and dioritic rocks from the N4 iron deposit, Serra dos Carajás, Pará, Brazil. Acta Geology Leopoldensia 17, 71-114.

Trendall, A.F., Basei, M.A.S., Laeter, J.R., Nelson, D.R., 1998. SHRIMP zircon U–Pb constraints on the age of the Carajás formation, Grão Pará group, Amazon Craton. Journal of South American Earth Sciences 11, 265–277.

Vasquez, L.V., Rosa-Costa, L.R., Silva, C.G., Ricci, P.F., Barbosa, J.O., Klein, E.L., Lopes, E.S., Macambira, E.B., Chaves, C.L., Carvalho, J.M., Oliveira, J.G., Anjos, G.C., Silva, H.R., 2008. Geologia e Recursos Minerais do Estado do Pará: Sistema de Informações Geográficas – SIG: texto explicativo dos mapas Geológico e Tectônico e de Recursos Minerais do Estado do Pará, 328p (in Portuguese).

Vernon, R.H., 2004. A practical guide to rock microstructure, third ed., Cambridge University press, Cambridge, 954p.

Table A - Supplementary U–Pb on zircon LA-MC-ICPMS analytical data for the granitoids of the Canaã dos Carajás area.

		Isotopic ratios								Ages					
AMR-102	Th/U	6/4 ratio	7/6 ratio	1s(%)	7/5 ratio	1s(%)	6/8 ratio	1s(%)	Rho	7/6 age	1s(%)	7/5 age	1s(%)	6/8 age	1s(%)	Conc (%)
28-Z9N	0,49	41619	0,22068	0,70	17,94974	1,69	0,58991	1,54	0,91	2985,7	11,2	2987,0	16,2	2989,1	36,8	100,1
41-Z12	0,18	23210	0,21726	0,68	17,48368	1,76	0,58364	1,63	0,92	2960,5	10,9	2961,8	16,9	2963,6	38,7	100,1
44-Z12B	0,16	16648	0,21279	0,73	17,26768	1,53	0,58856	1,34	0,87	2926,9	11,9	2949,8	14,7	2983,6	32,1	101,9
57-Z16N	0,22	8216	0,21687	0,91	17,71806	2,39	0,59255	2,21	0,92	2957,6	14,7	2974,6	22,9	2999,7	52,9	101,4
70-Z19B	0,20	14202	0,21491	0,85	17,35276	1,40	0,58562	1,12	0,78	2942,9	13,7	2954,5	13,5	2971,6	26,6	101,0
37-Z11N[2]	0,20	53542	0,20340	0,86	15,81130	1,23	0,56379	0,88	0,69	2853,7	13,9	2865,5	11,7	2882,3	20,4	101,0
69-Z19N¨	0,26	9233	0,22596	0,95	19,10705	2,19	0,61328	1,98	0,90	3023,7	15,3	3047,2	21,2	3083,1	48,5	102,0
04-Z1N*"	0,13	303	0,20609	0,57	14,28272	1,13	0,50263	0,96	0,85	2875,1	9,2	2768,7	10,6	2625,1	20,9	91,3
07-Z1B"*	0,13	1921	0,22259	1,11	17,43564	1,45	0,56812	0,93	0,62	2999,5	17,8	2959,1	13,9	2900,1	21,7	96,7
08-Z2"*	0,43	291596	0,20267	0,51	17,27087	0,95	0,61805	0,80	0,82	2847,8	8,4	2950,0	9,1	3102,2	19,7	108,9
16-Z5"*	0,19	39355	0,20457	0,83	14,88275	1,35	0,52765	1,06	0,78	2863,0	13,5	2807,8	12,8	2731,5	23,7	95,4
48-Z14"*	0,26	55122	0,21020	0,80	17,96988	1,15	0,62004	0,82	0,69	2907,1	13,0	2988,1	11,0	3110,1	20,3	107,0
49-Z14B"*	0,17	93659	0,21246	0,79	15,98196	1,26	0,54556	0,98	0,76	2924,4	12,7	2875,7	12,0	2806,7	22,3	96,0
56-Z16"*	0,20	21601	0,21318	0,98	15,55454	2,30	0,52920	2,09	0,90	2929,8	15,8	2849,8	22,0	2738,1	46,5	93,5
73-Z20[1]	0,21	3093	0,25473	2,25	24,51958	5,66	0,69813	5,19	0,92	3214,4	35,6	3289,3	55,2	3413,6	137,6	106,2
11-Z3N"	0,16	1313	0,19467	1,31	7,08415	1,83	0,26393	1,28	0,69	2782,0	21,5	2122,1	16,3	1509,9	17,2	54,3
12-Z3B"	0,17	5048	0,19202	0,63	1,45128	3,65	0,05482	3,60	0,98	2759,6	10,3	910,4	21,9	344,0	12,0	12,5
15-Z4"	0,22	2046	0,19410	0,83	9,41254	1,31	0,35171	1,01	0,76	2777,2	13,6	2379,1	12,0	1942,8	17,0	70,0
19-Z6N"	0,10	84565	0,20315	0,89	17,93629	1,89	0,64035	1,66	0,88	2851,7	14,6	2986,3	18,1	3190,4	41,8	111,9
20-Z6B"	0,02	84	0,18185	0,88	6,98187	1,37	0,27846	1,04	0,75	2669,8	14,6	2109,1	12,1	1583,6	14,6	59,3
24-Z7"	0,20	218	0,20515	2,35	13,26053	2,80	0,46880	1,53	0,54	2867,6	38,2	2698,4	26,4	2478,3	31,4	86,4
25-Z8"	0,18	420	0,16584	0,82	3,62325	1,59	0,15846	1,36	0,85	2516,1	13,8	1554,7	12,6	948,2	12,0	37,7
29-Z9B"	0,05	57	0,12729	2,17	1,93651	2,62	0,11034	1,47	0,55	2060,8	38,3	1093,8	17,6	674,7	9,4	32,7
32-Z10B"	0,21	75025	0,20913	0,99	18,82131	1,50	0,65274	1,13	0,74	2898,8	16,1	3032,7	14,5	3238,9	28,8	111,7
33-Z10N"	0,07	22627	0,19787	1,06	17,70956	1,98	0,64912	1,67	0,84	2808,7	17,3	2974,1	19,0	3224,8	42,4	114,8
36-Z11B"	0,09	125	0,48149	4,24	26,13456	7,04	0,39367	5,63	0,80	4185,5	62,6	3351,6	68,9	2139,8	102,5	51,1
45-Z13"	0,07	30	0,18328	0,96	4,73318	2,26	0,18730	2,05	0,90	2682,7	15,8	1773,1	19,0	1106,7	20,9	41,3
52-Z15"	0,13	898	0,13794	0,71	5,38694	1,16	0,28324	0,92	0,77	2201,5	12,3	1882,8	9,9	1607,7	13,1	73,0
53-Z15B"	0,19	7960	0,11055	0,76	3,99529	2,14	0,26211	2,00	0,93	1808,5	13,8	1633,2	17,4	1500,6	26,8	83,0
61-Z17B"	0,01	9	0,19827	0,75	4,28055	1,59	0,15658	1,40	0,88	2812,0	12,3	1689,6	13,1	937,8	12,3	33,3
62-Z17N"	0,12	107	0,22325	1,48	9,63540	2,25	0,31302	1,70	0,75	3004,3	23,7	2400,6	20,7	1755,6	26,1	58,4
65-Z18N"	0,50	192	0,28107	1,26	19,62262	2,39	0,50634	2,03	0,85	3368,9	19,6	3072,9	23,1	2641,0	44,1	78,4
66-Z18B"	0,01	10	0,21280	0,72	5,17617	1,39	0,17642	1,19	0,85	2927,0	11,6	1848,7	11,9	1047,4	11,5	35,8
74-Z20B"	0,22	327	0,17826	1,10	4,91256	1,50	0,19987	1,02	0,66	2636,8	18,2	1804,4	12,6	1174,6	11,0	44,5
77-Z21N"	0,14	4154	0,10579	2,23	1,48740	7,05	0,10197	6,69	0,95	1728,1	41,0	925,3	42,8	626,0	39,9	36,2
78-Z21B"	0,01	375	0,10466	1,38	1,72532	2,26	0,11956	1,79	0,79	1708,3	25,4	1018,0	14,5	728,0	12,3	42,6

Geographic coordinates = 9273289/628938

" discordance > 10%; "* discordance > 3%; [1] high error > 3%; [2] younger age; ¨inherited zircon

		Isotopic ratios								Ages					
AER-11A	Th/U	6/4 ratio	7/6 ratio	1s(%)	7/5 ratio	1s(%)	6/8 ratio	1s(%)	Rho	7/6 age	1s(%)	7/5 age	1s(%)	6/8 age	1s(%)	Conc (%)
05-Z1N	0,09	21043	0,20757	1,48	16,67551	2,04	0,58267	1,41	0,68	2886,6	24,0	2916,4	19,6	2959,6	33,5	102,5
18-Z5	0,22	32118	0,21311	0,88	17,20264	1,98	0,58545	1,77	0,89	2929,4	14,3	2946,2	19,0	2970,9	42,2	101,4
20-Z7B	0,12	20727	0,21122	0,75	17,07192	2,25	0,58621	2,13	0,94	2914,9	12,1	2938,9	21,6	2974,0	50,7	102,0
30-Z11N	0,13	36237	0,21438	0,70	16,91967	1,51	0,57241	1,34	0,88	2939,0	11,3	2930,3	14,5	2917,7	31,4	99,3
32-Z12N	0,04	13137	0,21306	0,76	16,92749	2,41	0,57621	2,29	0,95	2929,0	12,3	2930,7	23,1	2933,3	53,9	100,1
38-Z14B	0,04	41679	0,20924	0,64	16,47991	1,34	0,57122	1,18	0,87	2899,7	10,4	2905,1	12,8	2912,8	27,6	100,5
54-Z21	0,13	75580	0,20944	0,62	16,93366	1,00	0,58639	0,79	0,76	2901,2	10,1	2931,1	9,6	2974,8	18,7	102,5
17-Z4[2]	0,06	157646	0,20081	0,93	15,11850	1,87	0,54603	1,62	0,86	2832,8	15,1	2822,7	17,8	2808,6	36,9	99,1
33-Z12B[2]	0,07	652	0,20810	0,84	16,01323	1,40	0,55809	1,12	0,79	2890,8	13,6	2877,6	13,4	2858,7	25,9	98,9
51-Z19B[2]	0,17	60342	0,20703	0,61	15,89646	1,09	0,55689	0,91	0,81	2882,4	9,9	2870,6	10,4	2853,8	20,9	99,0
58-Z23B[2]	0,07	5953	0,20600	0,85	15,85891	2,07	0,55836	1,89	0,92	2874,3	13,8	2868,3	19,8	2859,8	43,7	99,5
27-Z10B"*	0,05	29681	0,20801	0,82	14,99406	1,32	0,52280	1,03	0,85	2890,1	13,3	2814,9	12,5	2711,1	22,7	93,8
48-Z17N"*	0,18	36179	0,22071	0,76	16,88474	1,64	0,55485	1,45	0,88	2985,9	12,3	2928,3	15,7	2845,3	33,5	95,3
55-Z21B"*	0,04	194337	0,20297	0,59	17,15680	0,91	0,61307	0,69	0,72	2850,2	9,6	2943,6	8,7	3082,3	17,0	108,1
19-Z6N[1]	0,07	16022	0,21391	0,91	17,95089	3,10	0,60863	2,97	0,96	2935,4	14,7	2987,1	29,9	3064,5	72,4	104,4
04-Z1B"	0,12	29576	0,19946	1,98	12,54431	2,91	0,45613	2,13	0,73	2821,8	32,0	2646,1	27,0	2422,4	42,9	85,8
06-Z1B2"	0,07	26852	0,19763	1,35	12,19059	1,87	0,44738	1,29	0,73	2806,7	21,9	2619,2	17,4	2383,6	25,7	84,9
12-Z2N2"	0,08	8300	0,21574	1,11	10,49542	5,21	0,35283	5,08	0,98	2949,2	17,8	2479,5	47,2	1948,1	85,0	66,1
13-Z2B"	0,05	14394	0,21529	0,75	8,05038	2,04	0,27120	1,90	0,93	2945,8	12,1	2236,7	18,3	1546,9	26,1	52,5
14-Z3I"	0,01	23661	0,21048	0,77	14,49962	1,68	0,49963	1,49	0,89	2909,2	12,4	2783,0	15,8	2612,2	32,0	89,8
15-Z3N"	0,05	30211	0,20346	1,14	4,21538	3,95	0,15027	3,78	0,97	2854,1	18,4	1677,0	31,9	902,5	31,8	31,6
24-Z8N"	0,15	11627	0,19987	1,10	12,71520	2,37	0,46140	2,09	0,88	2825,1	17,9	2658,8	22,0	2445,7	42,5	86,6
25-Z8B"	0,12	10183	0,19316	0,69	9,73502	1,91	0,36553	1,78	0,93	2769,2	11,2	2410,0	17,4	2008,3	30,7	72,5
26-Z9N"	0,04	12663	0,20346	0,93	8,63533	3,11	0,30782	2,96	0,98	2854,2	15,1	2300,3	27,9	1729,9	44,8	60,6
31-Z11B"	0,03	149180	0,15683	1,27	3,29761	5,87	0,15250	5,74	0,98	2421,8	21,5	1480,5	45,8	915,0	48,9	37,8
37-Z13B"	0,02	43938	0,18767	0,72	7,65177	2,29	0,29571	2,18	0,95	2721,9	11,9	2191,0	20,4	1670,0	32,0	61,4
38-Z13B2"	0,02	856	0,16163	0,68	4,52930	1,65	0,20325	1,47	0,91	2472,7	11,4	1736,4	13,6	1192,7	16,3	48,2
42-Z14N"	0,02	17372	0,12693	0,91	2,09056	1,82	0,11945	1,57	0,86	2055,9	16,0	1145,7	12,4	727,4	10,8	35,4
43-Z15"	0,08	56597	0,20343	0,62	13,23917	1,07	0,47199	0,87	0,79	2854,0	10,1	2696,9	10,0	2492,3	18,0	87,3
44-Z16"	0,06	34247	0,19095	0,94	10,31612	2,18	0,39183	1,97	0,94	2750,4	15,3	2463,6	20,0	2131,3	35,7	77,5
45-Z16N"	0,06	10673	0,20746	1,63	7,90106	3,70	0,27622	3,32	0,96	2885,8	26,2	2219,8	32,8	1572,3	46,2	54,5
49-Z17B"	0,22	83431	0,20006	0,66	13,21816	1,69	0,47919	1,56	0,92	2826,7	10,7	2695,4	15,9	2523,7	32,5	89,3
50-Z18"	0,04	1994	0,17582	1,02	4,63455	3,50	0,19118	3,32	0,96	2613,8	17,0	1755,5	28,8	1127,8	34,5	43,1
56-Z22B"	0,22	522	0,14912	0,75	4,44191	1,89	0,21604	1,67	0,91	2335,9	12,8	1720,2	15,5	1260,9	19,8	54,0
57-Z23"	0,08	21246	0,19186	0,88	10,64044	1,81	0,40222	1,59	0,91	2758,2	14,3	2492,2	16,7	2179,3	29,3	79,0
62-Z24"	0,05	1670	0,17458	0,82	7,54598	1,67	0,31349	1,45	0,86	2602,0	13,7	2178,5	14,9	1757,9	22,4	67,6
63-Z25N"	0,03	9846	0,19796	0,73	8,97133	1,52	0,32869	1,33	0,87	2809,4	11,9	2335,1	13,8	1832,0	21,2	65,2
64-Z25B"	0,07	1652	0,15794	0,85	5,02210	1,27	0,23061	0,94	0,81	2433,8	14,3	1823,1	10,7	1337,7	11,4	55,0
65-Z26"	0,06	14637	0,19113	0,73	11,56099	2,90	0,43871	2,80	0,98	2751,9	12,0	2569,5	26,8	2344,9	54,9	85,2

Geographic coordinates = 9290489/626932

" discordance > 10%; "* discordance > 5%; [1] high error > 3%; [2] younger age; ¨inherited zircon

		Isotopic ratios								Ages						
GRD-79C	Th/U	6/4 ratio	7/6 ratio	1s(%)	7/5 ratio	1s(%)	6/8 ratio	1s(%)	Rho	7/6 age	1s(%)	7/5 age	1s(%)	6/8 age	1s(%)	Conc (%)
04-Z1N	0,06	877	0,21	0,59	16,43	2,41	0,58	2,32	0,97	2876,15	9,58	2902,25	22,81	2940,03	54,91	102,22
19-Z4N	0,06	2180	0,19	2,27	8,15	3,11	0,32	2,12	0,68	2700,25	36,96	2247,55	27,77	1784,96	33,15	66,10
24-Z6N	0,06	188433	0,20	0,46	16,78	0,72	0,61	0,55	0,70	2834,20	7,54	2922,15	6,85	3051,54	13,30	107,67
32-Z9	0,10	910	0,19	0,73	11,50	1,72	0,45	1,55	0,90	2714,37	11,91	2564,54	15,98	2379,37	31,05	87,66
35-Z10N	0,06	72045	0,20	0,65	16,14	1,28	0,59	1,10	0,85	2810,24	10,66	2885,13	12,13	2993,64	26,19	106,53
43-Z12N	0,06	153337	0,20	0,60	15,49	0,99	0,56	0,79	0,77	2832,08	9,85	2846,14	9,45	2866,05	18,18	101,20
44-Z12B	0,00	134589	0,20	0,78	16,43	1,20	0,59	0,91	0,74	2844,57	12,76	2901,90	11,47	2985,24	21,67	104,95
52-Z14N	0,08	74674	0,19	1,23	10,40	2,71	0,40	2,41	0,89	2734,36	20,18	2470,68	25,07	2163,14	44,34	79,11
59-Z16N	0,09	75796	0,20	0,86	16,66	1,32	0,61	1,01	0,74	2822,86	13,94	2915,31	12,59	3051,10	24,40	108,09
71-Z19N	0,08	79529	0,19	1,13	11,81	2,07	0,45	1,73	0,83	2742,90	18,64	2589,65	19,40	2398,37	34,74	87,44
91-Z25N	0,13	36311	0,20	0,96	16,00	1,39	0,57	1,00	0,71	2849,02	15,59	2876,58	13,26	2916,12	23,57	102,36
16-Z3[2]	0,07	3522	0,19	2,25	13,39	3,19	0,52	2,27	0,71	2718,33	37,09	2707,21	30,17	2692,34	49,87	99,04
09-Z2N"	0,06	119063	0,20	0,76	16,48	1,09	0,61	0,78	0,68	2786,92	12,41	2904,79	10,38	3077,90	19,06	110,44
10-Z2B"	0,10	163	0,19	0,98	10,79	2,55	0,40	2,32	0,92	2775,29	16,03	2505,63	23,42	2186,66	43,47	78,79
20-Z4B"	0,01	128875	0,19	1,26	11,86	1,92	0,44	1,45	0,75	2779,51	20,47	2593,78	17,84	2362,78	28,67	85,01
23-Z5B"	0,04	230	0,12	1,36	2,31	2,26	0,13	1,66	0,77	2022,90	23,95	1216,69	15,88	814,78	13,76	40,28
27-Z6B"	0,04	58219	0,20	0,48	9,96	1,21	0,36	1,11	0,91	2830,57	7,79	2430,91	11,11	1982,87	18,95	70,05
28-Z7B"	0,04	1400	0,20	0,77	10,61	1,66	0,38	1,47	0,88	2854,79	12,46	2489,59	15,30	2067,25	26,00	72,41
31-Z8"	0,09	191	0,16	0,85	3,39	1,59	0,16	1,22	0,81	2409,57	14,44	1502,11	12,36	945,14	11,73	39,22
36-Z10B"	0,02	107971	0,19	0,59	16,16	0,90	0,60	0,68	0,71	2783,61	9,70	2886,03	8,58	3035,10	16,37	109,03
40-Z11"	0,05	555	0,19	0,55	9,18	1,97	0,35	1,87	0,96	2759,59	8,95	2355,81	17,84	1918,37	31,25	69,52
47-Z13N"	0,08	107540	0,20	0,92	16,35	1,37	0,61	1,02	0,73	2791,11	14,93	2897,52	13,03	3053,12	24,73	109,39
48-Z14B"	0,08	127	0,17	1,19	8,97	2,25	0,38	1,89	0,84	2558,93	19,74	2334,68	20,38	2086,90	34,05	81,55
51-Z14B"	0,03	102044	0,19	1,19	16,91	2,19	0,63	1,84	0,84	2773,92	19,41	2929,93	20,82	3162,42	45,89	114,01
56-Z15"	0,09	118	0,14	1,09	3,29	1,93	0,17	1,56	0,81	2190,12	18,77	1478,09	14,92	1034,04	15,23	47,21
60-Z16B"	0,10	108	0,17	0,84	8,29	1,31	0,36	0,97	0,73	2524,17	14,11	2263,25	11,81	1986,05	17,12	78,68
63-Z17N"	0,04	8344	0,21	0,97	9,55	1,82	0,33	1,53	0,84	2898,21	15,74	2392,63	16,69	1845,23	24,62	63,67
64-Z17B"	0,05	6519	0,20	0,72	10,56	1,91	0,38	1,77	0,92	2843,93	11,80	2485,09	17,71	2070,46	31,29	72,80
67-Z18N"	0,14	33051	0,22	0,80	15,35	1,35	0,52	1,09	0,80	2948,48	12,85	2837,13	12,89	2683,06	24,00	91,00
68-Z18B"	0,20	111	0,17	0,95	7,77	1,86	0,33	1,53	0,84	2578,94	15,81	2204,34	16,61	1824,54	25,39	70,75
72-Z19B"	0,10	93	0,17	1,25	9,22	1,62	0,39	0,99	0,60	2580,74	20,81	2360,42	14,75	2113,97	18,50	81,91
74-Z20N"	0,38	276174	0,20	1,75	16,93	2,20	0,63	1,34	0,60	2785,90	28,36	2930,95	20,91	3146,84	33,28	112,96
75-Z20B"	0,05	123983	0,19	2,02	16,28	2,38	0,61	1,25	0,52	2777,76	32,78	2893,48	22,51	3062,68	30,48	110,26
79-Z21"	0,19	289	0,17	1,20	9,51	1,96	0,40	1,51	0,77	2567,32	20,00	2388,41	17,84	2184,40	28,55	85,08
82-Z22"	0,17	1412	0,16	1,39	7,41	1,83	0,33	1,17	0,63	2481,10	23,32	2162,22	16,22	1842,66	18,91	74,27
83-Z22B"	0,13	445	0,20	0,78	10,74	1,18	0,40	0,89	0,73	2788,71	12,64	2500,94	10,94	2162,23	16,42	77,54
86-Z23N"	0,38	2720	0,21	0,92	18,33	1,32	0,64	0,95	0,70	2885,01	14,78	3007,33	12,67	3193,71	24,06	110,70
87-Z23B"	0,11	32	0,18	0,66	9,98	1,18	0,39	0,94	0,80	2694,14	10,83	2432,77	10,86	2132,79	17,83	79,16
90-Z24"	0,47	64115	0,21	0,63	17,70	1,07	0,61	0,87	0,79	2919,56	10,19	2973,83	10,25	3054,74	21,04	104,63
91-Z25B"	0,06	2381426	0,20	0,70	17,21	1,10	0,63	0,85	0,75	2804,84	11,36	2946,69	10,46	3158,90	21,07	112,62

Geographic coordinates = 9290740/633473

"not utilized for calculed upper intercepts age

		Isotopic ratios								Ages						
ARC-65	Th/U	6/4 ratio	7/6 ratio	1s(%)	7/5 ratio	1s(%)	6/8 ratio	1s(%)	Rho	7/6 age	1s(%)	7/5 age	1s(%)	6/8 age	1s(%)	Conc (%)
04-Z1	0,47	7274	0,20619	1,52	15,92448	2,78	0,56013	2,33	0,83	2875,9	24,8	2872,3	26,6	2867,2	53,9	99,7
05-Z2	0,43	12921	0,20649	1,51	16,00804	2,40	0,56226	1,87	0,77	2878,2	24,5	2877,3	23,0	2876,0	43,4	99,9
06-Z3B	0,40	36698	0,20240	1,51	15,63130	2,57	0,56013	2,08	0,81	2845,6	24,6	2854,5	24,5	2867,2	48,2	100,8
09-Z4B	0,57	146160	0,20132	1,58	15,64381	2,35	0,56359	1,75	0,74	2836,9	25,7	2855,3	22,5	2881,4	40,6	101,6
39-Z21	0,44	6739	0,20146	1,54	15,65075	2,37	0,56344	1,81	0,76	2838,0	25,1	2855,7	22,6	2880,8	42,0	101,5
40-Z22	0,46	38875	0,19765	1,24	15,22228	2,02	0,55857	1,59	0,78	2806,9	20,3	2829,2	19,2	2860,7	36,7	101,9
41-Z23	0,84	5659	0,19962	1,19	15,52558	2,36	0,56407	2,04	0,86	2823,1	19,4	2848,1	22,5	2883,4	47,4	102,1
42-Z24	0,96	19362	0,19931	1,17	15,52154	2,17	0,56481	1,83	0,84	2820,6	19,1	2847,8	20,7	2886,5	42,5	102,3
44-Z25N	0,53	5045	0,20836	1,27	15,96219	2,43	0,55561	2,07	0,85	2892,9	20,7	2874,5	23,2	2848,5	47,7	98,5
29-Z17[2]	0,64	3719	0,19080	1,79	13,82525	2,92	0,52552	2,31	0,79	2749,1	29,5	2737,8	27,7	2722,5	51,2	99,0
30-Z17B[2]	0,62	12286	0,18601	1,92	13,11260	2,88	0,51127	2,16	0,74	2707,2	31,6	2687,8	27,2	2662,0	47,0	98,3
37-Z20[2]	0,56	3694	0,19146	1,63	13,50541	2,89	0,51160	2,38	0,82	2754,7	26,7	2715,7	27,3	2663,4	52,0	96,7
36-Z19¨	0,95	33480	0,22014	1,68	18,31236	2,35	0,60332	1,64	0,69	2981,7	27,0	3006,3	22,6	3043,2	39,9	102,1
07-Z3N"*	0,62	35610	0,20018	1,51	13,62096	2,94	0,49350	2,53	0,86	2827,7	24,6	2723,7	27,8	2585,8	53,8	91,4
31-Z18"*	0,59	8056	0,19320	2,02	15,00280	2,93	0,56320	2,12	0,72	2769,6	32,7	2815,4	27,5	2879,8	49,1	104,0
38-Z20B"*	0,35	37656	0,19485	1,50	12,88019	3,24	0,47942	2,87	0,89	2783,5	24,6	2670,9	30,5	2524,8	59,9	90,7
25-Z13[1]	0,72	1836	0,19931	2,86	13,48966	6,99	0,49088	6,38	0,91	2820,5	46,7	2714,6	66,1	2574,5	135,3	91,3
43-Z25N[1]	0,54	5217	0,20630	1,59	15,97937	4,12	0,56176	3,80	0,92	2876,7	25,9	2875,6	39,3	2873,9	88,0	99,9
08-Z4N"	0,49	888	0,20518	3,40	2,93112	92,07	0,10361	90,38	1,00	2867,8	54,3	1390,0	530,7	635,5	534,1	22,2
10-Z5N"	0,44	8326	0,19893	3,31	16,95258	4,80	0,61808	3,48	0,84	2817,4	54,0	2932,2	46,0	3102,3	85,6	110,1
11-Z6N"	0,18	914	0,17488	3,28	16,39747	9,75	0,68004	9,18	0,94	2604,9	54,6	2900,3	93,3	3344,5	239,7	128,4
12-Z6B"	0,82	1012	0,20397	6,48	17,71808	43,32	0,63003	42,84	0,99	2858,2	105,5	2974,6	416,4	3149,7	1067,3	110,2
13-Z7N"	1,05	1156	0,19621	2,72	10,61893	17,97	0,39252	17,76	0,99	2794,9	44,6	2490,4	166,7	2134,5	322,7	76,4
14-Z7B"	0,33	1935	0,22001	45,32	20,95712	57,14	0,69085	34,80	0,84	2980,8	729,7	3136,6	553,8	3385,9	916,5	113,6
15-Z8"	0,15	290	0,21042	6,01	8,78115	106,82	0,30267	106,65	1,00	2908,7	97,3	2315,5	973,8	1704,5	1597,4	58,6
19-Z9N"	0,75	3135	0,18110	3,05	9,23623	17,08	0,36990	16,81	0,98	2662,9	50,6	2361,7	156,5	2028,9	292,5	76,2
20-Z9B"	0,40	1187	0,16169	3,37	5,22767	9,52	0,23450	8,90	0,94	2473,4	56,9	1857,1	81,1	1358,0	109,0	54,9
21-Z10B"	0,56	3174	0,22521	2,49	13,17115	9,45	0,42417	9,12	0,96	3018,3	40,0	2692,0	89,2	2279,4	175,1	75,5
22-Z12N"	0,29	414	0,21127	18,10	2,39456	226,31	0,08220	225,59	1,00	2915,3	293,1	1241,0	1621,0	509,3	1104,6	17,5
23-Z12N"	0,37	1045	0,19342	3,97	10,81623	12,72	0,40557	12,08	0,95	2771,5	65,2	2507,5	118,2	2194,6	224,8	79,2
24-Z12N"	0,68	10289	0,18975	2,23	11,20441	6,22	0,42825	5,81	0,93	2740,0	36,7	2540,3	58,0	2297,8	112,3	83,9
26-Z14"	0,29	875	0,24173	7,90	2,39324	168,84	0,07181	168,66	1,00	3131,4	125,6	1240,6	1209,1	447,0	728,4	14,3
27-Z15"	0,61	356	0,26007	6,45	5,41039	37,66	0,15088	37,11	0,99	3247,1	101,6	1886,5	322,8	905,9	313,6	27,9
28-16"	0,86	3244	0,20321	2,42	13,16054	15,19	0,46971	15,00	0,99	2852,2	39,4	2691,2	143,4	2482,3	309,0	87,0
35-Z18B"	0,64	15861	0,18372	1,94	10,57837	2,74	0,41761	1,94	0,70	2686,7	32,0	2486,8	25,4	2249,6	36,9	83,7

Geographic coordinates = 9292330/626105

" discordance > 10%; "* discordance > 5%; [1] high error > 3%; [2] younger age; ¨inherited zircon

		Isotopic ratios								Ages						
ARC-95A	Th/U	6/4 ratio	7/6 ratio	1s(%)	7/5 ratio	1s(%)	6/8 ratio	1s(%)	Rho	7/6 age	1s(%)	7/5 age	1s(%)	6/8 age	1s(%)	Conc (%)
03-Z1	0,40	108169	0,21	0,58	13,90	1,50	0,49	1,39	0,92	2873,74	9,39	2742,81	14,24	2568,54	29,40	89,38
11-Z5	0,50	79528	0,20	0,51	15,94	1,28	0,57	1,18	0,91	2862,64	8,37	2873,14	12,27	2888,12	27,38	100,89
12-Z6	0,58	205513	0,20	0,71	15,09	1,33	0,54	1,13	0,84	2861,84	11,48	2820,72	12,69	2763,54	25,41	96,57
17-Z9	0,28	132526	0,21	0,60	15,17	2,17	0,53	2,08	0,96	2884,54	9,78	2825,84	20,63	2744,29	46,48	95,14
18-Z10	0,30	70085	0,20	0,80	14,91	3,50	0,54	3,41	0,97	2828,00	13,06	2809,69	33,29	2784,24	77,01	98,45
19-Z11	0,56	84246	0,20	1,38	13,74	2,10	0,50	1,58	0,75	2812,84	22,48	2731,82	19,85	2623,59	34,13	93,27
23-Z12	0,51	47130	0,20	0,62	14,00	1,19	0,50	1,01	0,84	2853,63	10,07	2749,94	11,25	2610,95	21,75	91,50
24-Z13	0,33	56115	0,20	0,72	13,92	1,30	0,50	1,08	0,82	2830,92	11,82	2744,23	12,35	2627,97	23,38	92,83
25-Z14	0,29	67648	0,20	1,09	15,01	1,80	0,54	1,44	0,79	2833,14	17,72	2816,17	17,16	2792,53	32,60	98,57
29-Z16	0,39	46862	0,20	0,74	15,75	1,83	0,56	1,68	0,91	2859,41	12,07	2861,51	17,52	2864,49	38,81	100,18
30-Z17	0,41	48579	0,20	0,82	15,81	1,76	0,57	1,56	0,88	2844,39	13,31	2865,42	16,82	2895,42	36,41	101,79
36-Z21	0,44	57869	0,20	0,71	15,84	1,35	0,57	1,15	0,84	2837,97	11,56	2867,22	12,90	2909,04	26,90	102,50
26-Z15	0,11	38813	0,18	1,64	12,52	2,82	0,51	2,29	0,83	2649,58	27,26	2644,40	26,53	2637,63	49,65	99,55
04-Z2"	0,17	171707	0,24	1,48	12,12	2,98	0,36	2,59	0,87	3131,31	23,55	2613,44	27,95	1998,95	44,43	63,84
05-Z3"	0,35	77536	0,22	1,67	11,62	3,76	0,38	3,37	0,90	3012,11	26,82	2574,21	35,15	2055,85	59,28	68,25
06-Z4"	0,12	13816	0,24	4,45	8,14	6,10	0,24	4,16	0,85	3131,45	70,82	2246,17	55,13	1407,85	52,66	44,96
13-Z7"	0,08	21240	0,23	1,73	12,22	2,45	0,39	1,73	0,70	3027,19	27,76	2621,40	23,00	2129,06	31,45	70,33
14-Z8"	0,10	47737	0,19	1,50	10,03	2,52	0,38	2,02	0,82	2737,71	24,76	2437,73	23,29	2094,84	36,21	76,52
31-Z18"	0,22	450	0,22	1,21	10,64	2,26	0,35	1,91	0,84	2994,19	19,46	2492,44	20,96	1924,68	31,73	64,28
32-Z19"	0,15	10614	0,21	2,04	10,67	2,75	0,37	1,84	0,75	2908,45	33,09	2494,55	25,51	2018,76	31,86	69,41
35-Z20"	0,14	30013	0,19	0,37	9,35	1,09	0,36	1,03	0,94	2710,34	6,09	2372,65	10,02	1999,97	17,68	73,79
37-Z22"	0,19	32350	0,18	1,11	7,38	2,28	0,30	1,99	0,87	2646,23	18,46	2159,13	20,42	1685,09	29,57	63,68
38-Z23"	0,16	25614	0,19	1,49	10,14	2,60	0,39	2,13	0,85	2711,03	24,56	2447,64	24,00	2143,47	38,79	79,06

" Discordance > 11%

		Isotopic ratios								Ages						
ARC-100	Th/U	6/4 ratio	7/6 ratio	1s(%)	7/5 ratio	1s(%)	6/8 ratio	1s(%)	Rho	7/6 age	1s(%)	7/5 age	1s(%)	6/8 age	1s(%)	Conc (%)
29-Z18	0,39	1158	0,16	1,18	5,05	2,19	0,22	1,82	0,83	2494,04	19,76	1827,80	18,39	1301,81	21,70	52,20
04-Z2	0,45	51762	0,19	1,15	10,46	3,03	0,39	2,81	0,92	2777,69	18,70	2476,81	27,73	2127,07	50,67	76,58
05-Z3	0,34	2378	0,16	1,24	5,59	2,84	0,25	2,54	0,90	2499,69	20,67	1914,95	24,18	1422,85	32,57	56,92
16-Z9	0,13	235672	0,21	0,83	15,91	1,27	0,56	0,96	0,74	2883,49	13,46	2871,61	12,05	2854,69	22,03	99,00
21-Z12	0,38	136753	0,21	0,91	12,84	1,55	0,45	1,25	0,80	2872,87	14,75	2668,24	14,47	2406,77	25,04	83,78
23-Z14	0,62	45078	0,16	1,03	5,28	1,53	0,23	1,13	0,73	2505,82	17,17	1865,53	12,98	1346,53	13,78	53,74
27-Z16	0,07	2461	0,18	0,69	6,33	1,24	0,26	1,02	0,82	2632,97	11,36	2022,28	10,79	1479,75	13,60	56,20
28-Z17	0,28	60526	0,19	0,90	9,52	1,54	0,37	1,25	0,80	2698,57	14,75	2389,25	14,04	2043,72	21,84	75,73
36-Z22	0,23	7697	0,21	1,48	13,03	2,64	0,45	2,17	0,84	2923,83	23,82	2681,95	24,55	2373,07	43,08	81,16
40-Z24	0,29	67117	0,17	0,89	7,29	1,81	0,31	1,57	0,87	2583,33	14,85	2147,71	16,13	1722,53	23,76	66,68
41-Z25	0,16	1774	0,19	1,19	9,08	2,13	0,35	1,76	0,82	2712,03	19,65	2346,25	19,47	1949,20	29,66	71,87
46-Z28	0,51	126869	0,17	1,30	6,23	3,75	0,26	3,52	0,94	2595,47	21,73	2008,18	32,82	1488,27	46,76	57,34
47-Z29	0,59	80212	0,18	1,37	7,98	2,12	0,32	1,61	0,76	2658,06	22,74	2229,19	19,12	1793,05	25,28	67,46
03-Z1¨	0,65	106498	0,24	1,22	19,97	3,84	0,61	3,64	0,95	3089,93	19,45	3089,72	37,10	3089,40	89,30	99,98
15-Z8¨	0,55	131886	0,23	0,69	19,30	1,36	0,61	1,17	0,85	3060,52	11,01	3057,12	13,07	3051,95	28,49	99,72
17-Z10¨	0,39	118890	0,23	1,18	18,53	1,71	0,59	1,24	0,71	3026,54	18,86	3017,55	16,37	3004,07	29,66	99,26
22-Z13	0,18	676	0,17	0,92	5,55	1,59	0,24	1,28	0,80	2528,23	15,41	1909,15	13,57	1392,86	16,16	55,09
48-Z30	0,69	817	0,20	1,64	11,59	2,33	0,42	1,65	0,72	2826,27	26,75	2571,89	21,76	2261,77	31,54	80,03
10-Z6"	0,48	19	0,12	1,36	1,48	2,34	0,09	1,71	0,78	1883,17	24,21	922,47	14,08	574,47	10,47	30,51
24-Z15"	0,71	150	0,10	2,51	1,67	3,08	0,12	1,57	0,66	1609,58	46,11	995,47	19,35	740,56	12,44	46,01
06-Z4"	0,69	2307	0,11	3,39	1,71	4,18	0,11	2,43	0,74	1820,29	60,29	1011,08	26,42	679,99	15,77	37,36
34-Z20"	0,52	530	0,15	0,87	1,71	3,29	0,08	3,15	0,96	2357,06	14,83	1013,87	20,90	510,11	15,55	21,64
30-Z19"	0,57	29392	0,13	4,14	2,04	5,99	0,12	4,33	0,87	2073,18	71,25	1128,63	40,04	703,86	28,82	33,95
39-Z23"	0,45	238	0,18	2,26	2,06	4,79	0,08	4,22	0,88	2679,17	37,46	1134,15	32,70	505,19	20,50	18,86
09-Z5"	0,83	16460	0,14	0,72	2,39	1,44	0,13	1,25	0,86	2181,11	12,51	1238,21	10,28	770,14	9,08	35,31
42-Z26"	0,59	663	0,15	3,21	2,57	4,24	0,13	2,76	0,79	2291,73	55,21	1291,83	30,96	777,57	20,25	33,93
18-Z11"	0,77	213	0,14	1,51	2,84	2,26	0,15	1,54	0,73	2225,08	25,98	1366,83	16,80	886,58	13,84	39,84
11-Z7"	0,26	6090	0,14	1,27	2,87	2,00	0,15	1,55	0,77	2267,82	21,72	1375,32	14,99	875,50	12,68	38,61
45-Z27"	0,70	420	0,16	1,20	2,94	3,01	0,14	2,76	0,92	2405,20	20,35	1392,45	22,77	829,53	21,45	34,49
35-Z21"	0,42	22679	0,15	1,61	3,90	3,65	0,19	3,27	0,90	2311,55	27,29	1613,68	29,05	1134,32	33,97	49,07

Geographic coordinates = 9283659/599241

" Discordance > 50% 6/4<1000

		Isotopic ratios								Ages						
GRD-58	Th/U	$^{206}Pb/^{204}Pb$	7/6 ratio	1s(%)	7/5 ratio	1s(%)	6/8 ratio	1s(%)	Rho	7/6 age	1s(%)	7/5 age	1s(%)	6/8 age	1s(%)	Conc (%)
04-Z1B	1,46	11893	0,20211	1,10	16,06286	2,01	0,57640	1,69	0,83	2843,3	17,9	2880,5	19,2	2934,1	39,8	103,2
05-Z2B	1,29	9425	0,20225	1,02	16,03182	1,85	0,57489	1,54	0,83	2844,5	16,7	2878,7	17,7	2927,9	36,2	102,9
06-Z3B	0,89	4398	0,20417	2,08	16,38971	3,57	0,58220	2,90	0,91	2859,8	33,9	2899,8	34,1	2957,7	68,7	103,4
07-Z3N	1,33	5095	0,19878	1,32	15,52045	3,99	0,56627	3,77	0,94	2816,2	21,5	2847,7	38,1	2892,5	87,8	102,7
08-Z3B2	0,85	11639	0,20310	1,19	15,64391	3,92	0,55864	3,73	0,95	2851,3	19,3	2855,3	37,4	2861,0	86,3	100,3
09-Z4B	0,62	12124	0,20416	1,23	16,69532	3,27	0,59310	3,03	0,93	2859,7	20,0	2917,5	31,4	3002,0	72,8	105,0
30-Z16B´	0,89	5852	0,19483	2,17	15,36165	3,77	0,57186	3,08	0,88	2783,3	35,5	2837,9	35,9	2915,4	72,3	104,7
25-Z13N´	0,04	8820	0,19456	1,61	14,49152	3,28	0,54020	2,86	0,87	2781,1	26,4	2782,4	31,2	2784,3	64,6	100,1
35-Z18N´	0,07	6566	0,19109	1,81	14,80933	3,08	0,56207	2,50	0,81	2751,6	29,7	2803,1	29,3	2875,2	58,0	104,5
44-Z24B´	0,69	15292	0,18170	1,66	13,05752	3,27	0,52121	2,81	0,86	2668,4	27,6	2683,8	30,8	2704,3	62,1	101,3
40-Z20N"*	1,35	7304	0,18542	1,84	14,34486	5,31	0,56110	4,98	0,94	2701,9	30,4	2772,8	50,4	2871,2	115,4	106,3
55-Z28N"*	0,27	5346	0,20108	2,54	13,87906	4,65	0,50061	3,90	0,89	2835,0	41,4	2741,5	44,1	2616,4	83,8	92,3
22-Z10N"*	0,08	9705	0,18591	1,77	12,53853	3,23	0,48916	2,70	0,89	2706,3	29,2	2645,6	30,4	2567,1	57,2	94,9
26-Z13B"*	0,92	15426	0,19513	1,57	15,74362	2,64	0,58515	2,12	0,84	2785,9	25,7	2861,4	25,2	2969,7	50,5	106,6
27-Z14"*	0,05	45117	0,19543	1,48	16,26208	2,88	0,60350	2,47	0,86	2788,4	24,2	2892,3	27,5	3043,9	59,9	109,2
28-Z15"*	0,90	34535	0,19334	1,47	15,88206	2,35	0,59579	1,83	0,78	2770,8	24,1	2869,7	22,4	3012,8	44,1	108,7
43-Z23B"*	0,13	10123	0,18344	1,66	14,56312	2,84	0,57580	2,30	0,81	2684,2	27,5	2787,1	27,0	2931,6	54,2	109,2
19-Z8B´	0,96	9676	0,19800	1,57	15,50997	5,03	0,56813	4,77	0,95	2809,8	25,7	2847,1	47,9	2900,2	111,5	103,2
10-Z5N"	0,27	12521	0,19104	1,35	10,04916	2,77	0,38152	2,42	0,91	2751,1	22,2	2439,3	25,6	2083,4	43,1	75,7
16-Z7N"	0,40	7928	0,19756	1,75	6,59832	4,73	0,24223	4,40	0,93	2806,2	28,5	2059,1	41,7	1398,3	55,3	49,8
17-Z7B"	0,18	9840	0,17473	1,43	6,19944	4,17	0,25733	3,92	0,94	2603,5	23,9	2004,4	36,5	1476,1	51,7	56,7
18-Z8B"	1,00	5306	0,19555	3,12	17,48583	5,39	0,64852	4,40	0,92	2789,4	51,1	2961,9	51,8	3222,4	111,5	115,5
20-Z9N"	0,58	20098	0,17817	1,30	9,49249	2,27	0,38641	1,86	0,82	2635,9	21,6	2386,8	20,8	2106,1	33,4	79,9
21-Z9B"	0,89	3437	0,19646	1,64	16,99533	5,30	0,62740	5,05	0,95	2797,0	26,8	2934,6	50,9	3139,3	125,4	112,2
23-Z11N"	0,09	8506	0,19685	1,38	18,35067	3,62	0,67609	3,35	0,92	2800,3	22,5	3008,3	34,9	3329,4	87,2	118,9
24-Z12N"	0,13	50332	0,18488	1,28	11,07945	2,14	0,43463	1,71	0,80	2697,2	21,1	2529,8	19,9	2326,6	33,4	86,3
29-Z15B"	0,43	8725	0,17501	1,81	7,80602	4,68	0,32349	4,32	0,92	2606,2	30,1	2208,9	42,1	1806,8	68,0	69,3
31-Z17B"	0,29	12102	0,16922	1,91	5,44764	3,51	0,23349	2,94	0,84	2549,9	32,0	1892,4	30,1	1352,8	35,9	53,1
32-Z17N"	0,27	15227	0,15638	1,77	2,99027	3,29	0,13868	2,77	0,84	2416,9	30,0	1405,1	25,0	837,2	21,8	34,6
33-Z17B"	0,18	19978	0,14002	1,66	3,68442	2,86	0,19085	2,33	0,81	2227,4	28,7	1568,0	22,8	1126,0	24,1	50,5
34-Z18B"	0,51	414	0,17795	2,29	13,97620	3,66	0,56962	2,76	0,83	2633,9	37,6	2748,1	34,1	2906,3	66,4	110,3
41-Z21N"	0,73	2965	0,19086	1,69	18,78138	3,71	0,71371	3,30	0,89	2749,6	27,8	3030,7	35,8	3472,4	88,7	126,3
42-Z22N"	0,09	9430	0,17848	1,86	10,68781	3,19	0,43431	2,59	0,85	2638,8	30,9	2496,4	29,6	2325,1	50,5	88,1
45-Z24N"	0,32	11043	0,17171	1,67	9,52506	4,39	0,40232	4,06	0,92	2574,4	27,9	2390,0	40,4	2179,7	75,2	84,7
46-Z25N"	0,27	739	0,18813	9,07	1,83078	32,27	0,07058	30,22	0,99	2725,8	142,1	1056,6	192,5	439,7	130,3	16,1

Geographic coordinates = 9283956/627951

" discordance > 10%; "* discordance > 5%; ¹ high error > 5%; ² younger age; ¨inherited zircon

		Isotopic ratios								Ages						
GRD-59	Th/U	6/4 ratio	7/6 ratio	1s(%)	7/5 ratio	1s(%)	6/8 ratio	1s(%)	Rho	7/6 age	1s(%)	7/5 age	1s(%)	6/8 age	1s(%)	Conc (%)
06-Z2N	0,37	29242	0,19722	1,57	15,04689	2,44	0,55335	1,86	0,76	2803,3	25,7	2818,2	23,2	2839,1	42,7	101,3
10-Z3N	0,17	30592	0,20142	0,65	15,24121	1,39	0,54880	1,23	0,88	2837,7	10,7	2830,4	13,2	2820,2	28,0	99,4
12-Z4N	0,36	13087	0,19937	0,80	15,29950	1,53	0,55657	1,30	0,84	2821,0	13,1	2834,1	14,6	2852,4	30,0	101,1
37-Z15	0,10	11009	0,19981	1,14	15,25047	1,93	0,55357	1,56	0,85	2824,6	18,6	2831,0	18,4	2840,0	35,8	100,5
43-Z18N	0,55	30935	0,19797	0,85	15,35617	1,81	0,56256	1,60	0,88	2809,6	13,8	2837,6	17,3	2877,2	37,2	102,4
57-Z23N	0,23	7393	0,20039	0,77	15,46752	2,28	0,55981	2,14	0,94	2829,4	12,5	2844,5	21,7	2865,8	49,6	101,3
65-Z26	1,05	1809	0,20250	1,16	15,88365	2,56	0,56887	2,29	0,89	2846,5	18,9	2869,8	24,5	2903,2	53,5	102,0
71-Z30	0,20	15215	0,20135	1,39	15,12722	2,27	0,54490	1,79	0,78	2837,1	22,7	2823,3	21,6	2803,9	40,6	98,8
22-Z8N"*	0,32	4161	0,20363	0,69	14,09102	1,73	0,50187	1,59	0,91	2855,5	11,3	2755,9	16,4	2621,8	34,2	91,8
26-Z10N"*	0,59	3291	0,20084	0,81	13,50460	1,80	0,48768	1,61	0,89	2833,0	13,1	2715,6	17,0	2560,6	33,9	90,4
44-Z18B¹	0,56	36348	0,19722	0,87	15,33272	2,98	0,56386	2,86	0,96	2803,3	14,2	2836,1	28,5	2882,5	66,4	102,8
04-Z1N"	0,62	55	0,17088	2,53	5,77358	3,89	0,24505	2,81	0,74	2566,3	41,8	1942,5	33,2	1412,9	37,4	55,1
05-Z1B"	0,40	240	0,16024	2,25	4,62168	3,46	0,20918	2,45	0,74	2458,2	37,5	1753,2	28,5	1224,5	29,3	49,8
11-Z3B"	0,26	230	0,19374	0,64	9,69965	1,57	0,36311	1,43	0,91	2774,2	10,5	2406,7	14,5	1996,9	24,6	72,0
13-Z4B"	0,08	218	0,17383	2,20	3,35779	2,43	0,14010	1,03	0,64	2594,8	36,8	1494,6	19,0	845,2	8,1	32,6
14-Z5N"	0,19	420	0,21258	0,55	6,71487	1,70	0,22909	1,61	0,95	2925,3	8,9	2074,6	15,1	1329,7	19,4	45,5
15-Z5B"	0,11	19	0,19848	0,69	5,13416	1,89	0,18761	1,76	0,93	2813,8	11,2	1841,8	16,1	1108,4	18,0	39,4
16-Z6N"	0,17	2020	0,19974	0,67	7,55128	1,48	0,27419	1,32	0,89	2824,1	11,0	2179,1	13,3	1562,1	18,3	55,3
17-Z7N"	0,18	11758	0,20920	0,97	13,55423	2,79	0,46990	2,62	0,96	2899,4	15,7	2719,1	26,4	2483,1	54,0	85,6
20-Z7I"	0,30	7671	0,21631	0,83	10,68757	3,12	0,35834	3,00	0,96	2953,5	13,5	2496,3	28,9	1974,3	51,1	66,8
21-Z7B"	0,06	331	0,16530	0,80	4,12293	3,04	0,18089	2,93	0,96	2510,6	13,5	1658,9	24,8	1071,9	28,9	42,7
23-Z8B"	0,51	215	0,14981	1,65	1,42775	2,63	0,06912	2,05	0,90	2343,8	28,2	900,6	15,7	430,9	8,5	18,4
24-Z9N"	0,15	569	0,22065	0,85	3,54054	2,44	0,11638	2,29	0,94	2985,4	13,7	1536,3	19,3	709,7	15,4	23,8
25-Z9B"	0,17	106	0,21942	0,90	9,42790	3,55	0,31163	3,44	0,97	2976,4	14,5	2380,5	32,6	1748,7	52,6	58,8
27-Z10B"	0,22	673	0,20652	1,00	10,48679	1,92	0,36828	1,63	0,88	2878,4	16,3	2478,8	17,8	2021,3	28,4	70,2
30-Z11N"	0,23	888	0,20133	1,11	6,62393	2,27	0,23862	1,98	0,87	2837,0	18,0	2062,5	20,0	1379,5	24,6	48,6
31-Z11B"	0,45	21	0,16580	1,03	2,35106	1,87	0,10285	1,55	0,83	2515,6	17,4	1227,9	13,3	631,1	9,3	25,1
32-Z12N"	0,63	1246	0,19822	0,93	12,80660	2,04	0,46857	1,81	0,89	2811,6	15,2	2665,5	19,2	2477,3	37,3	88,1
33-Z12B"	0,39	278	0,15128	1,24	2,76790	2,09	0,13270	1,69	0,87	2360,4	21,1	1346,9	15,6	803,3	12,8	34,0
34-Z13B"	0,43	5928	0,19994	0,96	11,97399	1,88	0,43436	1,62	0,86	2825,7	15,6	2602,4	17,6	2325,3	31,6	82,3
35-Z14N"	0,35	18158	0,20094	0,87	12,22131	1,81	0,44111	1,58	0,87	2833,9	14,3	2621,5	17,0	2355,6	31,3	83,1
36-Z14B"	0,28	357	0,15707	0,94	3,43772	2,13	0,15873	1,91	0,90	2424,4	15,9	1513,1	16,7	949,7	16,9	39,2
38-Z16N"	0,18	19704	0,19005	1,02	10,67323	1,84	0,40731	1,54	0,83	2742,6	16,7	2495,1	17,1	2202,6	28,7	80,3
42-Z17"	0,15	1546	0,21326	1,05	12,18212	3,52	0,41430	3,36	0,95	2930,5	17,0	2618,5	33,0	2234,5	63,4	76,3
53-Z21N"	0,29	16757	0,20244	0,75	10,16931	2,04	0,36433	1,90	0,93	2846,0	12,2	2450,3	18,9	2002,7	32,7	70,4
54-Z21B"	0,15	463	0,14112	0,93	2,90264	2,12	0,14918	1,90	0,90	2241,0	16,2	1382,6	16,0	896,4	15,9	40,0
55-Z22N"	0,14	1315	0,19272	1,40	2,46973	4,17	0,09294	3,93	0,98	2765,5	22,9	1263,2	30,2	572,9	21,6	20,7
56-Z22B"	0,17	257	0,11727	1,06	1,75176	1,92	0,10834	1,50	0,81	1915,1	18,9	1027,8	12,4	663,1	10,1	34,6
58-Z24N"	0,37	1691	0,22639	0,92	5,63132	2,22	0,18040	2,02	0,91	3026,7	14,8	1920,9	19,1	1069,2	19,9	35,3
59-Z24B"	0,31	434	0,17136	1,28	3,10389	3,57	0,13137	3,33	0,96	2571,0	21,5	1433,7	27,4	795,7	24,9	30,9
60-Z25N"	0,37	415	0,22857	0,94	15,79890	2,52	0,50130	2,34	0,93	3042,1	15,0	2864,7	24,0	2619,4	50,3	86,1
64-Z25B"	0,28	484	0,21566	0,98	14,67055	1,99	0,49338	1,73	0,87	2948,5	15,8	2794,1	18,9	2585,3	36,8	87,7
66-Z27N"	0,25	9695	0,22201	1,58	11,87745	2,88	0,38802	2,41	0,93	2995,3	25,4	2594,8	27,0	2113,6	43,4	70,6
67-Z27B"	0,24	803	0,19370	0,97	7,40078	2,03	0,27711	1,79	0,88	2773,8	15,9	2161,1	18,2	1576,8	25,0	56,8
68-Z28"	0,51	125	0,18085	0,79	3,96834	2,66	0,15914	2,54	0,95	2660,7	13,1	1627,7	21,6	952,0	22,5	35,8
69-Z29N"	0,31	434	0,20032	0,86	5,94096	5,02	0,21510	4,95	0,99	2828,8	14,0	1967,2	43,6	1255,9	56,4	44,4
70-Z29B"	0,04	364	0,19397	1,20	6,27830	3,35	0,23474	3,13	0,96	2776,2	19,7	2015,4	29,4	1359,3	38,4	49,0
72-Z31"	0,41	22484	0,20395	1,29	12,99480	3,03	0,46212	2,74	0,90	2858,0	21,0	2679,3	28,6	2448,9	55,8	85,7

Geographic coordinates = 9291062/623281

" discordance > 10%; "* discordance > 5%; ¹ high error > 3%; ² younger age; ¨inherited zircon

		Isotopic ratios								Ages						
AMR-191	Th/U	6/4 ratio	7/6 ratio	1s(%)	7/5 ratio	1s(%)	6/8 ratio	1s(%)	Rho	7/6 age	1s(%)	7/5 age	1s(%)	6/8 age	1s(%)	Conc (%)
71-Z28	0,28	17613	0,19	1,03	12,18	1,97	0,47	1,68	0,85	2719,83	16,92	2618,21	18,50	2488,84	34,75	91,51
72-Z29	0,46	11441	0,19	1,40	12,36	1,98	0,48	1,40	0,70	2700,09	23,08	2632,41	18,61	2545,31	29,54	94,27
34-Z13B	0,46	27260	0,19	0,80	12,58	1,22	0,48	0,92	0,73	2746,10	13,13	2648,60	11,43	2522,88	19,13	91,87
23-Z9	0,26	20179	0,19	1,08	12,55	1,68	0,48	1,29	0,76	2727,07	17,79	2646,33	15,79	2542,03	27,01	93,21
46-Z17N	1,16	24005	0,19	0,86	12,76	1,57	0,49	1,31	0,83	2739,24	14,06	2662,42	14,64	2562,50	27,62	93,55
47-Z17B	0,71	11538	0,19	1,33	12,99	2,00	0,50	1,50	0,74	2732,72	21,97	2679,01	18,90	2608,41	32,08	95,45
29-Z12B	0,27	29178	0,18	1,09	12,20	1,55	0,48	1,10	0,70	2695,98	17,92	2619,70	14,44	2522,14	22,93	93,55
11-Z4N	0,49	30140	0,19	1,12	12,41	1,58	0,48	1,11	0,69	2707,26	18,49	2636,25	14,84	2544,74	23,40	94,00
27-Z10	0,26	26073	0,19	0,65	13,31	1,14	0,50	0,94	0,81	2752,87	10,65	2702,05	10,75	2634,63	20,24	95,71
22-Z8	0,25	222362	0,19	0,81	12,97	1,20	0,50	0,88	0,71	2723,99	13,41	2677,44	11,33	2616,24	19,01	96,04
70-Z27B	0,77	17237	0,19	0,85	13,51	1,62	0,51	1,38	0,84	2759,61	13,97	2715,80	15,31	2657,31	30,01	96,29
63-Z24	0,31	29400	0,19	0,78	13,40	1,48	0,51	1,25	0,84	2749,62	12,89	2708,53	13,95	2653,80	27,21	96,52
09-Z3B	0,27	49801	0,19	0,51	12,99	0,84	0,50	0,66	0,76	2717,64	8,37	2678,57	7,88	2627,13	14,34	96,67
51-Z20N	0,36	26286	0,19	0,57	13,95	1,03	0,53	0,85	0,81	2755,21	9,44	2746,56	9,71	2734,79	18,92	99,26
15-Z5N	0,27	19911	0,19	0,66	13,94	1,11	0,53	0,89	0,79	2754,07	10,81	2745,56	10,50	2734,00	19,86	99,27
52-Z20B	0,31	20113	0,19	0,74	14,04	1,15	0,53	0,88	0,74	2759,96	12,17	2752,22	10,89	2741,70	19,61	99,34
21-Z7	0,36	55672	0,19	0,58	14,18	1,20	0,53	1,05	0,86	2768,61	9,56	2761,69	11,36	2752,22	23,44	99,41
58-Z23N	0,50	139463	0,19	0,96	13,85	1,56	0,53	1,23	0,78	2745,86	15,77	2739,62	14,79	2731,17	27,44	99,47
45-Z17	0,16	13482	0,19	0,71	13,60	1,53	0,52	1,35	0,88	2744,68	11,62	2722,58	14,45	2692,88	29,81	98,11
28-Z11	0,22	497785	0,19	0,84	13,41	1,27	0,52	0,95	0,73	2725,55	13,78	2709,15	11,94	2687,21	20,91	98,59
04-Z1B	0,22	15124	0,19	1,32	13,41	2,32	0,52	1,90	0,82	2714,21	21,77	2709,14	21,90	2702,35	42,04	99,56
12-Z4B	0,45	32825	0,19	1,40	13,38	1,93	0,52	1,33	0,71	2701,60	23,09	2707,08	18,21	2714,42	29,38	100,47
59-Z23	0,35	35186	0,19	1,07	13,17	1,63	0,52	1,24	0,75	2700,97	17,60	2691,65	15,41	2679,26	27,13	99,20
17-Z6B	0,30	19048	0,18	1,14	13,17	1,68	0,52	1,24	0,72	2672,56	18,91	2691,60	15,90	2717,02	27,45	101,66
05-Z2	0,26	43686	0,18	1,10	13,10	1,52	0,52	1,06	0,68	2672,95	18,01	2686,82	14,26	2705,28	23,30	101,21
54-Z21B	0,26	43478	0,18	1,52	13,25	2,17	0,52	1,55	0,74	2681,81	25,18	2697,37	20,53	2718,19	34,42	101,36
16-Z5B	0,29	54663	0,18	0,85	13,44	1,23	0,53	0,89	0,70	2690,63	14,05	2710,76	11,62	2737,85	19,83	101,76
30-12B2²	0,25	69238	0,18	1,38	12,97	1,89	0,53	1,29	0,67	2629,83	22,92	2677,12	17,81	2740,18	28,82	104,20
65-Z25B²	0,27	32271	0,18	1,04	13,97	1,63	0,56	1,26	0,76	2672,07	17,04	2747,89	15,36	2852,27	29,05	106,74
64-Z25N²	0,37	231506	0,18	0,92	13,41	1,44	0,55	1,11	0,76	2617,74	15,30	2708,67	13,61	2832,25	25,40	108,19
36-Z14B²	0,26	38548	0,18	1,41	12,36	1,97	0,50	1,37	0,70	2636,86	23,30	2632,16	18,30	2626,05	29,39	99,59
53-Z21¨	0,19	34608	0,20	1,36	12,95	2,30	0,48	1,85	0,80	2807,03	22,22	2676,34	21,66	2506,82	38,49	89,31
57-Z22¨	0,86	19866	0,21	1,11	15,65	1,77	0,54	1,38	0,77	2909,80	17,93	2855,52	16,91	2779,23	31,23	95,51
69-Z27N¨	0,69	3790	0,21	1,21	16,87	1,83	0,57	1,37	0,74	2938,29	19,57	2927,31	17,54	2911,38	32,13	99,08
33-Z13N"	0,28	1205	0,21	0,77	6,84	2,21	0,24	2,04	0,93	2901,46	12,50	2091,42	19,36	1370,88	25,46	47,25
10-Z3N"	0,60	157	0,14	0,98	4,49	1,58	0,23	1,22	0,77	2281,18	16,84	1729,86	13,02	1311,63	14,61	57,50
35-Z14N"	0,29	480873	0,18	1,10	9,73	1,58	0,39	1,13	0,70	2673,07	18,10	2409,75	14,45	2110,68	20,39	78,96
18-Z6N"	0,43	479112	0,19	0,84	11,80	3,14	0,45	3,02	0,96	2735,23	13,82	2588,53	29,36	2405,31	60,67	87,94
03-Z1N"	0,22	1263	0,18	0,68	11,35	1,21	0,45	0,99	0,81	2693,51	11,19	2552,54	11,21	2378,93	19,83	88,32
48-Z19B"	0,27	12440	0,19	1,56	11,75	2,14	0,45	1,46	0,70	2723,66	25,74	2584,94	20,01	2411,74	29,38	88,55
66-Z26¹	0,97	21580	0,18	1,39	12,14	3,83	0,48	3,57	0,93	2689,51	22,91	2615,48	35,94	2520,94	74,51	93,73

Geographic coordinates = 9274706/636247

" discordance > 10%; "* discordance > 5%; ¹ high error > 5%; ² younger age; ¨inherited zircon

Table B - Supplementary Pb evaporation on zircon analytical data for the granitoids of the Canaã dos Carajás area.

Sample/grai	Evaporation Temperature	Ratios	$^{204}Pb/^{206}Pb$	2s	$^{208}Pb/^{206}Pb$	2s	$^{207}Pb/^{206}Pb)$	2s	Age (Ma)	2s
AER-11A/Biotite trondhjemite										
AER-11A/4	1500	36/36	0,000320	0,000013	0,02821	0,00068	0,21276	0,00046	2928	3,5
	1550	30/30	0,000315	0,000010	0,02912	0,00075	0,21320	0,00066	2930	5,0
	1580	14/38	0,000359	0,000004	0,02807	0,0004	0,21271	0,00051	2927	3,9
AER-11A/7	1500	14/14	0,000057	0,000002	0,03001	0,00024	0,21280	0,00051	2927	3,9
AER-11A/8	1500	38/38	0,000053	0,000002	0,04196	0,00025	0,21361	0,00044	2933	3,3
Geographic coordinates = 9290489S/626932W					MSWD = 2.6		$^{207}Pb/^{206}Pb$ mean age =		2929	3,0
GRD-79C/Biotite granodiorite										
GRD-79C/3	1500	16/16	0,000222	0,000034	0,055760	0,000730	0,204450	0,001030	2863	8,2
GRD-79C/4	1500	38/54	0,000133	0,000005	0,075850	0,000290	0,205180	0,000830	2868	6,6
GRD-79C/6	1550	32/60	0,000165	0,000010	0,102060	0,001690	0,205580	0,001050	2871	8,3
GRD-79C/1	1500	6/12	0,000172	0,000014	0,099170	0,000680	0,205560	0,000780	2871	6,2
Geographic coordinates = 9290740/633473					MSWD = 1.13		$^{207}Pb/^{206}Pb$ mean age =		2869	4,0
ARC-65A/Biotite-hornblende tonalit										
ARC-65A/3	1500	14/14	0,000074	0,000006	0,17098	0,00114	0,20617	0,00082	2876	6,5
ARC-65A/5	1450	30/34	0,000115	0,000008	0,17023	0,00046	0,20549	0,00032	2871	2,5
	1550	38/38	0,000091	0,000004	0,17438	0,00337	0,20564	0,00036	2872	2,8
ARC-65A/9	1450	38/38	0,000176	0,000016	0,15617	0,00052	0,20542	0,00047	2870	3,7
ARC-65A/1	1450	28/34	0,000027	0,000002	0,14404	0,00043	0,20583	0,00028	2873	2,2
	1550	6/6	0,000038	0,000014	0,14984	0,00124	0,20616	0,00062	2876	4,9
ARC-65A/1	1500	36/36	0,000031	0,000003	0,14933	0,0007	0,20568	0,00045	2872	3,6
Geographic coordinates = 9292330S/626105W					MSWD = 1.2		$^{207}Pb/^{206}Pb$ mean age =		2872	1,0
ERF-07C/Biotite granodiorite										
ERF-07C/2	1500	12/26	0,000076	0,000025	0,1787	0,00067	0,20485	0,00046	2866	3,7
ERF-07C/3	1500	14/58	0,000535	0,000020	0,1621	0,00073	0,20519	0,00042	2868	3,3
ERF-07C/5	1500	40/86	0,000028	0,000006	0,1617	0,00053	0,20523	0,00038	2869	3,0
ERF-07C/8	1500	36/92	0,000028	0,000004	0,1919	0,00192	0,20480	0,00048	2865	3,8
ERF-07C/1	1500	36/80	0,000031	0,000002	0,1606	0,00039	0,20540	0,00046	2870	3,7
Geographic coordinates = 9296314S/629055W					MSWD = 1.3		$^{207}Pb/^{206}Pb$ mean age =		2868	2,0
ARC-95A/Hornblende tonalite										
ARC-95A/2	1500	20/102	0,000030	0,000002	0,1208	0,00153	0,20315	0,0003	2852	2,4
ARC-95A/4	1550	74/112	0,000054	0,000005	0,1626	0,00064	0,20339	0,00022	2854	1,7
ARC-95A/5	1500	40/76	0,000009	0,000031	0,1234	0,00351	0,20314	0,00029	2852	2,3
ARC-95A/1	1550	28/68	0,000070	0,000005	0,1646	0,00096	0,20369	0,00028	2856	2,3
ARC-95A/1	1550	40/100	0,000074	0,000017	0,1109	0,00191	0,20306	0,00035	2851	2,8
Geographic coordinates = 9284670S/598962W					MSWD = 3.1		$^{207}Pb/^{206}Pb$ mean age =		2853	2,0

Table C- U-Pb SHRIMP isotopic data of zircon of investigated samples.

					Isotopic ratios				Ages			
	U	Th	Pb	4f206	^{207}Pb	^{207}Pb	^{206}Pb	^{208}Pb	^{206}Pb	^{207}Pb	error	disc.
spot	ppm	U	ppm	(%)	^{206}Pb	^{235}U	^{238}U	^{232}Th	^{238}U	^{206}Pb	corr.	%
AMR-187B – Hornblende syenogranite												
a.4-1	262	158	112.9	-0.01	0.18941 ± 0.32	13.1050 ± 1.38	0.5018 ± 1.35	0.1321 ± 1.44	2622 ± 29	2737 ± 5	0.973	4
a.4-2	336	217	146.0	0.01	0.18966 ± 0.25	13.2314 ± 1.44	0.5060 ± 1.42	0.1372 ± 1.52	2639 ± 31	2739 ± 4	0.985	4
a.5-1	379	286	159.9	0.00	0.18925 ± 0.28	12.8020 ± 1.44	0.4906 ± 1.42	0.1303 ± 1.55	2573 ± 30	2736 ± 5	0.982	6
a.6-1	462	308	203.7	0.01	0.19010 ± 0.26	13.4627 ± 1.44	0.5136 ± 1.42	0.1384 ± 1.47	2672 ± 31	2743 ± 4	0.984	3
a.7-1	323	184	147.2	0.04	0.18924 ± 0.30	13.8187 ± 1.46	0.5296 ± 1.43	0.1453 ± 1.52	2740 ± 32	2736 ± 5	0.979	0
a.7-2	203	144	92.6	0.02	0.18914 ± 0.54	13.8566 ± 1.57	0.5313 ± 1.48	0.1429 ± 1.77	2747 ± 33	2735 ± 9	0.939	0
a.8-1	440	419	199.0	0.03	0.19012 ± 0.21	13.7893 ± 1.42	0.5260 ± 1.40	0.1415 ± 1.46	2725 ± 31	2743 ± 4	0.989	1
a.10-1	396	279	179.4	0.02	0.18931 ± 0.22	13.7452 ± 1.43	0.5266 ± 1.41	0.1414 ± 1.45	2727 ± 31	2736 ± 4	0.988	0
ARC-109 – Hornblende-biotite syenogranite												
g.1-1	1254	646	135.3	0.08	0.09033 ± 0.87	1.5637 ± 1.73	0.1256 ± 1.49	0.0390 ± 1.86	762 ± 11	1433 ± 17	0.863	47
g.1-2	1906	905	153.5	0.12	0.06995 ± 0.57	0.9031 ± 1.38	0.0936 ± 1.26	0.0296 ± 1.42	577 ± 7	927 ± 12	0.911	38
g.4-1	554	292	198.6	0.03	0.18489 ± 0.73	10.6319 ± 1.79	0.4171 ± 1.63	0.1087 ± 2.06	2247 ± 31	2697 ± 12	0.913	17
g.5-1	995	862	692.4	0.02	0.19576 ± 0.27	21.8636 ± 1.50	0.8100 ± 1.47	0.2041 ± 1.50	3825 ± 43	2791 ± 4	0.984	-37
g.6-1	805	386	353.9	-0.01	0.17792 ± 0.34	12.5532 ± 1.56	0.5117 ± 1.52	0.1419 ± 1.67	2664 ± 33	2634 ± 6	0.976	-1
g.6-2	893	497	258.6	0.05	0.15638 ± 0.70	7.2623 ± 1.63	0.3368 ± 1.47	0.0972 ± 1.77	1871 ± 24	2417 ± 12	0.903	23
g.6-3	147	73	76.0	0.12	0.19043 ± 0.58	15.8043 ± 1.72	0.6019 ± 1.62	0.1591 ± 2.25	3038 ± 39	2746 ± 10	0.941	-11
g.7-1	1117	533	211.6	0.17	0.13043 ± 0.54	3.9572 ± 1.56	0.2200 ± 1.47	0.0636 ± 1.77	1282 ± 17	2104 ± 9	0.939	39
g.8-1	523	334	252.9	0.02	0.19067 ± 0.65	14.8105 ± 1.61	0.5634 ± 1.47	0.1470 ± 1.53	2880 ± 34	2748 ± 11	0.914	-5
g.8-2	184	97	92.9	0.03	0.18992 ± 0.54	15.3618 ± 1.71	0.5866 ± 1.62	0.1602 ± 1.87	2976 ± 39	2741 ± 9	0.949	-9
g.9-1	333	263	139.6	0.02	0.18749 ± 0.29	12.6072 ± 1.35	0.4877 ± 1.32	0.1285 ± 1.39	2561 ± 28	2720 ± 5	0.976	6
g.9-2	458	475	191.5	0.04	0.18959 ± 0.49	12.7160 ± 1.38	0.4864 ± 1.29	0.1277 ± 1.56	2555 ± 27	2739 ± 8	0.935	7
g.9-3	191	99	84.3	0.06	0.18827 ± 0.69	13.3102 ± 1.58	0.5128 ± 1.42	0.1355 ± 1.62	2668 ± 31	2727 ± 11	0.901	2
g.11-1	669	574	225.5	0.00	0.17511 ± 0.35	9.4661 ± 1.52	0.3921 ± 1.48	0.1120 ± 1.68	2132 ± 27	2607 ± 6	0.973	18
g.11-2	228	160	100.5	0.02	0.18925 ± 0.42	13.3974 ± 1.71	0.5134 ± 1.66	0.1364 ± 1.77	2671 ± 36	2736 ± 7	0.969	2
g.11-4	453	320	214.5	0.01	0.18807 ± 0.26	14.2811 ± 1.50	0.5507 ± 1.48	0.1431 ± 1.56	2828 ± 34	2725 ± 4	0.985	-4
GRD-47 – Biotite leucosyenogranite												
g.1-2	1906	905	153.5	0.12	0.06995 ± 0.57	0.90 ± 1.38	0.0936 ± 1.26	0.0296 ± 1.42	577 ± 7	927 ± 12	0.911	38
g.4-1	839	69	221.1	0.75	0.18501 ± 0.42	7.77 ± 1.30	0.3045 ± 1.23	0.1379 ± 5.26	1714 ± 19	2698 ± 7	0.947	36
g.7-1	850	123	325.0	0.11	0.19512 ± 0.22	11.96 ± 1.25	0.4445 ± 1.23	0.1941 ± 1.54	2371 ± 24	2786 ± 4	0.985	15
g.8-1	734	130	254.2	0.17	0.19304 ± 0.29	10.71 ± 1.28	0.4024 ± 1.25	0.1216 ± 1.83	2180 ± 23	2768 ± 5	0.974	21
g.9-1	333	263	139.6	0.02	0.18749 ± 0.29	12.61 ± 1.35	0.4877 ± 1.32	0.1285 ± 1.39	2561 ± 28	2720 ± 5	0.976	6
g.9-2	461	480	195.1	0.04	0.19032 ± 0.35	12.91 ± 1.34	0.4920 ± 1.30	0.1282 ± 1.35	2580 ± 28	2745 ± 6	0.965	6
g.9-3	191	99	84.3	0.06	0.18827 ± 0.69	13.31 ± 1.58	0.5128 ± 1.42	0.1355 ± 1.62	2668 ± 31	2727 ± 11	0.901	2
g.12-1	166	127	84.4	0.02	0.22496 ± 0.30	18.36 ± 1.35	0.5921 ± 1.32	0.1525 ± 1.40	2998 ± 32	3017 ± 5	0.974	1
g.13-1	962	416	274.8	0.14	0.18025 ± 0.26	8.26 ± 1.25	0.3322 ± 1.23	0.0812 ± 2.03	1849 ± 20	2655 ± 4	0.978	30
g.13-2	843	131	247.9	0.06	0.18403 ± 0.30	8.68 ± 1.28	0.3422 ± 1.24	0.1091 ± 1.73	1897 ± 20	2690 ± 5	0.973	29
g.14-1	1147	83	446.1	0.03	0.19240 ± 0.29	12.01 ± 1.28	0.4528 ± 1.25	0.1249 ± 2.37	2408 ± 25	2763 ± 5	0.974	13
h.5-1	590	325	227.1	0.16	0.19554 ± 0.29	12.06 ± 1.30	0.4474 ± 1.27	0.1127 ± 1.54	2384 ± 25	2789 ± 5	0.975	15
h.5-2	717	122	329.1	0.05	0.20082 ± 0.21	14.79 ± 1.31	0.5341 ± 1.29	0.1613 ± 1.48	2759 ± 29	2833 ± 3	0.987	3
h.7-1	279	238	139.6	0.01	0.23320 ± 0.37	18.71 ± 1.37	0.5820 ± 1.31	0.1482 ± 1.37	2957 ± 31	3074 ± 6	0.962	4
h.6-1	731	610	303.1	0.04	0.19705 ± 0.20	13.11 ± 1.29	0.4824 ± 1.27	0.1011 ± 1.39	2538 ± 27	2802 ± 3	0.987	9
h.9-1	766	129	299.2	0.00	0.19416 ± 0.23	12.17 ± 1.30	0.4546 ± 1.28	0.1252 ± 2.17	2416 ± 26	2778 ± 4	0.984	13
h.13-1	792	123	382.8	0.00	0.20075 ± 0.19	15.58 ± 1.30	0.5629 ± 1.28	0.1494 ± 1.41	2879 ± 30	2832 ± 3	0.989	-2
h.18-1	584	143	258.8	0.08	0.19962 ± 0.21	14.18 ± 1.31	0.5150 ± 1.30	0.1360 ± 1.50	2678 ± 28	2823 ± 3	0.987	5
h.18-2	1067	508	294.5	0.18	0.18353 ± 0.29	8.11 ± 1.30	0.3206 ± 1.27	0.0850 ± 1.41	1793 ± 20	2685 ± 5	0.975	33
h.19-1	729	109	370.0	0.12	0.20253 ± 0.19	16.49 ± 1.28	0.5905 ± 1.27	0.2172 ± 1.54	2992 ± 30	2847 ± 3	0.989	-5
h.19-2	640	140	272.8	0.14	0.19819 ± 0.23	13.54 ± 1.30	0.4956 ± 1.28	0.1326 ± 1.62	2595 ± 27	2811 ± 4	0.984	8

Notes: Isotopic ratios errors in %; All Pb in ratios are radiogenic component corrected for ^{204}Pb; disc. = discordance, as 100 - 100{t[$^{206}Pb/^{238}U$]/t[$^{207}Pb/^{206}Pb$]}; f206 = (common ^{206}Pb) / (total measured ^{206}Pb) based on measured ^{204}Pb; Uncertainties are 1σ.

Capítulo – 3

3. GEOCHEMISTRY AND PETROGENESIS OF THE GRANITES FROM THE CANAÃ DOS CARAJÁS AREA, CARAJÁS PROVINCE, BRAZIL: IMPLICATIONS FOR THE ORIGIN OF ARCHEAN GRANITES

Gilmara Regina Lima Feio

Roberto Dall'Agnol

Submetido: Lithos

Dear Mrs Feio,

Your submission entitled "Geochemistry and petrogenesis of the granites from the Canaã dos Carajás area, Carajás province, Brazil: implications for the origin of Archean granites" (Research Paper) has been received by Lithos.

Please note that submission of an article is understood to imply that the article is original and is not being considered for publication elsewhere. Submission also implies that all authors have approved the paper for release and are in agreement with its content.

You will be able to check on the progress of your paper by logging on to http://ees.elsevier.com/lithos/ as Author.

Your manuscript will be given a reference number in due course.

Thank you for submitting your work to this journal.

Kind regards,

Journal management
Lithos

Geochemistry and petrogenesis of the granites from the Canaã dos Carajás area, Carajás province, Brazil: implications for the origin of Archean granites

G.R.L Feio[1,2], R. Dall'Agnol[1,2]

[1]Grupo de Pesquisa Petrologia de Granitóides, Instituto de Geociências (IG), Universidade Federal do Pará (UFPA), Rua Augusto Corrêa, 01. CEP 66075-110. Brasil.

[2]Programa de Pós-graduação em Geologia e Geoquímica, IG - UFPA.

* Corresponding for author

Abstract

Four Mesoarchean (2.93 to 2.83 Ga) granite units, which encompass the Canaã dos Carajás, Bom Jesus, Cruzadão and Serra Dourada granites, and the Neoarchean Planalto suite (2.73 Ga) were recognized in the Canaã area of the Archean Carajás province. The Mesoarchean units are composed dominantly of biotite leucomonzogranites whereas the Planalto suite dominant rocks are biotite-hornblende monzogranites to syenogranites with total mafic content between 5% and 20%. The Planalto granites have ferroan character, are similar geochemically to reduced A-type granites and show a strong geochemical contrast with the Mesoarchean studied granites. The Canaã dos Carajás, Bom Jesus and the variety of the Cruzadão granite with higher La/Yb are geochemically more akin to the calc-alkaline granites, whereas the other varieties of the Cruzadão granite are transitional between calc-alkaline and alkaline granites. The Serra Dourada granite has an ambiguous geochemical character with some features similar to those of calc-alkaline granites and other to peraluminous granites. The Neoarchean Planalto suite granite has no counterpart in the Mesoarchean Rio Maria terrane of the Carajás province, neither in the Yilgarn and Dharwar cratons. The Mesoarchean granites described in the Canaã and Rio Maria domains of the Carajás province are also geochemically distinct. The Canaã dos Carajás and Bom Jesus granites of Canaã are similar to the High-Ca granites, whereas the Cruzadão and Serra Dourada are more akin to the Low-CaO granites of the Yilgarn craton. The geochemical characteristics of the Mesoarchean Canaã granites approach those of the biotite granite group of Dharwar but the latter are enriched in HFSE and HREE compared to the Mesoarchean granites of Canaã. The accentuated variation of the Sr/Y and $(La/Yb)_N$ ratios observed in the Canaã granites should reflect dominantly compositional differences in the sources of the granite magmas with a subordinate effect of pressure. Geochemical modeling suggests that partial melting of a mafic source similar in composition to the average of Early Proterozoic basalts or to the average lower continental crust could be able to give origin to the Bom Jesus granite and to the variety of the Cruzadão granite with higher $(La/Yb)_N$. The residue of melting will contain variable proportions of plagioclase, amphibole, garnet, clinopyroxene ± orthopyroxene, and ilmenite. In the other Canaã granites, plagioclase was dominant, garnet was probably an absent phase in the residue of melting and

the influence of amphibole was also apparently limited. A crustal environment and a pressure of 8 to 10 kbar is estimated for the generation of the granite magmas that left garnet as a residual phase. The pressure for the origin of the other granites was probably a little lower.

Keywords: Archean, granites, Carajás, Sr/Y, lower crust

1. Introduction

Archean cratons are composed dominantly of tonalitic-trondhjemitic-granodioritic series (TTG) associated with greenstone belts (Goodwin, 1991; Condie, 1993; Martin, 1994). However, other kind of granitoid rocks which include sanukitoid series (Stern and Hanson, 1989; Smithies and Champion, 2000; Moyen et al., 2003; Halla, 2005; Lobach-Zhuchenko et al., 2005; Oliveira et al., 2009; Heilimo et al., 2011) and diferent varieties of potassic granites (Sylvester, 1994; Davis et al., 1994; Champion and Sheraton, 1997; Frost et al., 1998; Smithies and Champion, 1999; Ishihara et al., 2002; Moyen et al., 2003; Whalen et al., 2004; Käpyaho et al., 2006; Jayananda et al., 2006; Champion and Smithies, 2007; Moyen, 2011; Almeida et al., submitted), are now recognized as important components of Archean cratons.

Sylvester (1994) stated that the Archean granites were more voluminous than previously admitted and there is increasing evidence in the literature of a large geochemical diversity of Archean granites (Champion and Sheraton, 1997; Moyen et al., 2003; Käpyaho et al., 2006; Jayananda et al., 2006; Champion and Smithies, 2007; Almeida et al., 2010, submitted). On the other hand, potassic granites are generally related to the late stages of tectonic stabilization of Archean cratons (Goodwin, 1991; Nisbet, 1987; Krooner, 1991; Davis et al., 1994). Thus, it is relevant for a clear understanding of the late Archean evolution a better geochemical characterization and the definition of the petrogenetic processes involved in the origin of different granites formed at that period.

We present in this paper a detailed geochemical characterization of five different varieties of granites distinguished in the Canaã area of the Carajás Archean province of the eastern Amazonian craton (Fig. 1a). These granites have Mesoarchean to Neoarchean ages and will be compared with those found in the adjacent Rio Maria terrane and with granites described in other Archean cratons in order to contribute to clarify the nature and possible origin of the Archean potassic granites. The meaning of whole rock Sr/Y and La/Yb ratios (Martin, 1999; Moyen, 2009; Halla et al., 2009; Almeida et al., 2010; He et al., 2011) for definition of sources and processes involved in magma origin is emphasized.

2. Geological and tectonic setting

The Carajás Province is the largest and best preserved Archean segment of the Amazonian craton (Fig. 1a). It is located in the southeastern part of the Amazonian craton (Fig. 1a, Machado et al., 1991; Santos et al., 2000; Tassinari and Macambira, 2004; Dall'Agnol et al., 2006) and two distinct domains separated by approximately E-W shear zones were distinguished on it (Fig. 1b; Vasquez et al., 2008). To the south, it is exposed the Mesoarchean Rio Maria granite-greenstone terrane (RMGGT; 3.0 to 2.86 Ga; Macambira and Lafon, 1995; Althoff et al., 2000; Souza et al., 2001; Almeida et al., 2011) and, to the north, the Carajás domain (3.0 to 2.55 Ga; Gibbs et al., 1986; Machado et al., 1991; Dall'Agnol et al., 2006; Vasquez et al., 2008). The latter domain corresponds approximately to the Itacaiúnas shear belt as defined by Araújo and Maia (1991) and Costa et al. (1995).

The Mesoarchean Rio Maria granite-greenstone terrane is composed of greenstone belts (3.0-2.90 Ga; Macambira and Lafon, 1995; Souza et al., 2001 and references therein) and several granitoid series: (1) An older TTG series (2.98-2.93 Ga; Macambira and Lancelot, 1996; Althoff et al., 2000; Leite et al., 2004; Almeida et al., 2011); (2) The sanukitoid Rio Maria suite (~2.87 Ga; Macambira, 1992; Oliveira, M.A. et al., 2009, 2010 and references therein); (3) An younger TTG series (~2.87-2.86 Ga; Leite et al., 2004; Almeida et al., 2011); (4) A high Sr- and Ba-bearing leucogranodiorite-granite suite (~2.87 Ga; Almeida et al., 2010); and (5) Potassic leucogranites of calc-alkaline affinity (~2.87-2.86 Ga; Leite et al., 1999, 2004; Almeida et al., submitted). Despite their diversity, the magmatic units of that terrane were generated in a relatively short period of ~120 Ma.

The Carajás domain comprises a southern 'Transition' sub-domain, formed by strongly deformed Mesoarchean to Neoarchean units, and a northern sub-domain which corresponds essentially to the Neoarchean Carajás basin. Most of the Archean granitoid and gneissic rocks of the 'Transition' sub-domain were generally grouped in the Xingu Complex (Fig. 1b). The border between the RMGGT and the Carajás domain is located to the North of the Sapucaia belt (Fig. 1b), where there is geophysical evidence of a major tectonic discontinuity which separates the strongly deformed 'Transition' sub-domain of the RMGGT.

The Neoarchean Carajás basin (Fig. 1b) is formed dominantly by banded iron formations and basalts with subordinate felsic volcanic rocks metamorphosed in greenschist facies conditions (Itacaiúnas Supergroup; 2.76-2.74 Ga; Machado et al., 1991; Trendall et al., 1998; Tallarico et al., 2005). These sequences are partially covered by the fluvial to marine siliciclastic deposits of the Águas Claras formation (Nogueira et al., 1995). Neoarchean

(~2.76-2.57 Ga) subalkaline granite plutons (Barros et al., 2004, 2009; Sardinha et al., 2004, 2006; Feio et al., submitted a) and mafic-ultramafic stratified bodies (Vasquez et al., 2008 and references therein) are intrusive in the Mesoarchean units and in the Itacaiúnas supergroup (Fig. 1b). These rocks are cross-cut by small stocks, sills, and dykes of Neoarchean hydrothermally altered gabbros.

Differently of the RMGGT, a large part of the evolution of the Carajás domain occurred during the Neoarchean when the Carajas basin and a widespread plutonic magmatism were formed. This implies that the tectonic stabilization of the RMGGT preceded that of the Carajás domain (Dall'Agnol et al., 2006). In this context, the 'Transition' sub-domain was interpreted as a probable Mesoarchean substratum, similar to the RMGGT, that was intensely affected by the magmatic and tectonic Neoarchean events recorded in the Carajás domain (Dall'Agnol et al., 2006 and references therein; Domingos, 2009). However, recent geological, geochemical and geochronological data obtained in the Canaã area (Feio et al., submitted b), in the northern part of the 'Transition' sub-domain, indicate that its evolution was distinct of that of the RMGGT. It is not possible to extrapolate this conclusion to all the 'Transition' sub-domain, but it suggests that the evolution of the two Archean domains of the Carajás province could be more distinct than previously admitted.

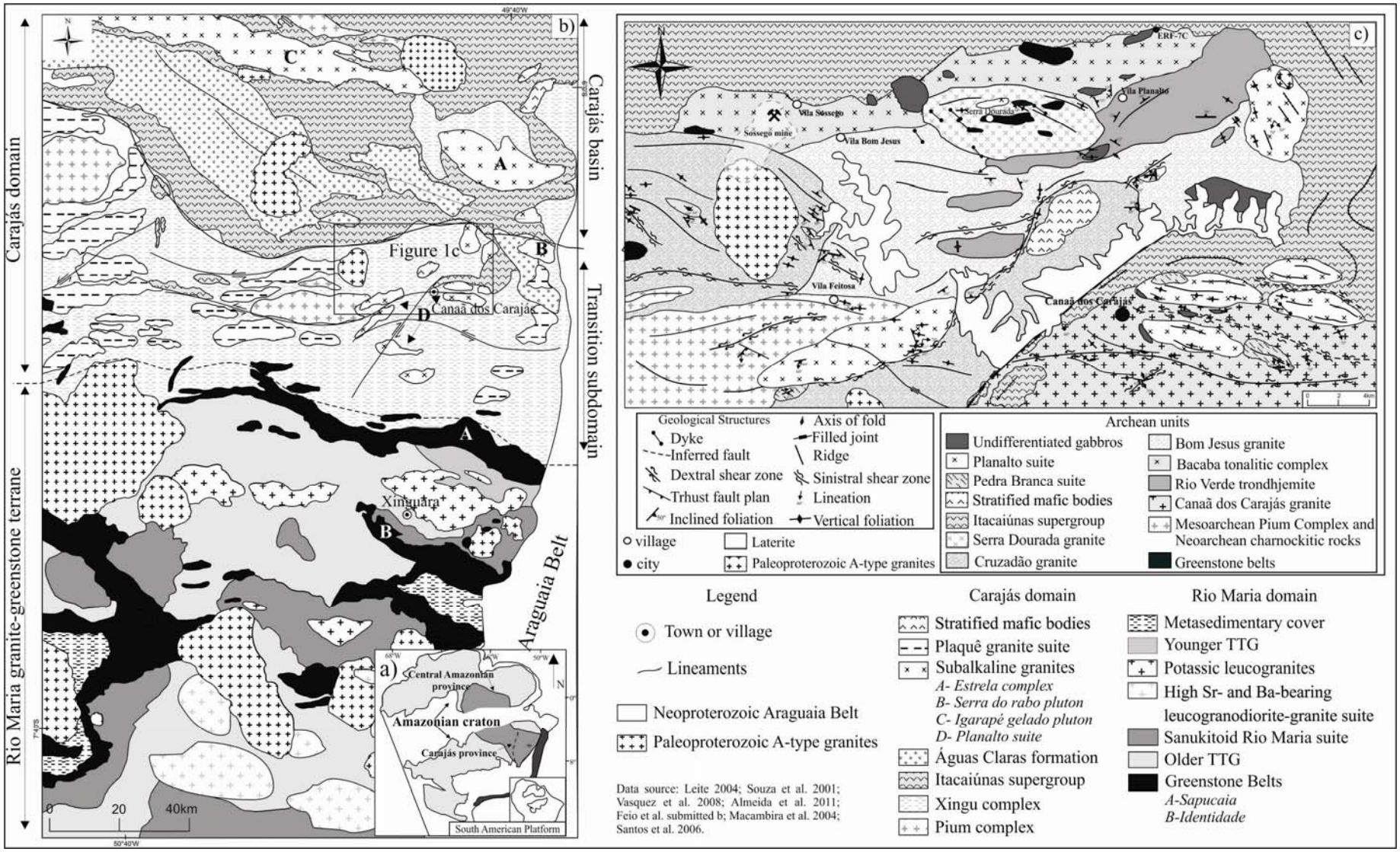

Figure 1 - (a) Location of the Carajás Province in the Amazonian craton; (b) Geological map of the Carajás Province, showing the location of the Canaã dos Carajás area and the approximate limits between the Rio Maria granite-greenstone terrane and the Carajás domain (dashed line), and the Carajás basin and 'Transitional' sub-domain (continuous lines); (c) Geological map of the Canaã dos Carajás area.

3. Geology and geochronology of the Canaã dos Carajás area

The Canaã dos Carajás area is located in the border between the Carajás basin and the 'Transition' sub-domain. A more detailed discussion about the geology, geochronology and crustal evolution of that area was presented by Feio et al. (submitted b) and additional geochronological data on the Planalto granite suite is given by Feio et al. (submitted a). The geological map of the Canaã area is shown in Figure 1b. The available geochronological information (Fig. 2) demonstrates that the main evolution of the Canaã crust was concentrated in the Mesoarchean and Neoarchean. The oldest units (ca. 3.0 to 2.93 Ga) are small remnants of greenstone belts, the Pium granulitic complex, the Canaã dos Carajás granite and local trondhjemitic occurrences (part of the Rio Verde trondhjemite). Other Mesoarchean units (ca. 2.87 to 2.83 Ga) include the Bacaba tonalitic complex, the major part of the Rio Verde trondhjemite, the Bom Jesus, Cruzadão, and Serra Dourada granites.

The Neoarchean units (mostly formed in between 2.76 and 2.70 Ga) are represented by the metavolcanics and banded iron formations of the Itacaiúnas supergroup, the Vermelho mafic-ultramafic stock, the tonalitic-trondhjemitic Pedra Branca suite, the Planalto suite granites, charnockitic rocks associated with the Pium complex, and a little younger (ca. 2.65 Ga) small stocks, dikes and sills of mafic rocks. Stocks of Paleoproterozoic (1.88 Ga) A-type anorogenic granites, e.g. the Rio Branco pluton in the west of the Canaã area, are locally intrusive in the Archean units.

Five distinct granite units (Fig. 2) with variable ages (2.93 to 2.73 Ga) were selected for the present study. They include (1) the Canaã dos Carajás granite, exposed in the southeastern part of the area; (2) the Bom Jesus granite in its central part; (3) the Cruzadão granite, with two different areas of occurrence, in the western and center-southern parts of the area; (4) the Serra Dourada granite, a stock located in the northern part of the area; and (5) the Planalto suite, represented by several stocks distributed along most of the area.

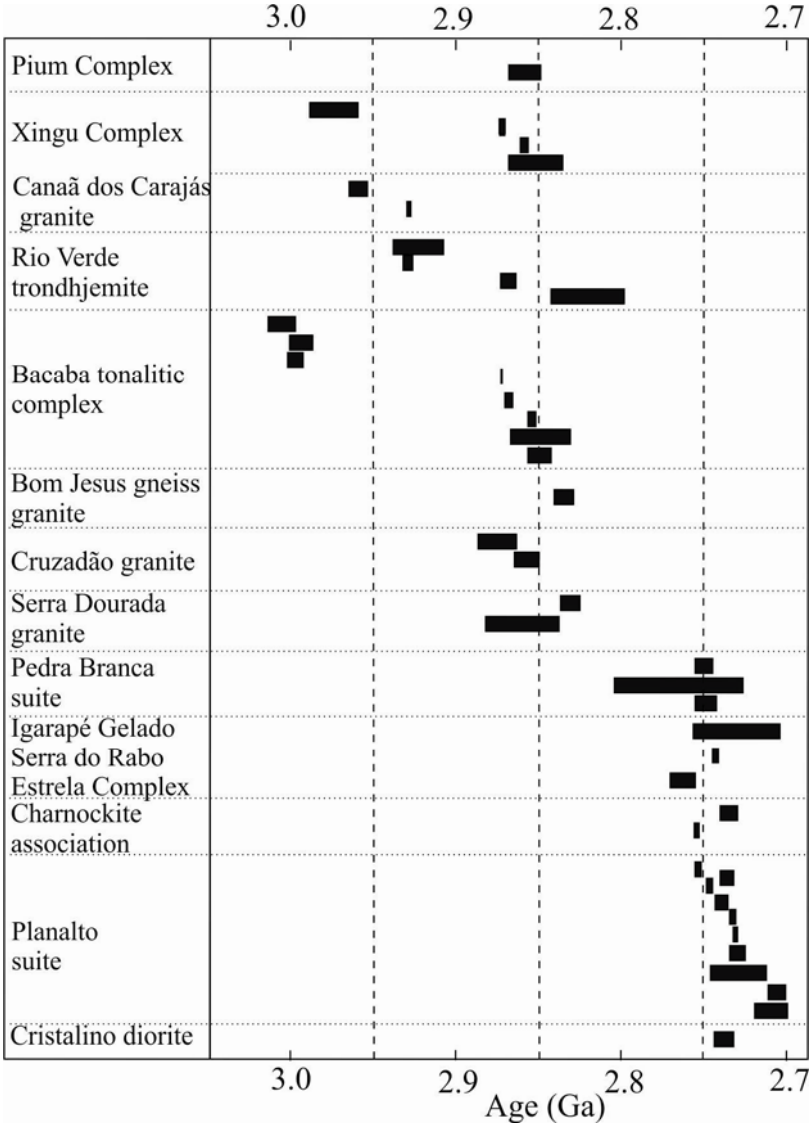

Figure 2 - Summary of geochronological data of the major units of the Carajás domain of the Carajás Province.

4. Geological and petrographic aspects of the Canaã dos Carajás granites

The studied granites are deformed and generally show penetrative foliation which follows the dominant NW-SE to W-E regional main trend (Fig. 1b). They were affected by important shear zones that locally define the limit of the granite bodies. The Serra Dourada is comparatively less deformed than the other granite units.

The modal compositions of representative samples of the five granite units (Table A in the supplemental data, and Fig. 3) demonstrate that the analyzed rocks are dominantly monzogranites, with subordinate granodiorite (Canaã dos Carajás) or syenogranite (Planalto suite, Bom Jesus and Cruzadão granites). Alkali feldspar granites are rare and limited to the Planalto suite. Except for some samples of the Planalto suite which can have hornblende as

the main mafic mineral and have total mafic content (M') generally between 5% and 20%, the remainder granite units are commonly composed of hololeucocratic rocks (M'< 5%) with biotite as the main mafic phase.

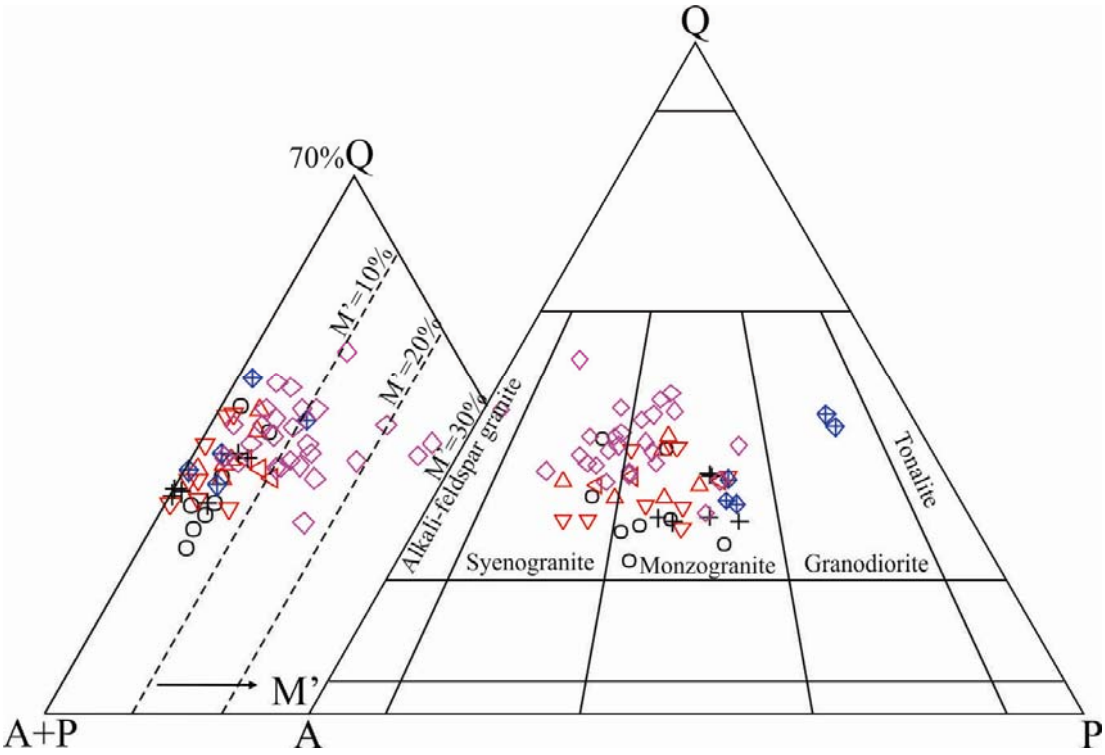

Figure 3 - QAP and Q-(A+P)-M' diagrams (fields of Le Maitre et al., 2002) for the Archean granites of the Canaã dos Carajás area.

4.1. Canaã dos Carajás granite

The Canaã dos Carajás granite forms a relatively large intrusion exposed in the southeastern part of the study area in the proximities of the Canaã dos Carajás town (Fig. 1c). Its western contact is limited by an important NE-SW lineament that is bordered by the southernmost extension of the Itacaiunas supergroup (Fig. 1c). The Canaã dos Carajás intrusion was affected by large approximately E-W shear zones and was intruded by the Pedra Branca and Planalto suite stocks. The contact relationships were not observed in the field but geochronological data are conclusive about the younger age of the latter units compared to the Canaã dos Carajás granite. Locally, the latter includes metric enclaves of amphibolite.

The Canaã dos Carajás granite show a penetrative, vertical NW-SE to E-W foliation which was locally crosscut by dextral and subordinate sinistral NE-SW oriented shear zones (Fig. 1c). A lineation dipping 60° to 70° to S or SE was also observed. The dominant foliation was folded and affected by faults oriented E-W dipping at high angle to S.

The granite is a strongly deformed and mylonitized, hololeucocratic rock (M'<5%). It displays gray color and medium- to fine-grained seriate texture. It is a biotite monzogranite to granodiorite, with zircon, magnetite, titanite ± apatite ± allanite as primary accessory minerals and muscovite, tourmaline, and chlorite as secondary ones. At the microscope, the texture is characterized by the presence of augen shaped plagioclase and alkali feldspar crystals enveloped by fine-grained recrystallized aggregates (core and mantle structures; Vernon, 2004). Quartz is strongly recrystallized and occurs as polygonal fine or elongated aggregates of grains. The biotite is oriented along the dominant foliation and contours the feldspar. Bulbous myrmekite (Phyllips, 1980) is common in the border of the larger alkali feldspar crystals.

4.2. Bom Jesus granite

The Bom Jesus granite is exposed in the central-eastern part of the mapped area (Fig. 1c). It consists essentially of banded and foliated granite oriented along NE-SW to EW with vertical or steep SE- to S-dips. Sinistral mylonitic shear zones crosscut the granite and, locally, isoclinals folds with SE-dipping axes were registered. The granite was submitted to an intense ductile deformation responsible for its gneissic aspect. In the center of the Canaã area, the Bom Jesus granite is intimately associated with the Rio Verde trondhjemite and both rocks show similar structures and occur in the field as intercalated bands or strips. The Bom Jesus granite contains enclaves of amphibolites but field relationships between it and the other granite units were not observed.

The Bom Jesus granite shows pink to gray color and fine- to medium- or medium- to coarse-grained seriated to porphyroclastic texture. It has monzogranite to syenogranite composition with biotite as the main mafic mineral. The accessory minerals are allanite, titanite, zircon, magnetite ± ilmenite, and apatite. The secondary mineralogy is chlorite, rutile, hematite, epidote, carbonates, scapolite, and muscovite. In thin section, the foliation observed in the granite is defined by the oriented micas, the oval shaped feldspars porphyroclasts and the elongated recrystallized quarts aggregates. K-feldspar and plagioclase form the porphyroclasts which are set in a fine-grained recrystallized matrix. Plagioclase grains generally display deformed curved twin lamellae and myrmekite intergrowths occur in the borders of K-feldspar grains.

4.3. Cruzadão granite

The Cruzadão granite shows dominant NW-SE- to EW-striking foliation and was affected by shear zones and mylonitized. In its occurrence of the western of the area, it is locally associated with hornblende tonalites which were tentatively correlated with the Bacaba tonalite complex (Feio et al., submitted b). In that area, both rocks define folded banded structures with intercalated bands of granitic and tonalitic composition which indicate that these rocks were submitted to similar ductile deformational processes. In the occurrence of the center-southern of the area, the Cruzadão granite defines a NE-SW-oriented strip (Fig. 1c) and is intruded by the Vermelho mafic body, a pluton of the Planalto suite and a small stock of the Pedra Branca suite. The field relationships between different units were not observed in the field and the local stratigraphy was defined with support of geochronological data.

The Cruzadão granite displays pink to gray color and coarse- to medium- or medium- to fine-grained seriated texture. It is a hololeucocratic (M'<7%), biotite monzogranite to syenogranite, with zircon, allanite, apatite, magnetite ± epidote ± titanite as common accessory minerals. Chlorite, epidote, muscovite ± carbonates are the secondary minerals. The Cruzadão granite is quite similar to the Bom Jesus granite in mineralogy and broad textural aspects. However, these two granites differ significantly in their geochemical signature and for this reason were distinguished in the present work.

4.4. Serra Dourada granite

The Serra Dourada granite is a sub-circular stock, located near the homonymous village in the northern part of the Canaã area (Fig. 1c). The major part of the stock is formed by little deformed rocks which shows a not pervasive EW-striking vertical foliation and is only locally affected by shear zones. This granite is intrusive in the Bacaba tonalitic complex, includes remnants of greenstone belts, and is intruded by a small body of the Planalto suite. It shows also a close spatial association with abundant Neoarchean dikes and sills of mafic rocks.

This granite displays pink color and medium- to coarse-grained or subordinate fine-grained texture. It has monzogranite composition and biotite, with accessory allanite, zircon ± magnetite and ilmenite as mafic minerals. Secondary phases, mostly related to hydrothermal alteration, are common, including albite, muscovite, biotite, chlorite, epidote, opaque, titanite, quartz, scapolite, and tourmaline. Pegmatite and aplitic veins cut the granite.

The plagioclase (calcic oligoclase - An_{30-20}) and alkali feldspar form subeuhedral crystals. The latter is perthitic and shows myrmekite quartz-plagioclase intergrowths along the borders

of its crystals. Quartz consists of locally fractured and partially recrystallized anhedral grains; biotite is interstitial to the feldspars and quartz.

4.5. Planalto suite granite

The Planalto suite consists of several lenticular granite stocks with less than 10 km in the largest dimension, located in the areas of stronger deformation and oriented concordantly to the dominant EW-trending regional structures or, eventually to NE-SW or NS (Fig. 1c). This Neoarchean Planalto suite is intrusive in the Mesoarchean granitoid units, in the mafic Pium complex, in the Neoarchean supracrustal Itacaiúnas supergroup (Fig. 1c) and is associated spatially with the Pium complex and the Pedra Branca suite. It was described in more detail by Feio et al. (submitted a).

The Planalto granite shows penetrative EW- to NNW-subvertical foliation locally accompanied by a high angle stretching mineral lineation and C-type shear bands. Mylonites are found along sinistral or subordinate dextral shear zones. The less deformed rocks preserve magmatic textures. The Planalto suite is composed of biotite-hornblende monzogranite to syenogranite, with subordinate alkali feldspar granite. Relics of clinopyroxene with coronae of amphibole are present in some samples. The primary accessory minerals are zircon, apatite, allanite, ilmenite ± magnetite ± titanite ± fluorite.

Most rocks display porphyroclasts of quartz, perthitic alkali-feldspar, and plagioclase, which show core-and-mantle microstructures. The quartz occurs also as ribbons and recrystallized aggregates. The plagioclase show curved twin plans and recrystallization to fine-grained polygonal aggregates of largely untwinned grains. Bulbous myrmekite intergrowths are found along the borders of alkali-feldspar grains. The amphibole occurs as medium-grained oval porphyroclasts or form oriented aggregates together with biotite and other mafic minerals. In the mylonites, the foliation is deflected around alkali-feldspar porphyroclasts and strain shadows are formed by the fine-grained recrystallized aggregates.

5. Geochemistry of the Canaã dos Carajás granites

49 samples of the different granite units of the Canaã area were selected for chemical analyses, including 3 samples from the Canaã dos Carajás, 8 samples from the Bom Jesus, 12 samples from the Cruzadão, 6 samples from the Serra Dourada and 20 samples from the Planalto granites. The chemical analyses were performed by ICP-ES for major elements and ICP-MS for trace-elements, including the rare-earth elements, at the Acme Analytical Laboratories Ltd. in Canada. The geochemistry of the Planalto suite granite was discussed in

detail by Feio et al. (submitted a) and only part of the available chemical analyses is presented here. A set of representative chemical analyses of the studied granites is given on Table 1.

5.1. Major and trace elements

Harker diagrams for selected major and trace elements (Figs. 4, 5) demonstrate that all analyzed samples of different granite units exhibit high silica contents with a restrict variation (70-76 wt. %). Two clearly distinct geochemical signatures can be identified in the Harker diagrams: Granites with relatively high Al_2O_3 contents (>13 wt. % to ca. 15 wt. %, Table 1, Fig. 4a) which includes the Canaã dos Carajás, Bom Jesus, Cruzadão, and Serra Dourada Mesoarchean granites, and the low-Al_2O_3 (11-13 wt. %), Neoarchean Planalto granite. The latter is enriched in FeO (Fig. 4c), Ba, Zr, Y, Nb, and impoverished in MgO (Fig. 4d), Na_2O (Fig. 4f), Sr, and Rb (Figs. 5c, b) compared to the high-Al_2O_3 granites. Among the latter, the geochemical contrasts are less marked but remain significant. The Canaã dos Carajás granite has relatively higher contents of Al_2O_3, CaO, and Na_2O (Figs. 4a, b, f) and lower contents of K_2O (Fig. 4e), Ba, Rb, Zr, Nb, and Y (Figs. 5a, b, d, e, f), compared to the other high-Al_2O_3 granites. The Serra Dourada granite has also relatively high Al_2O_3 and Na_2O contents, but a little lower than in the Canaã dos Carajás granite, and is enriched in Nb, and Y (Figs. 5e, f), and impoverished in Sr (Fig. 5c) compared with the Bom Jesus and Canaã dos Carajás granites. Finally, the Bom Jesus and Cruzadão granites, that show similar field aspects and ages, can be distinguished by their significant geochemical contrasts. CaO, K_2O, Ba, and Sr, are higher, and Rb, Nb, and Y contents are lower in the Bom Jesus granite compared to the Cruzadão one. There is also significant geochemical variation in the samples of the Cruzadão granite. Some rocks, as exemplified by samples ARC-141A, GRD-58A, and ARC-58B, have lower silica and are clearly more enriched in Zr, Nb, and Y compared to the dominant rocks of that unit (Figs. 5 d, e, f). Apparently the registered chemical contrasts in the Cruzadão granite are not related with the provenance of the samples, in the sense that samples with different geochemical signature occur in both the western and center-southern plutons.

The Rare Earth Elements (REE) patterns (Fig. 6) of different granite units show clear contrasts in the extent of Heavy-REE (HREE) fractionation and in the nature of the europium anomaly. The Canaã dos Carajás granite (Fig. 6a) has the lowest ∑REE contents (Table 1), show low to moderate fractionation of the HREE [(La/Yb)n = 7 to 21] and europium anomalies slightly positive or negative (Eu/Eu* = 1.1 to 0.7). The Bom Jesus granite samples are relatively enriched in Light-REE (LREE), show a strong fractionation of HREE [(La/Yb)n = 79 to 330], europium anomalies generally also slightly positive or negative (Eu/Eu* = 1.2 to

0.7 with two anomalous values of 1.8 and 0.5; Table 1) and a concave shape of the HREE branch (Fig. 6b) which suggests fractionation of amphibole during the granite magma evolution. The Cruzadão granite shows the higher ∑REE contents (Table 1) of the high-Al_2O_3 granite group, and two different REE patterns (Figs. 6c, d) were identified: (1) The first group shows accentuated HREE fractionation [(La/Yb)n = 78 to 120], but lower than that observed in the Bom Jesus granite, strongly negative europium anomalies (Eu/Eu* = 0.5 to 0.3; Table 1), and concave-shaped HREE patterns (Fig. 6c). (2) The second group has a moderate degree of HREE fractionation [(La/Yb)n = 11 to 56], and prominent negative europium anomalies (Eu/Eu* = 0.5 to 0.2; Table 1, Fig. 6d). The samples ARC-141A, GRD-58A, and ARC-58B, which are relatively enriched in HREE and show flat HREE branch patterns are those enriched in High-Field Strength Elements (HFSE; Table 1). The Serra Dourada granite displays low to moderate fractionation of HREE [(La/Yb)n = 9 to 63] and discrete to accentuate negative europium anomalies (Eu/Eu* = 0.8 to 0.4; Table 1, Fig. 6e). The Planalto suite has the highest ∑REE of the studied granites, is enriched in LREE but with low degree of HREE fractionation [(La/Yb)n = 6 to 17, Table 1], and show generally accentuate negative europium anomalies (Eu/Eu* = 0.7 to 0.3; Table 1, Fig. 6f).

Table 1 -Chemical composition of the Archean granites of the Canaã dos Carajás area

Sample	AMR-213*	AMR-102*	AMR-83B	ERF-123*	AER-16A	ERF-18C	AER-65A*	ARC-116	ERF-137	AE-47*	AER-65C	ARC-100*	ARF-9	ARC-113
Petrology	BGrd	BLMzG	BLMzG	BMzG	BMzG	BMzG	BMzG	BMzG	BLSG	BLSG	BMzG	BLSG	BSG	BLSG
Unidade	Canaã dos Carajás granite			Bom Jesus Granite								Cruzadão granite		
SiO2	70,56	72,44	72,93	71,83	72,89	72,92	73,63	73,81	74,02	74,43	74,87	70,90	71,34	74,34
TiO2	0,31	0,16	0,18	0,18	0,20	0,14	0,23	0,13	0,22	0,15	0,21	0,22	0,31	0,18
Al2O3	14,74	14,84	14,28	14,47	13,83	14,84	13,42	13,54	13,52	13,79	13,24	14,25	14,19	13,41
FeOt	3,03	1,55	1,74	1,39	1,80	1,38	1,61	1,48	1,53	1,03	1,30	2,55	1,93	1,29
Fe2O3t	3,37	1,72	1,93	1,55	2,00	1,53	1,79	1,65	1,70	1,15	1,44	2,83	2,14	1,43
MnO	0,01	0,04	0,03	0,01	0,02	0,01	0,01	0,01	0,02	0,01	0,02	0,03	0,02	0,01
MgO	0,77	0,37	0,38	0,41	0,47	0,34	0,33	0,30	0,40	0,23	0,25	0,48	0,59	0,26
CaO	1,50	2,02	1,60	1,59	1,51	1,94	1,60	1,27	1,24	1,56	1,29	0,76	1,29	0,98
Na2O	4,29	4,54	3,59	3,83	3,31	3,76	3,43	3,17	3,35	3,53	3,28	3,62	2,95	3,27
K2O	3,17	3,02	3,76	4,51	4,77	3,69	4,28	5,08	4,84	4,56	4,70	5,60	5,81	5,48
P2O5	0,08	0,05	0,05	0,07	0,08	0,06	0,05	0,05	0,06	0,06	0,04	0,12	0,04	0,04
LOI	1,00	0,70	0,70	1,30	0,70	0,60	1,00	0,70	0,40	0,40	1,00	0,80	1,00	0,40
Ba	961,0	684,0	837,0	1658,1	1410,6	1110,7	1547,0	1403,0	857,6	915,0	1379,1	1531,0	1419,0	783,0
Rb	108,7	77,6	132,5	140,1	135,2	121,1	151,0	120,2	211,1	135,2	160,9	227,5	207,9	281,4
Sr	202,3	282,4	220,8	462,5	531,7	424,7	330,5	640,1	201,2	194,0	261,0	343,0	186,2	182,4
Zr	125,6	89,4	90,6	167,4	267,2	133,3	240,5	238,1	141,1	110,6	210,2	293,2	303,0	186,8
Nb	6,9	4,9	6,9	5,8	4,1	3,6	5,1	1,3	7,4	3,2	3,4	3,7	12,1	13,9
Y	14,8	6,5	7,3	2,9	5,7	3,5	2,8	1,7	3,3	2,5	2,0	6,4	10,3	6,3
Th	9,9	5,3	5,2	62,6	36,8	14,8	32,1	31,7	36,0	2,6	31,9	67,0	71,8	72,6
U	2,0	0,7	1,8	6,7	0,7	0,9	1,7	0,9	1,7	1,2	2,7	3,1	4,6	21,9
Ta	0,8	0,4	1,4	2,7	1,2	0,3	1,9	0,1	2,3	0,2	1,1	0,3	0,4	0,8
Hf	4,1	2,9	2,7	4,5	6,4	3,9	6,9	6,9	4,4	3,4	6,4	7,9	8,5	5,6
V	29,0	11,0	20,0	19,0	22,0	20,0	13,0	19,0	16,0	21,0	10,0	31,0	24,0	8,0
Ga	15,7	18,9	16,8	17,9	18,9	18,9	17,5	15,3	19,8	17,3	16,3	18,2	17,5	17,4
Cu	28,4	0,8	19,3	2,5	6,5	99,7	2,9	10,6	8,7	7,0	3,1	165,5	24,9	27,5
Pb	3,5	2,8	7,7	11,0	8,9	15,3	5,7	10,1	10,9	2,9	5,5	18,7	38,6	20,8
Ni	8,1	2,2	2,6	5,4	5,2	3,7	1,5	2,3	4,7	4,5	2,6	6,1	5,3	2,9
Co	43,2	2,4	65,4	20,6	13,9	24,6	16,9	39,8	19,0	24,8	10,7	30,0	35,4	48,1
Zn	9,0	34,0	24,0	27,0	39,0	21,0	26,0	18,0	38,0	19,0	24,0	24,0	17,0	23,0
La	32,00	15,30	8,10	51,30	128,00	57,40	56,20	78,20	35,00	23,10	45,10	125,90	87,20	104,60
Ce	58,80	29,00	20,60	87,80	197,80	121,50	115,20	129,90	65,10	36,90	89,60	238,90	163,60	198,90
Pr	6,55	3,23	1,76	7,51	19,63	11,27	10,01	12,85	6,14	3,71	8,21	26,23	19,00	21,79
Nd	23,70	11,80	5,60	20,90	58,60	35,20	32,30	37,40	19,80	12,00	25,70	81,00	67,60	68,30
Sm	3,69	1,97	1,18	2,00	6,00	3,60	3,50	2,94	2,80	1,35	3,10	10,85	10,34	7,31
Eu	0,91	0,40	0,41	0,62	0,77	0,62	0,68	0,74	0,65	0,69	0,70	1,40	0,88	0,65
Gd	2,93	1,45	1,04	0,92	2,12	1,38	1,25	1,38	1,51	0,85	0,91	5,26	6,74	3,40
Tb	0,43	0,21	0,21	0,10	0,24	0,19	0,15	0,10	0,14	0,10	0,12	0,62	0,71	0,30
Dy	2,35	1,15	1,31	0,46	0,91	0,91	0,52	0,39	0,72	0,41	0,39	2,35	2,59	1,15
Ho	0,46	0,20	0,25	0,07	0,12	0,12	0,09	0,04	0,09	0,08	0,06	0,29	0,32	0,17
Er	1,36	0,54	0,73	0,25	0,32	0,27	0,25	0,13	0,29	0,19	0,20	0,70	0,67	0,48
Tm	0,19	0,07	0,12	0,05	0,05	0,05	0,05	0,02	0,05	0,03	0,05	0,13	0,09	0,10
Yb	1,27	0,52	0,79	0,24	0,30	0,33	0,30	0,17	0,29	0,21	0,20	0,91	0,52	0,73
Lu	0,20	0,06	0,13	0,04	0,05	0,05	0,06	0,03	0,03	0,03	0,04	0,13	0,07	0,12
K_2O/Na_2O	0,74	0,67	1,05	1,18	1,44	0,98	1,25	1,60	1,44	1,29	1,43	1,55	1,97	1,68
ACNK	1,12	1,03	1,11	1,03	1,04	1,08	1,02	1,04	1,04	1,02	1,03	1,06	1,05	1,02
FeOt/(FeOt+M	0,80	0,81	0,82	0,77	0,79	0,80	0,83	0,83	0,79	0,82	0,84	0,84	0,77	0,83
#Mg	0,31	0,30	0,28	0,34	0,32	0,31	0,27	0,26	0,32	0,28	0,26	0,25	0,35	0,26
Sr/Ba	0,21	0,41	0,26	0,28	0,38	0,38	0,21	0,46	0,23	0,21	0,19	0,22	0,13	0,23
Rb/Sr	0,54	0,27	0,60	0,30	0,25	0,29	0,46	0,19	1,05	0,70	0,62	0,66	1,12	1,54
Sr/Y	13,67	43,45	30,25	159,48	93,28	121,34	118,04	376,53	60,97	77,60	130,50	53,59	18,08	28,95
La/Yb	25,20	29,42	10,25	213,75	426,67	173,94	187,33	460,00	120,69	110,00	225,50	138,35	167,69	143,29
TREE	134,84	65,90	42,23	172,26	414,91	232,89	220,56	264,29	132,61	79,65	174,38	494,67	360,33	408,00
(La/Yb)N	18,07	21,11	7,35	153,32	306,05	124,77	134,37	329,96	86,57	78,90	161,75	99,24	120,29	102,78
(La/Sm)N	5,60	5,01	4,43	16,56	13,77	10,29	10,37	17,17	8,07	11,05	9,39	7,49	5,44	9,24
(Gd/Yb)N	1,91	2,31	1,09	3,17	5,85	3,46	3,45	6,72	4,31	3,35	3,76	4,78	10,72	3,85
Eu/Eu*	0,82	0,69	1,11	1,22	0,54	0,71	0,81	0,98	0,87	1,84	0,98	0,50	0,30	0,35

Cont. Table 1

Sample	ERF-109	ARC-141A	GRD-58A	ARC-58B	ARC-108	ERF-101	ARC-106A	ERF-102*	AER-30B	AER-59*	AER-47E	AER-27*	AER-30C	AER-57A
Petrology	BLMzG	BMzG	BSG	BSG	BLMzG	BLMzG	BMzG	BLSG	BMzG	BLMzG	BLMzG	LMzG	LMzG	LMzG
Unidade	Cruzadão granite								Serra Dourada Granite					
SiO2	72,61	70,63	70,92	71,08	72,31	73,51	73,56	74,10	72,32	72,35	73,85	74,61	75,07	75,40
TiO2	0,17	0,20	0,41	0,41	0,24	0,19	0,26	0,15	0,28	0,27	0,23	0,08	0,05	0,11
Al2O3	13,59	14,36	14,21	14,12	14,13	13,64	13,53	13,35	14,01	14,42	14,14	13,50	13,68	13,58
FeOt	1,40	2,21	2,44	2,22	1,48	1,54	2,03	1,13	2,12	1,93	1,90	1,17	0,69	0,82
Fe2O3t	1,56	2,46	2,71	2,47	1,64	1,71	2,26	1,26	2,36	2,15	2,11	1,30	0,77	0,91
MnO	0,02	0,02	0,03	0,03	0,01	0,02	0,02	0,02	0,01	0,01	0,04	0,01	0,01	0,01
MgO	0,27	0,54	0,61	0,57	0,62	0,33	0,35	0,29	0,44	0,39	0,35	0,25	0,08	0,09
CaO	0,95	1,31	1,61	1,62	0,54	0,98	1,05	1,03	1,34	1,94	1,59	0,26	0,41	1,16
Na2O	3,66	3,95	3,70	3,76	3,49	3,45	3,80	3,54	3,40	3,95	3,92	3,64	3,08	3,40
K2O	5,04	4,95	4,89	4,81	5,81	5,31	4,31	4,83	4,54	3,32	3,49	4,80	5,98	4,37
P2O5	0,05	0,09	0,15	0,13	0,06	0,06	0,06	0,05	0,10	0,12	0,08	0,04	0,02	0,01
LOI	2,00	1,30	0,60	0,70	0,90	0,70	0,60	1,30	1,00	1,00	0,10	1,40	0,80	0,90
Ba	638,9	365,0	885,0	934,0	1047,0	910,7	724,0	519,5	1299,7	610,1	764,5	911,2	561,4	710,0
Rb	269,7	388,2	232,0	232,0	215,0	192,1	281,9	152,8	227,2	172,3	194,8	149,4	253,3	134,9
Sr	124,8	89,4	233,6	238,5	115,5	130,8	119,4	200,0	193,9	205,2	180,6	60,3	64,8	148,3
Zr	205,4	238,2	302,2	345,9	233,3	229,8	231,4	146,3	235,0	148,6	198,7	78,2	54,3	74,0
Nb	10,7	30,9	39,3	38,9	27,0	7,9	30,4	8,6	18,4	15,9	14,0	25,3	19,9	7,8
Y	6,2	47,1	34,2	43,4	18,8	20,8	19,3	16,9	16,2	11,1	10,6	14,2	8,8	9,0
Th	62,4	57,3	29,0	28,3	38,3	71,8	23,4	63,4	41,8	16,8	35,8	25,4	14,8	55,2
U	18,4	23,4	9,0	15,8	9,9	6,5	9,6	18,1	9,5	14,4	10,5	14,0	7,7	14,9
Ta	2,3	3,5	7,7	4,6	2,6	2,5	2,3	2,6	6,8	1,3	1,3	14,0	7,3	0,9
Hf	6,9	7,2	7,9	9,0	6,4	7,2	7,1	5,0	6,7	4,3	6,2	2,8	2,9	2,4
V	16,0	10,0	27,0	26,0	14,0	12,0	16,0	11,0	21,0	16,0	9,0	6,0	5,0	5,0
Ga	19,0	21,7	18,5	19,5	19,6	18,2	21,1	16,2	20,5	22,3	21,0	18,5	19,5	17,6
Cu	5,6	4,1	8,8	14,2	18,2	5,0	63,4	4,8	39,3	135,3	18,8	66,5	21,9	17,1
Pb	21,7	13,2	9,8	10,5	7,9	23,8	7,1	14,1	21,5	13,4	18,4	3,3	6,5	10,6
Ni	2,2	6,1	5,2	5,2	6,4	2,1	3,4	2,4	7,1	10,7	2,1	6,9	1,5	3,4
Co	18,3	26,8	24,2	31,1	42,5	16,4	31,0	15,5	49,9	28,9	25,3	68,4	39,7	25,8
Zn	33,0	15,0	39,0	44,0	8,0	38,0	18,0	28,0	25,0	17,0	38,0	16,0	12,0	13,0
La	88,30	72,70	88,10	101,40	66,80	86,40	79,50	81,70	77,60	30,20	61,00	24,30	14,30	42,10
Ce	171,30	135,00	187,60	196,50	129,90	152,70	148,00	172,50	147,00	62,10	123,80	46,70	30,10	63,30
Pr	15,95	14,95	20,07	22,38	14,18	17,31	16,03	18,35	15,22	6,63	11,83	4,85	3,06	7,45
Nd	46,80	48,80	66,60	76,00	45,40	56,90	51,50	59,80	51,30	24,20	41,30	17,80	10,50	26,60
Sm	4,90	8,30	10,79	11,82	6,17	8,50	6,86	9,30	7,00	4,10	5,60	3,30	2,00	4,20
Eu	0,49	0,57	0,89	1,03	0,90	0,84	0,74	0,71	0,79	0,52	0,55	0,75	0,42	0,76
Gd	2,39	6,72	8,02	8,63	4,01	5,56	4,72	5,38	3,99	2,81	3,01	2,59	1,40	2,70
Tb	0,26	1,19	1,12	1,39	0,57	0,69	0,66	0,74	0,53	0,39	0,46	0,42	0,26	0,33
Dy	0,99	6,67	6,06	7,28	2,82	3,23	3,32	4,02	2,67	2,01	1,96	2,02	1,37	1,48
Ho	0,15	1,40	1,10	1,39	0,53	0,59	0,60	0,59	0,45	0,32	0,31	0,45	0,29	0,26
Er	0,59	4,27	3,17	3,89	1,56	1,55	1,54	1,51	1,33	1,01	0,87	1,42	0,89	0,68
Tm	0,10	0,73	0,45	0,61	0,26	0,21	0,25	0,20	0,20	0,14	0,13	0,22	0,18	0,12
Yb	0,81	4,61	2,99	3,75	1,81	1,10	1,50	1,22	1,52	0,94	0,69	1,61	1,17	0,71
Lu	0,13	0,64	0,40	0,47	0,26	0,17	0,22	0,19	0,22	0,15	0,13	0,24	0,16	0,10
K_2O/Na_2O	1,38	1,25	1,32	1,28	1,66	1,54	1,13	1,36	1,34	0,84	0,89	1,32	1,94	1,29
ACNK	1,03	1,01	0,99	0,98	1,09	1,03	1,05	1,03	1,08	1,06	1,08	1,16	1,11	1,09
FeOt/(FeOt+M	0,84	0,80	0,80	0,80	0,70	0,82	0,85	0,80	0,83	0,83	0,84	0,82	0,90	0,90
#Mg	0,26	0,30	0,31	0,31	0,43	0,28	0,23	0,31	0,27	0,26	0,25	0,28	0,17	0,16
Sr/Ba	0,20	0,24	0,26	0,26	0,11	0,14	0,16	0,38	0,15	0,34	0,24	0,07	0,12	0,21
Rb/Sr	2,16	4,34	0,99	0,97	1,86	1,47	2,36	0,76	1,17	0,84	1,08	2,48	3,91	0,91
Sr/Y	20,13	1,90	6,83	5,50	6,14	6,29	6,19	11,83	11,97	18,49	17,04	4,25	7,36	16,48
La/Yb	109,01	15,77	29,46	27,04	36,91	78,55	53,00	66,97	51,05	32,13	88,41	15,09	12,22	59,30
TREE	333,16	306,55	397,36	436,54	275,17	335,75	315,44	356,21	309,82	135,52	251,64	106,67	66,10	150,79
(La/Yb)N	78,19	11,31	21,14	19,40	26,47	56,34	38,02	48,04	36,62	23,05	63,41	10,83	8,77	42,53
(La/Sm)N	11,63	5,65	5,27	5,54	6,99	6,56	7,48	5,67	7,16	4,76	7,03	4,75	4,62	6,47
(Gd/Yb)N	2,44	1,21	2,22	1,90	1,83	4,18	2,60	3,65	2,17	2,47	3,61	1,33	0,99	3,15
Eu/Eu*	0,39	0,23	0,28	0,30	0,52	0,35	0,38	0,28	0,42	0,44	0,37	0,76	0,73	0,65

*Feio et al. submitted b

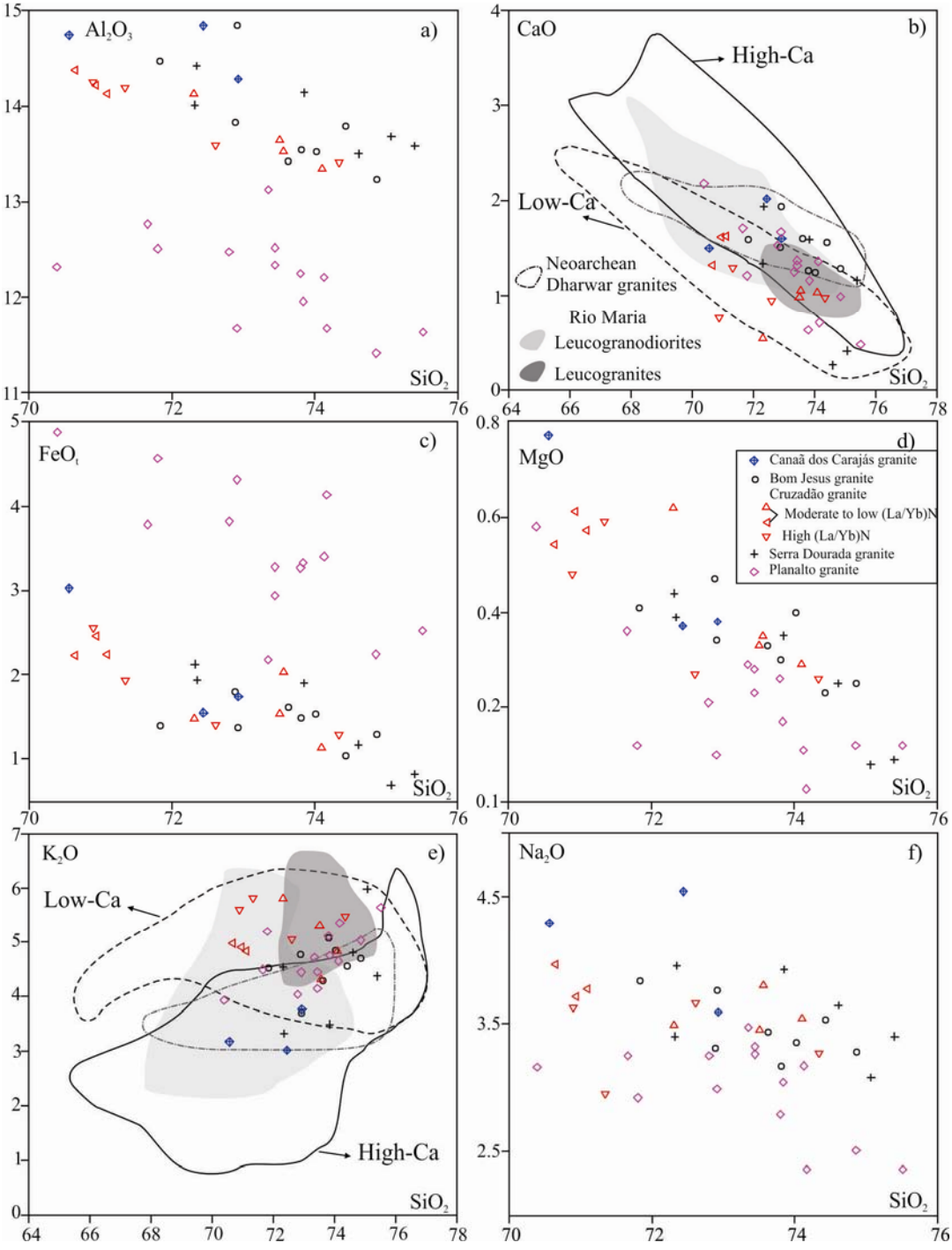

Figure 4 - Major elements Harker diagrams (oxides in wt. %) for the Archean granites of the Canaã dos Carajás area. In figures 3b and e, the fields of the Low-Ca and High-Ca Archean granites of the Yilgarn craton (Champion and Sheraton, 1997), the Neoarchean Dharwar granites (Jayananda et al., 2006), and the leucogranodiorite-leucogranite Guarantã suite (Almeida et al., 2010) and potassic leucogranites (Almeida et al., submitted) of Rio Maria are plotted for comparison.

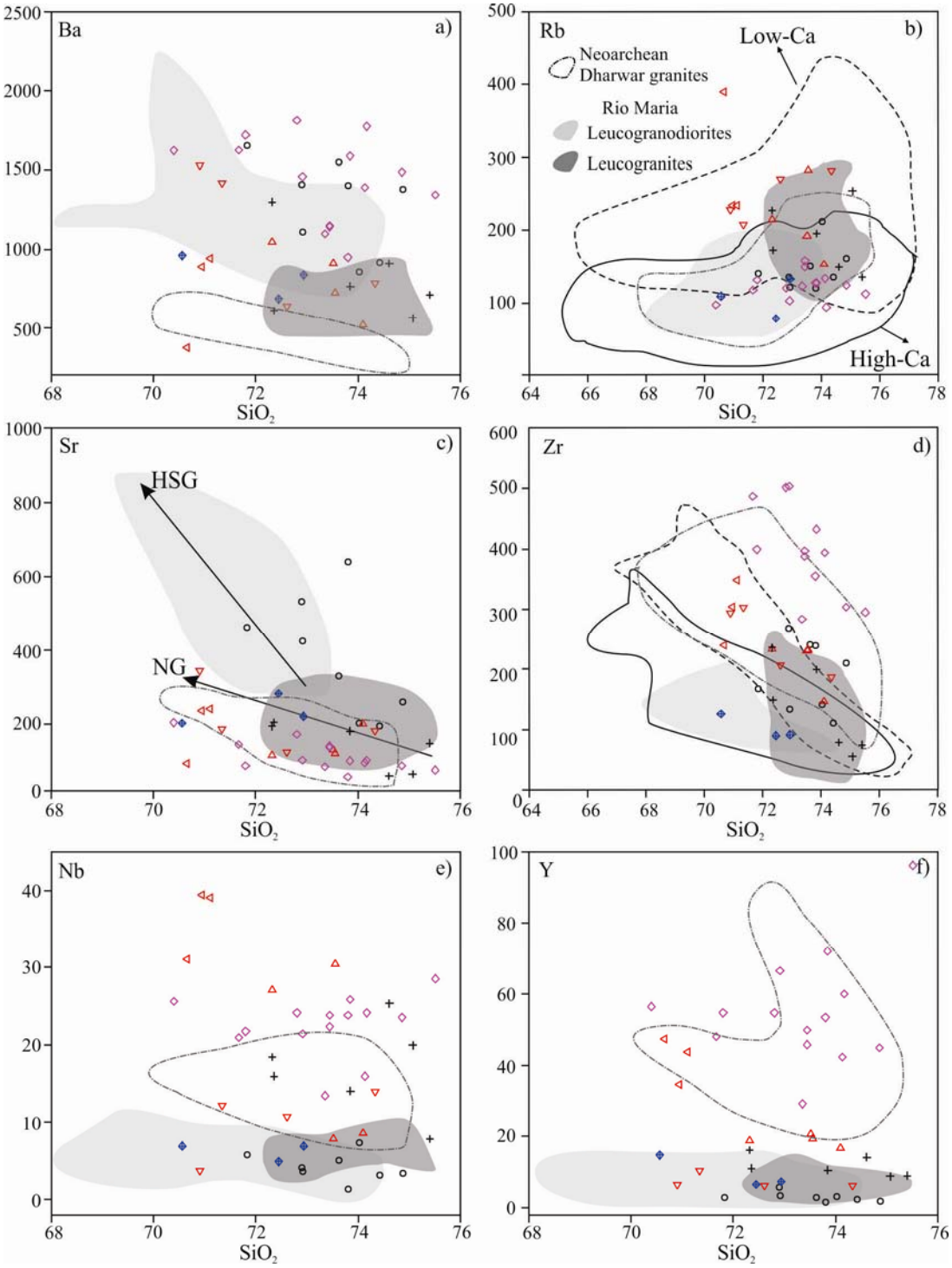

Figure 5 - Trace elements Harker diagrams (in ppm) for the Archean granites of the Canaã dos Carajás area. The fields of the Low-Ca and High-Ca of the Yilgarn craton (Champion and Sheraton, 1997), the Neoarchean Dharwar granites (Jayananda et al., 2006), the leucogranodiorite-leucogranite Guarantã suite (Almeida et al., 2010) and the potassic leucogranites (Almeida et al., submitted) of Rio Maria, and the trends (arrows in Figure 4c) of High-Sr/Y (HSG) and Normal granites (NG) of the Post-collisional granitoids from the Dabie orogen (He et al., 2011) are plotted for comparison.

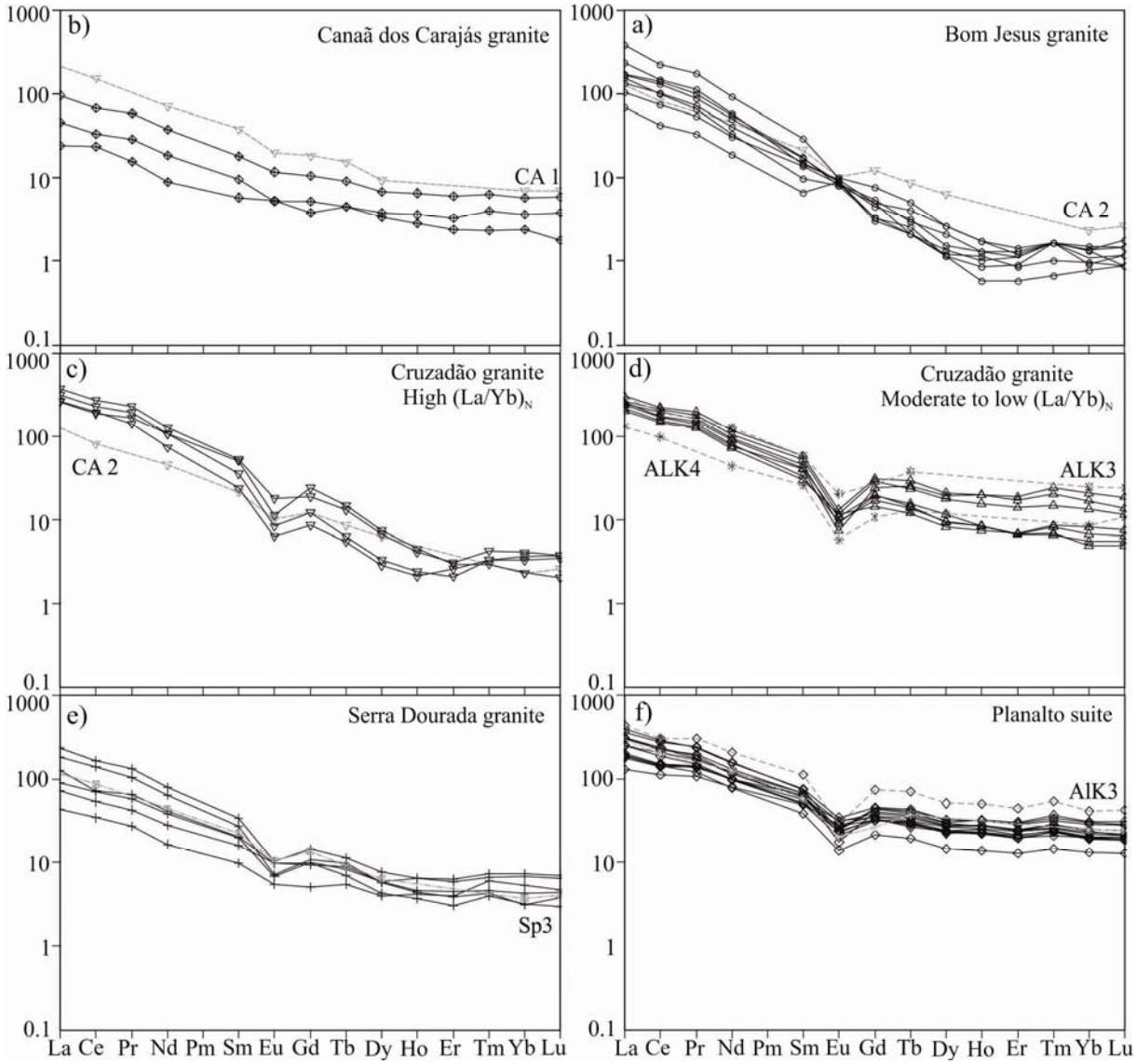

Figure 6 - REE patterns of the Archean granites of the Canaã dos Carajás area. Values normalized to chondrite after Nakamura (1974). The REE patterns (gray dashed lines) of average Archean granite types of Sylvester (1994) are shown for comparison. The Cruzadão granite varieties with high- and moderate to low $(La/Yb)_N$ ratios are separately plotted in figures 5c and 5d.

5.2. Magmatic series and classification of the Archean Canaã granites

The PQ diagram (Fig. 7a) shows that almost all analyzed samples are monzogranites or syenogranites with rare granodiorites. The Planalto suite granites are metaluminous to mildly peraluminous, whereas most of the high-Al_2O_3 granites are weakly peraluminous (cf. ACNK values in Table 1). In the $100*(MgO+FeO+TiO_2)/SiO_2$ vs. $(Al_2O_3+CaO)/(FeO+Na_2O+K_2O)$ diagram (Sylvester, 1989), the Planalto granites plot in the alkaline field and the other granites mostly in the calc-alkaline and strongly peraluminous or strongly fractionated fields (Fig. 7b). The exception is the Cruzadão granite that plots in the border between the calc-alkaline and alkaline fields. In the Al_2O_3 vs. FeOt/(FeOt+MgO)

diagram (Dall'Agnol and Oliveira, 2007), the Planalto granite plots in the reduced-A-type granite field and the other granites in the area of superposition of the oxidized-A-type and calc-alkaline fields (Fig. 7c). In the Na_2O vs. K_2O diagram it could be seen that almost all analyzed samples have $K_2O/Na_2O > 1$ (Fig. 7d, Table 1) and could be considered potassic granites, except for the Canaã dos Carajás granite that shows $K_2O/Na_2O < 1$ and has a more sodic character. In the Yb vs. Sr/Y plot (Fig. 7e), there is also a good discrimination between the studied granites. The low-Al_2O_3 Planalto granite has the highest Yb contents and can be easily distinguished of the other granites, except for the samples of the Cruzadão granite enriched in HFSE which approach the field defined by the Planalto granite in this diagram. The remainder samples of the Cruzadão granite, and those of the Canaã dos Carajás and Serra Dourada granites show similar distribution in this diagram due to their moderate Yb and Sr/Y values (Fig. 7e). Finally, the Bom Jesus granite has the highest Sr/Y ratios and the lowest Yb contents. Similar aspects can be observed in the La/Yb vs. Sr/Y diagram (Fig. 7f).

A comparison between the REE patterns and spidergrams (Fig. 8) of the analyzed rocks with the different types of Archean granites distinguished by Sylvester (1994) show that: (1) The Canaã dos Carajás granite is akin geochemically to the calc-alkaline granites of type 1 (CA1, Figs. 6a, 8a) of Sylvester (1994); (2) The Bom Jesus granite is more similar to the calc-alkaline granites of type 2 (CA2) of Sylvester (1994) but its REE patterns are generally devoid of negative europium anomalies and show a more accentuated fractionation of HREE and Y compared to the average composition of CA2 (Figs. 6b, 8b); (3) The comparison with the Cruzadão granite is a little more complex due to the chemical variations observed in this granite. The variety of this granite with stronger fractionation of HREE (Fig. 6c) has more geochemical affinity with the CA2 granites but it differs from them by the presence of positive anomalies of Th and U and negative anomaly of Sr (Fig. 8c). The Cruzadão granites relatively enriched in HREE (Fig. 6d) are similar to the alkaline granite types (ALK 3 or 4) of Sylvester (1994), as evidenced by the behavior of most incompatible elements (Fig. 8d), but the Cruzadão granites have comparatively higher Al_2O_3 contents; (4) The Serra Dourada granite REE pattern (Fig. 6e) and spidergram (Fig. 8e) suggest geochemical similarities with the strongly peraluminous granites of the type 3 of Sylvester (SP3); (5) The Planalto suite granites have clear geochemical affinities with the alkaline granites of the ALK3 subtype (Sylvester, 1994), as indicated by the REE patterns (Fig. 6f) and multi-element diagram (Fig. 8f).

The whole geochemical data obtained on the studied granites demonstrate that the Planalto granites have ferroan character and are similar geochemically to reduced A-type

granites. Feio et al. (submitted a) proposed to classify the biotite-hornblende granites of the Planalto suite as hydrated granites of the charnockitic rocks series based on their close association with rocks of the charnockitic series and emplacement in a syntectonic setting. Anyway, the strong geochemical contrast between the Neoarchean Planalto suite granites and the other studied granites is evident. Of the latter, the Canaã dos Carajás, Bom Jesus and part of the Cruzadão granites display geochemical signatures more akin to the calc-alkaline granites of CA1 (Canaã) or CA2 types (Bom Jesus and part of the Cruzadão). The second variety of the Cruzadão granite is clearly transitional between the calc-alkaline and alkaline granites and the alkaline character is reinforced in the samples enriched in HFSE and HREE. The Serra Dourada granite differs in some aspects of the calc-alkaline granites and the behavior of incompatible elements approaches that registered in the strongly peraluminous granites of SP3 subtype. However, the Nb and Y contents of the Serra Dourada are significantly higher than those observed in the SP3 granites and their ACNK ratios (<1.16 and generally <1.1) are significantly lower than the average of the SP3 granites (1.44; Sylvester, 1994). Other relevant aspects are: the modal mineralogy of the Serra Dourada granite do not show any evidence of a strong peraluminous character; the lack of inherited zircon in the dated sample of this unit (Feio et al., submitted b); and the positive εNd values yielded by the two analyzed samples of this granite. Thus, despite some geochemical evidence in favor of metasedimentary sources for the Serra Dourada granite, there are also indications of its derivation from more juvenile, possibly igneous sources.

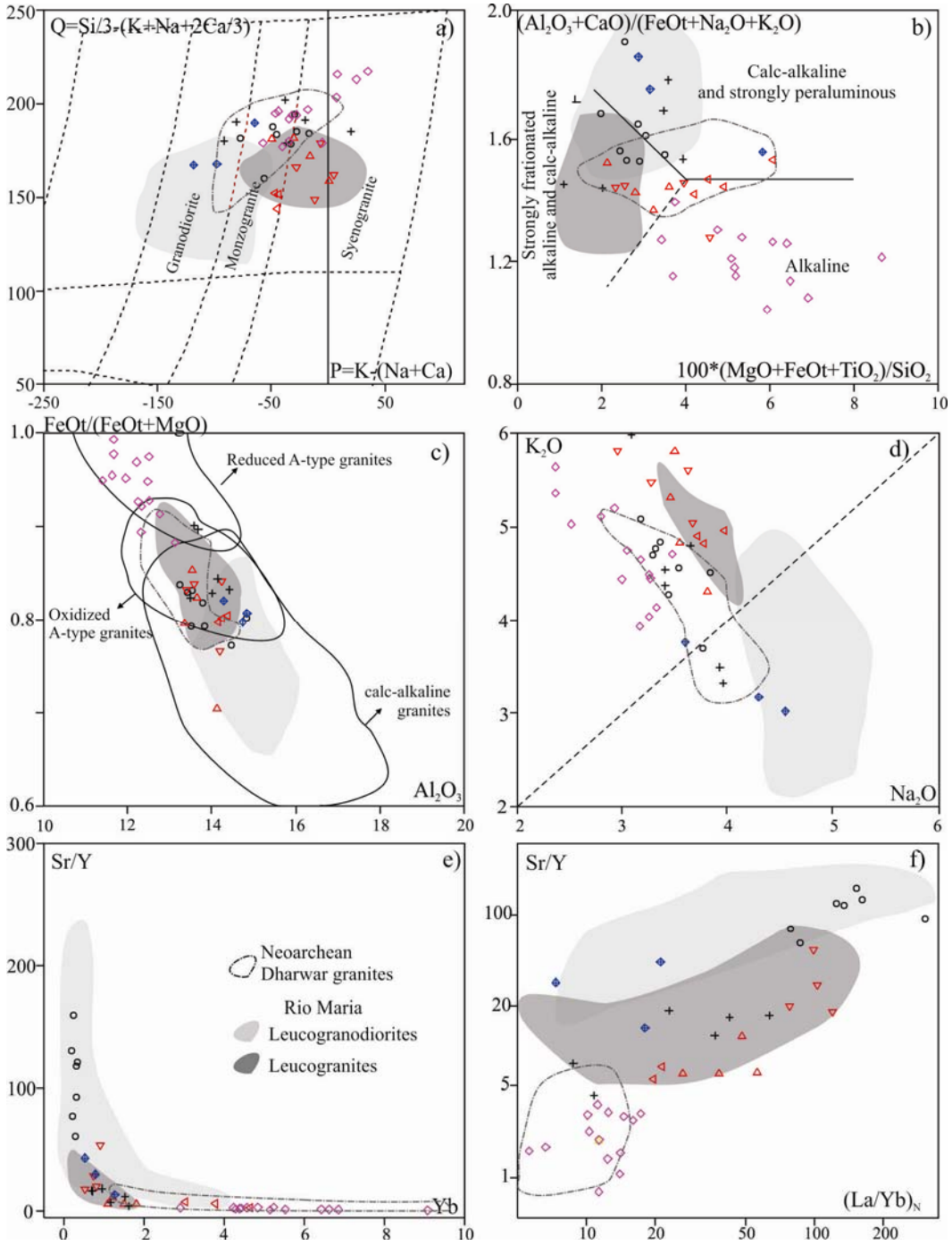

Figure 7 - Geochemical plots showing the distribution of the Archean granites of the Canaã dos Carajás area. (a) P-Q diagram (Debon and Le Fort, 1988); (b) $100*(MgO+FeOt+TiO_2)/SiO_2$ vs. $(Al_2O_3+CaO)/(FeOt+K_2O+Na_2O)$ diagram (Sylvester, 1989); (c) $FeOt/(FeOt+MgO)$ vs. Al_2O_3 diagram (fields of calc-alkaline and reduced and oxidized A-type granites of Dall'Agnol and Oliveira, 2007); (d) Na_2O vs. K_2O diagram; (e) Yb vs. Sr/Y diagram; (f) $(La/Yb)_N$ vs. Sr/Y diagram. The fields of leucogranodiorite to leucogranite of the Guarantã suite (Almeida et al., 2010) and potassic leucogranites (Almeida et al., submitted) of the Rio Maria terrane, and the Neoarchean Dharwar granites (Jayananda et al., 2006) are plotted for comparison.

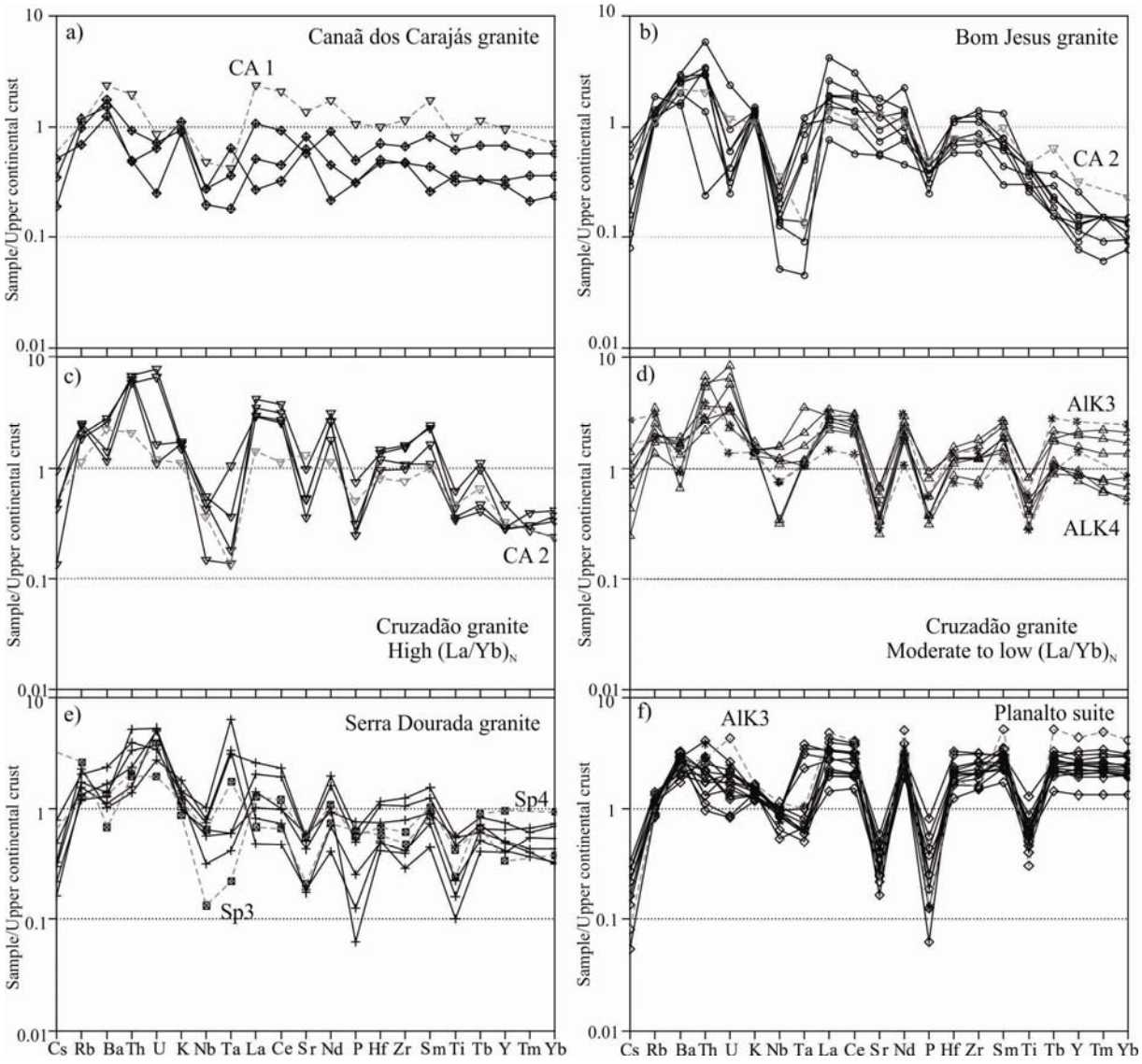

Figure 8 - Upper continental crust-normalized trace element diagram for (a) Canaã dos Carajás granite, with CA1 granite for comparison; (b) Bom Jesus granite, with CA2 granite for comparison; (c) Cruzadão granite with high $(La/Yb)_N$ ratio and the CA2 granite for comparison; (d) Cruzadão granite with moderate to low $(La/Yb)_N$ ratio and the ALK3 and ALK 4 granites for comparison; (e) Serra Dourada granite with the SP3 granite for comparison; and (f) Planalto suite in compare to ALK 3 granite.

6. Discussions

6.1. Comparison with other Archean granites

The granites of different Archean cratons have received increasing attention in the last years. At present, there is more information about their geochemistry and some broad classifications have also been proposed (Davis et al., 1994; Evans and Hanson, 1997; Champion and Sheraton, 1997; Frost et al., 1998; Champion and Smithies, 2003; Moyen et al., 2003; Jayananda et al., 2006; Almeida et al., 2010, submitted; Moyen, 2011) but the need for refinement of the geochemical characterization of these rocks is still evident.

The geochemical comparison between the granites of the Canaã area and those of other Archean cratons or domains will be limited in this paper to the Rio Maria granite-greenstone terrane, and the Yilgarn and Dharwar cratons. The geochemistry and petrogenesis of the Archean granites of the Rio Maria granite-greenstone terrane were summarized by Almeida et al. (2010, submitted) which distinguished essentially: (1) a leucogranodiorite-leucogranite group (Guarantã suite and related rocks) similar to the transitional TTG or high-Ca granites of the Yilgarn craton (Champion and Sheraton, 1997; Champion and Smithies, 2003); (2) potassic leucogranites (Xinguara and Mata Surrão plutons and related rocks) akin to the low-CaO granites or biotite granites of Yilgarn and Dharwar cratons, respectively. The comparison between the compositional variation of representative samples of these two groups of granites of Rio Maria and those of Canaã indicates that there is no a good equivalence between the mentioned granites. The PQ and Na_2O vs. K_2O plots (Figs. 7a, d) show that, except for the Canaã dos Carajás granite which has Na_2O/K_2O ratios > 1, the Canaã granites are distinct of the leucogranodiorite-leucogranite group of Rio Maria. This is shown in the PQ plot (Fig. 7a) by the total dominance of monzogranites in the analyzed Canaã granites. These contrasts can also be seen in some selected Harker diagrams (Figs. 4b, e; 5 a, b, c, d). Except for the Planalto suite granite which is clearly distinct because it has a more accentuated alkaline and reduced character (Figs. 5d, 7b, c, e), and has no counterpart in Rio Maria (Feio et al., submitted), in general, the remainder Canaã granites are more akin geochemically to the potassic granites of Rio Maria. However, there are also relevant differences between the Canaã granites and the potassic granites of Rio Maria. The Bom Jesus granite has CaO, Ba, Sr, and Sr/Y ratios (Figs. 4b, 5a, c, 7e) that are higher than those shown by the Rio Maria potassic leucogranites and its La/Yb ratios are higher than those registered in both groups of Rio Maria (Fig. 7f). Compared to the Yilgarn granites, the Canaã dos Carajás and Bom Jesus granites are similar to the High-Ca granites, whereas the Cruzadão and Serra Dourada are more akin to the Low-CaO granites. The Planalto suite granites apparently have no equivalent in the Yilgarn craton (Champion and Sheraton, 1997; Champion and Smithies, 2003).

In general, the geochemical characteristics of the Canaã granites approach those of the biotite granite group of Dharwar (Moyen et al., 2003). Granites equivalent to the two-mica and peralkaline granites were not identified in Canaã so far. Compared to the granites of Canaã and Rio Maria, the Neoarchean granites of the Dharwar craton studied by Jayananda et al. (2006) differ in geochemical signature of the leucogranodiorite-leucogranite group (Almeida et al., 2010) and are more akin to the potassic granites of Rio Maria and to the

various granites of Canaã (Figs. 5a, b, c, d, 7a, b, c, d). However, the Dharwar granites (Jayananda et al., 2006; their Table 2) show lower $(La/Yb)_N$ ratios (ca. 10) and Eu/Eu* (0.65 to 0.23) and are commonly enriched in CaO, and Zr, and impoverished in K_2O and Ba compared to the Canaã granites. The Dharwar granites are also characterized by low values of the Sr/Y ratio. Thus, they show a quite distinct distribution in the $(La/Yb)_N$ vs. Sr/Y plot compared to the Mesoarchean granites of Canaã and approach in this diagram the field defined by the Planalto suite granites (cf. Yb vs. Sr/Y plot, Fig. 7e). This indicates that the Neoarchean granites of Dharwar (Jayananda et al., 2006), despite their similarity with the CA1 and CA2 granites of Sylvester (1994), are relatively enriched in HFSE and HREE compared to the Mesoarchean granites of Canaã, except for the variety of the Cruzadão granite that is also enriched in the mentioned elements. On the other hand, the Planalto granites are enriched in Zr and Ba compared to the Dharwar granites, and differs also of the latter because they have a clear alkaline character (Fig. 7b) and are reduced granites (Fig. 7c).

6.2. Significance of the Sr/Y and $(La/Yb)_N$ ratios in the Archean Canaã granites

The relevance of the Sr/Y and $(La/Yb)_N$ ratios for petrogenetic interpretation of the origin of granitoid magmas was far recognized (Drummond and Defant, 1990; Martin, 1999) and has been recently emphasized (Moyen, 2009; Zhang et al., 2009; Almeida et al., 2010; He et al., 2011). The presence of garnet or plagioclase as dominant fractionating phase has been seen as determinant in the geochemical signature of granitoid magmas generated during the Archean and the presence or absence of these minerals in the melting residue or fractionate was attributed to variations of pressure (cf. Rapp et al., 1991; Rapp and Watson, 1995; Almeida et al., 2010). However, there is increasing evidence that other parameters than pressure and also different processes are able to explain the variations in the Sr/Y and $(La/Yb)_N$ ratios (Moyen, 2009; He et al., 2011, and references therein). Moyen (2009) argued that compositional variations in the source can be as relevant as pressure to determine the values of the mentioned ratios in granitoid magmas and emphasize that melting of normal crustal sources at pressures of 5 – 10 kbar could be able to generate magmas with high Sr/Y ratios.

The $(Dy/Yb)_N$ ratio and the behavior of Middle REE (MREE) give also indications about the influence of amphibole during the magma origin or fractionation. The decrease of that ratio and the presence of concave REE patterns for the HREE branch are strong indications of prominent amphibole fractionation (Moyen, 2009; He et al., 2011). The variations of Er contents face up to those of Sr and Ba can also give indications of the role of

garnet or plagioclase during the fractionation and allow a preliminary estimate of the possible influence of enriched-mantle sources in the origin of the granitoid magmas (Heilimo et al., 2010).

The $(La/Yb)_N$ vs. Sr/Y diagram (Fig. 7f) indicates that the Bom Jesus granite, despite its little higher $(La/Yb)_N$, approaches the High-Sr/Y granites (HSG), whereas the other Canaã granites are akin to the Normal granites (NG), both of He et al. (2011). However, one of the varieties of the Cruzadão granite also show significantly higher $(La/Yb)_N$. The $(La/Yb)_N$ vs. $(Dy/Yb)_N$ diagram (Fig. 9a) suggests that both garnet and amphibole were fractionated during the evolution of the Bom Jesus granite and the variety of the Cruzadão granite with higher $(La/Yb)_N$. In the triangular (Ba+Sr)/100 - 1/Er - Er plot (Fig. 9b), the Canaã Archean granites show a distinct distribution due essentially to strong variations in the Er contents which should reflect the varying influence of garnet as a fractionating phase. The Bom Jesus granite and the high-$(La/Yb)_N$ Cruzadão granite variety have lower contents of Er and contrast with the Planalto granite and the low $(La/Yb)_N$ varieties of the Cruzadão granite that are relatively enriched in that element. A similar geochemical behavior can be observed in the triangular Eu/Eu* - $(Al_2O_3+CaO)/20$ - Y/10 plot (Fig. 9c) where the Canaã granites can be distinguished by their simultaneous variations of Eu/Eu* and (Al_2O_3+CaO) vs. Y contents. The Bom Jesus and Canaã dos Carajás granites have the highest Eu/Eu* and $(Al_2O_3+CaO)/Y$ contents and the reverse is observed in the Planalto granite and in the varieties of the Cruzadão granite enriched in HREE and Y.

The geochemical behavior of the Canaã granites suggests that the evolution of their magmas was controlled by the fractionation of variable proportions of plagioclase ± amphibole ± garnet, among other phases. These magmas probably evolved at relatively low pressures (possibly 8 to 10 kbar) in a crustal environment. A remarkable influence of garnet and amphibole was restrict to the Bom Jesus granite and to the variety of the Cruzadão granite with higher $(La/Yb)_N$. In the remainder granites, plagioclase was dominant, garnet was more probably an absent phase in the residue of melting and the influence of amphibole was also apparently limited.

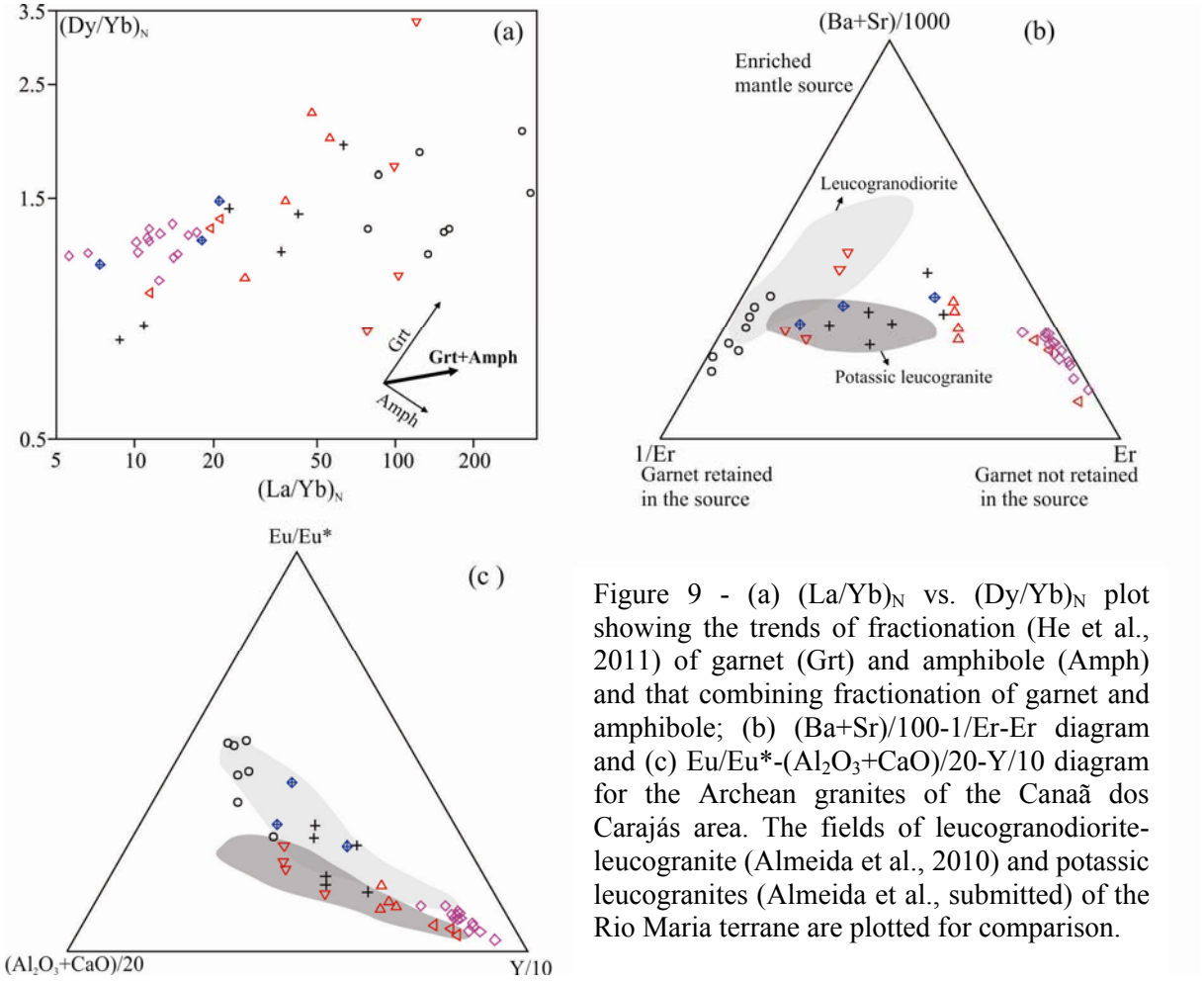

Figure 9 - (a) $(La/Yb)_N$ vs. $(Dy/Yb)_N$ plot showing the trends of fractionation (He et al., 2011) of garnet (Grt) and amphibole (Amph) and that combining fractionation of garnet and amphibole; (b) (Ba+Sr)/100-1/Er-Er diagram and (c) Eu/Eu*-(Al_2O_3+CaO)/20-Y/10 diagram for the Archean granites of the Canaã dos Carajás area. The fields of leucogranodiorite-leucogranite (Almeida et al., 2010) and potassic leucogranites (Almeida et al., submitted) of the Rio Maria terrane are plotted for comparison.

6.3. Origin of the Archean Canaã granite magmas

It was demonstrated in the previous discussion that variations in the proportions of garnet, amphibole, and plagioclase in the residue of melting or as fractionated phases were determinant to explain some outstanding geochemical differences observed in the Archean granites of Canaã. However, the possible sources of the granite magmas and the nature and proportion of other phases involved in the magma genesis were not discussed. Looking for answers to these questions, we employed batch melting geochemical modeling. The discussion was centered in the Bom Jesus and Cruzadão granites which have similar ages and deformational aspects but differ in their Sr/Y and $(La/Yb)_N$ ratios. The analyzed samples of these ~2.85 Ga granites yielded small positive εNd values (+ 0.12 to + 2.31) and T_{DM} model ages of 2932 to 2987 Ma (Feio et al., submitted b) possibly due to derivation of the granite magmas from juvenile sources with low time of crustal residence.

To test the possible magma sources of the mentioned granites we have made geochemical modeling for major and trace elements. The software Genesis 4.0 (Teixeira,

2005) was employed for modeling. Mineral-melt distribution coefficients applied for trace element modeling (Rollinson, 1993; Bédard, 2006) are given in the supplementary Table B. Rare earth elements were normalized according to Evensen (1978).

Several sources were tested for the Bom Jesus granite magma (the sample AER-65C was taken as representative of the original magma): (1) an average chemical composition of Early Archean graywackes, (2) an average chemical composition of Archean TTG, (3) an average chemical composition of Archean andesites (all of Condie, 1993) and (4) the average composition of the lower continental crust (Rudnick and Gao, 2003). The graywacke, TTG and andesite compositions gave bad fits for major element modeling. In the case of the graywacke, a high degree of melting was indicated (64%), and the fit for CaO, Na_2O, K_2O, and Ba was poor. For the TTG source, the fit for major elements was reasonable but that for trace elements, including REE, was very poor. Additional restrictions to a TTG source for granite magma generation were given for experimental studies (Watkins et al., 2007). An andesitic source would generate a TTG like melt better than a granitic one and the results of the modeling were also inconsistent. A source similar in composition to the average lower continental crust (Rudnick and Gao, 2003) could give origin to a melt with a good adjustment for major elements (Fig. 10a), except for K_2O, leaving as residual melting phases plagioclase (An60), amphibole, garnet, clinopyroxene, orthopyroxene and ilmenite (Table 2). The fit for trace elements (Fig. 10b) was generally good, except for Rb and Nb, and that for REE (Fig. 10c) was excellent.

The increasing evidence that crustal melting of mafic magmas is able to generate granitic liquids (Borg and Clynne, 1998; Xyaoyue et al., 2002; He et al., 2011) make us to test basaltic composition as possible sources for the Canaã granites. An Early Proterozoic basalt (Condie, 1993) was chosen for modeling, because it has a relatively high K_2O content compared to dominant Archean tholeiites and would be more suitable to generate granitic liquids. The adjustment for major elements was very good (r^2 = 0.034) and that for trace elements was good except for Nb, Y, and HREE, which were significantly higher in the melt compared to the Bom Jesus granite composition (Table 2; Figs. 10d, e, f). The residue was composed of hornblende and plagioclase (An60) with subordinate proportions of clinopyroxene, garnet, and ilmenite. The modeling indicate that for a better fit it would be necessary to retain a higher proportion of garnet in the residue, but this would imply significant changes in the mass balance and an inconsistent result will also be obtained. An alternative hypothesis is to admit that the original source was not identical in composition to the selected basalt in terms of trace elements.

Table 2 - Geochemical modeling data for the granites of the Canaã dos Carajás area.

	Original compositions			Modeling results		
	Source		Bom Jesus Granite	Co=Basalt	Co= Modified Basalt	Co=LCC
Oxides	Basalt	LCC	BJGr	BJGr	BJGr	BJGr
SiO_2	50,8	53,02	74,87	76,54	76,54	76,14
TiO_2	1,42	0,81	0,21	0,48	0,48	0,49
Al_2O_3	15,3	16,78	13,24	13,44	13,44	13,46
Fe2O3	10,56	9,43	1,45	1,28	1,28	1,8
MgO	6,9	7,19	0,25	0,27	0,27	0,26
CaO	9,6	9,52	1,29	1,04	1,04	1,29
Na_2O	2,7	2,63	3,28	3,05	3,05	3,59
K_2O	0,76	0,61	4,7	3,90	3,90	2,96
Ba	277	259	1379,1	1128,00	1128	1109
Rb	23	11	160,9	112,00	112	52,67
Sr	222	348	261	261,00	261	403
Zr	133	68	210,2	298,00	298	152
Nb	4.5 (2.3)	5	3,4	13,95	7,13	18,84
Y	32 (16)	16	2	10,78	5,39	3,59
La	11	8	45,1	36,09	36,09	29,97
Ce	27	20	89,6	58,74	58,74	48,74
Nd	15	11	25,7	18,60	18,6	16,66
Sm	3,8	2,8	3,1	3,02	3,02	2,52
Eu	1,3	1,1	0,7	1,13	1,13	1,11
Gd	4.22 (2.11)	3,1	0,91	2,30	1,14	1,53
Tb	0.72 (0.36)	0,48	0,12	0,38	0,19	0,22
Yb	2.7 (1.35)	1,5	0,2	0,92	0,44	0,31
Lu	0.45 (0.22)	0,25	0,04	0,19	0,09	0,07
F (%)				16	16	17
Residual phase/r^2				0,034	0,034	0,113
Hornblende				52,87	52,87	35,18
Plagioclase (An60)				33,65	33,65	38,21
Garnet				5,75	5,75	12,04
Clinopyroxene				6,22	6,22	7,94
Orthopyroxene						6,14
Ilmenite				1,51	1,51	0,49

In parentheses: Modified from Basalt of Condie (1993);

LCC - lower continental crust (Rudnick and Gao, 2003); BJ - Bom Jesus granite;

F(%) - % of melting; r^2 - sun of residue

As pointed out by Moyen (2009), the source composition could exert strong influence in the trace element composition of the melts and can explain large variations in the Sr/Y and La/Yb ratios. Hence, we have modified the composition of the Early Proterozoic basalt reducing the initial content of Nb, Y, and HREE to one half. The modeling with this modified composition gave also a good adjustment for trace elements (Figs. 10g, h). In fact, it is deduced that a source combining a major element composition similar to that of the Early Proterozoic basalt and a trace element composition akin to the average lower crust in terms of HFSE and HREE contents will be suitable to give origin to the Bom Jesus granite magma.

The results of modeling integrated to the previous evaluation of geochemical data indicate that the Bom Jesus granite magma could be derived of a mafic lower crustal source or of an average lower crust source leaving a residue with dominance of hornblende and plagioclase and subordinate clinopyroxene ± orthopyroxene, garnet, and ilmenite. This is consistent with the behavior of the studied granites in the $(La/Yb)_N$ and $(Dy/Yb)_N$ ratios (Fig. 9a). The influence of garnet should be lesser in the Cruzadão granite variety with higher values of $(La/Yb)_N$ and garnet is very probably absent in the residue of melting of the other studied granites. This reinforces our previous estimate of a maximum pressure range of 8 to 10 kbar to the magma generation. This pressure was possibly lower in the cases of the varieties relatively enriched in HREE of the Cruzadão granite and of the Serra Dourada and Planalto granites in which garnet was most probably absent as residual phase [cf. their distribution in the (Ba+Sr)/1000-1/Er-Er diagram; Fig. 9b]. This could also explain the relatively high K_2O/Na_2O ratios observed in these granites and their geochemical similarities with the Normal granites of He et al. (2011). Another relevant aspect is the negligible role of amphibole in the residue of melting of the sources of the low $(La/Yb)_N$ granites of Canaã as indicated by their REE patterns (Fig. 6).

Geochemical evidence suggests that the varieties of the Cruzadão granite are not comagmatic and that despite their similarities they could also be possibly not cogenetic. However, it is not possible at this stage to distinguish different domains for each variety of the Cruzadão granite and this justifies keeping it as a single unit.

The origin of the Planalto suite granite magmas was discussed by Feio et al. (submitted a) which concluded that melting of a mafic possibly granulitic source leaving plagioclase, clinopyroxene, orthopyroxene, magnetite, and ilmenite, in the residue was able to give origin to the Planalto granite magma. This model is consistent with the geochemical

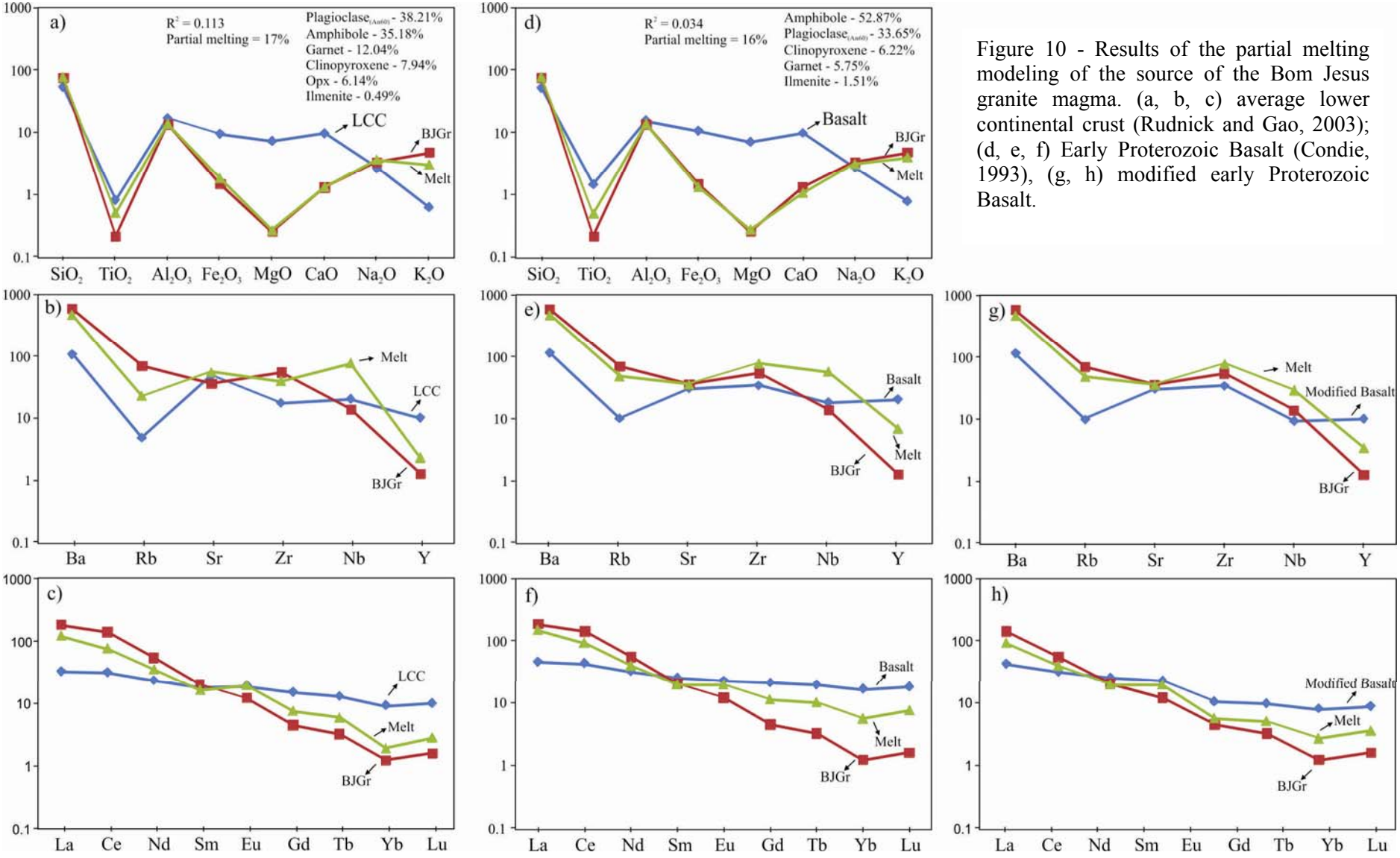

Figure 10 - Results of the partial melting modeling of the source of the Bom Jesus granite magma. (a, b, c) average lower continental crust (Rudnick and Gao, 2003); (d, e, f) Early Proterozoic Basalt (Condie, 1993), (g, h) modified early Proterozoic Basalt.

In the case of the Canaã dos Carajás granite, the few samples analyzed suggest that garnet could be a significant phase in the residue but the influence of amphibole was apparently negligible (Fig. 6a). Finally, admitting similar magmatic sources, the geochemical features of the Serra Dourada granite indicates to it a behavior intermediate between those of the Bom Jesus and high-HREE Cruzadão granites in terms of fractionated phases.

As discussed above, there are strong geochemical contrasts between the leucogranodiorite-leucogranites of the Rio Maria terrane and the Canaã granites (cf. Figs. 7d, 9b). This and the absence in Canaã of sanukitoid rocks make the model proposed by Almeida et al. (2010) unsuitable to explain the origin of the Archean Canaã granites.

7. Conclusions

1. Archean granites are the dominant exposed rocks in the Canaã area of the Carajás province. Five distinct granite units with ages varying between 2.93 and 2.73 Ga were recognized in that area. The Mesoarchean granites encompass the Canaã dos Carajás, Bom Jesus, Cruzadão and Serra Dourada granites and the Neoarchean granites are represented by the Planalto suite. The studied granites are deformed and generally show penetrative foliation which follows the dominant NW-SE to W-E regional main trend

2. The modal compositions of the Canaã granites are dominantly monzogranitic, with subordinate granodiorite (Canaã dos Carajás) or syenogranite (Planalto suite, Bom Jesus and Cruzadão granites). The Mesoarchean granites have biotite as the main mafic phase and are commonly composed of hololeucocratic rocks (mafic content < 5%). The Neoarchean Planalto granite has generally hornblende as the main mafic mineral and total mafic content between 5% and 20%.

3. The Planalto granites have ferroan character, are similar geochemically to reduced A-type granites and show a strong geochemical contrast with the Mesoarchean studied granites. The Canaã dos Carajás, Bom Jesus and the variety of the Cruzadão granite with higher La/Yb are geochemically more akin to the calc-alkaline granites of CA1 (Canaã granite) or CA2 types (Bom Jesus granite and part of the Cruzadão granite). The other varieties of the Cruzadão granite are transitional between calc-alkaline and alkaline granites and the alkaline character is reinforced in the samples relatively enriched in HFSE and HREE. The Serra Dourada granite has an ambiguous geochemical character with some features similar to those of calc-alkaline granites and other to the peraluminous granites of SP3 subtype.

4. The comparison between the Archean granites of Canaã and Rio Maria demonstrates that the Planalto suite granite has distinct age and geochemical signature and has no counterpart in

Rio Maria. The Mesoarchean Canaã granites differ also of the leucogranodiorite-leucogranite group and are more akin geochemically to the potassic granites of Rio Maria, although some relevant differences between the Canaã granites and the latter still exist. It is concluded that there is no a good equivalence between the Archean granites described in these two domains of the Carajás province.

Compared to the granites of the Yilgarn craton, the Canaã dos Carajás and Bom Jesus granites of Canaã are similar to the High-Ca granites, whereas the Cruzadão and Serra Dourada are more akin to the Low-CaO granites. The Planalto suite granites apparently have no equivalent in Yilgarn and Dharwar. The geochemical characteristics of the Mesoarchean Canaã granites approach those of the biotite granite group of Dharwar but the latter are relatively enriched in HFSE and HREE compared to the Mesoarchean granites of Canaã, except for the variety of the Cruzadão granite with low La/Yb and flat REE pattern. The two-mica and peralkaline granites of Dharwar have no equivalent in Canaã.

5. The Canaã granites show accentuated variation of the Sr/Y and $(La/Yb)_N$ ratios. It is concluded that the changes of these ratios are not essentially due to contrast in the pressures of magma generation. In fact, they should reflect dominantly compositional differences in the sources of the granite magmas with a subordinate effect of pressure.

6. The geochemical behavior and modeling of the Canaã granites suggests that the evolution of their magmas was controlled by the fractionation of variable proportions of plagioclase ± amphibole ± garnet, with subordinate clinopyroxene ± orthopyroxene + ilmenite. The best adjustment in the modeling of the Bom Jesus granite was obtained for: (1) a mafic source similar in composition to the average of Early Proterozoic basalts, but with lower contents of Nb, Y, and HREE; (2) A source similar in composition to the average lower continental crust. A significant influence of garnet and amphibole was restrict to the Bom Jesus granite and to the variety of the Cruzadão granite with higher $(La/Yb)_N$. In the other Canaã granites, plagioclase was dominant, garnet was probably an absent phase in the residue of melting and the influence of amphibole was also apparently limited.

7. The Bom Jesus and Canaã dos Carajás granites and the variety of the Cruzadão granite with higher $(La/Yb)_N$ magmas were probably generated at relatively low pressures, estimated at 8 to 10 kbar, in a crustal environment. The pressure for the origin of the varieties relatively enriched in HREE of the Cruzadão granite and of the Serra Dourada and Planalto granites was probably a little lower. Geochemical evidence suggests that the varieties of the Cruzadão granite are not comagmatic but it is not possible at this stage to distinguish different domains for each variety of that granite unit.

Acknowledgments

A.A.S. Leite, D.C. Oliveira, C.E.M Barros, and F.J. Althoff are acknowledged for participation in field work and A.S. Sardinha, A.K.B. Gomes, J.E.B. Soares and M.A. Oliveira for previous work in the studied area. This research received financial support from CNPq (R. Dall'Agnol – Grants 0550739/2001-7, 476075/2003-3, 1149 307469/2003-4, 484524/2007-0; PRONEX – Proc. 66.2103/1998-0; G.R.L. Feio – CNPq scholarship), and Federal University of Pará (UFPA). This paper is a contribution to the Brazilian Institute of Amazonia Geosciences (INCT program – CNPq/MCT/FAPESPA – Proc. 573733/2008-2) and to the project IGCP-SIDA 599.

References

Almeida, J.A.C., Dall'Agnol, R., Dias, S.B., Althoff, F.J., 2010. Origin of the Archean leucogranodiorite–granite suites: Evidence from the Rio Maria terrane and implications for granite magmatism in the Archean. Lithos 187, 201-221.

Almeida, J.A.C., Dall'Agnol, R., Oliveira, M.A., Macambira, M.J.B., Pimentel, M.M., Rämö, O.T., Guimarães, F.V., Leite, A.A.S., 2011. Zircon geochronology and geochemistry of the TTG suites of the Rio Maria granite-greenstone terrane: Implications for the growth of the Archean crust of Carajás Province, Brazil. Precambrian Research 120, 235-257.

Almeida, J.A.C., Dall'Agnol, R., Leite, A.A.S., submitted. Geochemistry and zircon geochronology of the Archean granite suites of the Rio Maria granite-greenstone terrane, Carajás Province, Brazil. Lithos.

Althoff, F.J., Barbey, P., Boullier, A.M., 2000. 2.8–3.0 Ga plutonism and deformation in the SE Amazonian craton: the Archean granitoids of Marajoara (Carajás Mineral province, Brazil). Precambrian Research 104, 187–206.

Araújo, O.J.B.; Maia, R.G.N., 1991. Programa de levantamentos geológicos básicos do Brasil, Serra dos Carajás, folha SB-22-Z-A, Estado do Pará. Texto explicativo, Brasília, DNPM/CPRM. 164p (in Portuguese).

Barros, C.E.M., Macambira, M.J.B., Barbey, P., Scheller, T., 2004. Dados isotópicos Pb-Pb em zircão (evaporação) e Sm-Nd do Complexo Granítico Estrela, Província Mineral de Carajás, Brasil: Implicações petrológicas e tectônicas. Revista Brasileira de Geociências 34, 531-538. (in portuguese).

Barros, C.E.M., Sardinha, A.S., Barbosa, J.P.O., Macambira M.J.B., 2009. Structure, Petrology, Geochemistry and zircon U/Pb and Pb/Pb geochronology of the synkinematic Archean (2.7 Ga) A-type granites from the Carajás Metallogenic Province, northern Brazil, Canadian Mineralogist 47, 1423-1440.

Bédard, J.H. 2006. A catalytic delamination-driven model for coupled genesis of Archaean crust and sub-continental lithospheric mantle. Geochimica et Cosmochimica Acta 70, 1188–1214

Borg, L.E., Clynne, M.A., 1998. Petrogenesis of Felsic Calc-alkaline Magmas from the Southernmost Cascades, California: Origin by Partial Melting of Basaltic Lower Crust. Journal of Petrology 39, 1197-1222.

Bédard, J.H., 2006. The catalytic delamination-driven model for coupled genesis of Archaean crust and sub-continental lithospheric mantle. Geochimica et Cosmochimica Acta 70, 1188–1214.

Champion, D.C., Sheraton, J.W., 1997. Geochemistry and Nd isotope systematics of Archean granites of the Eastern Goldfields, Yilgarn Craton, Australia: implications for crustal growth processes. Precambrian Research 83, 109-132.

Champion, D.C., Smithies, R.H., 2007. In: Van Kranendonk, M.J., Smithies, R.H., Bennett, V.C. (Eds.) Geochemistry of Paleoarchean Granites of the East Pilbara Terrane, Pilbara Craton, Western Australia: Implications for Early Archean Crustal Growth. Earth's Oldest Rocks, Developments in Precambrian Geology, vol. 15. Elsevier, Amsterdam, pp. 369–410.

Condie, K.C., 1993. Chemical composition and evolution of the upper continental crust: Contrasting results from surface samples and shales. Chemical Geology 104, 1-37.

Costa, J.B.S., Araújo, O.J.B., Santos, A., Jorge João, X.S., Macambira, M.J.B., Lafon, J.M., 1995. A Província Mineral de Carajás: aspectos tectono-estruturais, estratigráficos e geocronológicos. Boletim do Museu Paraense Emílio Goeldi 7, 199-235 (in Portuguese).

Dall'Agnol, R., Oliveira, M.A., Almeida, J.A.C., Althoff, F.J., Leite, A.A.S., Oliveira, D.C., Barros, C.E.M., 2006. Archean and Paleoproterozoic granitoids of the Carajás Metallogenic Province, eastern Amazonian Craton. In: Dall'Agnol, R., Rosa-Costa, L.T. and Klein, E.L. (Eds.) Symposium on magmatism, crustal evolution, and metallogenesis of the Amazonian Craton. Abstracts Volume and Field Trip Guide. Belém, PRONEX-UFPA-SBGNO, 99-150.

Dall'Agnol, R., Oliveira, D.C., 2007. Oxidized, magnetite-series, rapakivi-type granites of Carajás, Brazil: Implications for classification and petrogenesis of A-type granites. Lithos 93, 215–233.

Davis, W.J., Fryer, B.J., King, J.E., 1994. Geochemistry and evolution of Late Archaean plutonism and its significance to the tectonic development of the Slave Craton. Precambrian research 67, 207-241.

Debon, F. & Le Fort, P., 1988. A cationic classification of common plutonic rocks and their magmatic associations: principles, method, applications. Bulletin on Mineralogy 111, 493-510.

Drummond, M.S., Defant, M.J., 1990. A model for trondhjemite–tonalite–dacite genesis and crustal growth via slab melting: Archaean to modern comparisons. Journal of Geophysical Research 95, 21503–21521.

Domingos, F.H., 2009. The structural setting of the Canaã dos Carajás region and Sossego-Sequeirinho deposits, Carajás – Brazil. University of Durham, England, 483p. (Ph.D. Thesis).

Evans, O.C., Hanson, G.H., 1997. Late- to post-Archaean granitoids of the S.W. Superior Province: derivation through direct mantle melting. In: De Witt, M.J., Ashwall, L.D. (Eds.), Greenstone Belts. Oxford Univ. Press, pp. 280– 295.

Evensen, N.M., Hamilton, P.T., O'nions, R.K., 1978. Rare earth abundances in chondritic meteorites. Geochemical and Cosmochimica. Acta, 39: 55.64.

Feio, G.R.L., Dall'Agnol, R. Dantas, E.L. Macambira, M.J.B., Gomes, A.K.B., Sardinha, A.S., Santos, P.A., submitted a. Geochemistry, geochronology, and origin of the Neoarchean Planalto Granite suite, Carajás, Amazonian craton: A-type or hydrated charnockitic granites? Lithos.

Feio, G.R.L., Dall'Agnol, R. Dantas, E.L. Macambira, M.J.B., Santos, J.O.S., Althoff, F.J., Soares, J.E.B., submitted b. Archean granitoid magmatism in the Canaã dos Carajás area: implications for crustal evolution of the Carajás province, Amazonian craton, Brazil. Precambrian Research.

Frost, C.D. Frost, B.R., Chamberlain, K.R., Hulsebosch, T.P., 1998. Late Archean history of the Wyoming province as recorded by granitic magmatism in the Wind River Range, Wyoming. Precambrian Research 89, 145-173.

Gibbs, A.K., Wirth, K.R., Hirata, W.K., Olszewski Jr., W.J., 1986. Age and composition of the Grão Pará Group volcanics, Serra dos Carajás. Revista Brasileira de Geociências 16, 201–211.

Goodwin, A.M., 1991. Precambrian Geology: the dynamic evolution of the continental crust. Academic Press, London, 666 pp.

Halla, J., 2005. Late Archean high-Mg granitoids (sanukitoids) in the Southern Karelian craton, Eastern Finland. Lithos 79, 161–178.

Heilimo, E., Halla, J., Höltta, P., 2010. Discrimination and origin of the sanukitoid series: Geochemical constraints from the Neoarchean western Karelian Province (Finland). Lithos 115, 27-39.

Heilimo, E., Halla, J., Huhma, H., 2011. Single-grain zircon U–Pb age constraints of the western and eastern sanukitoid zones in the Finnish part of the Karelian Province. Lithos 121, 87–99.

He, Y., Li, S., Hoefs, J., Huang, F., Liu, S-A., Hou, Z., 2011. Post-collisional granitoids from the Dabie orogen: New evidence for partial melting of a thickened continental crust. Geochimica et Cosmochimica Acta 75, 3815–3838.

Ishihara, S., Robb, L., Anhaeusser, C.R., Imai, A., 2002. Granitoid Series in Terms of Magnetic Susceptibility: A Case Study from the Barberton Region, South Africa. Gondwana Research 5, 581-589.

Jayananda, M., Chardon, P., Peucaut, J-J., 2006. 2.61 Ga potassic granites and crustal reworking in the western Dharwar craton, southern India: Tectonic, geochronologic and geochemical constraints. Precambrian Research 150, 1–26.

Käpyaho, A., Mänttäari, I., Huhma, H., 2006. Growth of Archaean crust in the Kuhmo district, eastern Finland: U–Pb and Sm–Nd isotope constraints on plutonic rocks Precambrian Research 146, 95–119.

Leite, A.A.S., Dall'Agnol, R., Macambira, M.J.B., Althoff, F.J., 2004. Geologia e Geocronologia dos granitóides Arqueanos da região de Xinguara (PA) e suas implicações na evolução do Terreno Granito-Greenstone de Rio Maria. Revista Brasileira de Geociências 34, 447-458 (in Portuguese).

Le Maitre, R.W., Streckeisen, A.., Zanettin, B., Le Bas, M.J., Bonin, B., Bateman, P., Bellieni, G., Dudek, A., Efremova, J., Keller J., Lameyre J., Sabine P.A., Schmidt R., Sørensen H., Woolley A.R., 2002. Igneous Rocks. A Classification and Glossary of Terms. Recommendations of the International Union of Geological Sciences Subcommission on the systematics of igneous rocks. Cambridge University Press, Cambridge, 252 pp.

Lobach-Zhuchenko, S.B., Rollinson, H.R., Chekulaev, V.P., Arestova, N.A., Kovalenko, A.V., Ivanikov, V.V., Guseva, N.S., Sergeev, S.A., Matukov, D.I., Jarvis, K.E., 2005. The Archaean sanukitoid series of the Baltic Shield: geological setting, geochemical characteristics and implication for their origin. Lithos 79, 107–128.

Macambira, M.J.B., Lafon, J.M., 1995. Geocronologia da Província Mineral de Carajás; Síntese dos dados e novos desafios. Boletim do Museu Paraense Emílio Goeldi, série Ciências da Terra 7, 263-287 (in portuguese).

Macambira, M.J.B., Lancelot, J., 1996. Time constraints for the formation of the Archean Rio Maria crust, southeastern Amazonian Craton, Brazil. International Geology Review 38, 1134-1142.

Machado, N., Lindenmayer, Z.G., Krogh, T.E., Lindenmayer, D., 1991. U-Pb geochronology of Archean magmatism and basement reactivation in the Carajás area, Amazon shield, Brazil. Precambrian Research, 49, 329-354.

Martin, H., 1994. The Archean grey gneisses and the gneisses of continental crust. In: Condie, K. C. (ed.) Developments in precambrian geology 11. Archeancrustal evolution, Amsterdam, Elsevier. p. 205-259.

Martin, H., 1999. Adakitic magmas: modern analogues of Archaean granitoids Lithos 46, 411-429.

Moyen, J.-F., Martin, H., Jayananda, M., Auvray, B., 2003. Late Archaean granites: A typology based on the Dharwar Craton (India). Precambrian Research 127, 103-123.

Moyen, J.-F., 2009. High Sr/Y and La/Y ratios: The meaning of the “adakitic signature”. Lithos 112, 556–574.

Moyen, J.-F., 2011. Archean granitoids as Geodynamic markers. In: Jayananda, M., Ahmed, T., Chardon, D. (Eds.). International symposium on Precambrian Accretionary orogens and field workshop in the Dharwar craton, southern India, p. 88.

Nakamura N., 1974. Determination of REE, Ba, Fe, Mg, Na, and K in carbonaceous and ordinary chondrites. Geochimica et Cosmochimica Acta 38, 757-775.

Nisbet, E., 1987. The Young Earth: An Introdution to Archean Geology. Allen and Unwin, Boston, 402 pp.

Nogueira, A.C.R., Truckenbrodt W., Pinheiro, R.V.L., 1995. Formação Águas Claras, Pré-Cambriano da Serra dos Carajás: redescrição e redefinição litoestratigráfica. Boletim Museu Paraense Emílio Goeldi 7, 177-277 (in Portuguese).

Oliveira, M.A., Dall'Agnol, R., Althoff, F.J., Leite, A.A.S., 2009. Mesoarchean sanukitoid rocks of the Rio Maria Granite-Greenstone Terrane, Amazonian craton, Brazil. Journal of South American Earth Sciences 27, 146-160.

Rapp, R., Watson, E. B. and MIller, C. F., 1991. Partial melting of amphibolite/eclogite and the origin of Archean trondhjemites and tonalities. Precambrian Research 51, 1-25.

Rapp R. and Watson E. B., 1995. Dehydration melting of metabasalt at 8–32 kbar: implications for continental growth and crust-mantle recycling. Journal of Petrology. 36, 891–931.

Rollinson, H.R., 1993. Using Geochemical Data: Evaluation, Presentation, and Interpretation. New York, Longman, 352 p.

Rudnick R. L. and Gao S., 2003. Composition of the continental crust. In the Crust (ed. R.L. Rudnick), 3 Treatise on Geochemistry (eds. H.D. Holland and K.K. Turekian), Elsevier-Pergamon, Oxford. pp. 1–64.

Santos, J.O.S., Hartmann, L.A., Gaudette, H.E., Groves, D.I., McNaughton, N.J., Fletcher, I.R., 2000. A new understanding of the provinces of the Amazon Craton based on integration of field mapping and U-Pb and Sm-Nd geochronology. Gondwana Research 3, 453-488.

Sardinha, A.S., Dall'Agnol, R., Gomes, A.C.B., Macambira, M.J.B., Galarza, M.A., 2004. Geocronologia Pb-Pb e U-Pb em zircão de granitóides arqueanos da região de Canaã dos Carajás, Província Mineral de Carajás. In: Congresso Brasileiro de Geologia, 42, CDrom (in Portuguese).

Sardinha, A.S., Barros, C.E.M., Krymsky, R., 2006. Geology, Geochemistry, and U-Pb geochronology of the Archean (2.74 Ga) Serra do Rabo granite stocks, Carajás Province, northern Brazil. Journal of South American Earth Sciences 20, 327-339.

Smithies, R.H., and Champion, D.C., 1999, GSWA Annual Review, v. 1998-99, p. 45-49.

Smithies, R.H., Champion, D.C., 2000. The Archaean high-Mg diorite suite: links to tonalite–trondhjemite–granodiorite magmatism and implications for early Archaean crustal growth. Journal of Petrology 41, 1653– 1671.

Souza, Z.S., Potrel, A., Lafon, J.M., Althoff, F.J., Pimentel, M.M., Dall'Agnol, R., Oliveira, C.G., 2001. Nd, Pb and Sr isotopes in the Identidade Belt, an Archean greenstone belt of Rio Maria region (Carajás Province, Brazil): implications for the geodynamic evolution of the Amazonian Craton. Precambrian Research 109, 293–315.

Stern, R.A., Hanson, G.N., 1991. Archaean high-Mg granodiorites: a derivative of light rare earth enriched monzodiorite of mantle origin. Journal of Petrology 32, 201–238.

Sylvester, P.J., 1989. Post-collisional alkaline granites. Journal of Geology 97, 261–280.

Sylvester, P.J., 1994. Archaean granite plutons. In: Condie K. (ed.), Archean Crustal Evolution, Elsevier, Amsterdam, pp. 261–314.

Tallarico, F.H.B., Figueiredo, B.R., Groves, D.I., Kositcin, N., McNaughton, N.J., Fletcher, I.R., Rego, J.L., 2005. Geology and Shrimp U-Pb geochronology of the Igarapé Bahia deposit, Carajás

Copper-Gold belt, Brazil: an Archean (2.57 Ga) example of iron-oxide Cu-Au-(U-REE) mineralization. Economic Geology, 100, 7-28.

Tassinari, C.C.G., Macambira, M., 2004. A evolução tectônica do Craton Amazônico. In: Mantesso-Neto, V., Bartorelli, A., Carneiro, C.D.R., Brito Neves, B.B. (eds.). Geologia do Continente Sul Americano: Evolução da obra de Fernando Flávio Marques Almeida. São Paulo, p. 471-486 (in Portuguese).

Teixeira, L.R., 2005. Genesis versão 4.0. Aplicativo de modelamento geoquímico. Universidade Federal da Bahia (in Portuguese).

Trendall, A.F., Basei, M.A.S., Laeter, J.R., Nelson, D.R., 1998. SHRIMP zircon U–Pb constraints on the age of the Carajás formation, Grão Pará group, Amazon Craton. Journal of South American Earth Sciences 11, 265–277.

Vasquez, L.V., Rosa-Costa, L.R., Silva, C.G., Ricci, P.F., Barbosa, J.O., Klein, E.L., Lopes, E.S., Macambira, E.B., Chaves, C.L., Carvalho, J.M., Oliveira, J.G., Anjos, G.C., Silva, H.R., 2008. Geologia e Recursos Minerais do Estado do Pará: Sistema de Informações Geográficas – SIG: texto explicativo dos mapas Geológico e Tectônico e de Recursos Minerais do Estado do Pará, 328p (in Portuguese).

Watkins, J.M., Clemens, J.D., Treloar, P.J., 2007. Archaean TTGs as sources of younger granitic magmas: melting of sodic metatonalites at 0.6–1.2 GPa Contributions to Mineralogy and Petrology 154, 91–110.

Whalen, J.B.., Percival, J.A., Mc Nicoll, V.J., Longstaffe, F.J., 2004. Geochemical and isotopic (Nd–O) evidence bearing on the origin of late- to post-orogenic high-K granitoid rocks in the Western Superior Province: implications for late Archean tectonomagmatic processes. Precambrian Research 132, 303-326.

Xyaoyue, G., Xianhua, L., Zhigang, C., Wuping, L., 2002. Geochemistry and petrogenesis of Jurassic high Sr/low Y granitoids in eastern China: Constrains on crustal thickness. Chinese Science Bulletin 47, 962-968.

Zhang, S-B., Zheng, Y-F., Zhao, Z-F., Wu, Y-B., Yuan, H., Wu, F-Y., 2009. Origin of TTG-like rocks from anatexis of ancient lower crust: Geochemical evidence from Neoproterozoic granitoids in South China. Lithos 113, 347-368.

Sample	ARF-12A	AMR-213	AMR-83B	AMR-102	AMR-182	AER-16A	ERF-18C	AER-65A	AER-65C	AE-47	ERF-123	ERF-137	ARC-116	AER-30B	AER-59	AER-47E	AER-27	AER-30C	AER-57A
Petrology	LGdr	BGdr	BLMzG	BLMzG	BLMzG	BMzG	BMzG	BMzG	BMzG	BLSG	BMzG	BLSG	BMzG	BMzG	BLMzG	BLMzG	LMzG	LMzG	LMzG
Units	Canaã dos Carajás granite					Bom Jesus gneiss granite								Serra Dourada granite					
Quartz	43,6	38,3	29,7	33,8	31,6	25,6	23,7	27,2	21,6	40	27,2	30,6	36,7	33,1	33,6	27,2	29,2	28,4	28,7
Plagioclase	43,6	41,8	37,7	35,6	37,8	25,2	38,5	27,7	28,3	17,2	30,4	19,5	24,6	31,9	32	39,1	36,8	32,7	30,1
Alkali-felds	10,8	9,7	27,9	27,5	30,1	43,4	31,9	42	44,5	40,7	36,6	45	31,6	28,4	28,9	28,6	33,6	38,6	39,8
Hornblende	0	0	0	0	0	0	0	0	0	0	0	0	0	0	0	0	0	0	0
Biotite	1,6	9,6	4,5	2,8	0,4	4,8	3,3	2,5	2,2	1,5	5,2	3,8	4,9	5,1	0,4	3,5	n.d	n.d	0,1
Titanite	n.d	n.d	n.d	n.d	n.d	n.d	0	0,1	n.d	0	n.d	0	0	0	0	0	0	0	0
Zircon	n.d	n.d	n.d	n.d	n.d	n.d	n.d	0,1	n.d	n.d	n.d	0,1	0,1	0,1	n.d	n.d	n.d	n.d	n.d
Allanite	0	0	0	0	0	n.d	n.d	0,1	n.d	0	0	0,2	0,1	0,1	n.d	0	0	0	0
Apatite	n.d	n.d	n.d	n.d	n.d	n.d	n.d	n.d	n.d	n.d	n.d	n.d	n.d	n.d	n.d	n.d	n.d	n.d	n.d
Magmatic e	0,1	0	0	0	0	0	0	n.d	0	0	0	0	0	0	0	0	0	0	0
Opaques	0	0,5	0,1	0,2	n.d	0,6	0,3	0,2	0,9	0,6	0,3	0,4	1,6	1	1,7	1,2	0	0,2	0,6
Secondary	0	0	0	0	0	0	0	0	0	0	0	0	0	0	0	0	n.d	0	0
Chlorite	0	0	0	0	0	n.d	1,1	n.d	0	n.d	0,1	0,1	0,4	0	2,9	0,1	0,2	0	0,4
Muscovite	n.d	0,6	n.d	0,1	0,1	0	0	0	0	n.d	n.d	0	0	0	0	n.d	0	0	0
Escapolite	0	0	0	0	0	0	0,6	0	0,3	n.d	0	0	0	n.d	0,1	n.d	n.d	n.d	n.d
Fluorite	0	0	0	0	0	0	0	0	0	0	0	0	0	0	0	0	0	0	0
∑	99,7	100,5	99,9	100	100	99,6	99,4	99,9	97,8	100	99,8	99,7	100	99,7	99,6	99,7	99,8	99,9	99,7
Mafics	1,7	10,7	4,6	3,1	0,5	5,4	4,7	3	5,3	2,1	5,6	4,6	7	6,3	5	4,8	0,2	0,2	1,1

Sample	ARF-3	ARF-5	ARF-8	ARF-9	ARC-96	ARC-100	ARC-120	GRD-03A	ARC-106A	ARC-108	ERF-101	ERF-102	ERF-109	ARC-113	ERF-122	ARC-58B	ARC-141A
Petrology	LMzG	LMzG	LMzG	BSG	LMzG	BLSG	LMzG	LMzG	BMzG	BLMzG	BLMzG	BLSG	BLMzG	BLSG	BMzG	BSG	BMzG
Units	Cruzadão granite																
Quartz	27,2	38,8	30,2	26,6	38,5	27,8	30,3	35	36,8	39,4	32,3	31,6	30,3	33	31,3	30	32,5
Plagioclase	34,1	27,1	32,6	17	21,8	20,9	27,4	36,2	24,7	24,6	31,9	23	28,3	14,9	32,6	17,7	22,5
Alkali-felds	37,8	31,8	35,8	48,6	38,1	47,9	40,1	28	32,8	31,4	31,2	43,6	36	47,6	27,4	41,2	38,4
Hornblende	0	0	0	0	0	0	0	0	0	0	0	0	0	0	0	0	0
Biotite	n.d	0,4	0,1	6,6	n.d	0,4	0,3	0,2	4,6	1,6	3	0,9	1,5	1,6	6,2	7	4,4
Titanite	n.d	0	0	n.d	n.d	n.d	0	0	0	n.d	0,3	0,2	1	n.d	0,3	2	0,2
Zircon	n.d	n.d	n.d	0,1	n.d	n.d	0,2	n.d	n.d	0,2	n.d	n.d	n.d	0,2	n.d	0,1	0,1
Allanite	n.d	0	0	0,4	0	0,3	0	0	0,05	0,2	0,05	0,1	0,3	0,2	0,1	0,2	0,1
Apatite	n.d	n.d	n.d	0,2	0,2	n.d	n.d	n.d	n.d	n.d	n.d	n.d	n.d	n.d	n.d	n.d	n.d
Magmatic e	0	0,4	n.d	0,1	0	0,1	0,1	0	0	0	0	0	0	0	0	0,8	0
Opaques	0,1	n.d	n.d	0,1	1,1	0,5	1	0,2	0,6	0,3	0,4	0,2	1,1	0,3	1,8	0,7	1,1
Secondary	0	0	n.d	0	0,1	0	0	0	0	0	0	0	0	0	0	n.d	0
Chlorite	0,6	1	1	0,1	0	2,1	0,6	0,2	0,1	1,2	0,4	n.d	0,7	1,2	0	0,3	0,2
Muscovite	0	0	0	n.d	0	0	0	0	0,2	1,1	n.d	0	0,1	1,1	0	0	0
Escapolite	0	0	0	n.d	0	0	0	0	0	0	0	0	0	0	0	0	0
Fluorite	0	0,1	0	0	0	0	0	0	0,1	0	0	0	0	0	0	0	0
∑	99,8	99,6	99,7	99,8	99,8	100	100	99,8	99,95	100	99,55	99,6	99,3	100,1	99,7	100	99,5
Mafics	0,7	1,8	1,1	7,6	1,4	3,4	2,2	0,6	5,55	4,6	4,15	1,4	4,7	4,6	8,4	10,1	6,1

Table B - Representative composition of the minerals used in the modeling and partition coefficients for batch melting calculations.

	Amp	Plg_{An60}	Cpx	Grt	Opx	Ilm
SiO_2	45,08	52,96	50,92	39,35	55,06	0,51
TiO_2	1,56	0	0,42	0,32	0,17	50,44
Al_2O_3	8,83	29,72	2,02	21,41	4,17	0
FeOt	16,06	0,75	11,35	20,68	5,54	4,38
MgO	13,71	0	10,02	7,56	33,65	0,46
CaO	10,12	12,28	23,8	8,37	0,79	0,72
Na_2O	2,32	4,35	0,12	0	0	0
K_2O	0,33	0	0,08	0	0	0
Rb	0,06	0,071			0,003	0,025
Ba	0,05	0,23			0,003	0,018
Sr	0,39	1,8			0,009	0,0022
Nb	0,27	0,01				3
Zr	0,42	0,048		1,2	0,2	2,3
Y	2,50	0,03		35	1	0,037
La	0,32		0,056			0,015
Ce	0,56	0,12	0,092	0,25	0,15	0,012
Nd	1,30	0,08	0,23	0,53	0,22	0,01
Sm	2,10	0,067	0,455	2,7	0,27	0,09
Eu	1,80	0,34	0,474	1,5	0,17	0,01
Gd	2,50	0,63	0,556	10,5	0,34	0,011
Tb	2,60		0,57	11,9		0,018
Yb	1,80	0,067	0,542	39,9	0,86	0,13
Lu	1,60	0,06	0,506	29,6	0,9	0,19
	2*	1*	1*	1*	1*	2*

data source (Kd): 1*-Rollisson (1993); 2* - Bédard (2006)

Capítulo – 4

4 GEOCHEMISTRY, GEOCHRONOLOGY, AND ORIGIN OF THE NEOARCHEAN PLANALTO GRANITE SUITE, CARAJÁS, AMAZONIAN CRATON: A-TYPE OR HYDRATED CHARNOCKITIC GRANITES?

Gilmara Regina Lima Feio
Roberto Dall'Agnol
Elton L. Dantas
M.J.B. Macambira
A.C.B. Gomes
A.S. Sardinha
P.A. Santos
Submetido: Lithos

Author's Decision

Thank you for approving "Geochemistry, geochronology, and origin of the Neoarchean Planalto Granite suite, Carajás, Amazonian craton: A-type or hydrated charnockitic granites?".

View QC Results

Main Menu

Geochemistry, geochronology, and origin of the Neoarchean Planalto Granite suite, Carajás, Amazonian craton: A-type or hydrated charnockitic granites?

G.R.L Feio[1,2], R. Dall'Agnol[1], E.L. Dantas[3], M.J.B. Macambira[2,4], A.K.B. Gomes[1], A.S. Sardinha[1], P.A. Santos[1,2]

[1]Grupo de Pesquisa Petrologia de Granitóides, Instituto de Geociências (IG), Universidade Federal do Pará (UFPA), Rua Augusto Corrêa, 01. CEP 66075-110. Brasil.

[2]Programa de pós-graduação em Geologia e Geoquímica, IG - UFPA.

[3]Laboratório de Estudos Geocronológicos, Geodinâmicos e Ambientais, Universidade de Brasília, Brasília, DF, CEP 70910-900, Brasil.

[4]Laboratório de Geologia Isotópica, IG - UFPA.

Abstract

New whole rock geochemistry and LA-MC-ICPMS and Pb-evaporation geochronological data on zircon obtained in the Neoarchean Planalto suite granites and associated charnockitic rocks of the Canaã area of the Carajás province, eastern Amazonian craton, Brazil, indicate that: (a) The Pb-evaporation ages given by three samples of the Planalto suite are concentrated around 2733 Ma (2733 ± 2 Ma, 2731 ± 1 Ma and 2736 ± 4 Ma). The U-Pb LA-MC-ICPMS concordia ages obtained for the same samples are of 2729 ± 17 Ma, 2710 ± 10 Ma, and 2706 ± 5 Ma. The whole results indicate that the Planalto suite granites were crystallized in the time interval of 2730 to 2700 Ma; (b) The orthopyroxene-quartz gabbro associated with the Pium complex and Planalto suite yielded an U-Pb concordia age of 2735 ± 5 Ma assumed as its crystallization age. The Planalto granites have ferroan character and are similar geochemically to reduced A-type granites. In previous works, they have been classified as such, despite the fact that they are syntectonic. The tectonic setting and the association between the Planalto suite and charnockitic series led us to propose classifying these biotite-hornblende granites as hydrated granites of the charnockitic rocks series. The Planalto suite was derived by partial melting of mafic to intermediate tholeitic orthopyroxene-bearing rocks similar to those of the Pium complex. The orthopyroxene-quartz gabbros have chemical compositions compatible with their derivation from the Pium norite by partial melting, but this would require a high degree of melting. At 2.76 Ga, the upwelling of the asthenospheric mantle in an extensional setting propitiated the formation of the Carajás basin. Later on, at ca. 2.73-2.70 Ga, the heat input associated with underplate of mafic magma induced the partial melting of mafic to intermediate lower crustal rocks originating the Planalto and orthopyroxene-quartz gabbro magmas. The emplacement of these magmas was done under an active regional stress and associated with the major shear zones found in the Canaã dos Carajás area. It was probably coincident with the tectonic inversion of the Carajás basin. The close association between the Planalto suite and charnockitic rocks suggests similarity between its

evolution and that of the high temperature granite magmatism commonly found near the limits between distinct tectonic blocks or in their zone of interaction.

Keywords: A-type granite; charnockitic rocks; Archean; Carajás; Amazonian craton; geochronology; petrology

1. Introduction

A-type granites are a distinctive group of rocks of diversified magmatic origin (Loiselle and Wones, 1979; Collins et al., 1982; Whalen et al., 1987; Anderson and Bender, 1989; Eby, 1992; Rämo and Haapala, 2005; Bonin, 2007; Dall'Agnol and Oliveira, 2007). They are normally associated with anorogenic or post-collisional extensional tectonic settings (Whalen et al., 1987; Sylvester, 1989) and generally undeformed.

A-type granites are abundant in the Late-Paleoproterozoic and Mesoproterozoic, between 1900 and 1000 Ma, when most of the rapakivi granites and anorthosite-mangerite-charnockite-granite (AMCG) complexes were formed (Emslie, 1991; Rämö and Haapala, 1995). However, comparatively earlier Paleoproterozoic A-type intrusions aged of ~2.44 Ga occur in eastern Finland (Lauri et al., 2006) and, granite varieties that are relatively enriched in HFSE and show in this respect some affinity with A-type granites were also described in Archean terranes (Yilgarn craton; Champion and Sheraton, 1997). Archean granites associated with rocks of the charnockitic series have also been identified in the Kaapvaal, Siberian and Singhbhum-Orissa cratons and in the East Antarctic shield (Sheraton and Black, 1988; Moore et al., 1993; Misra et al., 2002; Larin et al., 2006). The occurrence of granites with A-type affinity is generally restricted to the Neoarchean, a time of vigorous crustal growth and reworking of older lithosphere (Percival, 1994; Sylvester, 1994).

Neoarchean granite bodies with A- type affinity have also been described in the Carajás Province, eastern Amazonian craton. They include the Estrela Complex and the Serra do Rabo and Igarapé Gelado plutons (Sardinha et al., 2006; Barros et al., 2009) which are exposed inside or to the northwestern of the Carajás basin. Moreover, immediately to the south of the Carajás basin, several elongated plutons with A-type characteristics have been reported and are grouped in the present paper in the Planalto Suite. This suite is spatially associated with charnockite rocks and peculiar sodic granitoids and is found only in the Carajás basin and adjacent areas being absent in the Mesoarchean Rio Maria granite-greenstone terrane, the southern domain of the Carajás province.

In this paper, we present geological, geochemical, geochronological, and Nd isotope data for the Archean granites of the Planalto suite of the Carajás Province. The new data are employed to discuss the petrogenesis of this Neoarchean granitoid magmatism, the complex relationships between A-type granites and charnockitic series and implications for understanding of the crustal evolution of the north domain of the Carajás Province.

2. Tectonical setting and regional geology

The Carajás Province corresponds to the major Archean crustal segment of the Amazonian craton (Fig.1a, Machado et al., 1991; Santos et al., 2000; Tassinari and Macambira, 2004; Dall'Agnol et al., 2006). It comprises two distinct tectonic domains, separated for approximately E-W shear zones (Fig. 1b; Vasquez et al., 2008): The Mesoarchean Rio Maria granite-greenstone terrane (RMGGT) to the south (3.0 to 2.86 Ga; Macambira and Lancelot, 1996; Souza et al., 2001; Leite et al., 2004; Almeida et al. 2010) and the Carajás domain to the north (3.0 to 2.55 Ga; Gibbs et al., 1986; Machado et al., 1991; Dall'Agnol et al., 2006). The Carajás domain corresponds approximately to the Itacaiúnas Shear Belt as defined by Araújo and Maia (1991) and Costa et al. (1995).

The limit between the RMGGT and the Carajás domain is located tentatively to the North of the Sapucaia belt (Fig. 1b). The Northern part of the Carajás domain corresponds to the Neoarchean Carajás basin (CB). Its southern part is composed dominantly of Meso to Neoarchean granitoids and the granulitic Pium complex. This part of the domain was denominated informally as 'Transition Domain', interpreted as a terrane probably similar to the RMGGT that was intensely affected by the magmatic and tectonic Neoarchean events recorded in the CB (Dall'Agnol et al., 2006 and references therein; Domingos, 2009).

The Mesoarchean Rio Maria granite-greenstone terrane is composed of greenstone belts (3.0-2.90 Ga; Macambira, 1992; Souza et al., 2001 and references therein) and several granitoid series: (1) An older TTG series (2.98-2.93 Ga; Macambira and Lancelot, 1996; Althoff et al., 2000; Leite et al., 2004; Almeida et al., submitted); (2) The sanukitoid Rio Maria suite (~2.87 Ga; Macambira, 1992; Oliveira et al., 2009, and references therein); (3) An younger TTG series (~2.87-2.86 Ga; Leite et al., 2004; Almeida et al., submitted); (4) A high Sr- and Ba-bearing leucogranodiorite-granite suite (~2.87 Ga, Almeida et al., 2010); and (5) Potassic leucogranites of calc-alkaline affinity (~2.87-2.86 Ga, Leite et al., 2004).

The southern part of the Carajás domain is formed by strongly deformed Mesoarchean to Neoarchean units, whereas its northern part corresponds essentially to the Neoarchean Carajás basin. This southern area has been poorly studied so far and the granitoid and gneissic

rocks were generally grouped in the Xingu Complex (Fig. 1b). In the Canaã area of the 'Transition Domain' (Fig. 1c), studied in more detail in the present work, the oldest rocks exposed are the granulites of the Pium Complex, with a protolith crystallization age of 3002 ± 14 Ma and granulite facies metamorphism at 2859 ± 9 Ma (Pidgeon et al., 2000), the Bacaba tonalite, with a crystallization age of 3005 ± 8 Ma (U-Pb LA-MC-ICPMS on zircon; Moreto et al., 2010), a gneissic leucogranite with ages variable between 3.0 and 2.93 Ga, the Canaã dos Carajás potassic leucogranite (~2.95 Ga) and trondhjemitic rocks (~2.93 Ga; geochronological data of G. R. L. Feio, unpublished data). These older units were followed by little deformed calc-alkaline diorite to granodiorite, and the Serra Dourada K-leucogranite (respectively, 2.87 Ga and 2.82 Ga; G. R. L. Feio, unpublished data).

The Neoarchean Carajás basin is formed by banded iron formations, accompanied by a bimodal volcanism (Itacaiúnas Supergroup; 2.76-2.74 Ga), metamorphosed in greenschist conditions, and was followed by the siliciclastic sedimentation (fluvial to marine deposits) of the Águas Claras formation. In the borders of the Carajás basin there are also several Neoarchean mafic-ultramafic stratified bodies (e.g., Vermelho in the Canaã area; Vasquez et al., 2008 and references therein), mineralized in nickel. Sills and dykes of Neoarchean gabbros cross-cut all these rocks.

The Neoarchean evolution of the Carajás domain is also marked by a widespread plutonic magmatism: (1) Charnockitic rocks, comprising quartz-norites to enderbites (Pb-evaporation on zircon age of 2754 ± 1 Ma; Gabriel et al., 2010), intimately associated with the Pium complex and until recently mistaken with it (Ricci and Carvalho, 2006). (2) The Pedra Branca suite, composed of ~2.75 Ga sodic granitoids (Gomes and Dall'Agnol, 2007) and spatially associated with the Planalto suite granites. (3) Subalkaline granites represented, in the Carajás basin, by the Estrela Granitic Complex (~2.76 Ga; Barros et al., 2009), Serra do Rabo (2.74 Ga; Sardinha et al., 2006), Igarapé Gelado (2.73 Ga; Barros et al., 2009), and Velho Salobo plutons (2.57 Ga; Machado et al., 1991). In the 'Transition Domain', similar granites were included in the Planalto Suite (Fig. 1b, c).

The tectonic setting and processes responsible for the origin and evolution of the Carajás basin are still controversial. Some authors advocate the hypothesis that it was related to a continental rift tectonic setting (Gibbs et al., 1986; Nogueira et al., 1995; Macambira, 2003; Dall'Agnol et al., 2006; Domingos, 2009). An alternative model admits a continental margin setting, which evolution was related to subduction processes (Teixeira and Egler, 1994; Barros et al., 2009; Lobato et al., 2006). However, the Itacaiúnas supergroup metavolcanic sequences are formed dominantly by a bimodal magmatism and abundant TTG

or calc-alkaline series are absent in the Neoarchean which is more consistent with a rift setting (Dall'Agnol et al., 2006). Additionally, Nd data on the Paleoproterozoic Serra dos Carajás suite indicate the existence of a Mesoarchean substratum in the Carajás region similar isotopically to that of the RMGGT (Dall'Agnol et al., 2005; cf. also Tassinari and Macambira, 2004). Hence, a rift tectonic setting is assumed for the Carajás basin that was later deformed and metamorphosed in low-grade conditions. Domingos (2009) admitted that the tectonic inversion of the Carajás basin involved a regional phase of sinistral transpression controlled by a general NNE-directed oblique shortening.

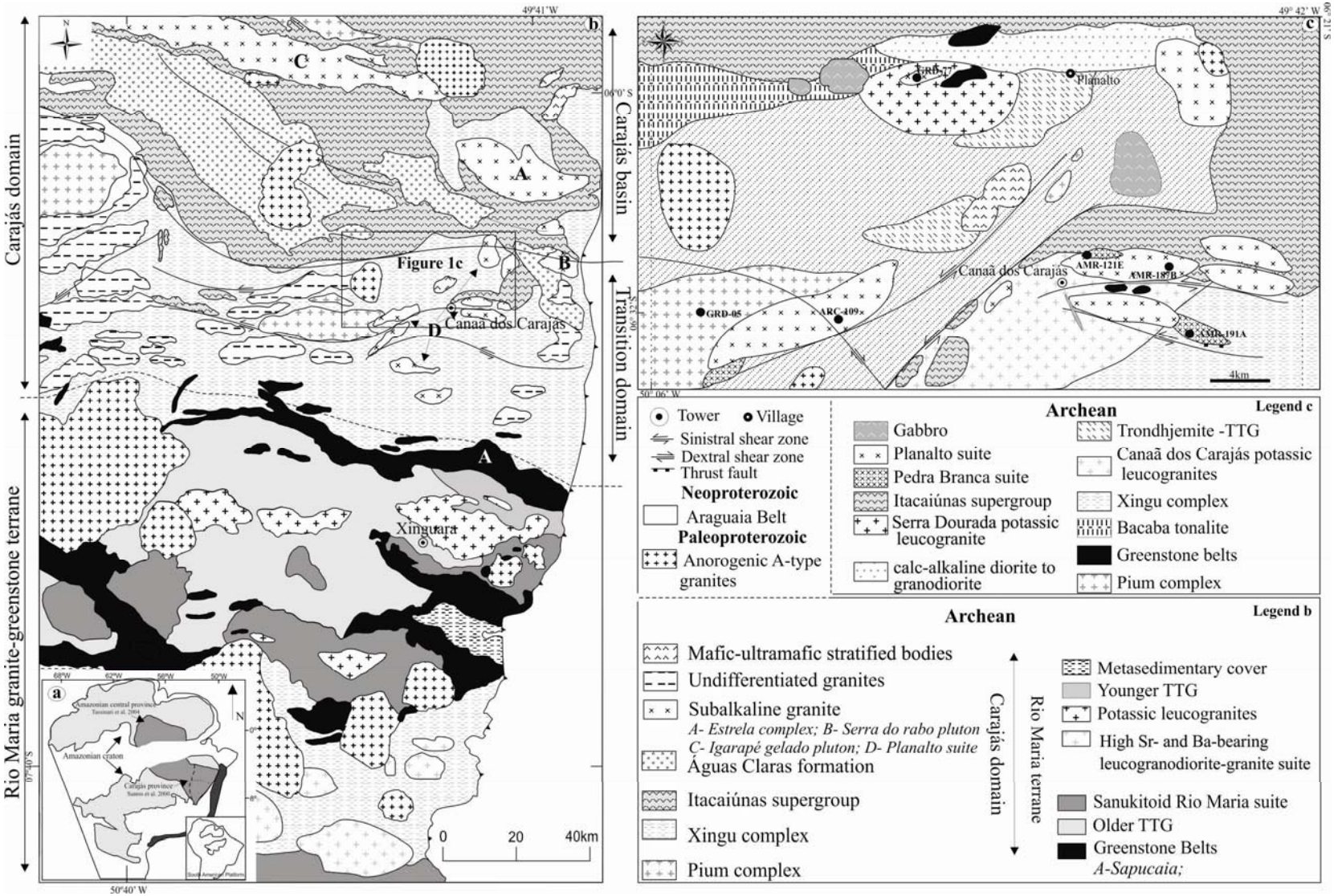

Figure 1 - (a) Location of the Carajás Province in the Amazonian craton; (b) Geological map of the Carajás Province, showing the location of the Canaã dos Carajás area and the approximate limits between the Rio Maria granite-greenstone terrane and the Carajás domain (dashed line), and the Carajás basin and transitional domain (continuous lines); (c) Geological map of the Canaã dos Carajás area, showing the location of the dated samples.

3. Geological features of the Planalto suite and associated units

3.1. Pium complex and associated charnockitic rocks

The Pium complex is restricted to the 'Transition Domain'. It was described as an orthopyroxene-bearing felsic to mafic granulitic complex (Araújo and Maia, 1991) that occurs as a number of elongate bodies, with maximum length of 35 km, parallel to the regional E–W foliation. In the type area, the Pium complex is composed dominantly of norite and gabbro with subordinate quartz-orthopyroxene-bearing rocks that could show massive or foliated aspect and generally display igneous textures modified by ductile deformation and recrystallization (Ricci and Carvalho, 2006; Santos and Oliveira, 2010). Field relationships between the mafic rocks and quartz gabbros, enderbites and charnockites indicate that the mafic rocks occur in several places as partially digested or assimilated enclaves (Araújo and Maia, 1991) or as high viscosity contrast angular enclaves (Santos and Oliveira, 2010) in the quartz-orthopyroxene-bearing rocks. These features suggest that the norite and gabbros were emplaced earlier and are possibly significantly older in time than the quartz-orthopyroxene-bearing rocks.

Pidgeon et al. (2000) dated an enderbite of the Pium complex by SHRIMP U-Pb on zircon and obtained an age of 3002 ± 14 Ma for the core zircons, interpreted as dating the crystallization of the protolith of the enderbite, while the rim zircons yielded a younger 2859 ± 9 Ma age that would correspond to the granulite facies metamorphism. However, the metamorphic character of the Pium complex and the significance of the ages obtained by Pidgeon et al. (2000) were challenged and a possible igneous origin for the orthopyroxene-bearing rocks of the type area was proposed (Ricci and Carvalho, 2006; Vasquez et al., 2008; Santos and Oliveira, 2010).

The igneous or metamorphic origin of the Pium complex remains a controversial question that it is beyond the scope of the present paper. Nevertheless, recent field work and geochronological data obtained in the area originally occupied by the Pium complex demonstrated the occurrence in it of Neoarchean charnockitic plutons composed essentially of leucoenderbites (2754 ± 1 Ma; Pb-evaporation on zircon; Gabriel et al., 2010). Similar ages have been also obtained for orthopyroxene-bearing quartz-gabbros spatially associated with the Pium complex (see geochronological section in the present paper). This indicates the existence of a generation of charnockitic rocks that is clearly younger than the rocks of the Pium complex studied by Pidgeon et al. (2000).

3.2. Pedra Branca suite

The Pedra Branca suite consists of small stocks (≤ 4km in the largest dimension) that occur spatially associated with the plutons of the Planalto Suite (Fig. 1c). Field relationships between the Pedra Branca suite and the Planalto suite and other older Archean units were not observed. It is composed of strongly deformed sodic granitoids (tonalite and trondhjemite), with hornblende and biotite as major mafic minerals, containing titanite, allanite, zircon, and apatite as accessory minerals, and, locally, relics of clinopyroxene (Gomes and Dall'Agnol, 2007).

The rocks of the Pedra Branca suite commonly show a magmatic banding, with alternation of decimeter- to meter-thick tonalitic and trondhjemitic bands and subvertical EW foliation related to a ductile deformation. Additionally, in the stock located in the southeastern part of the mapped area (Fig. 1c), a thrust fault with a high angle dipping to SSE intercept the primary foliation, indicating the action of a late NS-compressive strain (Gomes and Dall'Agnol, 2007).

Geochronological data for the AMR-191A trondhjemite sample of Pedra Branca suite yielded ages of 2749 ± 6 Ma and 2765 ± 39 Ma (respectively, Pb-evaporation on zircon and U-Pb on zircon by TIMS, discordia age; Sardinha et al., 2004; Pb-evaporation age recalculated for 2σ). Another sample of trondhjemite (AMR-121E) of a distinct body was analyzed by Pb-evaporation and U-Pb TIMS methods (Sardinha, A.S., unpublished data). The Pb-evaporation on zircon data did not present a good fit. The U-Pb TIMS results gave an upper intercept discordia age of 2737 ± 3 Ma (MSWD = 1.14; three zircon grains). Despite the uncertainties on the age of this unit, it should be probably comprised in the interval of 2.77 to 2.73 Ga.

3.3. Planalto suite

The Planalto suite consists of several E-W elongated lenticular granite plutons with less than 10 km in the largest dimension (Fig. 1c) generally limited by shear zones and oriented concordantly to the dominant EW-trending regional structures. These plutons are intrusive in the Mesoarchean gneissic and granitoid units, in the mafic Pium complex, and in the Neoarchean supracrustal Itacaiúnas supergroup (Fig. 1c), and are preferentially associated with the mafic rocks of the Pium complex, the charnockitic rocks and the Pedra Branca suite. The Planalto granite includes angular or partially digested enclaves of Pium mafic rocks (Fig. 2a, b). The Planalto and Pedra Branca granitoids show similar deformational features and both

and the charnockitic rocks were affected by the event responsible for the generation in the studied area of high angle thrust faults. However, the field relationships between the Planalto granites and the charnockitic rocks and the Pedra Branca suite are not conclusive.

The Planalto granites show penetrative EW-subvertical foliation sometimes accompanied by a remarkable high angle stretching mineral lineation and C-type shear bands. True mylonites are found along sinistral or subordinate dextral shear zones. The less-deformed rocks exhibit well-preserved magmatic texture. The granites are cut by decimeter- to meter-thick pegmatoid veins and by narrow aplitic and microgranite dikes. Besides the Pium mafic xenoliths, two different kind of enclaves were distinguished in the Planalto granite: (1) enclaves of a porphyritic rock, with medium-grained plagioclase phenocrysts in a dark-colored, fine-grained matrix; these enclaves are partially adsorbed in the contact with the granite and do not show the deformation features observed in the granite (Fig. 2c, d), suggesting that they are older rocks partially digested during the granite intrusion; (2) oval-shaped or quadratic enclaves of originally mafic or intermediate rocks that are now crowded with alkali-feldspar megacrysts probably dropped from the granite magma (Fig. 2e, f); these enclaves are interpreted as possible autholiths that have coexisted in the partial melting state with the granite and mingled with its magma.

The Planalto suite is composed of monzogranite to syenogranite with variable modal contents of hornblende and biotite. The primary accessory minerals are zircon, apatite, allanite, ilmenite ± magnetite ± titanite ± fluorite. Relics of clinopyroxene involved by amphibole are observed in some samples. The secondary minerals are epidote, muscovite, chlorite ± scapolite ± carbonate ± titanite ± tourmaline.

The less-deformed granites show pink to reddish color and a predominant coarse- or medium-grained equigranular to porphyritic texture, with euhedral alkali feldspar phenocrysts in a medium- to fine-grained matrix. Plagioclase (An_{25-17}), locally altered and mantled by alkali feldspar (Fig. 3a), is present in the porphyritic varieties. In a small, possibly epizonal body, quartz and alkali feldspar form granophyric intergrowths surrounding euhedral plagioclase, and biotite occurs as aggregates of euhedral crystals.

Most rocks display porphyroclasts of quartz, perthitic alkali-feldspar, and plagioclase, showing core-and-mantle microstructures. The quartz occurs also as ribbons and recrystallized aggregates (Fig. 3b). The plagioclase show deformed twinning and local recrystallization to fine-grained polygonal aggregates of largely untwined grains. Bulbous myrmekite is found commonly replacing the borders of alkali-feldspar grains. The amphibole occurs as medium-grained oval porphyroclasts (Fig. 3c) or form oriented aggregates together

with biotite and other mafic minerals. In the mylonites, the foliation is deflected around alkali-feldspar porphyroclasts and strain shadows are formed by the fine-grained recrystallized aggregates (Fig. 3d).

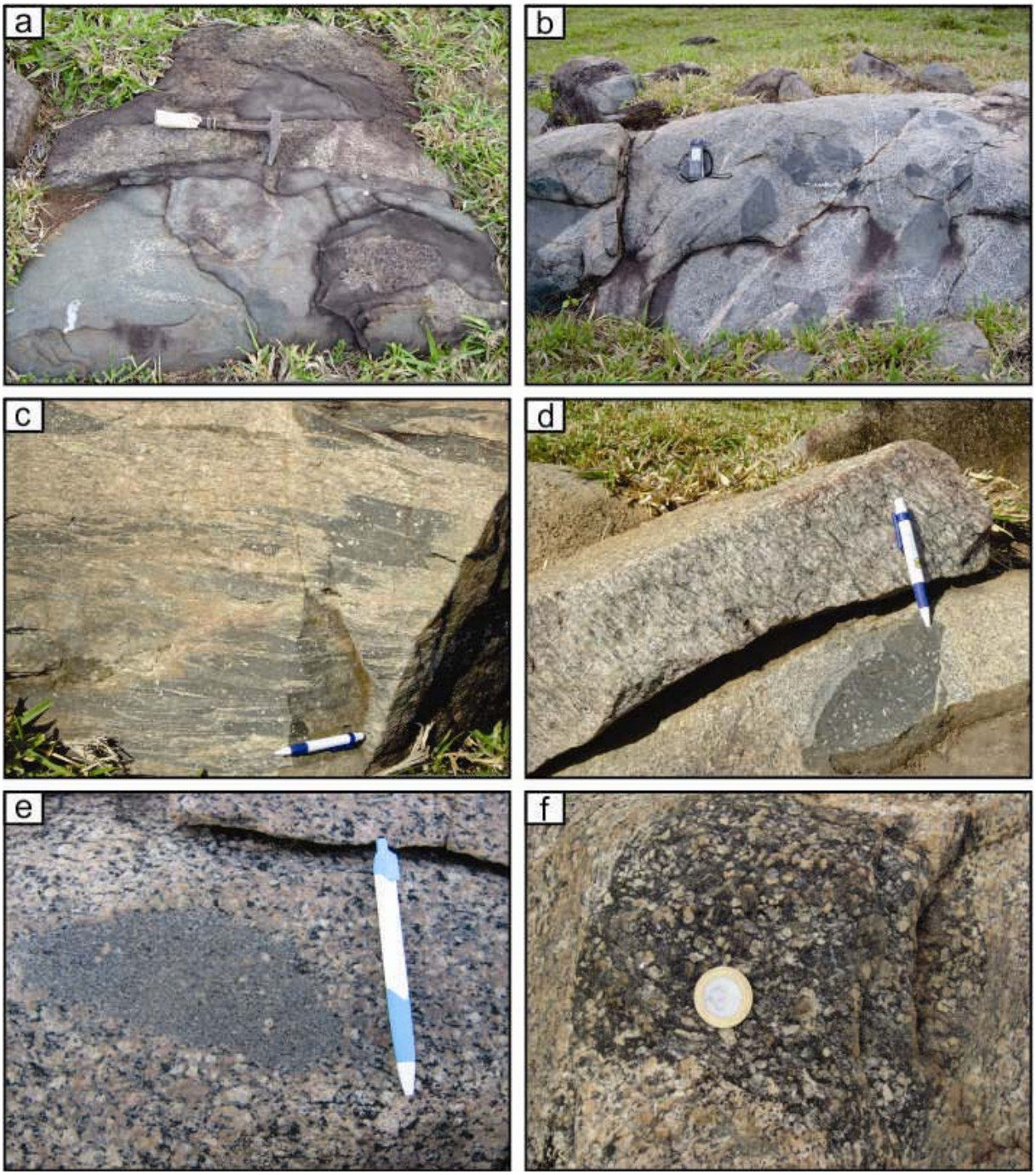

Figure 2 - Field aspects of the Planalto suite rocks (a, b) Angular, partially digested enclaves of Pium mafic rocks in the Planalto granite; (c, d) enclaves of an intermediate porphyritic rock partially adsorbed in the contact with the granite; (e, f) oval- or quadratic-shaped enclaves of mafic or intermediate rocks, crowded with dropped alkali-feldspar megacrysts of the granite.

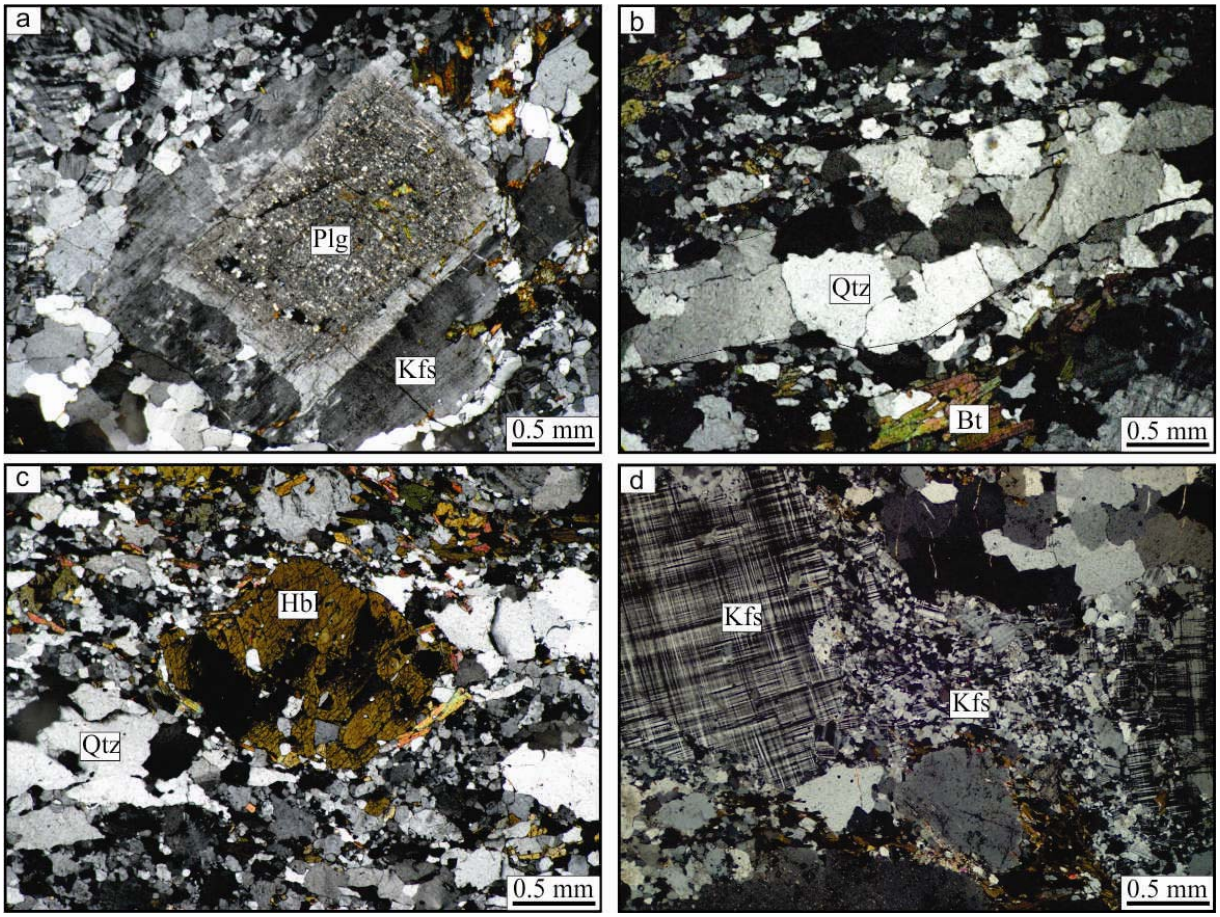

Figure 3 - Microscopic textures of the Planalto granite. (a) Plagioclase mantled by alkali feldspar; (b) recrystallized aggregates of quartz; (c) oval porphyroclast of amphibole with tails of recrystallized quartz in a mylonitized granite; (d) alkali-feldspar porphyroclasts showing strain shadows formed by the fine-grained recrystallized aggregates. Mineral abbreviations according to Kretz (1983).

4. Elemental Geochemistry

4.1. Pium Complex and associated charnockitic rocks

Representative chemical compositions of the Pium complex (Santos, 2009), including associated charnockitic rocks show variation from norite to quartz-gabbro and enderbite varieties. All analyzed samples display subalkaline tholeitic geochemical affinity.

According to Santos (2009), the noritic varieties have SiO_2 contents varying from 51 to 55 wt. %, moderate Al_2O_3 (14.4 to 15.9 wt. %), Mg# (0.44 to 0.56), and Ba, high CaO (7.1 to 10.0 wt. %), FeOt (8.2 to 11.1 wt %), Sr, and Zr, and low Nb and Rb. The quartz gabbro and enderbite show SiO_2 contents between (57.2 to 63.7 wt. %), moderate Al_2O_3 (13.2 to 17.6 wt. %) and Mg# (0.25 to 0.56), and significantly higher K_2O, Ba, Zr, and Y, compared to the norite. The FeO/(FeO+MgO) ratios vary from 0.58 to 0.69 in the norite and from 0.68 to 0.84 in the quartz gabbro and enderbite except for an anomalous value of 0.58.

All rock varieties display low $(La/Yb)_N$, generally between 5 and 14, indicating low fractionation of heavy rare earth elements (HREE). Most analyzed samples display discrete negative or more rarely positive Eu anomalies (Eu/Eu* varying generally between 0.8 and 1.18). The REE patterns are quite similar for the different rock varieties (Santos, 2009).

The only analyzed and dated quartz gabbro in the present work (sample GRD-05; Table 1) has SiO_2 content of 57.19 wt %. GRD-05 shows higher contents of TiO_2, FeOt, and K_2O, and lower of Al_2O_3 and MgO compared to rocks of the Pium complex with similar silica contents analyzed by Santos (2009). FeO/(FeO+MgO) is 0.82 for GRD-05 compared to 0.58 to 0.75 for the Pium rocks. The trace element contents of GRD-05 are not significantly different from those of the Pium complex similar rocks.

4.2. Planalto suite

Representative chemical compositions of the different plutons of the Planalto suite are given in Table 1. The granites of the suite show a restricted range of silica (70.4 to 75.7 wt. %) and relatively high K_2O contents (generally between 4.0 and 5.5 wt. %). They have typically low Al_2O_3 (Fig. 4a; 11.1-12.8 wt. %), CaO (Fig. 4b; 0.4-2.2 wt. %) and MgO (Fig. 4c; 0.03-0.58 wt. %) contents. The K_2O/Na_2O (Fig. 4d; 1.2-2.3) ratios are high and the FeOt/(FeOt+MgO) ratios are higher than 0.88, corresponding to those of ferroan granites (Frost et al., 2001). A/CNK values vary from 0.91 to 1.09, indicating the mildly metaluminous to peraluminous character of these granites (Fig. 5a, Table 1). The Planalto suite granites have high contents of Zr (Fig. 4e), Y, Nb, and heavy rare-earth elements (HREE) and show geochemical affinity with reduced A-type granites (Fig. 5b, 5c; Collins et al., 1982; Whalen et al., 1987; Eby, 1992; Dall'Agnol and Oliveira, 2007) and Archean alkaline granites (Fig. 5d; Sylvester, 1989, 1994). They show high Ba (Fig. 4f; 949-1928 ppm), low to moderate Sr (Fig. 4g; 35-204 ppm), and low Rb (Fig. 4h; 67-158 ppm) contents.

The REE patterns are similar for all analyzed samples that show low $(La/Yb)_N$ ratios (5-19; Table 1), resulting in relatively flat HREE patterns (Fig. 6), and variable negative Eu anomalies (Eu/Eu* = 0.31-0.86). Most of these anomalies are accentuated to moderate (Fig. 6a), but four samples show discrete negative Eu anomalies (Fig. 6b; Eu/Eu* = 0.81-0.86) and one sample (AMR-85A) show a positive Eu anomaly (Table 1; Fig. 6a). The Eu and Sr behavior of dominant samples indicates fractionation of plagioclase during the magma differentiation or its retention in the magma source. Moreover, the flat REE pattern and the absence of concave shape of the HREE branch suggest that garnet and/or hornblende where not important fractionating phases during the magma evolution.

Table 1 - Representative chemical compositions of the granites of the Planalto suite of the Canaã dos Carajás area.

Unit	Planalto suite																			Charnockite
Sample	AMR-152	ARC-147	ARC-144	ARC-109	AMR-209	AMR-137A	AMR-187B	AMR-85A	AMR-149	AER-72A	AMR-140	AC-4B	AMR-145	ARC-77	ARF-17	AMR-116	AMR-208A	ARC-104	AMR-171	AMR-177	GRD-05
Varieties	BHMzG	BHMzG	BHMzG	HBSG	BHMzG	BHSG	HSG	HSG	HBMzG	BMzG	BHMzG	BHSG	BHSG	BSG	HBSG	BHSG	BSG	BMzG	BSG	HAG	Opx-Qtz gabbro
SiO_2	70.39	71.35	71.41	71.66	71.80	72.80	72.91	73.25	73.28	73.35	73.44	73.44	73.45	73.80	73.84	74.13	74.17	74.86	75.51	75.62	57.19
TiO_2	0.64	0.38	0.52	0.44	0.28	0.38	0.31	0.29	0.41	0.28	0.32	0.35	0.42	0.29	0.30	0.25	0.23	0.20	0.15	0.14	1.85
Al_2O_3	12.32	13.44	12.61	12.77	12.51	12.48	11.67	12.47	11.13	13.13	12.52	12.34	11.69	12.25	11.96	12.21	11.67	11.41	11.63	12.01	13.04
Fe_2O_3t	5.42	3.50	4.35	4.21	5.07	4.25	4.80	3.87	4.67	2.42	3.27	3.65	4.69	3.64	3.71	3.79	4.60	2.49	2.80	2.39	12.70
MnO	0.07	0.04	0.04	0.03	0.04	0.05	0.05	0.02	0.05	0.02	0.04	0.04	0.07	0.02	0.04	0.05	0.02	0.02	0.02	0.02	0.12
MgO	0.58	0.32	0.46	0.36	0.12	0.21	0.10	0.10	0.25	0.29	0.23	0.28	0.25	0.26	0.17	0.11	0.03	0.12	0.12	0.03	2.51
CaO	2.18	1.74	2.15	1.71	1.21	1.53	1.67	1.30	1.46	1.25	1.32	1.37	1.37	0.63	1.16	1.36	0.71	0.99	0.48	0.43	5.84
Na_2O	3.16	3.55	3.20	3.25	2.92	3.25	2.99	3.58	2.95	3.47	3.26	3.32	2.88	2.79	3.04	3.17	2.36	2.51	2.36	3.42	3.41
K_2O	3.93	4.55	4.01	4.49	5.20	4.04	4.44	4.21	3.49	4.71	4.45	4.14	3.83	5.11	4.75	4.65	5.36	5.03	5.64	5.09	2.36
P_2O_5	0.13	0.09	0.10	0.09	0.04	0.04	0.04	0.04	0.05	0.06	0.04	0.07	0.08	0.03	0.04	0.03	0.01	0.02	0.02	<0.01	0.51
LOI	0.80	0.70	0.80	0.70	0.50	0.60	0.70	0.30	1.60	0.80	0.50	0.80	0.70	1.00	0.60	0.00	0.50	2.10	1.00	0.70	0.20
Total	99.62	99.66	99.65	99.71	99.69	99.63	99.68	99.43	99.34	99.78	99.39	99.80	99.43	99.82	99.61	99.75	99.66	99.75	99.73	99.85	99.73
Ba	1624	1914	1842	1627	1722	1814	1459	4626	1765	1099	1142	1150	1929	949	1589	1391	1777	1488	1344	499	1038.0
Rb	97	94	101	117	132	120	102	71	85	123	158	150	83	127	127	134	94	124	112	67	52.2
Sr	204	167	169	145	88	173	103	92	161	85	137	141	153	58	101	96	103	88	76	36	239.5
Zr	595	356	465	487	399	502	504	499	462	283	387	396	543	355	432	393	596	303	295	316	293.6
Nb	26	15	19	21	22	24	21	7	19	13	24	22	19	24	26	16	24	24	29	11	19.2
Y	56	27	32	48	55	55	66	16	35	29	50	46	44	53	72	42	60	45	96	26	42.2
Hf	18	9	11	13	10	14	14	10	12	7	12	12	15	10	12	11	19	9	11	9	7.6
Ta	5	1	1	1	1	7	1	0	6	2	8	8	6	1	2	1	2	2	2	1	1.2
Th	10	15	22	24	14	14	23	5	11	19	27	21	11	32	44	12	23	19	31	14	14.1
U	2	4	5	4	6	4	3	1	3	5	6	5	2	5	7	2	6	6	12	3	3.2
Ga	23	18	17	18	20	22	20	16	19	17	21	20	18	18	18	20	21	17	22	17	19.8
La	81.7	28.4	43.1	64.4	43.1	84.4	130.0	29.2	56.7	59.3	99.0	102.2	68.3	100.2	118.4	63.0	59.3	68.0	143.7	78.0	57.30
Ce	179.6	78.6	87.0	130.4	97.6	162.7	249.7	58.8	107.6	124.7	203.0	206.7	137.6	197.2	237.3	130.5	124.1	133.5	263.3	148.7	125.70
Pr	19.5	7.5	10.9	16.3	12.3	17.2	26.5	7.0	11.2	13.6	20.0	21.1	15.4	22.2	27.3	15.6	15.8	16.4	34.1	17.0	15.52
Nd	77.4	29.4	43.2	62.5	51.5	62.8	99.6	28.0	42.3	49.3	74.1	73.5	60.9	82.3	101.1	63.5	63.7	61.5	132.2	63.0	63.60
Sm	13.8	5.8	8.1	10.6	10.1	11.6	15.7	4.8	8.7	7.8	12.1	12.7	10.7	13.7	15.2	10.7	13.3	10.4	23.3	8.9	11.32
Eu	2.4	1.6	2.2	1.8	2.2	2.5	2.7	2.7	2.1	1.1	1.8	1.8	2.6	1.4	1.9	2.1	1.9	1.6	2.3	1.1	2.61
Gd	10.8	5.2	6.9	8.9	10.0	9.8	12.7	3.8	7.0	5.9	9.3	9.2	8.4	11.3	12.2	9.1	12.5	8.9	20.7	6.6	9.70
Tb	1.7	0.9	1.1	1.5	1.6	1.5	2.1	0.6	1.0	0.9	1.3	1.3	1.2	1.8	1.9	1.4	2.0	1.4	3.3	0.9	1.43
Dy	9.8	5.1	5.9	8.4	9.5	9.2	11.3	3.0	6.2	5.1	8.4	8.1	7.7	10.2	10.5	7.7	11.2	7.9	17.7	5.2	8.10
Ho	2.0	1.0	1.2	1.6	1.9	1.8	2.2	0.6	1.3	1.0	1.7	1.6	1.6	2.0	2.3	1.6	2.3	1.5	3.6	0.9	1.52
Er	5.6	2.9	3.3	4.7	5.4	5.3	6.8	1.9	3.7	2.9	4.9	4.5	4.5	5.5	6.9	4.5	6.5	4.4	10.1	2.9	4.26
Tm	0.9	0.5	0.5	0.7	0.8	0.8	1.0	0.3	0.5	0.4	0.7	0.7	0.6	0.8	1.1	0.6	1.0	0.7	1.6	0.4	0.62
Yb	5.2	3.0	3.1	4.6	5.5	4.8	6.6	1.9	3.7	2.9	4.4	4.2	4.0	5.1	6.9	4.4	6.4	4.3	9.1	2.9	3.96
Lu	0.7	0.4	0.5	0.7	0.8	0.7	1.0	0.3	0.5	0.4	0.6	0.6	0.6	0.8	1.1	0.7	1.0	0.6	1.5	0.4	0.58
FeOt/(FeOt+MgO)	0.89	0.91	0.89	0.91	0.97	0.95	0.98	0.97	0.94	0.88	0.93	0.92	0.94	0.93	0.95	0.97	0.99	0.95	0.95	0.99	0.82
K_2O/Na_2O	1.24	1.28	1.25	1.38	1.78	1.24	1.48	1.18	1.18	1.36	1.37	1.25	1.33	1.83	1.56	1.47	2.27	2.00	2.39	1.49	0.69
Eu/Eu*	0.58	0.85	0.86	0.56	0.65	0.68	0.56	1.88	0.81	0.47	0.50	0.48	0.81	0.32	0.41	0.63	0.45	0.51	0.31	0.41	0.74
(La/Yb)N	11.18	6.88	9.91	10.13	5.60	12.51	14.09	11.14	10.90	14.62	16.07	17.33	12.37	13.98	12.40	10.29	6.63	11.37	11.35	19.03	10.38
A/CNK	0.92	0.96	0.93	0.96	0.99	1.00	0.91	0.97	0.99	1.00	1.00	0.99	1.03	1.09	0.98	0.96	1.06	1.00	1.07	1.01	0.69

BHMzG – Biotite-hornblende monzogranite; HBSG – Hornblende-biotite syenogranite; BHSG – Biotite-hornblende syenogranite; HSG – Hornblende syenogranite; BMzG – Biotite monzogranite; BSG – Biotite syenogranite; HAG – Hornblende biotite syenogranite; opx - orthopyroxene; qtz – quartz.

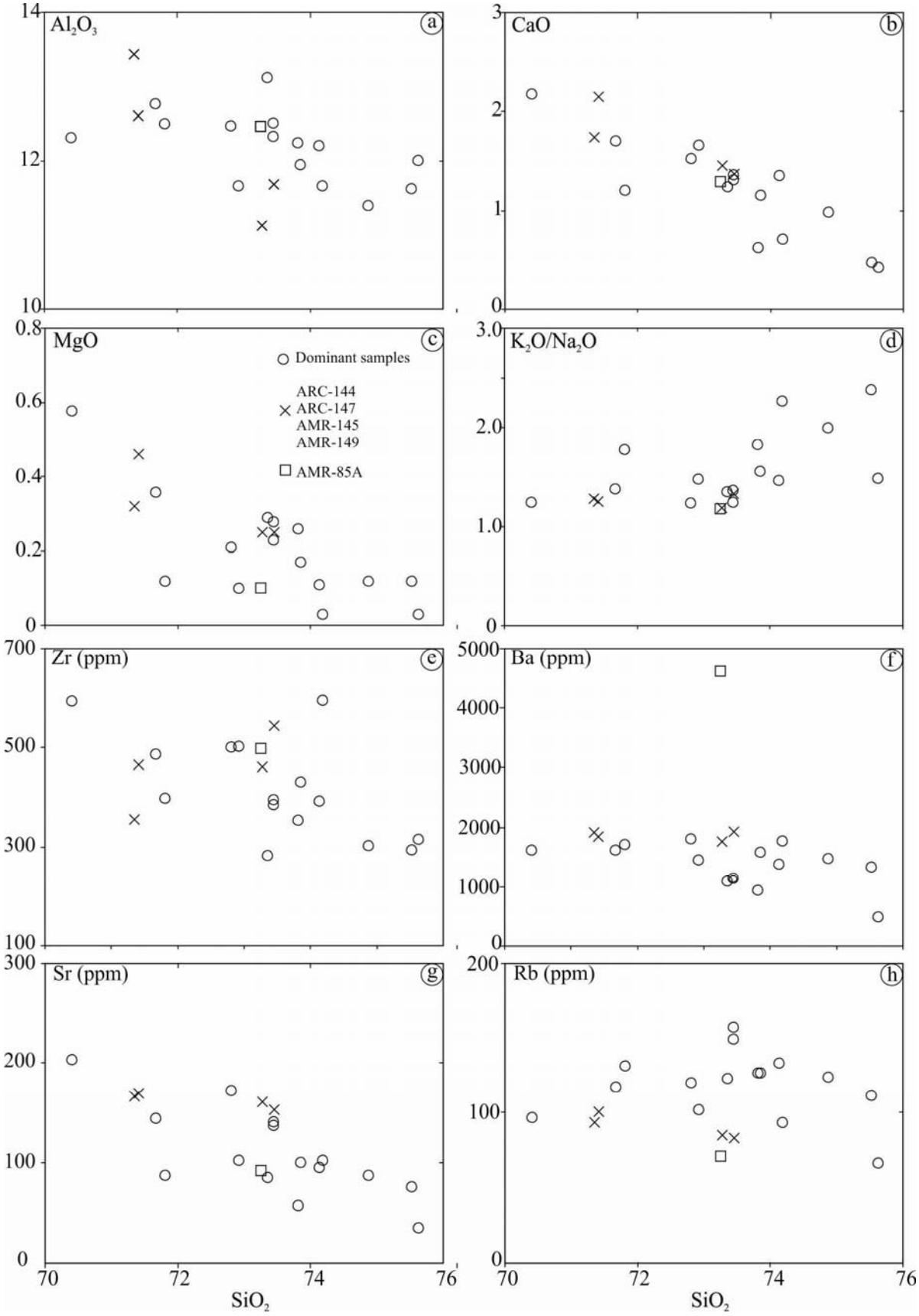

Figure 4 - Harker diagrams for the granites of the Planalto suite.

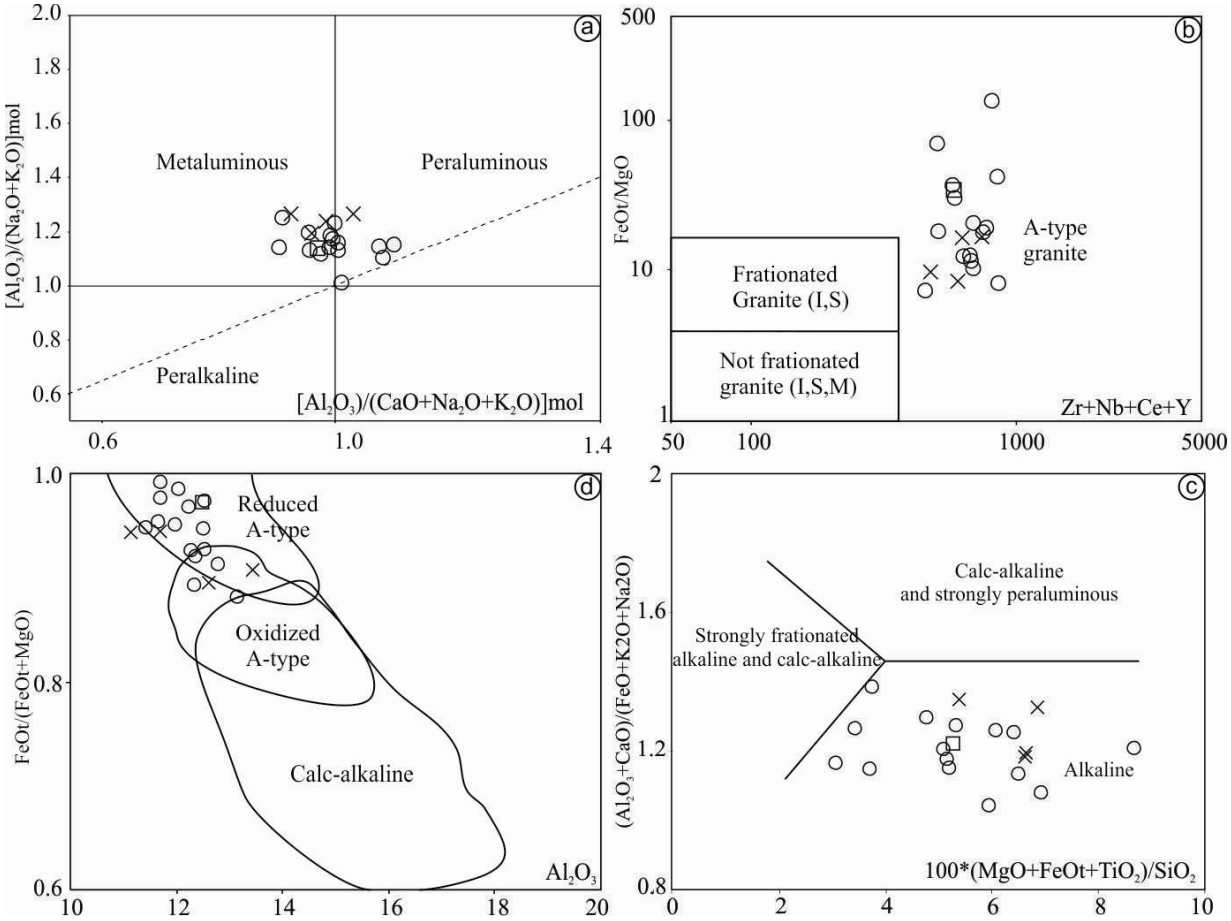

Figure 5 - Geochemical plot showing the distribution of the samples of the Planalto suites of the Canaã dos Carajás area. (a) $[Al_2O_3/(CaO + Na_2O + K_2O)]$mol vs. $[Al_2O_3/(K_2O + Na_2O)]$mol diagram (Shand, 1950); (b) Zr+Nb+Ce+Y vs. FeO/MgO diagram of Whalen et al. (1987); (c) Major element discrimination diagram for leucogranites (Sylvester, 1989); (d) FeOt/(FeOt+MgO) vs. $Al_2O_3/(K_2O/Na_2O)$ showing the compositional fields of calc-alkaline and A-type granites, and reduced and oxidized A-type granites (Dall'Agnol and Oliveira, 2007).

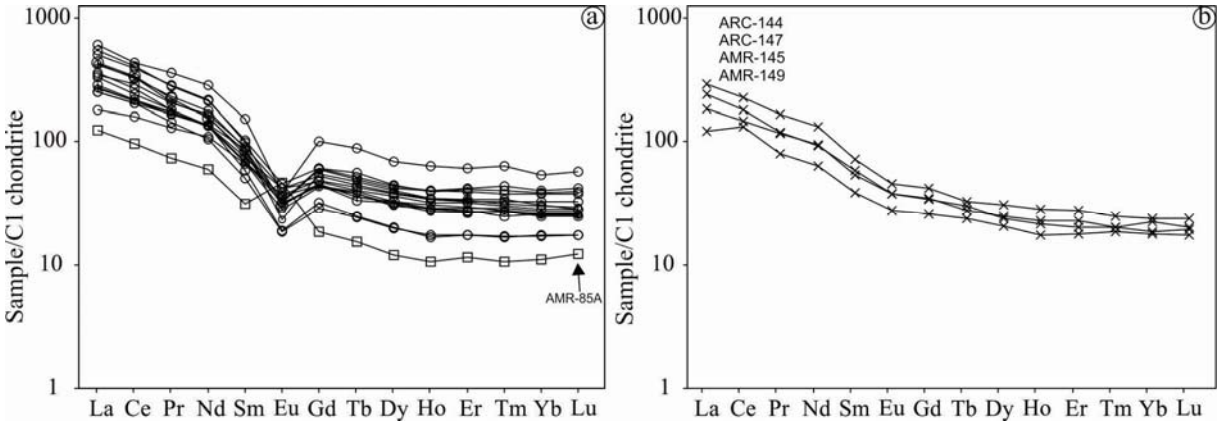

Figure 6 - REE patterns of the granites of the Planalto suite of the Canaã dos Carajás area: Values normalized to chondrite after Evensen et al. (1978).

5. Geochronology and Isotopic data

The location of the four dated samples is shown in Figure 1c and their geographical coordinates and the analytical results are given in the Table presented as supplementary data. The dated samples are representative of: (1) two plutons and of a small stock of the Planalto Suite; (2) a local occurrence of a charnockitic rock in the principal domain of the Pium complex. The four dated rocks and one additional sample of the Planalto granite were analyzed for Nd isotopes (Table 2).

5.1. Pb evaporation and U-Pb LA-MC-ICPMS Geochronology

5.1.1. Planalto Suite

Hornblende syenogranite (AMR-187B) - Zircon crystals are prismatic with slightly rounded edges, pale brown color, translucent to transparent, and intensely fractured. Under cathodoluminescence (CL), two populations of zircon crystals (Fig. 7a) were distinguished: (1) Low-CL dark crystals that correspond to the more brownish grains; (2) bright crystals showing marked oscillatory zoning and sometimes gray shade cores and low-CL darker rims that locally form convolute zones in the crystals.

For the Pb evaporation method, 18 crystals were analyzed and six (Fig. 8a) were used to calculate a $^{207}Pb/^{206}Pb$ mean age of 2733 ± 2 Ma with a MSWD = 0.92. Some analyses haven been discarded because they present high common Pb ($^{204}Pb/^{206}Pb>0.0004$) but most of them were rejected because they did not give a good fit with the assumed plateau age or have a limited number of analyses in the block (these criteria were employed in all samples analyzed for the Pb evaporation method).

The two distinct populations of zircon crystals and the core and outer zones were also analyzed by the U-Pb LA-MC-ICPMS method on zircon. The obtained results indicate similar ages for the different populations and zones. Thirty-four zircon grains were analyzed and, after treatment of the analytical results, ten spot analyzes yielded a discordant upper intercept age of 2713 ± 19 Ma (MSWD of 5.4; Fig. 9a) and five analyzes define a concordia age of 2729 ± 17 Ma (MSWD of 1.7; Fig. 9a).

Hornblende-biotite syenogranite (ARC-109) - This sample has elongated, euhedral, prismatic, translucent to transparent zircons with pale pink color, and sparse inclusions and fractures. Under cathodoluminescence, the zircon crystals (Fig. 7b) show most commonly irregular and apparently corroded dark gray cores surrounded by larger outer zones with well developed oscillatory zoning and local dark rims similar to those seen in AMR-187B. Eight

zircon crystals were analyzed and six (Fig. 8b) of them were used for calculate a $^{207}Pb/^{206}Pb$ mean age of 2731 ± 1 Ma (MSWD=2.0).

The U–Pb LA-MC-ICPMS method was also employed for this sample and the distinct cores and outer zones of the zircon crystals were analyzed (Fig. 9b). Fifteen selected analyzes provided a concordia age of 2710 ± 10 Ma (MSWD of 8.1). Taking in separate core and outer zones analyzes the obtained ages are, respectively, of 2716 ± 14 Ma (MSWD of 0.36) and 2703 ± 4 Ma (MSWD of 11.6), which are superposed within errors.

Biotite syenogranite (GRD-77) - the zircon crystals are colorless, transparent, prismatic and euhedral. CL images (Fig. 7c) show that the crystals are relatively more homogeneous than those of the other Planalto samples. They display strongly marked oscillatory zoning with local gray irregular cores and rare thin darker rims. Six zircon crystals were analyzed by the Pb evaporation method and yielded a $^{207}Pb/^{206}Pb$ mean age of 2736 ± 4 Ma with MSWD=3.0 (Fig. 8c). Twenty-seven zircon grains were also analyzed by the LA-MC-ICPMS method and the obtained results (Fig. 9c) indicate for ten selected zircons a discordia age of 2689 ± 23 Ma (MSWD of 5.1) and five analyzed grains defined a concordia age of 2706 ± 5 Ma (MSWD of 3.9).

The Pb-evaporation zircon ages obtained for the three samples of the Planalto granite are extremely similar (2733 ± 2 Ma, 2731 ± 1 Ma and 2736 ± 4 Ma). These ages are 10 to 20 Ma younger that those of other occurrences of the Planalto suite dated by the same method, as exemplified by the pluton of its type area (2747 ± 2 Ma, Huhn et al., 1999) and by stocks of the Transition zone in the southern part of the Carajás domain (2754 ± 2 Ma, Silva et al., 2010; 2748 ± 2 Ma and 2749 ± 3 Ma, Souza et al., 2010). Other granites similar to the Planalto suite, the Estrela complex, the Igarapé Gelado and the Serra do Rabo plutons, yielded, respectively, zircon ages of 2763 ± 7 Ma and 2731 ± 26 Ma (Pb-evaporation; Barros et al., 2009) and of 2743 ± 2 Ma (U-Pb TIMS age; Sardinha et al., 2006).

The ages obtained for the Planalto suite by the U-Pb LA-MC-ICPMS method show relatively larger variation. The samples AMR-187B, ARC-109 and GRD-77 gave, respectively, concordia ages of 2729 ± 17 Ma, 2710 ± 10 Ma and 2706 ± 5 Ma. The core and outer zones of zircon grains did not show significant age differences. The age of sample AMR-187B is superposed with those given by the Pb evaporation method, whereas those of the two other dated samples are 10 to 20 Ma younger. The whole results indicate that the Planalto suite granites were crystallized in the interval of 2730 to 2700 Ma. This time interval is a little lower than the ages available in the literature for similar granites of the Carajás province.

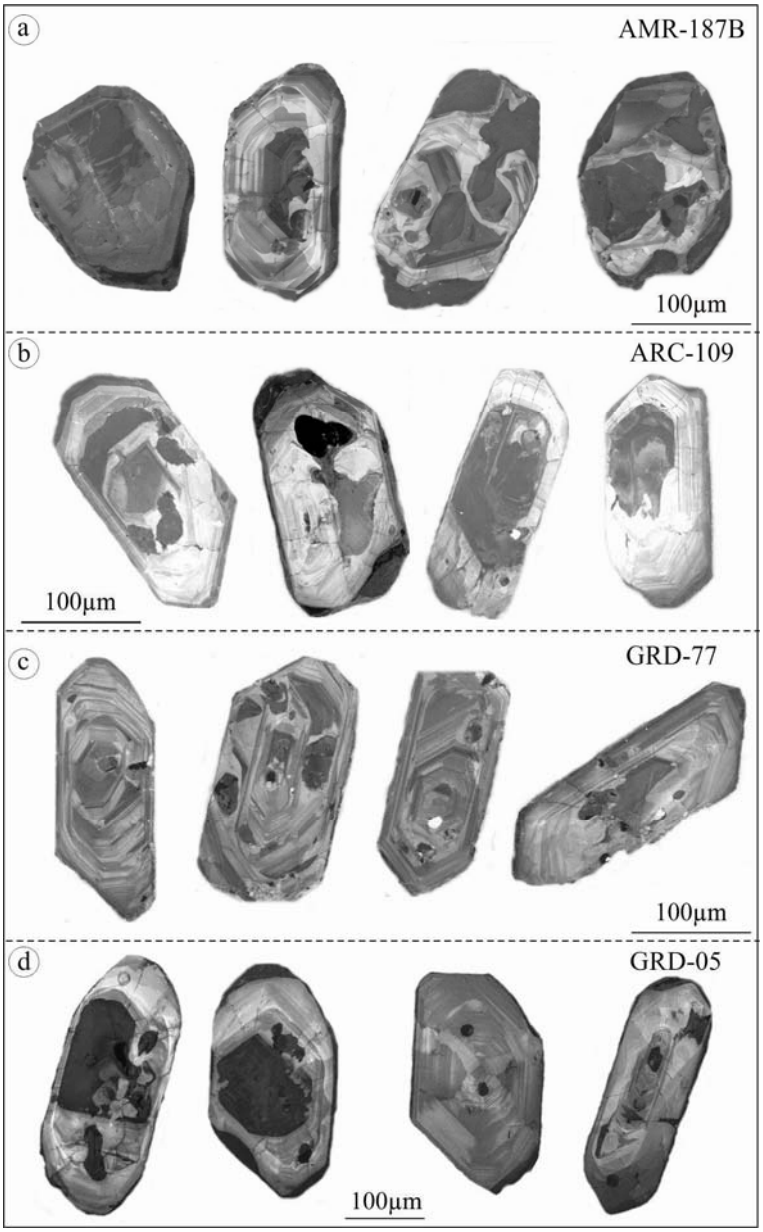

Figure 7 - Cathodoluminescence (CL) images of zircon crystals from samples (a) hornblende syenogranite (AMR-187B), (b) hornblende-biotite syenogranite (ARC-109), and (c) biotite syenogranite (GRD-77) of the Planalto suite; (d) orthopyroxene-quartz gabbro (GRD-05) of the charnockitic association.

5.1.2. Charnockitic rocks

The sample GRD-05 of the orthopyroxene-quartz gabbro was selected for U-Pb LA-MC-ICPMS dating. Zircon crystals display commonly prismatic shape with well defined but rounded edges, light pink color and transparent. Cathodoluminescence images reveal the presence of gray cores surrounded by lighter outer zones with irregular oscillatory or convolute zoning (Fig. 7d). 25 zircon grains were analyzed and whenever possible core and outer zones were analyzed in each crystal. The analyses done in 17 crystals were discarded

employing the criteria mentioned in Appendix B. In the ten analyzed crystals we have not been able to obtain core and outer zone analyzes in the same crystal. The whole data indicate a concordia age (Fig. 9d) of 2735 ± 5 Ma (MSWD=0.42). We have evaluated also independently analyzes of cores and outer zones, resulting, respectively, concordia ages of 2738 ± 6 Ma (MSWD=0.43) and 2731 ± 7 Ma (MSWD=3.9) which are superposed within errors.

These data indicate that there is no significant contrast on age between the gray cores and outer zones of the analyzed zircon crystals and we consider the age of 2735 ± 5 Ma as representative of the crystallization of the orthopyroxene-quartz gabbro. This age is entirely distinct of the ages assumed for the Pium complex (Pidgeon et al., 2000) and superposed within error with the age yielded by the zircon crystals of the Planalto granite.

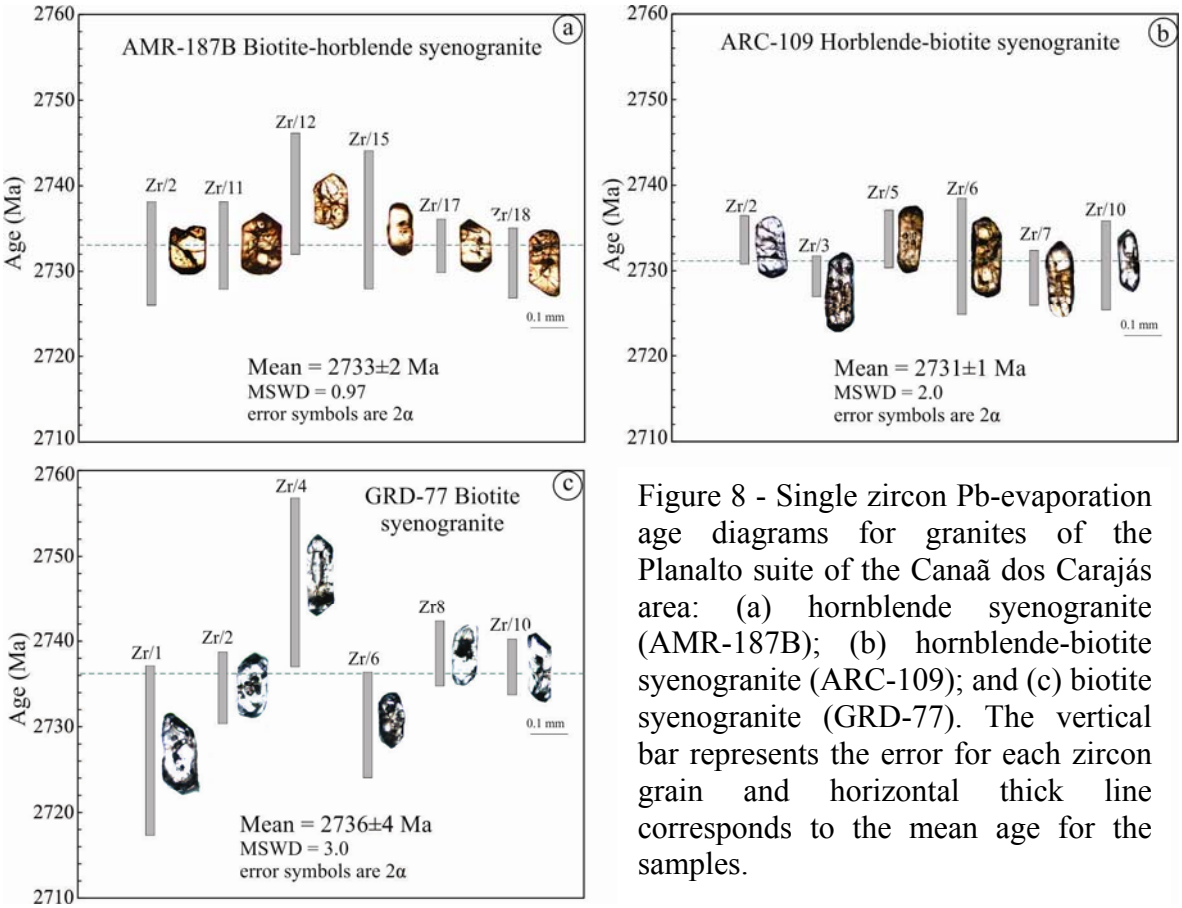

Figure 8 - Single zircon Pb-evaporation age diagrams for granites of the Planalto suite of the Canaã dos Carajás area: (a) hornblende syenogranite (AMR-187B); (b) hornblende-biotite syenogranite (ARC-109); and (c) biotite syenogranite (GRD-77). The vertical bar represents the error for each zircon grain and horizontal thick line corresponds to the mean age for the samples.

5.2. Nd isotopic data

The Nd isotope analyses of the Planalto granites gave εNd(t) values varying from -1.1 to -2.5 and corresponding T_{DM} ages from 2975 to 3084 Ma (Table 2). The GRD-05 sample of

the orthopyroxene-quartz gabbro yielded an εNd(t) value of -1.59 and a T_{DM} age of 3049 Ma (Table 2).

The whole Nd data are quite similar for the Planalto suite and charnockitic rock in terms of their εNd(t) values, all slightly negative, and T_{DM} ages concentrated around 3000 Ma. This suggests that the Planalto and the charnockitic rocks are not juvenile rocks and derived from older crustal protoliths separated from the mantle at ca. 3000 Ma. These new Nd isotope results are largely superposed with those available for the Estrela complex (Barros et al., 2009).

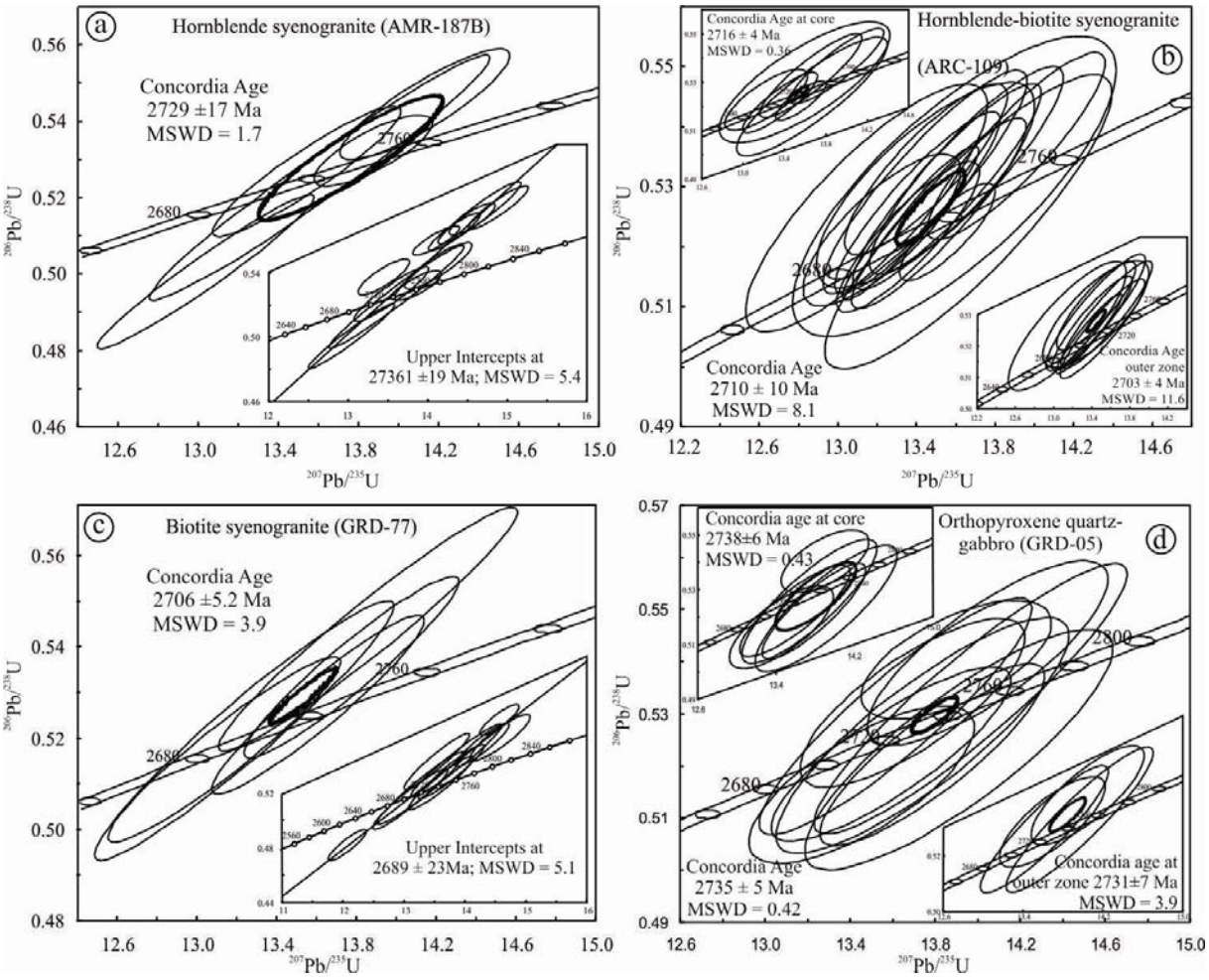

Figure 9 - LA-MC-ICPMS U–Pb concordia diagram for the samples of the Planalto suite [(a) AMR-187B; (b) ARC-109; (c) GRD-77] and orthopyroxene-quartz gabbro [(d) GRD-05].

Table 2 - Sm-Nd isotopic data for the Planalto suite and orthopyroxene-quartz gabbro of the Canaã dos Carajás area.

Sample	Sm (ppm)	Nd (ppm)	$^{147}Sm/^{144}Nd$	$^{143}Nd/^{144}Nd$ (±2σ)	$f_{(Sm/Nd)}$	$\varepsilon_{Nd(0)}$	$\varepsilon_{Nd(t)}$	$T_{DM}(Ma)$
2.71 Ga Planalto suite								
ARC-108	6.0	42.0	0.0867	0.510573 (9)	-0.5592	-40.3	-1.93	2996
ARC-109	11.4	63.0	0.1089	0.511013 (7)	-0.4464	-31.7	-1.08	2988
AMR-187B	17.1	100.5	0.1027	0.510901 (17)	-0.4779	-33.9	-1.10	2975
GRD-77	13.4	77.3	0.1048	0.510868 (23)	-0.4672	-34.5	-2.49	3084
2.73 Ga Orthopyroxene-quartz gabbro								
GRD-05	11.8	64.6	0.1102	0.510999 (7)	-0.4398	-32.0	-1.59	3049

6. Discussion

6.1. Origin of the Planalto suite and associated rocks

To test the hypotheses of origin and magmatic evolution of the Planalto granite and orthopyroxene-quartz gabbro we have made geochemical modeling for major and trace elements. The software Genesis 4.0 (Teixeira, 2005) was employed for modeling. Mineral-melt distribution coefficients applied for trace element modeling (Rollinson, 1993) are available over request to the authors. Rare earth elements were normalized according to Evensen (1978).

6.1.1. Planalto Suite

Geochemical modeling was focused on the biotite-hornblende monzogranite (HBMzG) and the hornblende-biotite syenogranite (HBSG). The available Nd isotope data on the subalkaline granites of the Estrela Complex (Barros et al., 2009) and those of the Planalto suite (this work; Table 2) are almost all negative and comprised between -0.42 and -2.49. Model ages calculated from the depleted-mantle evolution curve (De Paolo, 1981) vary from 2.97 to 3.19 Ga. These data suggest that the subalkaline granites of the Carajás domain were derived from a source separated from the mantle during the Mesoarchean and are not Neoarchean juvenile magmas (cf. Barros et al., 2009). The hypothesis of intense contamination of a juvenile magma by upper crustal components can be discarded in the case of the Planalto suite by the lack of geological evidence of interaction between the granite magmas and supracrustal country rocks.

The isotope data indicate that the Planalto magmas should be derived from the partial melting of older crustal rocks. Several models have been proposed to advocate a crustal

source for A-type or similar granites: (1) melting of metaluminous diorite-tonalite-granodiorite sources (Anderson and Bender, 1989; Patiño Douce, 1997; Dall'Agnol et al., 2005); (2) variable degrees of partial melting of a dry granulite residue depleted by prior extraction of granitic melt (Collins et al., 1982; Clemens et al., 1986; Whalen et al., 1987); (3) partial melting of a dehydrated non-depleted mafic to intermediate 'charnockitized' lower crust with very low water activities and fO_2 and at high temperatures (>900º C; Landerberger and Collins, 1996); (4) partial melting of undepleted tholeiitic basalts and their differentiated equivalents (Frost and Frost, 2011).

The Mesoarchean granite suites identified in the Canaã area (Gneissic granites, Canaã dos Carajás granite, and Serra Dourada granite) can be discarded as the possible magma sources, because they show similar silica contents and are too evolved geochemically compared to the Planalto suite to be compatible with its source. A similar reasoning can be applied to the older trondhjemites (~2.93 Ga) and to the younger sodic Pedra Branca suite. The remainder potential sources exposed in the Canaã area are the 2.87 Ga diorite-granodiorite expanded series and the Pium complex (Fig. 1c). The latter is intimately linked with the Planalto suite and this makes more plausible a genetic relationship between them.

To verify the possible sources, a first approach was to test if the partial melting of the diorite-granodiorite unit was able to generate liquid compositions similar to those of the Planalto suite. A diorite and a tonalite sample (59.18 and 62.89 wt. % of SiO2, respectively) were tested and both samples gave very bad fit for major elements. It was concluded that the derivation of the Planalto magmas by partial melting of the diorite-granodiorite unit is highly improbable.

To test the Pium complex rocks as a source for the Planalto magmas, we have devised several equilibrium batch melting models. The results of the modeling are presented in Table 3 and Figures 10 and 11. They demonstrate that the norite and associated quartz gabbro of the Pium Complex are both viable candidates for the source of the Planalto magmas. The melting of these rocks was able to generate liquids similar in composition to ARC-109 and AMR-152, respectively a hornblende-biotite syenogranite and a biotite-hornblende monzogranite of the Planalto suite. In the case of the norite sample, the degree of melting varies from 28 to 30% and for the quartz gabbro from 37 to 39%. The residual phases for the norite as a source were $plagioclase_{(An40)}$, clinopyroxene, orthopyroxene, magnetite, and ilmenite. The same residual phases, with the participation of a small amount of phlogopite in the residue were obtained for the quartz gabbro (Table 3).

The geochemical modeling suggests that the Planalto suite could be derived by partial melting of mafic to intermediate tholeitic orthopyroxene-bearing rocks similar to those of the Pium complex. This kind of source would more probably lead to reduced magmas (cf. Frost and Frost, 2011), which is consistent with the high FeOt/(FeOt+MgO) ratios of the Planalto Suite (> 0.88; Table 3).

The possible factors controlling the differentiation of the Planalto magmas were also evaluated by modeling. We have tested the evolution by fractional crystallization of the monzogranites to the syenogranites found in the same plutons. We have tested the samples AMR-209 (biotite-hornblende monzogranite) and AMR-208 (biotite syenogranite) of a pluton of the southeastern part of the area as initial and derived liquid, respectively. The models are consistent for major elements and less conclusive or inconsistent for trace elements. The same model was applied for the samples AMR-152 (biotite-hornblende monzogranite) and AMR-137 (biotite-hornblende syenogranite) of the type area of the Planalto granite and the results obtained were similar. The major element fractional crystallization model indicates that a low degree of fractionation would be necessary to generate the more evolved liquids.

This is consistent with the little difference in the degree of melting necessary to originate liquids of monzogranite and syenogranite composition from a more mafic protolith (Table 3). It is also noteworthy that the silica contents of monzogranites (70.39-74.86 wt. %) and syenogranites (71.66-75.51 wt. %) are largely superposed (Table 1). These evidences and the fact that there are no clear record of internal zoning in the plutons indicate that the monzogranites and syenogranites are more probably derived from small variations in the melting degree of the same sources and not by fractional crystallization. These sources were similar geochemically to the mafic and intermediate rocks of the Pium complex.

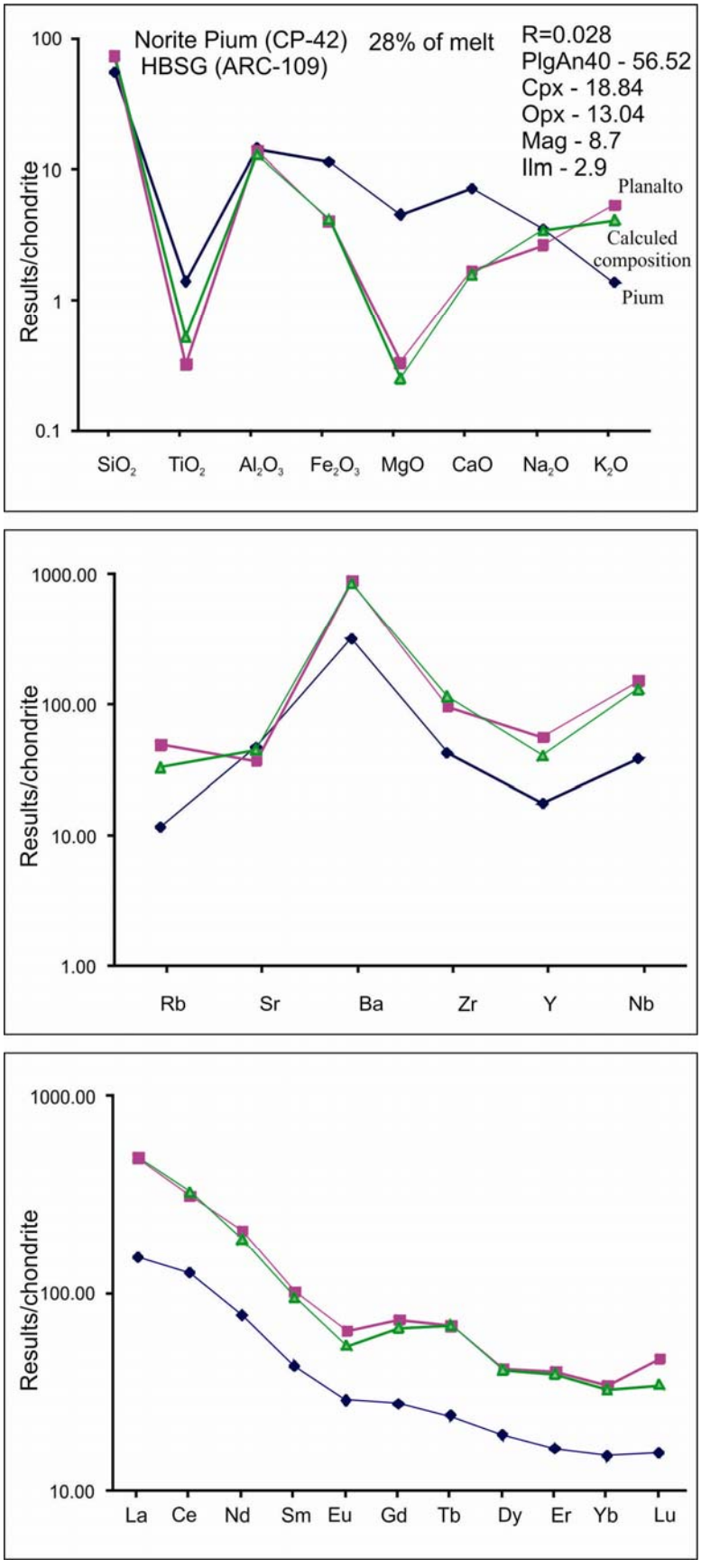

Figure 10 - Partial melting modeling of the Pium complex norite as a source of the Planalto granite magmas.

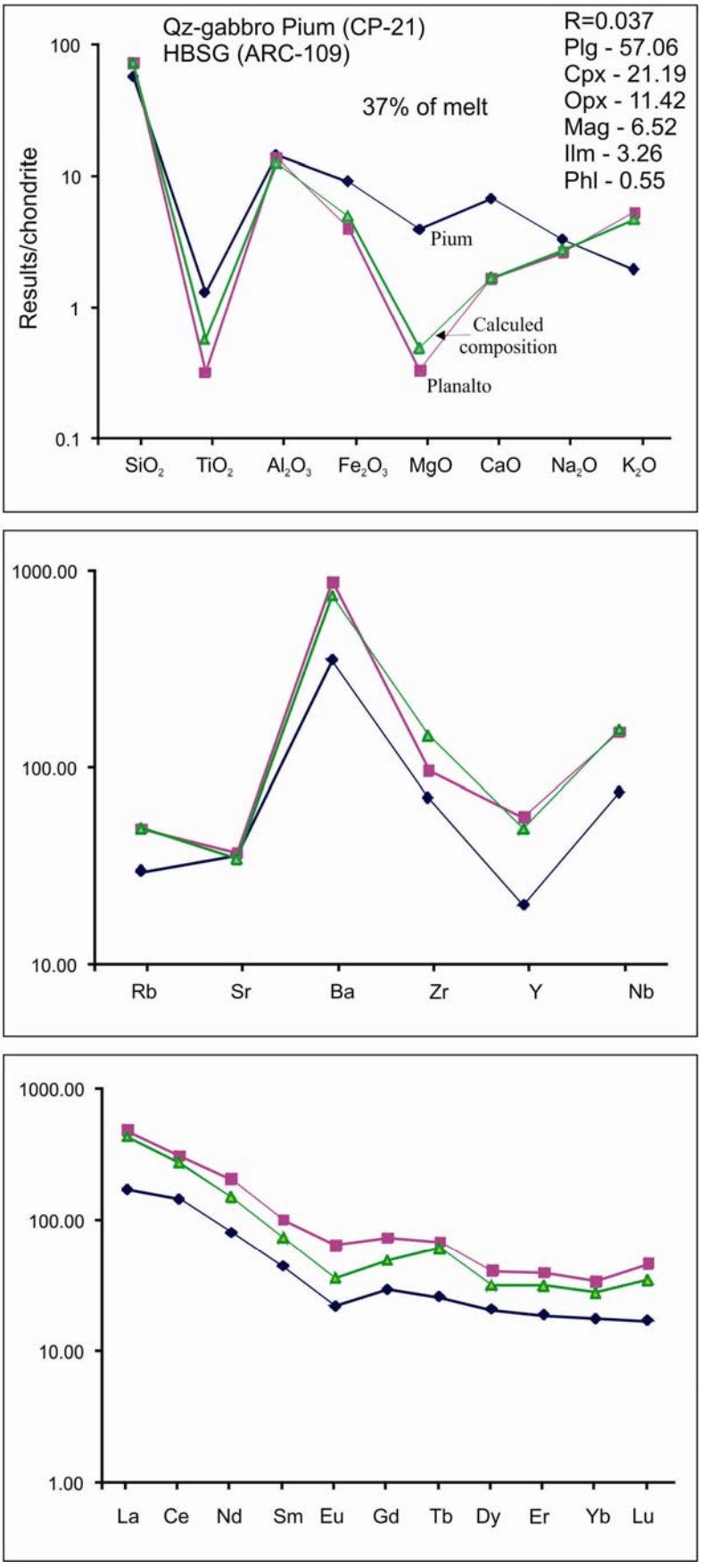

Figure 11 - Partial melting modeling of the Pium complex quartz gabbro as a source of the Planalto granite magmas.

Table 3 - Geochemical modeling data for the granitoids of the Canaã dos Carajás area.

	Original composition					(Co=CP-42)[1]		(Co=CP-21)[2]		(Co=CP-42)[3]
Samples	CP-42*	CP-21*	GRD-05	ARC-109	AMR-152	ARC109	AMR-152	ARC-109	AMR-152	GRD-05
Lithologies	Norite	Qtz gabbro	Qtz gabbro	HBSG	BHMzG	PM	PM	PM	PM	PM
SiO_2	54.96	57.65	57.19	72.51	70.39	73.15	70.99	72.22	71.5	57.66
TiO_2	1.38	1.3	1.85	0.32	0.64	0.52	0.67	0.57	0.69	1.87
Al2O3	14.39	14.4	13.04	13.81	12.32	12.86	12.51	12.57	12.61	13.12
Fe_2O_3	11.34	9.2	12.7	4.03	5.42	4.15	5.71	4.98	5.57	12.93
MgO	4.51	3.98	2.51	0.33	0.58	0.25	0.68	0.49	0.58	2.72
CaO	7.16	6.83	5.84	1.68	2.18	1.577	2.32	1.69	2.2	5.92
Na_2O	3.47	3.3	3.41	2.64	3.16	3.4	3.28	2.77	2.83	3.9
K_2O	1.36	1.96	2.36	5.31	3.93	4.1	3.84	4.71	4.01	1.89
Rb	26.9	69.1	52.2	114	97.1	77.21	65.19	115	88.43	36.7
Sr	340	263.3	239.5	269	203.9	328	331	252	242	334
Ba	772	845	1038	2119	1624.3	2040	1762	1812	1666	1017
Zr	164.8	270.8	293.6	374	594.5	446	380	564	493	221
Y	27.6	31.3	42.2	88.25	56.4	63.88	56.65	77.46	70.38	35.4
Nb	9.6	18.4	19.2	37.19	25.6	32.13	26.17	38.53	26.46	12.88
La	36.8	42.4	57.3	119	81.7	120	98.01	107	104	51.08
Ce	80.3	92.9	125.7	199	179.6	208	179	177	168	107
Nd	36.3	38.4	63.6	98.39	77.4	89.04	77.33	71.63	72.13	48.5
Sm	6.52	6.84	11.32	15.58	13.8	14.54	12.85	11.36	11.12	8.59
Eu	1.64	1.27	2.61	3.74	2.41	3.13	2.87	2.11	2.03	2.04
Gd	5.55	5.99	9.7	14.97	10.8	13.6	11.91	10.15	9.82	7.3
Tb	0.89	0.97	1.43	2.56	1.68	2.56	2.13	2.29	2.35	1.23
Dy	4.81	5.27	8.1	10.47	9.79	10.35	9.22	8.15	8.26	6.27
Er	2.69	3.11	4.26	6.62	5.59	6.45	5.68	5.27	5.13	3.49
Yb	2.45	2.9	3.96	5.62	5.24	5.36	4.78	4.64	4.58	3.13
Lu	0.39	0.43	0.58	1.18	0.71	0.87	0.77	0.89	0.87	0.5
Residue (%)										
Plagioclase An60						–	–	–	–	57.44
Plagioclase An40						56.52	56.07	57.06	60.71	–
Clinopyroxene						18.84	18.87	21.19	21.43	14.45
Orthopyroxene						13.04	12.87	11.42	8.93	23.07
Ilmenite						2.9	3.19	3.26	1.79	0.14
Magnetite						8.7	9.01	6.52	5.36	4.9
Phlogopite						–	–	0.55	1.79	–
r2						0.028	0.001	0.034	0.025	0.234
Degree of melting						28	30	37	39	72

1 - Partial melting (PM) - norite of Pium Complex to Planalto suite

2 - Partial melting - quartz gabbro of Pium Complex to Planalto suite

3- Partial melting- norite to quartz gabbro of charnockitic association;

* Chemical composition from Santos (2010)

Co- Composition of the source

HBSG-Hornblende-biotite syenogranite; BHMzG - Biotite-hornblende monzogranite; Qtz -Quartz

6.1.2. Charnockitic rocks

The relationships between the Pium norite (CP-42; Santos, 2009) and the Neoarchean quartz gabbros were also verified by modeling. The orthopyroxene-bearing quartz gabbro (GRD-05) of the charnockitic association could possibly result of the partial melting of the norite, leaving as residual phases the same minerals observed in the case of the Planalto granites. However, in the residue the plagioclase is labradorite, orthopyroxene is more abundant than clinopyroxene and the required degree of melting attained 72% (Table 3). It is concluded that the quartz gabbros have chemical compositions compatible with their derivation from the Pium norite by partial melting processes, but this would require a high degree of melting implying a quite high temperature.

6.2. Planalto Suite: A-type or hydrated charnockite rocks?

The Planalto suite and similar granites of the Carajás province have geochemical affinities with alkaline Archean granites and reduced-A-type granites and have ferroan character. However, all these rocks are foliated, deformed, and interpreted as synkinematic granites, in the sense that they were strongly deformed during their emplacement (Barros et al., 2009). In this respect, they differ from classical A-type granites that are essentially related to extensional settings and generally little deformed.

On the other hand, the Planalto suite is associated closely with 'granulitic' and charnockitic rocks, and a granulitic source was admitted for the Estrela complex, Serra do Rabo and Igarapé Gelado plutons (Barros et al., 2009). Frost and Frost (2008, their Fig. 11) advocate that biotite-hornblende granites associated with charnockitic rocks could be produced by residual melts of the charnockite magma evolution. These residual melts will be hydrated, enriched in fluids and granitic in composition and will be formed at lower crustal levels compared to the associated charnockitic rocks which could represent, at least in part, dry cumulates of the original magma. Mafic underplate, probably in an extensional tectonic setting, would be responsible for the melting of the crust and release of CO_2 and H_2O for higher levels. The general characteristics described in this particular geological setting are also shown by the Planalto and similar suites of the Carajás province with the difference that these are synkinematic granites possibly related to collision better than formed in an extensional setting (Barros et al., 2009).

Frost and Frost (2008) argue that the hydrated biotite-hornblende granitoids associated with charnockites can be ferroan or magnesian in character and related, respectively, to mafic

underplate in extensional settings or to arc-related sources. It was also proposed that the term A-type granite should be replaced by ferroan granites (Frost and Frost, 2011). Accepting this broad definition, the Planalto suite and similar granites of the Carajás province could be classified as A-type on the basis of their major and trace element signature including ferroan character (high HFSE and FeO/(FeO+MgO), low Al_2O_3 and CaO; Figs. 4 and 5). However, the structural features of the studied granites and their close association with charnockitic rocks are intriguing and denote a tectonic setting distinct to that generally admitted for A-type granites. This aspect and the large geochemical variation observed in the granitoids associated with charnockitic series could be seen as a restriction for the classification of their ferroan varieties as A-type granites. An alternative would be to classify these biotite-hornblende granites of the Planalto suite as hydrated granites of the charnockitic rocks series, independent of their FeO/(FeO+MgO) ratios.

It is concluded that it is relevant to make further studies on hydrated biotite-hornblende A-type like granites associated with charnockitic rock series to attain a better understanding of their geochemistry, origin and classification. These granites occur in several cratons and are common in the Late Archean (Sheraton and Black, 1988; Moore et al., 1993; Misra et al., 2002; Larin et al., 2006). By the moment, we prefer to classify the studied granites of the Planalto suite as hydrated granites associated with charnockitic series. However, if a largest and open definition of A-type or ferroan granites is adopted, they could also be classified as such. The only restriction to the classification of them as A-type granites is that it would imply to admit the formation of this kind of granite in synkinematic settings.

6.3. Tectonic significance of the Planalto Suite and similar granites

It is commonly accepted that A-type granite formed in a crustal extensional environment and occurred in both post-orogenic and/or anorogenic settings (Collins et al., 1982; Whalen et al., 1987; Sylvester, 1989; Bonin, 2007; Dall'Agnol et al., 2005). However, in the Carajás province, it was recognized the occurrence of syntectonic or synkinematic Archean A-type granites contemporaneous to compressional stages (Barros et al., 2009; Domingos, 2009). The emplacement model proposed for the Estrela complex, situated in the Carajás basin, involved recurrent injection of batches of magmas with the filling of the magma chamber promoting lateral expansion and flattening of the peripheral earlier pulses and adjacent country rocks (Barros et al., 2009). In the Canaã dos Carajás area of the 'Transition domain', it was admitted that a regional phase of sinistral transpression was accompanied by magmatism forming the E-W elongated, foliated A-type granites of the

Planalto suite. Transpression produced a penetrative ductile fabric and most of the strain was accommodated in shear zones (Domingos, 2009). Araújo and Maia (1991) stated that the Pium complex and the granites now included in the Planalto suite correspond to deep crustal rocks transported along shear zones to comparatively shallower crustal levels.

Accepting that the Carajás basin was formed at ca. 2.76 Ga (age admitted for the metavolcanic rocks of the Itacaiúnas supergroup filling the basin; Gibbs et al., 1986; Machado et al., 1991) and was related to a rift that evolved in a continental tectonic setting, regarding the ages admitted for the Estrela complex (2763 ± 7 Ma; Barros et al., 2009) and those available in the literature for the Planalto suite (2747 ± 2 Ma, Huhn et al., 1999; 2754 ± 2 Ma, Silva et al., 2010; 2748 ± 2 Ma, 2749 ± 3 Ma, Souza et al., 2010), there is a problem to accommodate the extensional setting necessary for the development of the basin and the compressional setting implied in the syntectonic emplacement of the Estrela complex, Planalto suite and similar granites. The mentioned ages for the formation and filling of the basin are too close to the ages admitted for the granites that evolved in a compressional setting. If correct, this would imply that the opening and inversion of the Carajás basin would be almost coincident in time. However, the age interval of 2730 to 2700 Ma obtained in this work for the crystallization and emplacement of the Planalto granite is significantly younger and more suitable for the inversion from an extensional to a compressional setting. Therefore, we can speculate that the Planalto suite magmas were formed by the partial melting of mafic lower crustal rocks during the tectonic inversion of the Carajás basin. The resulting magmas should have initiated their crystallization at relatively deep crustal levels and were more probably largely crystallized during their emplacement in the upper crust. Their emplacement was done under an active regional shear and associated with the major shear zones found in the Canaã dos Carajás area (Araújo and Maia, 1991; Domingos, 2009). These features explain the major structural features observed in the Planalto granite including its penetrative foliation and local stretching lineation.

On the other hand, the close association between the Planalto suite and the Pium complex and charnockitic rocks suggest a possible similarity between its evolution and that of the high temperature granite magmatism of the Mesoproterozoic Musgrave province of Central Australia (Smithies et al., 2010). In that province, there are widespread metaluminous and ferroan rocks ranging from alkali-calcic to calc-alkalic, with affinities with A-type granites, and including an orthopyroxene-bearing (charnockitic) primary mineralogy. Their evolution was attributed by Smithies et al. (2010) to MASH (melting, assimilation, storage, and homogenization) processes. The same model cannot be easily adapted for the Carajás

region but both provinces have in common the formation of charnockites and associated granites triggered by the underplating of mafic magmas in the base of the crust. Another aspect in common between both provinces, and also registered in the Limpopo belt (Rapopo, 2010), is the generation of this kind of rock association near the limits between distinct tectonic blocks or in their zone of interaction (Smithies et al., 2010).

7. Conclusions

1. The new LA-MC-ICPMS and Pb-evaporation geochronological data on zircon obtained indicate that: (a) The orthopyroxene-quartz gabbro associated with the Pium complex and Planalto suite has an age of 2735 ± 5 Ma (average concordia age with little age variation in the zircon cores and outer zones of, respectively, 2738 ± 6 Ma and 2731 ± 7 Ma), assumed as its crystallization age. (b) The Pb-evaporation ages given by three samples of the Planalto suite are concentrated around 2733 Ma (2733 ± 2 Ma, 2731 ± 1 Ma and 2736 ± 4 Ma). The U-Pb LA-MC-ICPMS concordia ages obtained for the same samples are of 2729 ± 17 Ma, 2710 ± 10 Ma, and 2706 ± 5 Ma. The first age is superposed with those given by the Pb evaporation method, whereas the two other dated samples are 10 to 20 Ma younger. The whole results indicate that the Planalto suite granites were crystallized in the time interval of 2730 to 2700 Ma, implying a little lower age than those available in the literature for similar granites of the Carajás province.

2. The Planalto suite granites have ferroan character and are similar geochemically to reduced A-type granites. Plagioclase was retained in the melting residue of the magma and garnet and hornblende where not important fractionating phases during the magma evolution. In previous works, these Archean granites and similar rocks of the Carajás province have been classified as A-type granites. However, the structural features of these units denote a syntectonic setting distinct to that generally admitted for A-type granites. This aspect and the large geochemical variation observed in the granitoids associated with charnockitic series was seen as a restriction for the classification of these ferroan granites as A-type granites. We propose, alternatively, to classify the granites of the Planalto suite as hydrated granites of the charnockitic series. The need for further studies on hydrated biotite-hornblende A-type like granites associated with the charnockitic series to attain a better understanding of their geochemistry, origin and classification was emphasized.

3. The Planalto suite was derived by partial melting of mafic to intermediate tholeitic orthopyroxene-bearing rocks similar to those of the Pium complex. The dominant

monzogranite and syenogranite varieties were derived from small variations in the melting degree of the same sources rather than by fractional crystallization.

4. The orthopyroxene-quartz gabbros have chemical compositions compatible with their derivation from the Pium norite by partial melting, but this would require a high degree of melting implying a quite high temperature for the magma generation.

5. At 2.76 Ga, the upwelling of the asthenospheric mantle in an extensional setting propitiated the formation of the Carajás basin. Later on, at ca. 2.73-2.70 Ga, the heat input associated with underplate of mafic magma would make possible the partial melting of mafic to intermediate lower crustal rocks originating the Planalto and orthopyroxene-quartz gabbro magmas. These magmas should have initiated their crystallization at relatively deep crustal levels and were largely crystallized during their emplacement in the upper crust. Their emplacement was done under an active regional stress and associated with the major shear zones found in the Canaã dos Carajás area. It was probably coincident with the tectonic inversion of the Carajás basin. Moreover, the close association between the Planalto suite and charnockitic rocks suggests similarity between its evolution and that of the high temperature granite magmatism commonly found near the limits between distinct tectonic blocks or in their zone of interaction.

Acknowledgements

F.J. Althoff, C.E.M Barros, A.A.S. Leite, D.C. Oliveira, M.A. Oliveira are acknowledged for support in geological mapping work and J.E.B. Soares for previous work in the studied area. The authors thank to: R.D. Santos and D.C. Oliveira for unpublished geochemical data of the Pium complex; M.A. Galarza Toro for his assistance for obtainment of the single zircon Pb-evaporation analyses; and M. Matteini, B. Lima, and J.A.C. Almeida for their assistance on LA-MC-ICPMS analyses; O.T. Rämö for discussions about geochronological data and petrogenesis. C.N. Lamarão and I.M.O. Ramalho are also thanked for their assistance in the cathodoluminescence imaging. This research received financial support from CNPq (R. Dall'Agnol – Grants 0550739/2001-7, 476075/2003-3, 307469/2003-4, 484524/2007-0; PRONEX – Proc. 66.2103/1998-0; G.R.L Feio – CNPq scholarship), and Federal University of Pará (UFPA). This paper is a contribution to the Brazilian Institute of Amazonia Geosciences (INCT program –CNPq/MCT/FAPESPA – Proc. 573733/2008-2).

Appendix -

A- Analytical procedures for whole-rock chemical analyses **-** The chemical analyses for major elements and for trace-elements, including the REE, were performed by ICP-ES and ICP-MS, respectively, at the Acme Analytical Laboratories Ltd. in Canada.

Sm–Nd isotopic analyses followed the method described by Gioia and Pimentel (2000). They were performed at the Geochronology Laboratory of the University of Brasília. Whole rock powders (ca. 50 mg) were mixed with ^{149}Sm–^{150}Nd spike solution and dissolved in Savillex capsules. Sm and Nd extraction of whole rock samples followed conventional cation exchange techniques, using teflon columns containing LN-Spec resin (HDEHP–diethylhexyl phosphoric acid supported on PTFE powder). Sm and Nd samples were loaded on Re evaporation filaments of double filament assemblies and the isotopic measurements were carried out on a multi-collector Finnigan MAT 262 mass spectrometer in static mode. Uncertainties for Sm/Nd and $^{143}Nd/^{144}Nd$ ratios are better than ± 0.5% (2σ) and ± 0.005% (2σ), respectively, based on repeated analyses of international rock standards BHVO-1 and BCR-1. The $^{143}Nd/^{144}Nd$ ratios were normalized to $^{146}Nd/^{144}Nd$ of 0.7219 and the decay constant used was 6.54×10^{-12} to $^{-1}$. The T_{DM} values were calculated using the model of DePaolo (1981).

B- Analytical methods of Geochronology - Samples ARC-109, GRD-77, and AMR-187B (Planalto suite) and GRD-05 (orthopyroxene-quartz gabbro) were selected for geochronological studies. All samples of the Planalto suite were analyzed by the Pb-Pb method and also by LA-MC-ICPMS. GRD-05 was analyzed only by LA-MC-ICPMS. Zircon concentrates were extracted from ca. 10 kg rock samples using conventional gravimetric methods of heavy mineral separation and magnetic (Frantz isodynamic separator) techniques at the Geochronology Laboratory of the University of Pará (Pará-Iso). Final purification was achieved by hand selecting through a binocular microscope and the zircon grains of each sample were then photographed under reflected light. For U-Pb LA-MC-ICPMS analyses, the zircons grains of each sample were mounted in epoxy resin, polished, and. their internal structures were examined by cathodoluminescence (CL) imaging technique in a scanning electron microscope LEO 1430 at the Scanning Electron Microscopy Laboratory of the Geosciences Institute of Federal University of Pará (UFPA).

For the Pb-evaporation method (Kober, 1987), individual selected zircon grains were encapsulated in the Re-filament used for evaporation, which was placed directly in front of the ionization filament. The Pb is extracted by heating in three evaporation steps at

temperatures of 1450º, 1500º, and 1550 °C and loaded on an ionization filament. The Pb intensities were measured by each peak stepping through the 206–207–208–206–207–204 mass sequence for five mass scans, defining one data block with eight $^{207}Pb/^{206}Pb$ ratios. The weighted $^{207}Pb/^{206}Pb$ mean for each block is corrected for common Pb using appropriate age values derived from the two-stage model of Stacey and Kramers (1975), and results with $^{204}Pb/^{206}Pb$ ratios higher than 0.0004 and those that scatter more than two standard deviations from the average age value were discarded. The calculated age for a single zircon grain and its error, according to Gaudette et al. (1998), is the weighted mean and standard error of the accepted blocks of data. The ages are presented with 2σ error.

The U–Pb LA-MC-ICPMS analyses were carried out using a New Wave UP213 Nd:YAG laser (λ - 213 nm), linked to a Thermo Finnigan Neptune multi-collector ICPMS at the Geochronology Laboratory of the University of Brasília. The analytical procedures were described by Buhn et al. (2009). The laser was run at a frequency of 10 Hz and energy of 0.4 mJ/pulse, ablation time of 40 s and a spot size of 30 μm in diameter. Plotting of U–Pb data was performed by ISOPLOT (Ludwig, 2001) and errors for isotopic ratios are presented at the 1σ level.

The analyses have been carried out using raster ablation method (Bühn et al., 2009) to prevent laser induced mass bias fractionation. The U-Pb raw data are translated to an Excel spreadsheet for data reduction and, when necessary, the laser induced mass bias was corrected using the method of Kosler et al. (2002). Common lead (^{204}Pb) interference and background correction, when necessary were carried out by monitoring the ^{202}Hg and 204 mass ($^{204}Hg+^{204}Pb$) during the analytical sessions and using a model Pb composition (Stacey and Kramers, 1975) when necessary. Reported errors are propagated by quadratic addition $[(2SD^2+2SE^2)^{1/2}]$ of external reproducibility and within-run precision. The external reproducibility is represented by the standard deviation (SD) obtained by repeated analyses (n=20, ~ 0.8% for $^{207}Pb/^{206}Pb$ and ~ 1% for $^{206}Pb/^{238}U$) of standard zircon GJ-1, performed during analytical session, and the within-run precision is represented by the standard error (SE) that was calculated for each analysis.

For the exclusion of spot analyzes on the calculation of U-Pb ages we have employed the general criteria adopted in the literature: (1) the common lead content (the $^{206}Pb/^{204}Pb$ ratio should not be lower than 1000); (2) the degree of discordance (not using data where the discordance is higher than 10%); (3) the analytical precision (not using the data where the isotopic ratios have error greater than 3%). These general criteria were refined for each specific sample.

References

Almeida, J.A.C., Dall'Agnol, R., Dias, S.B., Althoff, F.J., 2010. Origin of the Archean leucogranodiorite–granite suites: Evidence from the Rio Maria terrane and implications for granite magmatism in the Archean. Lithos 120, 235-257.

Almeida, J.A.C., Dall'Agnol, R., Oliveira, M.A., Macambira, M.J.B., Pimentel, M.M., Rämö, O.T., Guimarães, F.V., Leite, A.A.S., submitted. Zircon geochronology and geochemistry of the TTG suites of the Rio Maria granite-greenstone terrane: Implications for the growth of the Archean crust of Carajás Province, Brazil. Precambrian Research.

Althoff, F.J., Barbey, P., Boullier, A.M., 2000. 2.8–3.0 Ga plutonism and deformation in the SE Amazonian craton: the Archean granitoids of Marajoara (Carajás Mineral province, Brazil). Precambrian Research 104, 187–206.

Anderson, J.L., Bender, B., 1989. Nature and origin of Proterozoic A-type granitic magmatism in the southwestern United States of America. Lithos 23, 19-52

Araújo, O.J.B.; Maia, R.G.N., 1991. Programa de levantamentos geológicos básicos do Brasil, Serra dos Carajás, folha SB-22-Z-A, Estado do Pará. Texto explicativo, Brasília, DNPM/CPRM. 164p (in Portuguese).

Barros, C.E.M., Sardinha, A.S., Barbosa, J.P.O., Macambira M.J.B., 2009. Structure, Petrology, Geochemistry and zircon U/Pb and Pb/Pb geochronology of the synkinematic Archean (2.7 Ga) A-type granites from the Carajás Metallogenic Province, northern Brazil, Canadian Mineralogist 47, 1423-1440.

Bonin, B., 2007. A-type granites and related rocks: Evolution of a concept, problems and prospects. Lithos 97, 1–29.

Buhn, B., Pimentel, M.M., Matteini, M., Dantas, E.L., 2009. High spatial resolution analysis of Pb and U isotopes for geochronology by laser ablation multi-collector inductively coupled plasma mass spectrometry (LA-MC-ICP-MS). Anais Academia Brasileira de Ciências 81, 1–16.

Champion, D.C., Sheraton, J.W., 1997. Geochemistry and Nd isotope systematics of Archean granites of the Eastern Goldfields, Yilgarn Craton, Australia: implications for crustal growth processes. Precambrian Research 83, 109-132.

Clemens, J.D., Holloway, J.R., White, A.J.R., 1986. Origin of the A-type granite: experimental constraints. American Mineralogist 71, 317–324.

Collins, W.J., Beams, S.D., White, A.J.R., Chappell, B.W., 1982. Nature and origin of A-type granites with particular reference to southeastern Australia. Contributions to Mineralogy and Petrology 80, 189–200.

Costa, J.B.S., Araújo, O.J.B., Santos, A., Jorge João, X.S., Macambira, M.J.B., Lafon, J.M., 1995. A Província Mineral de Carajás: aspectos tectono-estruturais, estratigráficos e geocronológicos. Boletim do Museu Paraense Emílio Goeldi 7, 199-235 (in Portuguese).

Dall'Agnol, R., Oliveira, D.C., 2007. Oxidized, magnetite-series, rapakivi-type granites of Carajás, Brazil: Implications for classification and petrogenesis of A-type granites. Lithos 93, 215–233.

Dall'Agnol, R., Oliveira, M.A., Almeida, J.A.C., Althoff, F.J., Leite, A.A.S., Oliveira, D.C., Barros, C.E.M., 2006. Archean and Paleoproterozoic granitoids of the Carajás Metallogenic Province, eastern Amazonian Craton. In: Dall'Agnol, R., Rosa-Costa, L.T. and Klein, E.L. (Eds.) Symposium on magmatism, crustal evolution, and metallogenesis of the Amazonian Craton. Abstracts Volume and Field Trip Guide. Belém, PRONEX-UFPA-SBGNO, 99-150.

Dall'Agnol, R., Teixeira, N.P., Rämö, O.T., Moura, C.A.V., Macambira, M.J.B., Oliveira, D.C., 2005. Petrogenesis of the Paleoproterozoic, rapakivi, A-type granites of the Archean Carajás Metallogenic Province, Brazil. Lithos 80, 01-129.

De Paolo, D.J., 1981. Neodymium isotope in the Colorado Front Range and crust–mantle evolution in the Proterozoic. Nature 291, 193– 196.

Domingos, F.H., 2009. The structural setting of the Canaã dos Carajás region and Sossego-Sequeirinho deposits, Carajás – Brazil. University of Durham, England, 483p. (Ph.D. Thesis)

Eby, G.N., 1992. Chemical subdivision of the A-type granitoids: petrogenetic and tectonic implications. Geology 20, 641–644.

Emslie, R.F., 1991. Granitoids of rapakivi granite-anorthosite and related associations. Precambrian Research 51, 173-192.

Evensen, N.M., Hamilton, P.T., O'Nions, R.K., 1978. Rare earth abondances in chondritic meteorites. Geochimica et Cosmochimica Acta 39, 55-64.

Frost, B.R., Barnes, C., Collins, W., Arculus, R., Ellis, D., Frost, C., 2001. A chemical classification for granitic rocks. Journal of Petrology 42, 2033–2048.

Frost, C.D., Frost, B.R., 2008. On charnockites. Gondwana Research 13, 30–44.

Frost, C.D., Frost, B.R., 2011. On ferroan (A-type) granitoids: their compositional variability and modes of origin. Journal of Petrology 32, 39-53.

Gabriel, E.O., Oliveira, D.C., Macambira, M.J.B., 2010. Caracterização geológica, petrográfica e geocronológica de ortopiroxênio-trondhjemitos (leucoenderbitos) da região de Vila Cedere III, Canaã dos Carajás-PA, Província Mineral de Carajás. In: SBG, Congresso Brasileiro de Geologia, 45, CDrom (in Portuguese).

Gaudette, H.E., Lafon, J.M., Macambira, M.J.B., Moura, C.A.V., Scheller, T., 1998. Comparison of single filament Pb evaporation/ionization zircon ages with conventional U-/Pb results: examples from the Precambrian of Brazil. Journal of South American Earth Sciences 11, 351-363.

Gibbs, A.K., Wirth, K.R., Hirata, W.K., Olszewski Jr., W.J., 1986. Age and composition of the Grão Pará Group volcanics, Serra dos Carajás. Revista Brasileira de Geociências 16, 201–211.

Gioia, S.M.C.L., Pimentel, M.M., 2000. The Sm-Nd Isotopic Method in the Geochronology Laboratory of the University of Brasília. Anais da Academia Brasileira de Ciências 72, 219-246.

Gomes, A.C.B., Dall'Agnol, R., 2007. Nova associação tonalítica-trondhjemítica Neoarqueana na região de Canaã dos Carajás: TTG com altos conteúdos de Ti, Zr e Y. Revista Brasileira de Geociências 37, 182-193 (in Portuguese).

Huhn, S.B., Macambira, M.J.B., Dall'Agnol, R., 1999. Geologia e geocronologia Pb/Pb do granito alcalino arqueano Planalto, região da Serra do Rabo, Carajás-PA. In: Simpósio de Geologia da Amazônia, 6, 463-466 (in Portuguese).

Kober, B., 1987. Single-grain evaporation combined with Pb+ emitter bedding for $^{207}Pb/^{206}Pb$ age investigations using thermal ion mass spectrometry, and implications to zirconology. Contributions to Mineralogy and Petrology 96, 63-71.

Kosler, J., Fonneland, H., Sylvester, P., Tubrett, M. & Pedersen, R.B., 2002. U-Pb dating of detrital zircons for sediment provenance studies - a comparison of laser ablation ICPMS and SIMS techniques. Chemical Geology 182, 605-618.

Kretz, R., 1983. Symbols for rock-forming minerals. American Mineralogist 68, 277-279.

Landerberger, B., Collins, W.J., 1996. Derivation of A-type granites from a dehydrated charnockitic lower crust: evidence from the Chaelundi complex, eastern Australia. Journal of Petrology 37, 145-170.

Larin, A.M., Kotov, A.B., Sal'nikova, E.B., Glebovitskii, V.A., Sukhanov, M.K. Yakovleva, S.Z. Kovach, V.P., Berezhnaya, N.G. Velikoslavinskii, S.D., Tolkachev, M.D., 2006. The Kalar Compex, Aldan–Stanovoi Shield, an Ancient Anorthosite–Mangerite–Charnockite–Granite Association: Geochronologic, Geochemical, and Isotopic–Geochemical Characteristics. Petrology 14, 2–20.

Lauri, L.S., Rämö, O.T., Huhmab, H., Mänttärib, I., Räsänenc, J., 2006. Petrogenesis of silicic magmatism related to the ~ 2.44 Ga rifting of Archean crust in Koillismaa, eastern Finland. Lithos 86, 137-166.

Leite, A.A.S., Dall'Agnol, R., Macambira, M.J.B., Althoff, F.J., 2004. Geologia e Geocronologia dos granitóides Arqueanos da região de Xinguara (PA) e suas implicações na evolução do Terreno Granito-Greenstone de Rio Maria. Revista Brasileira de Geociências 34, 447-458 (in Portuguese).

Lobato, L.M., Rosière, C.A., Silva, R.C.F., Zucchetti, M., Baars, F.J., Sedane, J.C.S., Javier Rios, F., Pimentel, M., Mendes, G.E., Monteiro, A.M., 2006. A mineralização hidrotermal de ferro da Província Mineral de Carajás – controle estrutural e contexto na evolução metalogenética da província. In: Marini, O.J., Queiroz, E.T., Ramos, B.W. (Eds.) Caracterização de Depósitos Minerais em Distritos Mineiros da Amazônia, DNPM, CT-Mineral / FINEP, ADIMB, pp. 25-92 (in Portuguese).

Loiselle, M.C., Wones, D.R., 1979. Characteristics and origin of anorogenic granites. Geological Society of America, Abstracts 11, 468.

Ludwig, K.R., 2001. User's manual for Isoplot/Ex Version 2.49 A geochronological toolkit for Microsoft Excel. Berkeley Geochronological Center Special Publication 1, 1-55.

Macambira, M.J.B. 1992. Chronologie U/Pb, Rb/Sr, K/Ar et croissance de la croûte continentale dans L'Amazonie du sud-est; exemple de la région de Rio Maria, Province de Carajas, Brésil. Université Montpellier II - France. 212p. (Ph.D. thesis; in French)

Macambira, J.B., 2003. O ambiente deposicional da Formação Carajás e uma proposta de modelo evolutivo para a Bacia Grão Pará. Universidade de Campinas – São Paulo. 217p. (Ph.D. thesis; in Portuguese)

Macambira, M.J.B., Lancelot, J., 1996. Time constraints for the formation of the Archean Rio Maria crust, southeastern Amazonian Craton, Brazil. International Geology Review 38, 1134-1142.

Machado, N., Lindenmayer, Z.G., Krogh, T.E., Lindenmayer, D., 1991. U-Pb geochronology of Archean magmatism and basement reactivation in the Carajás area, Amazon shield, Brazil. Precambrian Research, 49, 329-354.

Misra, S., Sarkar, S.S., Ghosh, S. 2002. Evolution of Mayurbhanj granite pluton, eastern Singhbhum, India: a case study of petrogenesis of an A-type granite in bimodal association. Journal of Asian Earth Sciences 20, 965-989.

Moore, M., Davis, D.W., Robb, L.J., Jacson, M.C., Globler, D.F., 1993. Archean rapakivi granite-anorthosite-ryolite complex in the Witwatersrand basin hinterland, Southern Africa. Geology 21, 1031-1034.

Moreto, C.P.N., Monteiro, L.V.S., Xavier, R.P., Souza Filho, C.R., 2010. Geocronologia U-Pb das rochas hospedeiras mesoarqueanas (3.0 e 2.86 Ga) do depósito de óxido de ferro-cobre-ouro bacaba, Província Mineral de Carajás. In: SBG, Congresso Brasileiro de Geologia, 45, CDrom (in Portuguese).

Nogueira, A.C.R., Truckenbrodt W., Pinheiro, R.V.L., 1995. Formação Águas Claras, Pré-Cambriano da Serra dos Carajás: redescrição e redefinição litoestratigráfica. Boletim Museu Paraense Emílio Goeldi 7, 177-277 (in Portuguese).

Oliveira, M.A., Dall'Agnol, R., Althoff, F.J., Leite, A.A.S., 2009. Mesoarchean sanukitoid rocks of the Rio Maria Granite-Greenstone Terrane, Amazonian craton, Brazil. Journal of South American Earth Sciences 27, 146-160.

Patiño Douce, A.E., 1997. Generation of metaluminous A-type granites by low-pressure melting of calc-alkaline granitoids, Geology 25, 743-746.

Percival, J.A., 1994. Archean high-grade metamorphism. In: Condie, K.C., (Ed.). Archean Crustal Evolution, Elsevier, Amsterdam, pp. 357–410.

Pidgeon, R.T., Macambira, M.J.B., Lafon, J.M., 2000. Th-U-Pb isotopic systems and internal structures of complex zircons from an enderbite from the Pium Complex, Carajás Province, Brazil: evidence for the ages of granulites facies metamorphism and the protolith of the enderbite. Chemical Geology 166, 159-171.

Rapopo, M., 2010. Petrogenesis of the Matok pluton, South Africa: implications on the heat source that induced regional metamorphism in the Southern Marginal Zone of the Limpopo Belt. University of Stellenbosch, South Africa, 117p. (Master thesis).

Ricci, P.S.F., Carvalho, M.A., 2006. Rocks of the Pium-Area, Carajás Block, Brazil – A Deep seated High-T Gabbroic Pluton (Charnockitoid-Like) with Xenoliths of Enderbitic Gneisses Dated at 3002 Ma – The Basement Problem Revisited. In: Simpósio de Geologia da Amazônia 8, CDroom (in Portuguese).

Rollinson, H.R., 1993. Using Geochemical Data: Evaluation, Presentation, and Interpretation. New York, Longman, 352 p.

Santos, J.O.S., Hartmann, L.A., Gaudette, H.E., Groves, D.I., McNaughton, N.J., Fletcher, I.R., 2000. A new understanding of the provinces of the Amazon Craton based on integration of field mapping and U-Pb and Sm-Nd geochronology. Gondwana Research 3, 453-488.

Santos, R.D. 2009. Geologia, petrografia e caracterização geoquímica das rochas máficas (granulitos?) do Complexo Pium – regiões de Vila Feitosa e Cedere III, Canaã dos Carajás – Província mineral de Carajás. Trabalho de conclusão de curso, Universidade Federal do Pará, 73p (in Portuguese).

Santos, R.D., Oliveira, D.C., 2010. Geologia, petrografia e caracterização geoquímica das rochas máficas do Complexo Pium - Província mineral de Carajás. In: Congresso Brasileiro de Geologia, 45, CDrom (in Portuguese).

Sardinha, A.S., Barros, C.E.M., Krymsky, R., 2006. Geology, Geochemistry, and U-Pb geochronology of the Archean (2.74 Ga) Serra do Rabo granite stocks, Carajás Province, northern Brazil. Journal of South American Earth Sciences 20, 327-339.

Sardinha, A.S., Dall'Agnol, R., Gomes, A.C.B., Macambira, M.J.B., Galarza, M.A., 2004. Geocronologia Pb-Pb e U-Pb em zircão de granitóides arqueanos da região de Canaã dos Carajás, Província Mineral de Carajás. In: Congresso Brasileiro de Geologia, 42, CDrom (in Portuguese).

Sheraton, J.W., Black, L.P., 1988. Chemical evolution of granitic rocks in the East Antarctic Shield, with particular reference to post-orogenic granites. Lithos 21, 37-52.

Silva, M.L.T., Oliveira, D.C., Macambira, M.J.B., 2010. Geologia, petrografia e geocronologia do magmatismo de alto K da região de vila Jussara, Água Azul do Norte - Província Mineral de Carajás. In: Congresso Brasileiro de Geologia, 45, CDrom (in Portuguese).

Smithies, R.H., Howard, H.M., Evins, P.M., Kirkland, C.L., Kelsey, D.E., Hand, M., Wingate, M.T.D., Collins, A.S., Belousova, E. and Allchurch, S. (2010). Geochemistry, geochronology and petrogenesis of Mesoproterozoic felsic rocks in the western Musgrave Province of central Australia, and implication for the Mesoproterozoic tectonic evolution of the region. Geological Survey of Western Australia, Report 106, 73p.

Souza, M.C., Oliveira, D.C., Macambira, M.J.B., Galarza, M.A., 2010. Geologia, petrografia e geocronologia do granito de alto K da região de Velha Canadá, município de Água Azul do Norte - Província Mineral de Carajás. In: Congresso Brasileiro de Geologia, 45, CDrom (in Portuguese).

Souza, Z.S., Potrel, A., Lafon, J.M., Althoff, F.J., Pimentel, M.M., Dall'Agnol, R., Oliveira, C.G., 2001. Nd, Pb and Sr isotopes in the Identidade Belt, an Archean greenstone belt of Rio Maria region (Carajás Province, Brazil): implications for the geodynamic evolution of the Amazonian Craton. Precambrian Research 109, 293–315.

Stacey, J.S., Kramers, J.D., 1975. Approximation of terrestrial lead isotope evolution by a two stage model. Earth and Planetary Science Letters 26, 207–221.

Sylvester, P.J., 1989. Post-collisional alkaline granites. Journal of Geology 97, 261–280.

Sylvester, P.J., 1994. Archaean granite plutons. In: Condie K. (ed.), Archean Crustal Evolution, Elsevier, Amsterdam, pp. 261–314.

Tassinari, C.C.G., Macambira, M., 2004. A evolução tectônica do Craton Amazônico. In: Mantesso-Neto, V., Bartorelli, A., Carneiro, C.D.R., Brito Neves, B.B. (eds.). Geologia do Continente Sul Americano: Evolução da obra de Fernando Flávio Marques Almeida. São Paulo, p. 471-486 (in Portuguese).

Teixeira, J.B.G., Eggler, D.H., 1994. Petrology, geochemistry, and tectonic setting of Archean basaltic and dioritic rocks from the N4 iron deposit, Serra dos Carajás, Pará, Brazil. Acta Geology Leopoldensia 17, 71-114.

Teixeira, L.R., 2005. Genesis versão 4.0. Aplicativo de modelamento geoquímico. Universidade Federal da Bahia (in Portuguese).

Vasquez, L.V., Rosa-Costa, L.R., Silva, C.G., Ricci, P.F., Barbosa, J.O., Klein, E.L., Lopes, E.S., Macambira, E.B., Chaves, C.L., Carvalho, J.M., Oliveira, J.G., Anjos, G.C., Silva, H.R., 2008. Geologia e Recursos Minerais do Estado do Pará: Sistema de Informações Geográficas – SIG: texto explicativo dos mapas Geológico e Tectônico e de Recursos Minerais do Estado do Pará, 328p (in Portuguese).

Whalen, J.B., Currie, K.L., Chappell, B.W., 1987. A-types granites: geochemical characteristics, discrimination and petrogenesis, Contributions of Mineralogy and Petrology 95, 407–419.

Supplementary data - Pb evaporation on zircon analytical data for the granitoids of the Canaã dos Carajás area.

Sample/grain	Evaporation Temperature	Ratios	$^{204}Pb/^{206}Pb$	2s	$^{208}Pb/^{206}Pb$	2s	$(^{207}Pb/^{206}Pb)c$	2s	Age (Ma)	2s
AMR187/02	1550	16/16	0.000080	0.000032	0.170590	0.001250	0.188830	0.000710	2732	6
AMR187/11	1550	30/30	0.000102	0.000001	0.172580	0.000570	0.188850	0.000590	2733	5
AMR187/12	1500	16/16	0.000036	0.000024	0.167590	0.000970	0.189600	0.000790	2739	7
AMR187/15	1500	26/26	0.000009	0.000003	0.173200	0.000820	0.189260	0.000940	2736	8
AMR187/17	1500	36/36	0.000005	0.000002	0.153040	0.000630	0.188860	0.000350	2733	3
AMR187/18	1500	40/40	0.000002	0.000000	0.157090	0.000350	0.188620	0.000440	2731	4
Geographic coordinates = 9278743/635270					MSWD = 0.92		$^{207}Pb/^{206}Pb$ mean age =		2733	2

Sample/grain	Evaporation Temperature	Ratios	$^{204}Pb/^{206}Pb$	2s	$^{208}Pb/^{206}Pb$	2s	$(^{207}Pb/^{206}Pb)c$	2s	Age (Ma)	2s
ARC109/2	1550	34/50	0.000025	0.000003	0.164650	0.000410	0.188960	0.000310	2734	3
ARC109/3	1550	30/80	0.000025	0.000007	0.153870	0.000560	0.188480	0.000250	2729	2
ARC109/5	1550	26/66	0.000050	0.000006	0.152370	0.000390	0.188980	0.000370	2734	3
ARC109/6	1550	66/78	0.000012	0.000006	0.179240	0.001070	0.188740	0.000770	2732	7
ARC109/7	1500	14/28	0.000056	0.000008	0.183840	0.002310	0.188450	0.000360	2729	3
AR109/10	1500	24/30	0.000037	0.000013	0.147690	0.000700	0.188620	0.000580	2731	5
Geographic coordinates = 9275089/612681					MSWD = 2.0		$^{207}Pb/^{206}Pb$ mean age =		2731	1

Sample/grain	Evaporation Temperature	Ratios	$^{204}Pb/^{206}Pb$	2s	$^{208}Pb/^{206}Pb$	2s	$(^{207}Pb/^{206}Pb)c$	2s	Age (Ma)	2s
GRD77/1	1500	22/30	0.000063	0.000074	0.177240	0.001990	0.188240	0.001110	2727	10
GRD77/2	1450	16/16	0.000001	0.000002	0.256680	0.010730	0.189070	0.000460	2735	4
GRD77/4	1500	22/48	0.000010	0.000002	0.192350	0.000650	0.190500	0.001130	2747	10
GRD77/6	1500	8/14	0.000003	0.000002	0.175160	0.010420	0.188580	0.000690	2730	6
GRD77/8	1500	40/58	0.000058	0.000013	0.169470	0.000520	0.189550	0.000420	2739	4
GRD77/10	1550	32/74	0.000274	0.000003	0.219100	0.001180	0.189360	0.000360	2737	3
Geographic coordinates = 9291660/618604					MSWD = 3.0		$^{207}Pb/^{206}Pb$ mean age =		2736	4

Supplementary data - U–Pb on zircon LA-MC-ICPMS analytical data for the granitoids of the Canaã dos Carajás area.

	Isotopic ratios									Ages						
AMR-187	Th/U	6/4 ratio	7/6 ratio	1s(%)	7/5 ratio	1s(%)	6/8 ratio	1s(%)	Rho	7/6 age	1s(Ma)	7/5 age	1s(Ma)	6/8 age	1s(Ma)	Conc (%)
03-Z1	0.46	4166	0.18791	0.54	13.6067	2.56	0.5252	2.5	0.98	2723.9	8.9	2722.7	24.2	2721.1	55.5	99.9
04-Z2	0.30	1569	0.18902	0.50	13.8736	0.87	0.5323	0.7	0.79	2733.7	8.2	2741.1	8.2	2751.2	15.9	100.6
23-Z16	0.39	5668	0.18826	0.57	14.1315	1.23	0.5444	1.1	0.88	2727.0	9.3	2758.6	11.6	2801.9	24.7	102.7
24-Z17	0.37	7549	0.18639	0.52	13.5395	1.42	0.5268	1.3	0.93	2710.6	8.5	2718.0	13.4	2728.1	29.4	100.6
07-Z5	0.41	2880	0.18889	0.42	13.0395	1.70	0.5007	1.6	0.97	2732.6	6.8	2682.5	16.0	2616.6	35.4	98.0
09-Z7"*	0.39	2817	0.18381	0.36	14.3321	0.93	0.5655	0.9	0.91	2687.6	6.0	2771.9	8.8	2889.4	19.9	107.5
10-Z8"*	0.39	8320	0.18261	0.54	14.1036	0.85	0.5601	0.7	0.86	2676.7	8.9	2756.7	8.0	2867.2	15.2	107.1
15-Z11"*	0.34	6334	0.18411	0.40	14.5594	0.81	0.5735	0.7	0.85	2690.3	6.6	2786.9	7.7	2922.3	16.6	108.6
19-Z15"*	0.44	15391	0.18145	0.50	13.4452	0.98	0.5374	0.8	0.84	2666.1	8.3	2711.4	9.2	2772.7	19.0	104.0
28-Z21"*	0.34	7482	0.18592	0.40	14.8880	1.03	0.5808	0.9	0.91	2706.4	6.6	2808.1	9.7	2951.9	22.3	109.1
29-Z22"*	0.35	4786	0.18403	0.46	14.6508	1.45	0.5774	1.4	0.95	2689.5	7.7	2792.8	13.7	2938.1	32.4	109.2
17-Z13[1]	0.16	2185	0.16112	2.99	11.0596	5.64	0.4978	4.8	0.85	2467.4	49.6	2528.2	51.2	2604.5	101.7	105.6
05-Z3"	0.29	4779	0.19258	0.90	16.1677	2.09	0.6089	1.9	0.90	2764.3	14.7	2886.8	19.8	3065.6	45.9	110.9
06-Z4"	0.17	2069	0.14292	3.97	4.5430	5.13	0.2305	3.2	0.85	2262.9	68.4	1738.9	42.7	1337.4	39.2	59.1
08-Z6"	0.08	2608	0.13061	1.83	1.8839	15.08	0.1046	15.0	0.99	2106.2	32.2	1075.4	100.0	641.3	91.3	30.4
13-Z9"	0.35	6461	0.18621	0.43	15.2727	1.00	0.5948	0.9	0.89	2709.0	7.1	2832.4	9.5	3009.0	21.6	111.1
14-Z10"	0.37	5011	0.18666	1.06	17.0564	2.06	0.6627	1.8	0.85	2712.9	17.5	2938.0	19.8	3277.8	45.5	120.8
16-Z12"	0.40	3766	0.18442	0.71	15.5844	1.32	0.6129	1.1	0.93	2693.0	11.7	2851.7	12.5	3081.6	27.2	114.4
18-Z14"	0.29	5503	0.19563	0.85	19.1280	2.15	0.7091	2.0	0.92	2790.1	13.9	3048.3	20.7	3455.2	52.7	123.8
25-Z18"	0.43	5142	0.18567	0.63	15.2618	1.43	0.5961	1.3	0.89	2704.2	10.4	2831.7	13.5	3014.3	30.8	111.5
26-Z19"	0.02	1129	0.08999	4.29	1.2596	6.36	0.1015	4.7	0.91	1425.3	82.0	827.7	36.0	623.3	27.9	43.7
27-Z20"	0.28	8240	0.18184	0.51	11.2345	1.05	0.4481	0.9	0.86	2669.8	8.4	2542.8	9.8	2386.7	18.3	89.4
30-Z23"	0.34	6327	0.18897	0.73	15.7414	1.93	0.6041	1.8	0.96	2733.2	12.0	2861.2	18.3	3046.5	43.2	111.5
33-Z24"	0.04	5396	0.12606	0.92	2.9624	1.40	0.1704	1.1	0.74	2043.7	16.2	1398.0	10.6	1014.5	9.9	49.6
34-Z25"	0.45	10052	0.18713	0.63	18.1657	1.58	0.7041	1.5	0.91	2717.1	10.5	2998.6	15.2	3436.1	38.6	126.5
35-Z26"	0.26	1873	0.18037	0.60	15.3183	1.22	0.6159	1.1	0.86	2656.3	10.0	2835.2	11.7	3093.7	26.2	116.5
36-Z27"	0.26	8147	0.18114	1.15	10.6804	5.74	0.4276	5.6	0.99	2663.3	19.1	2495.7	53.3	2295.0	108.7	86.2
37-Z28"	0.40	8940	0.18253	0.65	15.4231	1.10	0.6128	0.9	0.78	2676.0	10.8	2841.7	10.4	3081.4	21.6	115.2
38-Z29"	0.51	16159	0.18141	0.41	15.4753	0.78	0.6187	0.7	0.81	2665.8	6.8	2845.0	7.4	3104.7	16.2	116.5
39-Z30"	0.53	9848	0.17944	0.42	14.6299	1.69	0.5913	1.6	0.97	2647.7	7.0	2791.5	16.0	2994.8	39.1	113.1
43-Z31"	0.10	22887	0.16759	1.58	7.4389	3.43	0.3219	3.0	0.89	2533.7	26.6	2165.7	30.7	1799.1	47.7	71.0
44-Z32"	0.45	12140	0.18506	0.41	16.2730	1.14	0.6378	1.1	0.93	2698.7	6.7	2893.0	10.9	3180.3	26.8	117.8
45-Z33"	0.14	3722	0.16324	0.64	7.1012	2.20	0.3155	2.1	0.96	2489.5	10.8	2124.2	19.6	1767.7	32.5	71.0
46-Z34"	0.44	9445	0.18311	0.49	16.5098	0.98	0.6539	0.8	0.90	2681.2	8.1	2906.8	9.4	3243.6	21.7	121.0

"discordance >10%; [1]high error (>3%); ¨inherited zircon; "* discordance >3%

	Isotopic ratios									Ages						
ARC-109	Th/U	6/4 ratio	7/6 ratio	1s(%)	7/5 ratio	1s(%)	6/8 ratio	1s(%)	Rho	7/6 age	1s(Ma)	7/5 age	1s(Ma)	6/8 age	1s(Ma)	Conc (%)
16-Z4N	0.51	361704	0.18792	0.60	13.9081	1.33	0.5368	1.188	0.888	2724.04	9.813	2743.47	12.59	2769.94	26.74	101.685
23-Z6N	0.33	116543	0.1857	0.52	13.3563	1.11	0.5216	0.983	0.875	2704.48	8.548	2705.17	10.5	2706.1	21.72	100.06
27-Z7	0.30	95132	0.18588	0.64	13.6534	1.48	0.5327	1.329	0.895	2706.03	10.62	2725.97	13.97	2752.96	29.77	101.734
49-Z13	0.23	55799	0.18597	1.55	13.5919	2.48	0.5301	1.928	0.774	2706.87	25.65	2721.7	23.42	2741.73	43.05	101.288
52-Z14N	0.29	152878	0.18908	1.05	13.6640	2.18	0.5241	1.915	0.875	2734.15	17.22	2726.7	20.64	2716.66	42.44	99.36
57 Z16N	0.02	339479	0.18821	0.37	13.5571	0.74	0.5224	0.636	0.831	2726.56	6.111	2719.28	6.942	2709.49	14.05	99.3741
80-Z22N	0.31	59986	0.19015	0.46	13.6962	1.24	0.5224	1.15	0.924	2743.48	7.541	2728.93	11.72	2709.32	25.44	98.7551
04-Z1N"*	0.35	110847	0.18454	0.64	13.8048	1.28	0.5426	1.11	0.858	2694.08	10.5	2736.41	12.05	2794.13	25.11	103.714
43-Z11N"*	0.13	243658	0.18024	0.63	13.1897	1.55	0.5307	1.419	0.911	2655.1	10.42	2693.32	14.65	2744.55	31.72	103.369
44-Z12N"*	0.33	191063	0.1777	1.37	13.1972	1.96	0.5386	1.408	0.708	2631.54	22.74	2693.86	18.53	2777.7	31.77	105.554
85 Z24N"*	0.48	200244	0.18402	0.34	13.7400	1.08	0.5415	1.027	0.946	2689.4	5.599	2731.95	10.19	2789.89	23.22	103.736
03-Z1B	0.23	165565	0.18435	0.51	13.4038	1.28	0.5273	1.172	0.911	2692.39	8.496	2708.53	12.1	2730.2	26.1	101.404
07-Z2B	0.20	131875	0.18549	0.57	13.5558	1.44	0.5300	1.326	0.914	2702.58	9.457	2719.18	13.66	2741.59	29.61	101.443
08-Z3B	0.24	121265	0.18368	0.66	13.4418	1.58	0.5308	1.435	0.905	2686.35	10.93	2711.2	14.93	2744.68	32.08	102.171
12-Z4B	0.26	88443	0.18301	0.62	13.4475	1.25	0.5329	1.09	0.86	2680.35	10.26	2711.6	11.85	2753.75	24.43	102.739
20-Z5B	0.25	167452	0.18507	0.33	13.3701	1.05	0.5240	0.999	0.946	2698.86	5.436	2706.15	9.937	2715.93	22.14	100.632
40-Z11B	0.23	115701	0.17891	1.18	12.3941	1.89	0.5024	1.475	0.774	2642.75	19.58	2634.73	17.74	2624.31	31.79	99.3022
68-Z19B	0.29	115338	0.18108	1.05	13.1444	1.92	0.5265	1.604	0.833	2662.77	17.34	2690.08	18.07	2726.56	35.66	102.396
72-Z20B	0.24	62418	0.18388	1.06	13.4440	1.69	0.5303	1.318	0.771	2688.18	17.48	2711.36	15.97	2742.57	29.45	102.023
75-Z21B	0.25	87735	0.18649	0.53	13.5137	1.35	0.5256	1.237	0.915	2711.44	8.733	2716.24	12.72	2722.71	27.47	100.416
89 Z25B	0.21	82810	0.18845	0.35	13.9733	0.99	0.5378	0.923	0.93	2728.68	5.687	2747.9	9.336	2774.14	20.8	101.666
88 Z24B	0.23	75148	0.18532	0.33	13.0772	1.06	0.5118	1.002	0.945	2701.08	5.484	2685.24	9.908	2664.25	21.82	98.6367
36-Z10B"*	0.31	256802	0.17653	1.43	13.1268	2.07	0.5393	1.506	0.719	2620.57	23.53	2688.81	19.39	2780.52	33.93	106.104
39-Z10B2"*	0.23	322700	0.1795	0.91	13.1295	1.49	0.5305	1.182	0.781	2648.22	15.07	2689.01	14	2743.6	26.37	103.601
48-Z12B"*	0.23	370617	0.18077	0.82	13.5639	1.68	0.5442	1.472	0.869	2659.91	13.53	2719.75	15.81	2801.04	33.35	105.306
60-Z16B"*	0.23	405104	0.18338	0.50	14.2600	0.89	0.5640	0.74	0.803	2683.67	8.241	2767.16	8.464	2883.09	17.2	107.431
61-Z17B"*	0.28	114881	0.17952	1.04	11.6781	2.28	0.4718	2.028	0.888	2648.44	17.25	2578.95	21.31	2491.45	41.9	94.0727
77-Z22B"*	0.23	103781	0.18219	1.04	11.8858	1.73	0.4732	1.378	0.79	2672.86	17.23	2595.45	16.17	2497.44	28.53	93.4367
32-Z8B[1]	0.21	151442	0.1809	0.83	12.1116	3.88	0.4856	3.79	0.977	2661.13	13.81	2613.08	36.4	2551.53	79.86	95.8811
81-Z23B[1]	0.28	127239	0.17728	1.20	12.4673	3.17	0.5100	2.93	0.925	2627.61	19.97	2640.27	29.76	2656.81	63.79	101.111
81-Z23B[1]	0.28	127600	0.17679	1.21	12.5379	3.15	0.5144	2.905	0.922	2622.96	20.13	2645.57	29.59	2675.24	63.6	101.993
11-Z3N"	0.29	6309	0.20452	0.61	9.8073	1.82	0.3478	1.718	0.941	2862.62	9.885	2416.83	16.79	1924.01	28.58	67.2115
19-Z5N"	0.50	134766	0.10332	2.76	1.8569	5.82	0.1303	5.122	0.88	1684.63	51.01	1065.89	38.41	789.842	38.08	46.885
24-Z6B"	0.09	12311	0.16788	1.41	7.4323	3.56	0.3211	3.272	0.918	2536.66	23.6	2164.86	31.87	1794.99	51.26	70.7619
24-Z6B"	0.09	12311	0.16788	1.41	7.4323	3.56	0.3211	3.272	0.918	2536.66	23.6	2164.86	31.87	1794.99	51.26	70.7619
28-Z8N"	0.33	117930	0.18291	1.40	14.6501	2.46	0.5809	2.016	0.817	2679.39	23.23	2792.79	23.35	2952.48	47.75	110.192
53-Z14B"	0.18	263489	0.14119	1.87	3.4310	4.01	0.1762	3.545	0.884	2241.9	32.34	1511.52	31.52	1046.4	34.24	46.6746
56-Z15B"	0.26	58250	0.18834	1.09	15.5433	1.88	0.5985	1.524	0.807	2727.74	18.01	2849.14	17.9	3023.95	36.79	110.859
67-Z18N"	0.41	176951	0.16487	0.93	8.6630	2.78	0.3811	2.619	0.941	2506.26	15.72	2303.19	25.31	2081.32	46.59	83.0448
71-Z20N"	0.35	63784	0.16464	0.97	8.1520	2.15	0.3591	1.919	0.89	2503.86	16.33	2248.03	19.45	1977.98	32.69	78.9973

		Isotopic ratios								Ages						
GRD-77	Th/U	6/4 ratio	7/6 ratio	1s(%)	7/5 ratio	1s(%)	6/8 ratio	1s(%)	Rho	7/6 age	1s(Ma)	7/5 age	1s(Ma)	6/8 age	1s(Ma)	Conc (%)
03-Z1	0.54	4016	0.18715	0.52	13.6062	1.60	0.5273	1.515	0.944	2717.26	8.537	2722.69	15.15	2730.03	33.72	100.47
09-Z7	0.36	3825	0.18404	0.65	13.2378	2.32	0.5217	2.223	0.959	2689.58	10.72	2696.76	21.86	2706.35	49.13	100.624
10-Z8	0.37	4165	0.18415	0.85	13.1388	1.81	0.5175	1.601	0.947	2690.58	14.12	2689.67	17.13	2688.47	35.2	99.9216
18-Z14	0.47	3752	0.18655	0.51	13.7753	1.60	0.5355	1.515	0.946	2712.02	8.374	2734.38	15.13	2764.76	34.06	101.945
07-Z5"*	0.42	4269	0.1842	0.42	14.5649	0.91	0.5735	0.805	0.872	2691.06	6.887	2787.25	8.598	2922.08	18.93	108.585
13-Z9"*	0.50	6420	0.18658	0.49	14.2815	1.27	0.5551	1.163	0.916	2712.28	8.111	2768.59	11.94	2846.5	26.76	104.949
19-Z15"*	0.53	9140	0.18164	0.46	12.0689	1.07	0.4819	0.964	0.895	2667.86	7.553	2609.77	9.996	2535.58	20.2	95.042
25-Z18"*	0.38	3170	0.18861	0.62	14.5754	1.39	0.5605	1.232	0.886	2730.1	10.24	2787.93	13.08	2868.56	28.57	105.072
26-Z19"*	0.37	3880	0.18483	0.92	13.8588	2.21	0.5438	2.004	0.965	2696.66	15.04	2740.11	20.71	2799.45	45.5	103.812
33-Z24"*	0.44	12781	0.18075	0.51	13.5357	1.61	0.5431	1.527	0.948	2659.74	8.35	2717.78	15.11	2796.55	34.59	105.144
04-Z2"	0.43	5810	0.18631	0.35	15.3083	0.82	0.5959	0.738	0.888	2709.83	5.733	2834.62	7.771	3013.42	17.75	111.203
05-Z3"	0.32	1933	0.18758	0.45	15.6765	1.23	0.6061	1.141	0.925	2721.02	7.466	2857.29	11.72	3054.52	27.76	112.256
06-Z4"	0.38	3643	0.18747	0.60	15.7961	1.30	0.6111	1.153	0.936	2720.12	9.881	2864.54	12.41	3074.38	28.2	113.024
08-Z6"	0.40	2558	0.18805	0.50	17.8283	1.28	0.6876	1.177	0.915	2725.2	8.275	2980.52	12.3	3373.42	30.92	123.786
14-Z10"	0.64	3075	0.14134	1.56	3.6298	2.82	0.1863	2.355	0.832	2243.69	26.91	1556.09	22.48	1101.07	23.84	49.0742
15-Z11"	0.28	4532	0.18121	0.45	11.0548	1.78	0.4424	1.723	0.967	2664.02	7.403	2527.76	16.57	2361.56	34.06	88.6465
16-Z12"	0.45	3963	0.1901	0.49	16.1244	0.90	0.6152	0.761	0.88	2743.04	8.015	2884.2	8.637	3090.68	18.68	112.674
17-Z13"	0.50	8963	0.18683	0.48	15.2222	1.48	0.5909	1.394	0.942	2714.44	7.97	2829.24	13.98	2993.17	33.34	110.268
23-Z16"	0.36	3696	0.18556	0.50	15.1664	1.06	0.5928	0.933	0.87	2703.17	8.227	2825.75	10.06	3000.75	22.42	111.009
24-Z17"	0.29	3135	0.18839	0.53	16.9425	1.35	0.6522	1.241	0.916	2728.19	8.682	2931.59	12.93	3236.96	31.58	118.649
27-Z20"	0.40	3085	0.18606	0.53	16.3530	1.19	0.6374	1.065	0.888	2707.65	8.742	2897.67	11.39	3178.96	26.74	117.407
28-Z21"	0.37	6134	0.19231	0.40	17.7058	0.99	0.6677	0.903	0.905	2762.03	6.555	2973.89	9.49	3297.16	23.31	119.375
29-Z22"	0.35	2106	0.18688	0.51	17.0723	1.10	0.6626	0.973	0.876	2714.87	8.386	2938.91	10.53	3277.16	24.99	120.712
30-Z23"	0.36	4840	0.18549	0.82	15.0195	1.36	0.5872	1.081	0.89	2702.62	13.6	2816.47	12.94	2978.25	25.78	110.199
34-Z25"	0.37	3114	0.18545	0.53	15.2555	1.32	0.5966	1.215	0.913	2702.23	8.695	2831.33	12.62	3016.2	29.26	111.619
35-Z26"	0.49	5180	0.18467	0.43	15.1110	1.40	0.5935	1.329	0.95	2695.31	7.064	2822.26	13.3	3003.4	31.92	111.431
36-Z27"	0.41	2838	0.19114	2.26	20.7287	3.41	0.7865	2.557	0.908	2752.01	37.07	3125.99	33.03	3740.7	72.58	135.926

		Isotopic ratios								Ages						
GRD-05	Th/U	6/4 ratio	7/6 ratio	1s(%)	7/5 ratio	1s(%)	6/8 ratio	1s(%)	Rho	7/6 age	1s(Ma)	7/5 age	1s(Ma)	6/8 age	1s(Ma)	Conc (%)
Core																
31-Z14N	0.22	19257	0.2	1.06	13.7395	2.05	0.5258	1.8	0.9	2737.9	17.5	2731.9	19.4	2723.9	39.0	99.5
38-Z17	0.31	135861	0.2	0.77	13.7866	1.57	0.5222	1.4	0.9	2754.9	12.7	2735.2	14.8	2708.5	30.2	98.3
40-Z19	0.32	30610	0.2	1.14	13.9115	2.13	0.5232	1.8	0.8	2766.7	18.7	2743.7	20.2	2712.5	39.9	98.0
43-Z20N	0.26	10343	0.2	1.08	13.4535	1.61	0.5164	1.2	0.7	2733.0	17.7	2712.0	15.2	2683.9	26.2	98.2
50-Z23	0.22	36055	0.2	1.00	13.8996	1.32	0.5404	0.9	0.6	2712.0	16.5	2742.9	12.5	2785.1	19.4	102.7
52-Z25	0.18	10380	0.2	1.08	13.5919	1.69	0.5223	1.3	0.8	2731.2	17.6	2721.7	15.9	2708.9	28.9	99.2
08-Z3N"*	0.25	34073	0.2	0.73	13.5222	1.31	0.5365	1.08	0.82	2678.54	12.14	2716.84	12.38	2768.65	24.41	103.36
10-Z4"*	0.30	31491	0.2	0.61	13.7390	1.07	0.5494	0.9	0.8	2665.4	10.1	2731.9	10.1	2822.7	20.0	105.9
17-Z7N"*	0.17	61651	0.2	0.85	13.5555	1.66	0.5601	1.4	0.9	2611.0	14.1	2719.2	15.7	2867.1	33.1	109.8
39-Z18"*	0.24	18083	0.2	0.95	14.0750	1.60	0.5451	1.3	0.8	2718.2	15.7	2754.8	15.1	2805.0	29.2	103.2
05-Z1B	0.15	11428	0.2	0.98	13.6931	1.58	0.5321	1.2	0.8	2712.8	16.1	2728.7	14.9	2750.3	27.8	101.4
26-Z10B	0.17	18207	0.2	0.80	13.6146	1.92	0.5296	1.8	0.9	2711.2	13.2	2723.3	18.2	2739.6	39.1	101.0
32-Z14B	0.21	14415	0.2	0.97	14.0473	1.65	0.5417	1.3	0.8	2725.4	16.0	2752.9	15.6	2790.5	30.2	102.4
34-Z15B	0.16	20312	0.2	0.83	13.9683	2.15	0.5329	2.0	0.9	2743.1	13.7	2747.6	20.4	2753.7	44.5	100.4
09-Z3B"*	0.23	152653	0.2	0.70	13.2109	1.14	0.5352	0.9	0.8	2643.9	11.7	2694.8	10.8	2763.3	20.3	104.5
22-Z9B"*	0.25	15559	0.2	0.67	13.7063	1.42	0.5405	1.2	0.9	2688.6	11.1	2729.6	13.4	2785.5	28.2	103.6
45-Z21B"*	0.22	14706	0.2	1.07	13.8248	1.79	0.5407	1.4	0.8	2702.2	17.7	2737.8	17.0	2786.3	32.5	103.1
04-Z1N"	0.05	270479	0.1	1.09	5.4029	1.58	0.2828	1.1	0.7	2209.4	19.0	1885.3	13.5	1605.3	16.1	72.7
15-Z6N"	0.13	8961	0.2	0.60	13.5998	1.60	0.5769	1.5	0.9	2567.1	10.1	2722.2	15.1	2936.3	34.8	114.4
16-Z6B"	0.15	3475	0.2	0.75	11.1027	2.23	0.4317	2.1	0.9	2711.7	12.3	2531.8	20.7	2313.5	40.8	85.3
37-Z16N"	0.05	82540	0.2	0.74	5.6507	1.25	0.2611	1.0	0.8	2423.1	12.5	1923.9	10.7	1495.5	13.4	61.7
44-Z20B"	0.22	243576	0.2	0.92	15.0182	1.24	0.6217	0.8	0.6	2608.0	15.3	2816.4	11.8	3116.6	20.4	119.5
46-Z22"	0.43	156540	0.2	1.08	15.3706	1.45	0.6337	1.0	0.7	2614.7	18.0	2838.5	13.8	3164.3	24.2	121.0
Geographic coordinates = 9275825/602992																

5. CONCLUSÕES E CONSIDERAÇÕES FINAIS

1. O mapeamento geológico sistemático, aliado a estudos petrográficos, geoquímicos e geocronológicos realizados na área de Canaã dos Carajás, permitiu a identificação de diversos tipos de granitóides, antes inseridos no Complexo Xingu.

2. Quatro principais eventos magmáticos, três de idade Mesoarqueana e um de idade Neoarqueana, foram distinguidos: (1) em 3,05-3,0 Ga, houve a formação do protólito do complexo de Pium e de rochas com idades semelhantes, como indicado por zircões herdados encontrados em unidades diferentes; (2) o segundo evento (2,96-2,93 Ga) foi marcado pela cristalização do granito Canaã dos Carajás e pela formação de rochas mais antigas do Trondhjemito Rio Verde; (3) no terceiro evento (2,87-2,83 Ga), houve a formação do Complexo tonalítico Bacaba, do Trondhjemito Rio Verde e dos granitos Cruzadão, Bom Jesus e Serra Dourada; (4) no Neoarqueano, em 2,75-2,73 Ga, um grande evento magmático foi responsável pela origem das suítes Planalto e Pedra Branca; e de rochas charnoquíticas.

3. Em termos de assinatura geoquímica, dois grupos de granitóides foram distinguidos na área de Canaã: (1) Unidades tonalíticas-trondhjemíticas que abrangem o Trondhjemito Rio Verde, o Complexo tonalítico Bacaba e a suíte Pedra Branca; e (2) graníticas, que incluem os granitos Canaã dos Carajás, Bom Jesus, Cruzadão, Serra Dourada e Planalto. O Complexo tonalítico Bacaba e a suíte Pedra Branca são distintos geoquimicamente das típicas associações TTG Arqueanas, enquanto o Trondhjemito Rio Verde apresenta afinidade com a mesma. Os granitos Canaã dos Carajás, Bom Jesus e a variedade do granito Cruzadão com alta razão La/Yb assemelham-se aos granitos cálcico-alcalinos tipo CA1 (Granito Canaã do Carajás) ou CA2 (Granito Bom Jesus e parte do Granito Cruzadão). As outras variedades do Granito Cruzadão são transicionais entre os tipos cálcico-alcalino e alcalino, caráter reforçado pelo enriquecimento de HFSE e ETRP em algumas amostras. O granito Serra Dourada apresenta características geoquímicas semelhantes às de granitos cálcio-alcalino ou peraluminosos do subtipo SP3. O granito Planalto apresenta caráter ferroso e são geoquimicamente similares aos granitos reduzidos tipo-A. O ambiente sin-tectônico e a intima relação do Granito Planalto com rochas charnoquíticas, levo-nos a classificá-los como granitos hidratados da série charnoquítica.

4. O magmatismo granitóide Arqueano da área de Canaã dos Carajás difere significativamente daquele encontrado em clássicos crátons arqueanos, incluindo o Rio Maria Terrane, porque magmatismo TTG não é abundante, rochas sanukitóides são ausentes e as rochas graníticas dominam. A Suíte Neoarqueana Planalto não apresenta correspondente no Terreno Rio Maria da Província Carajás, nem, aparentemente, nos crátons Yilgarn e Dharwar. Os contrastes entre

a área de Canaã e o Terreno granito-*greenstone* Rio Maria não favorecem uma evolução tectônica comum para estes dois domínios Arqueanos da Província de Carajás.

5. A crosta arqueana de Canaã não tem caráter juvenil e a curva de evolução do Nd sugere a existência de uma crosta pouco mais velha na área Canaã comparada com a de Rio Maria. A crosta da área de Canaã existia pelo menos desde o Mesoarqueano (ca. 3,2-3,0 Ga) e foi fortemente retrabalhada durante o Neoarqueano (2,75-2,70 Ga). Um terreno similar a crosta de Canaã ou mesmo uma extensão do mesmo corresponde ao substrato da Bacia Neoarqueana Carajás.

6. A evolução Neoarqueana da Província Carajás é marcada pela ascensão do manto astenosférico em um ambiente extensional, que propiciou a formação da Bacia Carajás. Entre 2,73-2,70 Ga, a entrada de calor associado com a colocação de magma máfico na base da crosta induziu a fusão parcial de rochas de composição máfica a intermediária originando os granitóides das suítes Planalto e Pedra Branca, e de rochas charnoquíticas. A estreita associação entre a suíte Planalto e rochas charnoquíticas sugerem um magmatismo formado em altas temperaturas encontradas em limites de blocos tectônicos ou em sua zona de interação.

REFERÊNCIAS

Almeida, J.A.C., Dall'Agnol, R., Dias, S.B., Althoff, F.J. 2010. Origin of the Archean leucogranodiorite–granite suites: Evidence from the Rio Maria terrane and implications for granite magmatism in the Archean. Lithos 187: 201-221.

Almeida, J.A.C., Dall'Agnol, R., Oliveira, M.A., Macambira, M.J.B., Pimentel, M.M., Rämö, O.T., Guimarães, F.V., Leite, A.A.S. 2011. Zircon geochronology and geochemistry of the TTG suites of the Rio Maria granite-greenstone terrane: Implications for the growth of the Archean crust of Carajás Province, Brazil. Precambrian Research 120: 235-257.

Almeida, J.A.C., Dall'Agnol, R., Leite, A.A.S. submitted. Geochemistry and zircon geochronology of the Archean granite suites of the Rio Maria granite-greenstone terrane, Carajás Province, Brazil. Lithos.

Althoff, F.J., Dall'AgnoL, R., Souza, Z.S. 1991. Região de Marajoara – SE do Pará: prolongamento dos terrenos arqueanos de Rio Maria ou retrabalhamento? In: SBG, Simpósio de Geologia da Amazônia, 3, Belém, Anais p. 130-141.

Althoff, F.J., Barbey, P., Boullier, A.M., Dall'Agnol, R. 1995. Composição e estrutura dos granitóides arqueanos da região de Marajoara. Boletim do Museu Paraense Emílio Goeldi - Série Ciências da Terra, 7:5-26

Althoff, F.J., Barbey, P.; Boullier, A.M. 2000. 2.8-3.0 Ga plutonism and deformation in the SE Amazonian craton: the Archean granitoids of Marajoara (Carajás Mineral province, Brazil). Precambrian Research, 104:187-206.

Araújo, O.J.B., Maia, R.G.N. 1991. Programa de levantamentos geológicos básicos do Brasil, Serra dos Carajás, folha SB-22-Z-A, Estado do Pará. Texto explicativo, Brasília, DNPM/CPRM. 164p.

Araújo, O.J.B., Maia, R.G.N., Jorge JOÃO, X.S., Costa, J.B.S. 1988. A megaestrutura arqueana da Folha Serra dos Carajás. In: CONGRESSO LATINO-AMERICANO DE GEOLOGIA, 7, Belém. Anais, Belém: SBG, p.324-338.

Avelar, V.G., Lafon, J.M., Correi,a JR, F.C., Macambira, E.M.B. 1999. O Magmatismo arqueano da região de Tucumã-Província Mineral de Carajás: novos resultados geocronológicos. Revista Brasileira de Geociências. 29(2): 454-460.

Barbosa, J.P.O. 2004. Geologia Estrutural, Geoquímica, Petrografia e Geocronologia de granitóides da região do Igarapé Gelado, norte da Província Mineral de Carajás. Universidade Federal do Pará, 96p (Dissertação de Mestrado).

Barros, C.E.M., Dall'agnol, R., Barbey, P., Boullier, A.M. 1997. Geochemistry of the Estrela Granite Complex, Carajás region, Brazil: an example of an Archean A-type granitoid. Journal of South American Earth Sciences, 10(3-4): 321-330.

Barros, C.E.M.; Macambira, M.J.B.; Barbey, P. 2001. Idade de zircão do Complexo Granítico Estrela: relações entre magmatismo, deformação e metamorfismo na Província Mineral de Carajás. In: SIMPÓSIO DE GEOLOGIA DA AMAZÔNIA, 7, Belém. Resumos Expandidos. Belém: SBG. P. 17-20.

Barros, C.E.M., Macambira, M.J.B., Barbey, P., Scheller, T. 2004. Dados isotópicos Pb-Pb em zircão (evaporação) e Sm-Nd do Complexo Granítico Estrela, Província Mineral de Carajás, Brasil: Implicações petrológicas e tectônicas. Revista Brasileira de Geociências 34: 531-538.

Barros, C.E.M., Sardinha, A.S., Barbosa, J.P.O., Macambira M.J.B. 2009. Structure, Petrology, Geochemistry and zircon U/Pb and Pb/Pb geochronology of the synkinematic Archean (2.7 Ga) A-type granites from the Carajás Metallogenic Province, northern Brazil, Canadian Mineralogist 47: 1423-1440.

Bühn, B., Pimentel, M.P., Matteini, M. Dantas, E.L. 2009. High spatial resolution analysis of Pb and U isotopes for geochronology by laser ablation multi-collector inductively coupled plasma mass spectrometry (LA-MC-ICP-MS). Anais da Academia Brasileira de Ciências 81(1): 99-114.

Chayes, F. 1956. Petrografic modal analysis: an elementary statistical appraisal. New York, John Wiley e Sons. 113 p.

Cordani, U.G., Sato, K. 1999. Crustal evolution of the South america Plataform, based on Nd isotopic systematics on granitoids rocks. Episodes, 22(3): 167-173.

Costa, J.B.S., Araújo, O.J.B., Santos, A., Jorge João X.S., Macambira, M.J.B., Lafon, J.M. 1995. A Província Mineral de Carajás: aspectos tectono-estruturais, estratigráficos e geocronológicos. Boletim do Museu Paraense Emílio Goeldi, série Ciências da Terra, 7:199-235.

Costa, J.B.S., Hasui, Y. 1997. Evolução geológica da Amazônia. Contribuições à Geologia da Amazônia, p. 16-90.

Compston, W., Williams, I.S., Kirschvink, J.L., Zichao, Z., Guogan, M., 1992. Zircon ages for the Early Cambrian timescale. Journal of Geological Society, London 149, 171–184.

CVRD. 1974. Distrito Ferrífero da Serra dos Carajás. In: 26º CONGRESSO BRASILEIRO DE GEOLOGIA. Belém. Resumo: SBGNO, 2: 78-80.

Dall'Agnol, R., Souza, Z.S., Althoff, F. J., Barros, C.E.M., Leite, A.A.S., Jorge João, X.S. 1997. General aspects of the granitogenesis of the Carajás metallogenic province. In: INTERNATIONAL SYMPOSIUM ON GRANITES AND ASSOCIATED MINERALIZATIONS, 2. Excution Guide..., Salvador, p. 135-161.

Dall'Agnol, R.; Rämö, O.T.; Magalhães, M.S.; Macambira, M.J.B. 1999. Petrology of the anorogenic, oxidised Jamon and Musa granites, Amazonian craton: implications for the genesis of Proterozoic A-type granites. Lithos 46:431-462.

Dall'Agnol, R., Teixeira, N.P., Rämö, O.T., Moura, C.A.V., Macambira, M.J.B., Oliveira, D.C. 2005. Petrogenesis of the Paleoproterozoic, rapakivi, A-type granites of the Archean Carajás Metallogenic Province, Brazil. Lithos 80: 01-129.

Dall'Agnol, R., Oliveira, M.A. Almeida, J.A.C., Althoff, F.J. Leite, A.A.S., Oliveira, D.C., Barros, C.E.M. 2006. Archean and paleoproterozoic granitoids of the carajás metallogenic province, eastern amazonian cráton. In: SYMPOSIUM ON MAGMATISMO, CRUSTAL EVOLUTION, AND METALLOGENESIS OF THE AMAZONIAN CRATON, Excution Guide, Belém, p. 99-150.

Dall Agnol, R., Almeida, J.C.A., Oliveira, M.A., Leite, A.A.S., Althoff, F.J. 2011. In: Jayananda, M., Ahmed, T., Chardon, D. (eds). International symposiun on Precambrian Accretionary Orogens and Fields workshop in the Dharwar craton Southern India. p. 112.

DOCEGEO (Rio Doce Geologia e Mineração - Distrito Amazônia) 1988. Revisão litoestratigráfica da Província Mineral de Carajás, Pará. In: SBG, Congresso Brasileiro de Geologia, 35, Belém. Anexos..., vol. Província Mineral de Carajás - Litoestratigrafia e Principais Depósitos Minerais. p. 11-54.

Duarte, K.D, Pereira, E.D., Dall'Agnol, R., Lafon, J.M. 1991. Geologia e geocronologia do Granito Mata Surrão - sudoeste de Rio Maria (Pa). In: SIMPÓSIO DE GEOLOGIA DA AMAZÔNIA, 3, Belém, SBG, Anais... p. 7-20.

Duarte, K.D., Dall'Agnol, R. 1996. Geologia e geoquímica do leucogranito arqueano potássico Mata Surrão, terreno granito-greenstone de Rio Maria, Pará. Boletim IG - USP, 18: 113-115 (publ. esp.).

Farias, N.F., Santos, A.B.S., Biagini, D.O., Vieira, E.A.P., Martins, L.P.B., Saueressig, R. 1984. Jazidas Cu-Zn da área Pojuca, Serra dos Carajás, PA. In: SBG, Congresso Brasileiro de Geologia, 33, Rio de Janeiro, Anais, 8: 3658-3668.

Galarza, M.A., Macambira, M.J.B., Villas, R.N.,2008. Dating and isotopic characteristics (Pb and S) of the Fe oxide–Cu–Au–U–REE Igarapé Bahia ore deposit, Carajás mineral province, Pará state, Brazil. Journal of South American Earth Sciences 25: 377-397.

Gastal, M.C.P. 1987. Mapeamento e petrologia do Maciço Granítico Musa: Rio Maria, sudeste do Pará. Belém, Universidade Federal do Pará. 342p. (Tese de Mestrado).

Gaudette, H.E., Lafon, J.M., Macambiram M.J.B., Moura, C.A.V., Scheller, T.,1998. Comparison of single filament Pb evaporation/ionization zircon ages with conventional U-Pb results: examples from the Precambrian of Brazil. J. South. Amer. Earth Sci., 11: 351-363.

Gibbs, A.K., Wirth, K.R., Hirata, W.K., Olszewski Jr., W.J.,1986. Age and composition of the Grão Pará Group volcanics, Serra dos Carajás. Revista Brasileira de Geociências 16: 201–211.

Gioia, S.M.C.L., Pimente, M.M. 2000. The Sm-Nd Isotopic Method in the Geochronology Laboratory of the University of Brasília. Anais da Academia Brasileira de Ciências, 72(2): 219-246.

Gomes, A.C.B. 2003. Geologia, Petrografia e Geoquímica dos granitóides de Canaã dos Carajás, SE do Estado do Pará. Belém, Universidade Federal do Pará, Centro de Geociências, 160p. (Dissertação de Mestrado).

Gomes, A.C.B., Dall'Agnol, R. 2007. Nova associação tonalítica-trondhjemítica Neoarqueana na região de Canaã dos Carajás: TTG com altos conteúdos de Ti, Zr e Y. Revista Brasileira de Geociências 37: 182-193 (in Portuguese).

Hirata W.K.; Rigon J.C.; Kadekaru K.; Cordeiro A.A.C.; Meireles E.M. 1982. Geologia regional da Província Mineral de Carajás. In: SIMP. GEOL. AMAZ., 1., Belém. Anais... SBG. v.1, p. 100-110.

Huhn S. R. B. Santos A. B. S., Amaral A. F., Ledsham E. J., Gouveia J. L., Martins L. B. P., Montalvão R.M.G., Costa V.G. 1988. O terreno granito-greenstone da região de Rio Maria - sul do Pará. In: CONGR. BRAS. GEOL., 35., Belém, Anais. Belém,v. 3:1438-1453.

Huhn, S.B., Macambira, M.J.B., Dall'Agnol, R. 1999. Geologia e geocronologia Pb/Pb do granito alcalino arqueano Planalto, região da Serra do Rabo, Carajás-PA. In: Simpósio de Geologia da Amazônia, 6: 463-466 (in Portuguese).

Hutchinson C.S. 1974. Laboratory Handbook of Petrographic Techniques. Wiley, New York.

Jorge João, X.S., Lobato, T.A., Marques, S.M.T.G., Brim, R.J.P., Araújo, E.S., 1991. Geoquímica. In: O.J.B. ARAÚJO, R.G.N. MAIA (Eds.), Serra dos Carajás, Folha SB.22-Z-A - Estado do Pará. CPRM/DNPM, Brasilia, pp. 79-95. (Programa Levantamento Geológicos Básicos do Brasil, Projeto especial mapas de recursos minerais, de solos e de vegetação para a área do Programa Grande Carajás).

Kober, B. 1987. Single-grain evaporation combined with Pb+ emitter bedding for $^{207}Pb/^{206}Pb$ age investigations using thermal ion mass spectrometry, and implications to zirconology. Contributions to Mineralogy and Petrology 96: 63-71.

Lafon, J.M.; Macambira, M.J.B.; Pidgeon, R.T. 2000. Zircon U-Pb SHRIMP dating of Neoarchean magmatism in the southwestern part of the Carajás Province (eastern Amazonian Craton, Brazil). In: INTERNATIONAL GEOLOGICAL CONGRESS, 31., 2000, Rio de Janeiro. Abstracts… Rio de Janeiro, 2000. 1 CD-ROM.

Lamarão, C.N., Dall'Agnol, R., Pimentel, M.M. 2005. Nd isotopic composition of Paleoproterozoic volcanic and granitoid rocks of Vila Riozinho: implications of the crustal evolution of the Tapajós gold province, Amazon craton. Journal of South American Earth Sciences, 18: 277-292.

Le Maitre, R.W., Streckeisen, A.., Zanettin, B., Le Bas, M.J., Bonin, B., Bateman, P., Bellieni, G., Dudek, A., Efremova, J., Keller J., Lameyre J., Sabine P.A., Schmidt R., Sørensen H., Woolley A.R. 2002. Igneous Rocks. A Classification and Glossary of Terms. Recommendations of the International Union of Geological Sciences Subcommission on the systematics of igneous rocks. Cambridge University Press, Cambridge, 252 pp.

Leite, A.A.S., Dall'Agnol, R., Althoff, F.J. 1997. Geologia e petrografia do maciço granítico Arqueano Xinguara e de suas encaixantes - SE do Pará. Boletim do Museu Paraense Emílio Goeldi - Série Ciência da Terra. 9: 43-81.

Leite, A.A.S. 2001. Geoquímica, petrogênese e evolução estrutural dos granitóides arqueanos da região de Xinguara, SE do Cráton Amazônico. Belém, Universidade Federal do Pará, Centro de Geociências. (Tese de Doutorado).

Leite, A.A.S., Dall'Agnol, R., Macambira, M.J.B., Althoff, F.J., 2004. Geologia e Geocronologia dos granitóides Arqueanos da região de Xinguara (PA) e suas implicações na evolução do Terreno Granito-Greenstone de Rio Maria. Revista Brasileira de Geociências 34: 447-458 (in Portuguese).

Lindenmayer Z.G., Fyfe, W.S., Bocalon V.L.S. 1994. Nota Preliminar sobre as Intrusões Granitóides do Depósito de Cobre do Salobo, Carajás. Acta Geol. Leopold., 40(7):153-184.

Lindenmayer, Z.G., Fleck, A., Gomes, C.H., Santos, A.B.S., Caron, R., Castro Paula, F., Laux, J.H., Pimentel, M.M., Sardinha, A.S. 2005. Caracterização geológica do alvo Estrela (Cu-Au), Serra dos Carajás, Pará. In: MARINI, O.J.; QUEITOZ, E.T.; RAMOS, B.W. Caracterização de depósitos minerais em distritos mineiros da Amazônia, P. 157-226.

Lobato, L.M., Rosière, C.A., Silva, R.C.F., Zucchetti, M., Baars, F.J., Sedane, J.C.S., Javier Rios, F., Pimentel, M., Mendes, G.E., Monteiro, A.M. 2005. A mineralização hidrotermal de ferro da Província Mineral de Carajás – controle estrutural e contexto na evolução metalogenética da província. In: Marini, O.J., Queiroz, E.T., Ramos, B.W. (Eds.). Caracterização de Depósitos Minerais em Distritos Mineiros da Amazônia, DNPM, CT-Mineral / FINEP, ADIMB, pp. 25-92 (in Portuguese).

Ludwig, K.R. 2002. Squid 1.02, a user's manual. Berkeley Geochronological Center Special Publication 2 (Berkeley, California, USA), 21 pp.

Macambira, M.J.B. 1992. Chronologie U/Pb, Rb/Sr, K/Ar et croissance de la croûte continentale dans L'Amazonie du sud-est; exemple de la région de Rio Maria, Province de Carajas, Brésil. Université Montpellier II - France. 212p. (Ph.D. thesis; in French)

Macambira, M.J.B., Lafon, J.M. 1995. Geocronologia da Província Mineral de Carajás; Síntese dos dados e novos desafios. Boletim do Museu Paraense Emílio Goeldi 7: 263-287 (in Portuguese).

Macambira, M.J.B., Lancelot, J. 1996. Time constraints for the formation of the Archean Rio Maria crust, southeastern Amazonian Craton, Brazil. International Geology Review 38, 1134-1142.

Macambira, E.M.B., Vale A.G. 1997. Programa Levantamentos Geológicos Básicos do Brasil. São Felix do Xingu. Folha SB.22-Y-B. Estado do Pará. DNPM/CPRM. Brasília.384p.

Macambira, E.M.B., Tassinari, C.C.G., 1998. Estudos Sm/Nd no complexo máfico-ultramáfico da Serra da Onça – sul do Pará: implicações geocronológicas e geotectônicas. In: CONGRESSO BRASILEIRO DE GEOLOGIA, 40., 1998, Belo Horizonte. Anais... Belo Horizonte: SBG-Núcleo Minas Gerais, 1998. p. 463.

Macambira, M.J.B., Costa, J.B.S., Althoff, F.J., Lafon, J.M., Melo, J.C.V., Santos, A. 2000. New geochronological data for the Rio Maria TTG terrane, implications for the time contraints of the crustal formation of the Carajás province, Brazil. In: INTERNATIONAL GEOLOGICAL CONGRESS, 31st, Rio de Janeiro, 2000, CD-ron abstract volume.

Macambira, M.J.B., Barros, C.E.M., Silva, D.C.C., Santos, M.C.C. 2001. Novos dados geológicos e geocronológicos para a região ao norte da Província de Carajás, evidências para o estabelecimento do limite Arqueano-Paleoproterozóico no sudeste do Cráton Amazônico. Simpósio de Geologia da Amazônia, vol. 7, Sociedade Brasileira de Geologia, Belém, Brazil, Resumos Expandidos, cdrom.

Macambira J.B. 2003. O ambiente deposicional da Formação Carajás e uma proposta de modelo evolutivo para a Bacia Grão Pará. 217 f. Tese (Doutorado) - Instituto de Geociências, Universidade Estadual de Campinas.

Macambira, M.J., Vasquez, M.L.., Silva, D.C.C., Galarza, M.A., Barros, C.E.M., Camelo, J.F. 2009. Crustal growth of the central-eastern Paleoproterozoic domain, SW Amazonian craton: Juvenile accretion vs. Reworking. Journal of South American Earth Sciences 27: 235–246

Machado, N., Lindenmayer, Z.G., Krogh, T.E., Lindenmayer, D. 1991. U-Pb geochronology of Archean magmatism and basement reactivation in the Carajás area, Amazon shield, Brazil. Precambrian Research 49, 329-354.

Medeiros, H., Dall'Agnol, R. 1988. Petrologia da porção leste do Batólito Granodiorítico Rio Maria, sudeste do Pará. In: CONGRESSO BRASILEIRO DE GEOLOGIA, 35, Belém. Anais... SBG. 3: 1488-1499.

Meireles, E.M.; Hirata, W.K.; Amaral, A.F.; Medeiros, C.A., P; Gato, W.C. 1984. Geologia das Folhas Carajás e Rio Verde, Província Mineral dos Carajás, Estado do Pará. In: CONGRESSO BRASILEIRO DE GEOLOGIA, 33. Rio de Janeiro, 1984. Anais... Rio de Janeiro, SBG. 5: 2164-2174.

Meirelles, M.R., Dardene, M.A. 1991. Vulcanismo basáltico de afinidade shoshonítica em ambiente de arco Arqueano, Grupo Grão-Pará, Serra dos Carajás, Estado do Pará. In: CONGR. BRAS. GEOL., 33, Rio de Janeiro, 1991. Anais... Rio de Janeiro, SBG, 5: 2164-2174.

Moreto, C.P.N., Monteiro, L.V.S. Xavier, R.P., Amaral, W.S., Santos, T.J.S., Juliani, C., Souza Filho, C.R. 2011. Mesoarchean (3.0 and 2.86 Ga) host rocks of the iron oxide–Cu–Au Bacaba deposit, Carajás Mineral Province: U–Pb geochronology and metallogenetic implications. Mineralium Deposita, DOI 10.1007/s00126-011-0352-9.

Mougeot, R., Respaut, J.P., Brique, L., Ledru, P., Milesi J.P., Lerouge, C., Marcoux, E., Huhn, S.B., Macambira, M.J.B. 1996. Isotope geochemistry constrains for Cu, Au mineralizations and evolution of the Carajás Province (Para, Brazil). In: SBG, Congresso Brasileiro de Geologia, 39, Salvador, Anais, 7, 321-324 (in Portuguese).

Neves, A.P., Vale, A.G. 1999. Programa Levantamentos Geológicos Básicos do Brasil. Folha SC.22-X-A Redenção. Estado do Pará e Tocantins. Escala 1:250.000 – CPRM, Brasilia.

Nogueira, A.C.R., Truckenbrodt, W., Pinheiro, R.V.L. 1995. Formação Águas Claras, Pré-Cambriano da Serra dos Carajás: redescrição e redefinição litoestratigráfica. Bol. Mus. Par. Em. Goeldi, Ciênc. da Terra, (7), pg. 177-277.

Oliveira, E.M., Lafon, J.M., Gioia, S.M.C.L., Pimentel, M.M. 2008. Datação Sm-Nd em rocha total e granada do metamorfismo granulítico da região de Tartarugal Grande, Amapá Central. Revista Brasileira de Geologia 38(1), 114-127 (in Portuguese).

Oliveira, M.A. 2003. Caracterização petrográfica, estudo de susceptibilidade magnéticae natureza dos minerais óxidos de Fe e Ti do Granito Planalto, Serra dos Carajás-PA. Belém: Centro de Geociência, Universidade Federal do Pará, 47p. Trabalho de Conclusão de Curso.

Oliveira, M.A., Dall'Agnol, R., Althoff, F. 2006. Petrografia e Geoquímica do Granodiorito Rio Maria da Região de Bannach e Comparações com as demais ocorrências no Terreno Granito-Greenstone De Rio Maria – Pará, Revista Brasileira de Geologia, pg. 313 – 326.

Oliveira, M.A., Dall'Agnol, R., Althoff, F.J., Leite, A.A.S. 2009. Mesoarchean sanukitoid rocks of the Rio Maria Granite-Greenstone Terrane, Amazonian craton, Brazil. Journal of South American Earth Sciences 27, 146-160.

Oliveira, D.C., Santos, P.J.L., Gabriel, E.O., Rodrigues, D.S., Faresin, A.C., Silva, M.L.T., Sousa, S.D., Santos, R.V., Silva, A.C., Souza, M.C., Santos, R.D., Macambira, M.J.B. 2010. Aspectos geológicos e geocronológicos das rochas magmáticas e metamórficas da região entre os municípios de Água Azul do Norte e Canaã dos Carajás – Província Mineral de Carajás, In: SBG, Congresso Brasileiro de Geologia, 45, CDrom (in Portuguese).

Passchier, C.W., Trouw, R.A.J. 1996. Microtectonics. Berlin, Springer-Verlag. 289p.

Pidgeon, R.T., Macambira, M.J.B., Lafon, J.M. 2000. Th-U-Pb isotopic systems and internal structures of complex zircons from an enderbite from the Pium Complex, Carajás Province, Brazil: evidence for the ages of granulites facies metamorphism and the protolith of the enderbite. Chemical Geology 166, 159-171.

Pimentel, M.M., Machado, N. 1994. Geocronologia U-Pb dos Terrenos granito-greenstone de Rio Maria, Pará. In: Congresso Brasileiro de Geologia, 38, Camboriú, 1988. Boletim de Resumos Expandidos. Camboriú, SBG. p. 390-391.

Ramö, O.T., Dall'Agnol, R., Macamira, M.J.B., Leite, A.A.S., Oliveira, D.C. 2002. 1.88 Ga oxidized A-type granites of the Rio Maria region, eastern Amazonian Craton, Brazil: positively anorogenic, Journal of Geology, 110: 603–610.

Ricci, P.S.F., Carvalho, M.A. 2006. Rocks of the Pium-Area, Carajás Block, Brazil – A Deep seated High-T Gabbroic Pluton (Charnockitoid-Like) with Xenoliths of Enderbitic Gneisses Dated at 3002 Ma – The Basement Problem Revisited. In: VIII Simpósio de Geologia da Amazônia, CDroom (in Portuguese).

Rodrigues, E.M.S., Lafon, J.M., Scheller, T. 1992. Geocronologia Pb-Pb em rochas totais da Província Mineral de Carajás: primeiros resultados. In: CONGRESSO BRASILEIRO DE GEOLOGIA, 37., São Paulo. Resumos... São Paulo: SBG, 1992. 2: 183-184.

Rolando, A.P., Macambira, M.J.B. 2002. Geocronologia dos granitóides arqueanos da região da Serra do Inajá, novas evidências sobre a formação da crosta continental no sudeste do Cráton Amazônico, SSE Pará. In: CONGRESSO BRASILEIRO DE GEOLOGIA, 41, João Pessoa. Boletim de Resumos Expandidos. João Pessoa, SBGeo, p. 525.

Rolando, A.P., Macambira, M.J.B. 2003. Archean crust formation in Inajá range area, SSE of Amazonian Craton, Brazil, based on zircon ages and Nd isotopes. In: South American Symposium on Isotope Geology, 4, Expanded Abstract. Salvador, cdrom.

Rosa-Costa, L.T. 2006. Geocronologia 207 Pb/ 206 Pb, Sm-Nd, U-Th-Pb E 40 Ar-39 Ar do segmento sudeste do Escudo das Guianas: evolução crustal e termocronologia do evento transamazônico. 226 f. Tese de Doutorado, Instituto de Geociências, Universidade Federal do Pará, Belém.

Rosa-Costa, L.T., Ricci, P. S. F., Lafon, J. M., Vasquez, M. L., Carvalho, J. M. A., Klein, E. L., Macambira, E.M.B. 2003. Geology and geochronology of Archean and Paleoproterozoic domais of southwestern Amapá and northwestern Pará, Brazil, southestern Guiana shield. In: BRGM (Eds). Géologie de la France. N°2-3-4:101-120.

Rosa Costa, L.T, Lafon, J.M. Delor, C. 2006. Zircon geochronology and Sm–Nd isotopic study: Further constraints for the Archean and Paleoproterozoic geodynamical evolution of the southeastern Guiana Shield, north of Amazonian Craton, Brazil, Gondwana Research, 10: 277–300.

Santos, J.O.S., Hartmann, L.A., Gaudette, H.E., Groves, D.I., McNaughton, N.J., Fletcher, I.R. 2000. A new understanding of the provinces of the Amazon Craton based on integration of field mapping and U-Pb and Sm-Nd geochronology. Gondwana Research 3: 453-488.

Santos, R.D., Oliveira, D.C., Borges, R.M.K. 2008. Geologia e Petrografia das rochas máficas e ultramáficas do complexo Pium-Província Mineral de Carajás. In: CONGRESSO BRASILEIRO DE GEOLOGIA, 44, Curitiba. Anais, SBGeo, p. 535.

Santos, R.D., Oliveira, D.C. 2010. Geologia, petrografia e caracterização geoquímica das rochas máficas do Complexo Pium - Província mineral de Carajás. In: Congresso Brasileiro de Geologia, 45, CDrom (in Portuguese).

Sardinha, A.S. 2005. Geocronologia das séries magmáticas e evolução crustal da região de Canaã dos Carajás, Província Mineral de Carajás-PA. Belém. Universidade Federal do Pará, Instituto de Geociências. Exame de Qualificação (Tese de Doutoramento).

Sardinha, A.S., Dall'Agnol, R., Gomes, A.C.B., Macambira, M.J.B., Galarza, M.A., 2004. Geocronologia Pb-Pb e U-Pb em zircão de granitóides arqueanos da região de Canaã dos Carajás, Província Mineral de Carajás. In: Congresso Brasileiro de Geologia, 42, CDrom (in Portuguese).

Sardinha, A.S., Barros, C.E.M., Krymsky, R., 2006. Geology, Geochemistry, and U-Pb geochronology of the Archean (2.74 Ga) Serra do Rabo granite stocks, Carajás Province, northern Brazil. Journal of South American Earth Sciences 20: 327-339.

Silva, M.G., Teixeira, J.B.G., Pimentel, M.M., Vasconcelos, P.M., Arielo, A., Rochaw. J.S.F. 2005. Geologia e mineralização de Fe-Cu-Au do alvo GT-46 (Igarapé Cinzento), Carajás. In: MARINI O.J., QUEITOZ E.T., RAMOS B.W. Caracterização de depósitos minerais em distritos mineiros da Amazônia, P. 97-151.

Stacey J.S., Kramers J.D. 1975. Approximation of terrestrial lead isotopic evolution by a two stage model, Earth Planet. Sci. Lett. 26 (1975), pp. 207–221.

Soares, J.E.B., 2002. Geologia, Petrografia e Geoquímica das rochas granitóides arqueanas da região de Serra Dourada, Canaã dos Carajás (PA). Belém. Universidade Federal do Pará, Instituto de Geociências. Exame de Qualificação (Tese de Doutoramento).

Souza, Z. S., Medeiros, H., Althoff, F. J., Dall'Agnol, R. 1990. Geologia do terreno granito - greenstone arqueano da região de Rio Maria, sudeste do Pará. In: 36º Congresso Brasileiro de Geologia, 1990, Natal. Anais, Natal : Sociedade Brasileira de Geologia, Núcleo Nordeste, 1990. 6: 2913-2928.

Souza, Z.S. 1994. Geologia e petrogênese do "Greenstone Belt" Identidade: implicações sobre a evolução geodinâmica do terreno granito- "greenstone" de Rio Maria, SE do Pará. Belém, Universidade Federal do Pará. 2 v. (Tese de Doutorado em Geoquímica e Petrologia).

Souza, S.Z., Dall'Agnol, R., Althoff, F.J., Leite, A.A.S., Barros, C.E.M. 1996. Carajás mineral province: geological, geochronological and tectonic contrasts on the Archean evolution of the Rio Maria Granite- Greenstone Terrain and the Carajás block. In: Symposium Archean Terrane South American Platform, Brasília, extended abstracts, Brasília, SBG, pp. 31-32.

Souza, Z.S., Dall´Agnol, R., Oliveira, C.G, Huhn, S.R.B. 1997. Geochemistry and Petrogenesis of metavolcanic rocks from Archaean Greenstone Belts: Rio Maria Region (Southeast Pará, Brazil). Revista Brasileira de Geociências, 27(2): 169-180.

Souza, Z.S., Potrel, A., Lafon, J.M., Althoff, F.J., Pimentel, M.M., Dall'Agnol, R., Oliveira, C.G., 2001. Nd, Pb and Sr isotopes in the Identidade Belt, an Archean greenstone belt of Rio Maria region (Carajás Province, Brazil): implications for the geodynamic evolution of the Amazonian Craton. Precambrian Research 109: 293–315.

Stern, R., G.N. Hanson and S.B. Shirley. 1989. Petrogenisis of Mantle derived LILE-enriched Archaean Monzodiorite, Trackyandesites (Sanukitoids) in southern Superior Province." Canadian Journal of Earth Sciences, 26: 1688-1712.

Tallarico, F.H.B., Figueiredo, B.R., Groves, D.I., Kositcin, N., MCNaughton, N.J., Fletcher, I.R., Rego, J.L. 2005. Geology and Shrimp U-Pb geochronology of the Igarapé Bahia deposit, Carajás Copper-Gold belt, Brazil: an Archean (2.57 Ga) example of iron-oxide Cu-Au-(U-REE) mineralization. Econ. Geol., 100:7-28.

Tassinari, C.C.G., Macambira, M.J.B. 1999. Geochronological provinces of the Amazonian Craton. Episodes, 22(3): 174-182.

Tassinari, C.C.G., Macambira, M. 2004. A evolução tectônica do Craton Amazônico. In: Mantesso-Neto, V., Bartorelli, A., Carneiro, C.D.R., Brito Neves, B.B. (eds.). Geologia do Continente Sul Americano: Evolução da obra de Fernando Flávio Marques Almeida. São Paulo, p. 471-486.

Tassinari, T., Tachibana, J., Tulio, M., Lívio, R., Gaia, C. 2005. Geologia isotópica aplicada nas mineralizações de Cu-Au do greenstone belt da Serra dos Gradaús, Província Mineral de Carajás,

Cráton Amazônico: exemplo de mineralizações policíclicas. In: SIMPÓSIO BRASILEIRO DE METALOGENIA, 1., Gramado, RS. Resumos... Porto Alegre: SBG/SEG/SGMTM-MME, 2005. 1 CD-ROM.

Teixeira, W., Tassinari, C.C.G., Cordani, U.G., Kawashita, K. 1989. A review of the geochronology of the Amazonian Craton: tectonic implications. Precambrian Research 42: 213–227.

Teixeira N.P., Betencourt J.S., Moura C.A.V., Dall'Agnol R., Macambira E.M.B. 2002. Pb-Pb geochronology and Sm-Nd isotopic composition of the Velho Guilherme Intrusive Suite and volcanic rocks of the Uatumã Group, south-southeast Pará - Brazil. Precambrian Research, 119(1-4):257-275.

Teixeira, J.B.G., Eggler, D.H. 1994. Petrology, geochemistry, and tectonic setting of Archean basaltic and dioritic rocks from the N4 iron deposit, Serra dos Carajás, Pará, Brazil. Acta Geologica Leopoldensia, 17:71-114.

Vasquez, M.L., Macambira, M.J.B., Galarza, M.A. 2005. Granitóides transamazônicos da Região Iriri-Xingu, Pará - Novos dados geológicos e geocronológicos. In: HORBE, A.M.C., SOUZA, V.S. (Coord). Contribuições à geologia da Amazônia. Manaus: SBG-Núcleo Norte, 4: 16-31.

Vasquez, M.L., Macambira, M.J.B. Armstrong, R.A. 2008a. Zircon geochronology of granitoids from the western Bacajá domain, southeastern Amazonian craton, Brazil: Neoarchean to Orosirian evolution. Precambrian Research, 161(3-4): pg. 279-302.

Vasquez, L.V., Rosa-Costa, L.R., Silva, C.G., Ricci, P.F., Barbosa, J.O., Klein, E.L., Lopes, E.S., Macambira, E.B., Chaves, C.L., Carvalho, J.M., Oliveira, J.G., Anjos, G.C., Silva, H.R. 2008b. Geologia e Recursos Minerais do Estado do Pará: Sistema de Informações Geográficas – SIG: texto explicativo dos mapas Geológico e Tectônico e de Recursos Minerais do Estado do Pará, 328p (in Portuguese).

Vernon, R.H. 2004. A practical guide to rock microstructure, third ed., Cambridge University press, Cambridge, 954p.

Wirth, K. R., Gibbs, A. K., Olszewski Jr., W.J. 1986. U-Pb zircon ages of the Grão Pará group and Serra dos Carajás granite, Para, Brazil. Revsta Brasileira de Geociências, 16 (2):195-200.

UNIVERSIDADE FEDERAL DO PARÁ
INSTITUTO DE GEOCIÊNCIAS
PROGRAMA DE PÓS-GRADUAÇÃO EM GEOLOGIA E GEOQUÍMICA

UNIVERSIDADE FEDERAL DO PARÁ
PROGRAMA DE PÓS-GRADUAÇÃO EM GEOLOGIA E GEOQUÍMICA
TESE APROVADA COM DISTINÇÃO
Instituto de Geociências

PARECER

Sobre a Defesa Pública da Tese de Doutorado de
GILMARA REGINA LIMA FEIO

A banca examinadora da tese de doutorado de **GILMARA REGINA LIMA FEIO** intitulada **"MAGMATISMO GRANITÓIDE ARQUEANO DA ÁREA DE CANAÃ DOS CARAJÁS: IMPLICAÇÕES PARA A EVOLUÇÃO CRUSTAL DA PROVÍNCIA CARAJÁS"**, *composta pelos Professores Doutores* **Roberto Dall' Agnol** (Orientador-UFPA) **Elson Paiva de Oliveira (UNICAMP) Ignez de Pinho Guimarães (UFPE), Jean Michel Lafon (UFPA), Cláudio Nery Lamarão (UFPA)** após a apresentação oral e arguição da candidata, emite o seguinte parecer:

A candidata fez uma apresentação pública clara, bem estruturada e de conteúdo atualizado e relevante. Na argüição, a candidata mostrou segurança, domínio do assunto e maturidade científica, respondendo adequadamente aos questionamentos dos membros da banca examinadora.

O documento, elaborado na forma de agregação de três artigos científicos, submetidos a revistas especializadas internacionais, constitui uma contribuição valiosa para o entendimento do magmatismo da região de Canaã dos Carajás e da evolução geodinâmica da Província Mineral de Carajás.

Com base no exposto, a banca examinadora, por unanimidade, considera a candidata aprovada com **Distinção**.

Belém, 16 de agosto de 2011.

Prof. Dr. Roberto Dall' Agnol
Membro (Orientador-UFPA)

Prof. Dra. Ignez de Pinho Guimarães
Membro (UFPE)

Prof. Dr. Elson Paiva de Oliveira
Membro (UNICAMP)

Prof. Dr. Jean Michel Lafon
Membro (UFPA)

Prof. Dr. Cláudio Nery Lamarão
Membro (UFPA)